

**Impact of gamma-aminobutyric acid receptor-associated protein
(GABARAP) on carcinogen-induced tumorigenesis**

Dissertation

in partial fulfilment of the requirements for the academic degree of

doctor rerum naturalium (Dr. rer. nat)

**submitted to the Faculty Council of the School of Medicine
at Friedrich Schiller University of Jena**

by M.Sc. Firas Subhi Salah

born on 10. April 1977 in Diyala, Iraq

Reviewers

1. Prof. Dr. med. Iver Petersen

Institute of Pathology, University Hospital - Friedrich Schiller University Jena

2. Prof. Dr. Rolf Bräuer

Institute of Pathology, University Hospital - Friedrich Schiller University Jena

3. Prof. Dr. rer. nat. Regine Schneider-Stock

Experimental Tumorpathology, Institute of Pathology, University of Erlangen

Date of the public disputation: 03/02/2015

Contents

List of abbreviations	I
Zusammenfassung	III
Summary	VI
1. Introduction	1
1.1 GABARAP	1
1.2 Autophagy	3
1.2.1 Role of autophagy in cellular homeostasis and survival	8
1.2.2 Role of autophagy and GABARAP in tumorigenesis	9
1.2.3 Role of autophagy in cancer cell metabolism	13
1.3 Autophagy and apoptosis	15
1.4 Autophagy and immune response	19
1.5 Chemical carcinogens	22
1.5.1 Immunosuppression and immunotoxicity of carcinogen (DMBA)	24
1.5.2 Carcinogen, autophagy and DNA damage	25
1.6 Aims of the study	27
2. Materials and Methods	28
2.1 Materials	28
2.1.1 Chemicals	28
2.1.2 PCR and cell culture reagents	29
2.1.3 Kits and assays	30
2.1.4 Laboratory equipment and consumables	30
2.1.5 Immunohistochemistry and Western blot primary antibodies	31
2.1.6 Secondary antibodies	32
2.1.7 ELISA antibodies	32
2.1.8 Cytokine standards	32
2.1.9 Genotype primer sequences	32
2.1.10 Quantitative reverse transcriptase PCR (qRT-PCR) primer sequences ...	33
2.1.11 Primer sequences for mutation analysis	33
2.1.12 Solutions and buffers	33
2.2 Methods	36
2.2.1 Animals	36
2.2.2 Genotyping of GABARAP knockout mice	36
2.2.2.1 Genomic DNA extraction	36
2.2.2.2 PCR amplification	37
2.2.2.3 Agarose gel electrophoresis	37
2.2.3 Carcinogen treatment	38
2.2.3.1 DMBA treatment	38
2.2.3.2 ENU treatment	39

2.2.3.3	Hormone stimulation and MNU treatment	39
2.2.3.4	MNU and DMBA treatment	39
2.2.4	Tumor and tissue specimens	40
2.2.4.1	Haematoxylin and eosin (H & E) staining	40
2.2.4.2	Immunohistochemistry (IHC)	40
2.2.4.3	TUNEL assay	40
2.2.5	Immunology experiments	41
2.2.5.1	Cytokine analysis from lymphocyte cell cultures	41
2.2.5.2	Cytokine analysis from macrophage cell cultures	42
2.2.5.3	Cell surface marker analysis for splenocytes by FACS	42
2.2.6	Whole mount analysis of mammary glands	44
2.2.7	Microarray gene expression profiling analysis of mammary glands	44
2.2.7.1	Quality control of total RNA	45
2.2.7.2	Library preparation and WTA amplification of RNA	46
2.2.7.3	ULS-Labeling	46
2.2.7.4	Hybridization of Agilent Whole Genome Oligo Microarrays	46
2.2.7.5	Scanning results	47
2.2.7.6	Image and data analysis	47
2.2.8	Reverse transcription polymerase chain reaction (RT-PCR)	47
2.2.8.1	RNA isolation	47
2.2.8.2	Complementary DNA (cDNA) synthesis	48
2.2.8.3	Quantitative reverse transcriptase PCR (qRT-PCR)	48
2.2.9	Fibroblasts isolation and treatment	49
2.2.9.1	Primary culture of mouse embryonic fibroblasts (MEFs)	49
2.2.9.2	Mouse embryonic fibroblasts (MEFs) treatment	49
2.2.10	Analysis of proteins	49
2.2.10.1	Protein extraction and measurement	49
2.2.10.2	Western blot analysis	50
2.2.11	B16 melanoma cell inoculation	51
2.2.12	Mutation analysis	52
2.2.12.1	DNA extraction	52
2.2.12.2	Polymerase chain reaction (PCR)	53
2.2.12.3	Agarose gel electrophoresis	53
2.2.12.4	Purification of PCR products for sequencing	53
2.2.12.5	Sequencing and result analysis	54
2.2.13	Statistical analysis	54
3.	Results	55
3.1	GABARAP knockout mice exhibited low tumor formation	55
3.2	GABARAP knockout mice reduced the survival after different carcinogen treatments	58

3.3	High sensitivity of GABARAP KO mice to immunotoxicity of DMBA	60
3.4	DMBA treatment enhanced cell death in splenocytes of GABARAP KO mice	63
3.5	GABARAP-deficient immune cells showed high cytokine secretion	65
3.6	GABARAP deficiency reduced the growth of mammary glands after DMBA treatment	69
3.7	Gene expression profiling indicated differential expression of tumor suppressor gene Xaf1 in mammary glands of GABARAP KO mice	72
3.8	Xaf1 highly expressed in organs of GABARAP KO mice	77
3.9	DNA damage repair impaired in GABARAP-deficient fibroblasts	79
3.10	GABARAP knockout inhibited proliferation of inoculated B16 melanoma cells	81
3.11	GABARAP-deficient tumors did not exhibit Ras mutation	81
4.	Discussion	84
4.1	Less tumor formation in GABARAP KO mice	84
4.2	High sensitivity of GABARAP KO mice upon carcinogens treatment	85
4.3	Enhancement of cytokine secretion in GABARAP-deficient immune cells	87
4.4	Inhibition of epithelial growth in mammary glands of GABARAP KO mice after DMBA treatment	89
4.5	Gene expression profiling indicated differential expression of tumor suppressor and apoptosis inducer genes in GABARAP KO mice	90
4.6	Impairment of DNA damage repair in GABARAP-deficient MEFs	95
4.7	<i>In vivo</i> inhibition of B16 melanoma cells growth in GABARAP KO mice	97
4.8	Absence of Ras mutation in DMBA-induced tumors of GABARAP KO mice	97
4.9	Conclusions	98
5.	References	101
6.	Appendix	124
6.1	Acknowledgment	124
6.2	Curriculum vitae	126
6.3	List of publication and presentations	127
6.4	Ehrenwörtliche Erklärung	128

List of abbreviations

AhR	Aryl hydrocarbon receptor
APS	Ammonium persulfate
Atg	Autophagy-related gene
ATP	Adenosine triphosphate
B16	Mouse melanoma cell line
Bax	BCL2-associated X protein
Bcl-2	B-cell lymphoma 2
Beclin-1	Homolog of yeast autophagy-related gene 6
Bid	BH3 interacting-domain death agonist
CD4	Cluster of differentiation 4
CD8	Cluster of differentiation 8
cDNA	Complementary deoxyribonucleic acid
CKO	Control knockout
CPT	Camptothecin
CQ	Chloroquine
CTL	Cytotoxic T-lymphocytes
CWT	Control wild-type
DDR	DNA damage response
DKO	DMBA-treated knockout
DMBA	7,12-Dimethylbenz(a)anthracene
DMSO	Dimethyl sulfoxide
DNA	Deoxyribonucleic acid
DSB	Double strand breaks
DWT	DMBA-treated wild-type
EBSS	Earle's balanced salt solution
EDTA	Ethylenediaminetetraacetic acid
ELISA	Enzyme-linked immunosorbent assay
EMT	Epithelial-mesenchymal transition
ENU	N-Ethyl-N-nitrosourea
ER	Endoplasmic reticulum
FACS	Fluorescence-activated cell sorting
FFPE	Formalin-fixed paraffin-embedded
FIP200	FAK family-interacting protein of 200 kDa
GABARAP	Gamma (γ)-aminobutyric acid type A (GABA _A) receptor-associated protein
GAPDH	Glyceraldehyde-3-phosphate dehydrogenase
H-ras	Harvey rat sarcoma viral oncogene homolog
i.m.	Intramuscular
i.p.	Intraperitoneal
IAPs	Inhibitor of apoptotic proteins
IFN- γ	Interferon gamma
IL-1 β	Interleukin 1 beta
IL-2	Interleukin 2
IL-6	Interleukin 6

Irf	Interferon regulatory factor
KO	Knockout
K-ras	Kirsten rat sarcoma viral oncogene homolog
LC3	Microtubule-associated protein light chain 3
LPS	Lipopolysaccharide
MAP1LC3	Microtubule-associated protein light chain 3
MCA	Methylcholanthrene
MEFs	Mouse embryonic fibroblasts
MNU	N-Methyl-N-nitrosourea
MPA	Medroxyprogesterone acetate
mRNA	Messenger RNA
mTOR	Mammalian target of rapamycin
NF- κ B	Nuclear factor of kappa light polypeptide gene enhancer in B cells
NK	Natural killer cell
NLRs	Nod-like receptors
p62/SQSTM1	Sequestosome-1
PAH	Polycyclic aromatic hydrocarbon
PAS	Phagophore assembly site
PBS	Phosphate-buffered saline
PCR	Polymerase chain reaction
PE	Phosphatidylethanolamine
PI3K-III	Class III phosphatidylinositol 3-kinase complex
qRT-PCR	Quantitative reverse transcriptase polymerase chain reaction
Ras	Rat sarcoma
RIPA	Radio-immuno-precipitation assay
RNA	Ribonucleic acid
ROS	Reactive oxygen species
RT-PCR	Reverse transcriptase polymerase chain reaction
SD	Standard deviation
SEM	Standard error of the mean
siRNA	Small interfering ribonucleic acid
TAE	Tris-acetate-EDTA
TBST	Tris-buffered saline and Tween 20
TEMED	Tetramethylethylenediamine
TLRs	Toll-like receptors
TNF α	Tumor necrosis factor alpha
TRAIL	Tumor necrosis factor related apoptosis inducing ligand
Tregs	Regulatory T cells
ULK1	UNC-51-like kinases 1
Wt	Wild-type
Xaf1	X-linked inhibitor of apoptosis protein associated factor 1
Xiap	X-linked inhibitor of apoptosis protein

ZUSAMMENFASSUNG

Grundlage Autophagie ist ein grundlegender, evolutionär konservierter zellulärer Prozess, der in die Initiation und Progression der Tumorbildung einbezogen ist. Dabei sind sowohl onkogene Effekte bekannt, während in anderen Fällen diese Prozesse zur Tumorsuppression beitragen. GABARAP spielt bei der Autophagie eine wesentliche Rolle, indem es an der Reifung der Autophagosomen beteiligt ist. Die Funktion von GABARAP bei der Tumorgenese ist jedoch bisher nicht geklärt. Während GABARAP in allen normalen Geweben exprimiert wird, ist das Vorkommen in Tumorgewebe sehr unterschiedlich. In einer früheren Studie der Arbeitsgruppe konnte gezeigt werden, dass GABARAP beim Brustkrebs als Tumorsuppressor fungiert. Hier sollte nun die generelle Bedeutung von GABARAP in der Kanzerogen-induzierten Tumorgenese näher untersucht werden.

Methoden Die Untersuchungen erfolgten vorwiegend an GABARAP-knockout (KO)-Mäusen, bei denen die spontane sowie die durch verschiedene Kanzerogene induzierte Tumorbildung analysiert wurde. Als Kontrollen dienten C57BL/6-Wildtyp-Mäuse. In den beiden Versuchstiergruppen wurde außerdem das Wachstum von inokulierten syngenischen Tumorzellen (B16-Melanomzellen) verfolgt. In Milzen und im Brustdrüsengewebe wurden die Proliferations- (Ki-67) und Apotoseraten (TUNEL-Assay) bestimmt. Mit der Flow-Zytometrie wurden die Milzzell-Populationen bestimmt und in Überständen von kultivierten Peritoneal-Makrophagen und Milz-Lymphozyten wurde mittels ELISA die Zytokinsekretion gemessen. In Totalpräparaten von Brustdrüsen von Mäusen, die mit dem Kanzerogen DMBA behandelt worden waren, wurde die Proliferation von Epithelzellen und das Auswachsen und Verzweigen der Ausführungsgänge untersucht. Mittels Analysen des Gesamt-Genoms (Agilent Whole Mouse Genome Array) und quantitativer RT-PCR wurden Veränderungen der Genexpression analysiert und mögliche molekulare Mechanismen identifiziert, die durch die GABARAP-Defizienz und die Kanzerogenbehandlung induziert werden. Durch Behandlung von isolierten embryonalen Mausfibroblasten (MEFs) mit den genotoxischen Agenzien DMBA und Camptothecin (CPT) wurde mittels Western-Blotting die Bedeutung von GABARAP im Autophagieprozess und bei der Reparatur von DNA-Schäden untersucht. In DMBA-induzierten Tumoren wurden schließlich noch H-ras-Mutationen analysiert.

Ergebnisse Im Vergleich zu WT-Kontrollen war in GABARAP-KO-Mäusen die spontane und die DMBA-induzierte Tumorentwicklung signifikant geringer ausgeprägt. Nach der Kanzerogenbehandlung wurden verschiedene phänotypische Veränderungen beobachtet, so z.B. ein reduziertes Überleben der Tiere und eine hohe Toxizität von DMBA für Milzzellen

(deutlich verringertes Volumen der Milz und der Zellzahl). FACS-Analysen zeigten, dass diese Verringerung alle Zellpopulationen betraf, d.h. kein selektiver Einfluss auf bestimmte Populationen stattfand. Die Verringerung der Zahl der Milzzellen nach DMBA-Behandlung war dabei in GABARAP-KO-Mäusen deutlich stärker ausgeprägt als in den WT-Kontrollen. Makrophagen aus GABARAP-KO-Mäusen produzierten nach DMBA-Behandlung signifikant höhere Mengen der proinflammatorischen Zytokine IL-1 β und IL-6 als Zellen von WT-Kontrollen, bei den Milz-Lymphozyten war in ähnlicher Weise nach Stimulation mit Anti-CD3 die Sekretion von IL-2 und IFN- γ erhöht. In Brustdrüsenpräparaten aus GABARAP-KO-Mäusen war nach DMBA-Behandlung die Proliferation der epithelialen Zellen und das Auswachsen und Verzweigen der Ausführungsgänge signifikant geringer als in WT-Kontrollen. Im Brustdrüsengewebe und in der Milz waren darüber hinaus die zelluläre Proliferation (Ki-67) verringert und die Apoptose (Zahl TUNEL-positiver Zellen) erhöht. Genexpressions-Analysen und qRT-PCR belegten im Brustdrüsengewebe von GABARAP-KO-Mäusen sowie in Milz, Leber, Lunge und Niere eine hohe und differentielle Expression des Tumorsuppressor- und Apoptoseinducer-Gens Xaf1. Darüber hinaus waren verschiedene Zelltod-Gene (Bid, Apaf1, Bax, Tnfrs10b, Ripk1 und Siva1) und die Zellzyklus-Inhibitoren Cdkn1a (p21) und Cdkn2c (p18) hochreguliert. In GABARAP-defizienten MEFs war nach Behandlung mit DMBA und CPT die Reparatur von DNA-Schäden beeinträchtigt, wie die Akkumulation von phosphoryliertem γ H2AX und des Autophagiemarkers p62 sowie die Verringerung der Cyclin D1-Proteine belegen. In GABARAP-KO-Mäusen war auch das Tumorstadium nach Inokulation von B16-Melanomzellen reduziert. Mutationsanalysen haben gezeigt, dass bei GABARAP-KO-Mäusen in den DMBA-induzierten Tumoren keine H-ras-Mutationen nachweisbar sind, im Gegensatz zu 5 Mutationen, die in den 14 Tumoren bei den WT-Kontrollen auftraten.

Schlussfolgerung Unsere Ergebnisse zeigen, dass GABARAP auf unterschiedliche Weise in die Hemmung der Tumorgenese einbezogen sein könnte. Die in GABARAP-KO-Mäusen nach DMBA-Behandlung beobachtete Modulation der Immunreaktivität lässt vermuten, dass GABARAP bei der Steigerung der Anti-Tumor-Immunität eine Rolle spielt, wie die erhöhte Sekretion von IL-1 β , IL-2, IL-6 und IFN- γ zeigen. Die hohe Expression von Xaf1 in GABARAP-KO-Mäusen könnte nach genotoxischen Einflüssen die zelluläre Todesrate erhöhen und auf diese Weise die Tumorbildung verhindern sowie das Wachstum/Verzweigen des Brustdrüsengewebes hemmen. Die Beeinträchtigung der Reparatur von DNA-Schäden in GABARAP-defizienten MEFs wiederum lässt vermuten, dass GABARAP auch in diesem Prozess eine wichtige Rolle spielt. Bei GABARAP-Mangel könnte so der Zellzyklusarrest

gefördert werden, der nach Behandlung mit genotoxischen Agenzien auftritt. Die Hemmung des Wachstums von inokulierten Melanomzellen und das Fehlen von H-ras-Mutationen in den DMBA-induzierten Tumoren bei GABARAP-KO-Mäusen unterstreichen die besondere Bedeutung von GABARAP für die Tumorprogression.

SUMMARY

Background: Autophagy is a basic, evolutionary conserved cellular process has been linked with tumor initiation and progression. In some instances, it may serve as oncogene, whereas in others, it contributes to tumor suppression. GABARAP has an essential role in the autophagic process through its involvement in the maturation of the autophagosome. The role of GABARAP in tumorigenesis is not yet clarified. It is ubiquitously expressed in all tested normal tissues, while its expression in tumors is divers. A previous study of our group revealed that GABARAP may function as a tumor suppressor in breast cancer. Here the general impact of GABARAP should now be examined in the carcinogen-induced tumor formation.

Methods: GABARAP knockout (KO) mice were used as the main experimental substrate. They were investigated for spontaneous and induced tumorigenesis by applying different carcinogens to the GABARAP KO and C57BL/6 control mice. Furthermore, the growth of inoculated syngeneic tumor cells (B16 melanoma) was monitored. Murine spleen and mammary gland tissue was investigated for proliferation and apoptosis by using Ki-67 immunostaining and the TUNEL assay. Peritoneal macrophages and splenic lymphocytes were isolated and cultured. Flow cytometry and ELISA were implemented to detect the populations of splenocytes and measure their cytokine secretion. Mammary gland whole mount analysis was carried out to investigate the proliferation of epithelial cells and ductal branching after treatment with the carcinogen DMBA. Agilent Whole Mouse Genome expression analysis and quantitative reverse transcriptase PCR (qRT-PCR) were performed to analyse the alteration of gene expression and to identify candidate molecular mechanisms being affected by GABARAP knockout and carcinogen treatment. Mouse embryonic fibroblasts (MEFs) were cultured and treated with the genotoxic agents DMBA and camptothecin (CPT) to reveal the role of GABARAP in autophagy and DNA damage repair by using western blotting. H-ras mutation analysis was performed in the DMBA-induced tumors.

Results: GABARAP KO mice exhibited significantly less tumor formation after DMBA treatment and less spontaneous tumor growth. Several phenotypic changes were observed in GABARAP KO mice upon carcinogen treatment: reduction in animal survival and high toxicity of DMBA to splenocytes represented by decrease of the spleen volume and the total cell number. FACS analysis revealed that the decreased number of splenocyte populations was in agreement with the reduction in total cell number and there was no discrimination for

the effect of DMBA on particular cell types. However, the reduction of splenocytes was more profound in GABARAP KO mice. GABARAP-deficient macrophages of DMBA-treated mice produced higher levels of proinflammatory cytokines (IL-1 β and IL-6) compared to wild-type counterparts. Moreover, GABARAP-deficient lymphocytes of DMBA-treated mice enhanced the immune response through increasing the production of IL-2 and IFN- γ upon CD3 stimulation. Mammary glands of GABARAP KO mice showed a significant reduction in epithelial cell proliferation and ductal branching after DMBA treatment. Mammary gland and spleen sections revealed a decrease of proliferation cells and an increase of positive cells in the TUNEL assay. Gene expression profiling and qRT-PCR manifested a high and a differential expression of tumor suppressor and apoptosis inducer gene Xaf1 in mammary glands of GABARAP KO mice as well as in the spleen, liver, lung and kidney. Moreover, several cell death genes (Bid, Apaf1, Bax, Tnfrsf10b, Ripk1 and Siva1) and cell cycle inhibitors (Cdkn1a (p21) and Cdkn2c (p18)) were upregulated. GABARAP-deficient MEFs treated with DMBA and CPT showed impairment in DNA damage repair through accumulation of phosphorylated γ H2AX which was accompanied by accumulation of the autophagy marker p62 and downregulation of the Cyclin D1 protein. Reduced tumor growth in GABARAP KO mice was also evident after B16 melanoma cell inoculation. Furthermore, mutation analysis of DMBA-induced tumors revealed no H-ras mutation in the tumors of GABARAP KO mice compared to 5 mutations in 14 tumors of the wild-type mice.

Conclusion: Our results indicated different aspects for the role of GABARAP in the inhibition of tumorigenesis. The immunomodulation by GABARAP deficiency upon DMBA treatment suggests the involvement of GABARAP in the enhancement of anti-tumor immune response by increasing IL-1 β , IL-6, IL-2 and IFN- γ . High Xaf1 expression in GABARAP KO mice may mediate increased cellular death upon genotoxic insult thereby preventing tumor formation and favoring inhibition of growth/branching of the mammary glandular tissue. Impairment of DNA damage repair in GABARAP-deficient MEFs suggests that GABARAP plays an important role in this process and that its deficiency promotes cell cycle arrest after treatment with genotoxic agents. Inhibition of inoculated B16 melanoma cell growth and absence of H-ras mutation in DMBA-induced tumors of GABARAP KO mice further underscores the importance of GABARAP in tumor progression.

1. Introduction

1.1 GABARAP

Gamma (γ)-aminobutyric acid type A (GABA_A) receptor-associated protein (GABARAP) is an evolutionarily highly conserved gene family from yeast to mammals and ubiquitously expressed in a wide range of organisms and tissues. The amino acid level for mammalian forms of GABARAP showed 100% identity suggesting that the function of this gene is essential or beneficial in mammals (Mohrlüder *et al.*, 2009). GABARAP, a cytoplasmic protein of 14 kDa, belongs to a gene family including GEC1 (glandular epithelial cell protein 1) or GABARAPL1; GATE-16 (Golgi associated ATPase enhancer of 16 kDa) or GABARAPL2 or GEF-2 (Ganglioside expression factor 2); GABARAPL3; LC3 (Microtubule-associated protein light chain 3); yeast Apg8 or Aut7p; and *Caenorhabditis elegans* (*C. elegans*) LGGs (LC3, GABARAP and GATE-16) protein (Chen and Olsen, 2007). GABARAP was previously described acting as a trafficking molecule for different receptors like the GABA_A receptor, a major inhibitory neurotransmitter in cortical neurons, or the transferrin receptor, a type II integral membrane protein responsible for delivery of iron-laden transferrin to the endosomal compartment (Wang *et al.*, 1999; Chen *et al.*, 2000; Green *et al.*, 2002). It is involved in the transport of proteins or vesicles from intracellular pools to the cell surface through its interaction with microtubules, tubulin, and N-ethylmaleimide-sensitive factor (NSF), an ATPase and chaperone that activates soluble NSF attachment protein receptor (SNARE) proteins in membrane fusion events (Wang and Olsen, 2000; Coyle *et al.*, 2002; Kittler *et al.*, 2001). The N-terminus of GABARAP is highly positively charged and features a putative tubulin-binding motif. GABARAP was identified in a yeast two-hybrid search for proteins that bind to the loop of the GABA_A receptor and has been implicated in the clustering of these receptors (Wang *et al.*, 1999; Chen *et al.*, 2000), thus GABARAP mediated inhibitory neurotransmission in mammalian through its interaction with the γ 2 subunit of GABA_A receptors in the central nervous system. In subsequent studies, GABARAP was shown to increase the cell-surface expression of GABA_A receptors, implying that GABARAP might be an important factor regulating the intracellular trafficking of GABA_A receptors (Leil *et al.*, 2004; Boileau *et al.*, 2005; Chen *et al.*, 2005). Furthermore, it has been reported that GABARAP binds to the C-terminal region and thereby inhibits Ost-III, a splice variant of the guanine nucleotide exchange factor Ost, suppressing Rac-1-dependent negative regulation of transferrin receptor endocytosis (Ieguchi *et al.*, 2007). Sequence analysis showed similarity between GABARAP and light chain-3 of microtubule-associated proteins 1A and 1B at the NH₂-terminus, whereas the COOH-terminal part of the GABARAP

protein is thought to interact with the target protein (Wang *et al.*, 1999). Figure 1 represents schematic protein structure of GABARAP indicating the alpha helix and beta sheet domains (Bavro *et al.*, 2002).

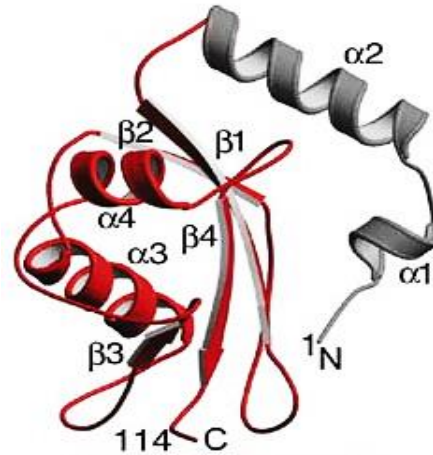


Figure 1. Ribbon presentation of the GABARAP structure. The N-terminal region (N) is shown in grey, the core structure displaying a conserved ubiquitin-like fold is shown in red and Carboxyl terminal ends is indicated as C (Source: Bavro *et al.*, 2002).

By using yeast two-hybrid analyses and/or coimmunoprecipitation assays, GABARAP has been found to interact directly with several proteins. For instance, GABARAP interacts with: P130 / phospholipase C-related inactive protein (PRIP); one of the essential factors in the dynamic regulation of GABA_A receptor expression at inhibitory synapses (Kanematsu *et al.*, 2002), transferrin receptor (TfR); a carrier protein needed for the import of iron into the cell through receptor-mediated endocytosis (Green *et al.*, 2002), glutamate receptor-interacting protein 1 (GRIP1); a synaptic protein that plays an important role in trafficking, synaptic targeting and recycling of glutamate receptors (Kittler *et al.*, 2004), DEAD box polypeptide 47 (DDX47); an RNA helicase implicated in pre-mRNA splicing or ribosome biogenesis (Lee *et al.*, 2005), Ras-related protein 24 (RAB24); one of the small GTP-binding proteins that are involved in vesicular transport and fusion events (Wu *et al.*, 2006), and calreticulin (CRT); a multifunctional protein known as a luminal Ca²⁺ dependent chaperone located in the endoplasmic reticulum (ER) (Mohrlüder *et al.*, 2007). Finally, Schwarten *et al.* (2009) have been identified BNIP3L / Nip-like protein x (Nix) as a direct interaction partner of GABARAP. BNIP3L (Bcl-2 and adenovirus E1B 19 kDa interacting protein-like), is commonly known to be implicated in apoptosis and known to localize to mitochondria, ER and the nuclear envelope (Imazu *et al.*, 1999; Ohi *et al.*, 1999; Yussman *et al.*, 2002).

1.2 Autophagy

The cellular homeostasis requires for a constant turnover of continuous synthesis of cellular components and clearance of damaged or superfluous proteins and organelles. Eukaryotic cells have developed two degradation pathways to achieve this homeostasis and controlling the balance between anabolism and catabolism in order to have a normal cell growth and development. These degradation pathways are the ubiquitin-proteasome system (UPS) and the lysosomal pathway. Proteasomal degradation has high selectivity; generally the proteasome recognizes only ubiquitinated substrates, which are primarily short-lived proteins, that's mean the proteasome only has the ability to degrade proteins; it is unable to degrade damaged organelles (Ciechanover, 2005; Cuervo *et al.*, 2005). The lysosomal degradation does not follow such a simple pattern as the proteasomal pathway; it is mainly supported by autophagy (Mizushima and Komatsu, 2011). The term autophagy derived from the Greek words “auto” and “phagy” which means “self” and “eating”, this term was coined by de Duve in 1963 when he described the presence of single- or double-membrane vesicles that contain parts of the cytoplasm and organelles (De Duve and Wattiaux, 1966).

Autophagy is an intracellular pathway for bulk degradation of proteins and organelles within the lysosome/vacuole. It is used for recycling cytoplasm to generate macromolecular building blocks and energy under stress conditions (Feng *et al.*, 2014). There are three primary types of autophagy (Fig. 2) (Wirawan *et al.*, 2012): macroautophagy (hereafter referred as autophagy), microautophagy and chaperone-mediated autophagy (CMA). Both macroautophagy and microautophagy can be selective or nonselective. Nonselective autophagy is used for the turnover of bulk cytoplasm under starvation conditions, whereas selective autophagy specifically targets damaged or dispensable organelles, including mitochondria and peroxisomes, as well as invasive microbes. The CMA degrades only soluble targeted proteins in a selective manner (Feng *et al.*, 2014). Autophagy is initiated by the formation of a cup shaped membrane (termed “phagophore”), suggested to originate from the ER (Hayashi-Nishino *et al.*, 2009; Yla-Anttila *et al.*, 2009). The phagophore enwraps parts of the cytoplasm to form a double-membrane vesicle, called autophagosome, which eventually fuses with the lysosomes/vacuole (Fig. 2). Autophagy was initially revealed in mammalian systems, but the molecular identification of it has been expanded and differentiated through genetic screening of autophagy-defective mutants in *Saccharomyces cerevisiae* (Tsukada and Ohsumi, 1993; Thumm *et al.*, 1994).

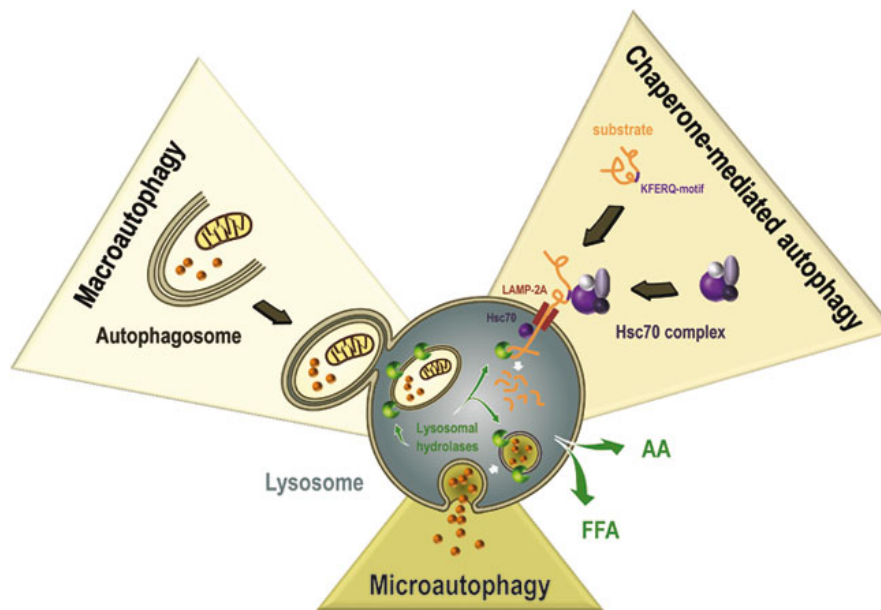


Figure 2. Schematic representation of the types of autophagy. *Microautophagy: the cargos are sequestered by direct invagination of the lysosome membrane. Chaperone-mediated autophagy: the protein transported by chaperone hsc70 complex to the lysosome membrane. Macroautophagy: the most distinguishing feature is the initiation of isolated membrane (phagophore) that encloses and isolates the cytoplasmic components by formation the autophagosome which eventually fuses with the lysosomes/vacuole (Wirawan et al., 2012).*

In 1997, the first autophagy-specific gene, APG1 (now Atg1 (Klionsky et al., 2003)), was identified, and the corresponding gene product, Apg1/Atg1, was characterized as a Ser/Thr protein kinase (Matsuura et al., 1997). Subsequently, multiple laboratories discovered more than thirty autophagy-related (Atg) genes in the autophagy machinery. The morphology of the autophagy process is essentially the same in yeast, plants and animals. The mammalian autophagy pathway can be divided into six discrete steps: initiation, nucleation, elongation, closure, autophagosome maturation and degradation by fusion with the lysosome (Kang et al., 2011). A critical regulator of autophagy is the serine/threonine kinase mTOR (mammalian target of rapamycin). The mTOR pathway involves two functional complexes: mTORC1 and mTORC2 (Fig. 3). The rapamycin-sensitive mTOR complex 1 (mTORC1) is composed of mTOR catalytic subunit, raptor (regulatory associated protein of mTOR, a protein that acts as a scaffold for the mTOR-mediated phosphorylation of mTOR substrates), GβL, PRAS40 (proline-rich Akt substrate of 40 kDa), and Deptor (DEP domain-containing mTOR-interacting protein) (Fig. 3). This complex functions as a nutrient/energy/redox sensor and controls protein synthesis (Kim et al., 2002; Hay and Sonenberg, 2004; Laplante and Sabatini, 2009). The other mTOR complex, mTORC2, which is less sensitive to rapamycin, includes mTOR, rictor (rapamycin-insensitive companion of mTOR), GβL, Sin1 (SAPK-interacting protein 1), PRR5/Protor-1 (protein observed with rictor), and Deptor (Fig. 3). The

mTORC2 promotes cellular survival by phosphorylating the Ser473 of Akt/PKB and also functions as an important regulator of cytoskeletal organization and metabolism (Sarbasov *et al.*, 2006; Laplante and Sabatini, 2009).

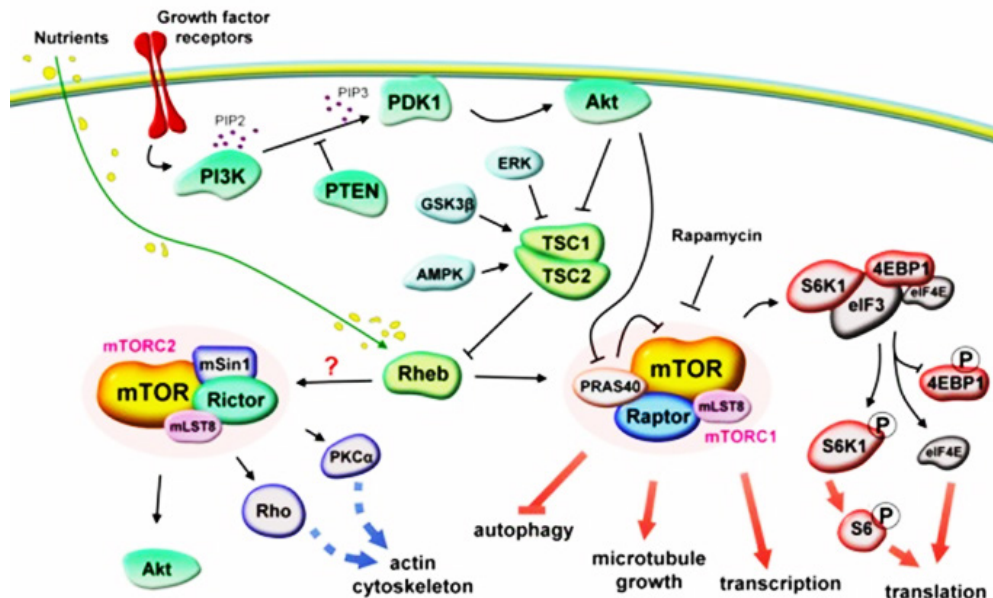


Figure 3. Schematic representation of mTOR signaling network

(Source: <http://www.iimcb.gov.pl/Jaworski-Laboratory-research-focus.html>)

ULK1 (homolog of yeast Atg1), Atg13, and FIP200 (FAK family-interacting protein of 200 kDa) form a stable complex that signals to the autophagic machinery downstream of mTORC1. In nutrient-rich states, mTORC1 forms a complex with ULK1/2 kinase, mAtg13, FIP200 and Atg101. mTOR phosphorylates ULK1 and Atg13 and thereby keeps the kinase activity of ULK1 in check. Under starvation conditions or if the AMP-to-ATP ratio increases or upon treatment with rapamycin (mTOR inhibitor), mTORC1 dissociates from the ULK complex resulting in the activation of ULK1 (the inhibitory phosphorylation of ULK1 is lost). ULK1 then autophosphorylates and activates Atg13 and FIP200 to initiate autophagy. The activated ULK complex localizes to the developing phagophore (Jung *et al.*, 2009; Mehrpour *et al.* 2010).

Another important nutrient-sensitive entry route to autophagy signaling is the class III phosphatidylinositol 3-kinase complex (PI3K-III) consisting of hVps34, Beclin-1 (yeast Atg6) and p150/hVps35. Phosphatidylinositol-3-phosphate is bound to its core partner Beclin-1 and p150/hVps35. The complex is found on the phagophore and might facilitate recruitment of other Atgs to the developing vesicle (Funderburk *et al.*, 2010; Rosenfeldt and Ryan, 2011). Moreover, the autophagy pathway can be stimulated by multiple forms of cellular stress apart

from nutrient or growth factor deprivation, for instance hypoxia, reactive oxygen species, DNA damage, protein aggregates, damaged organelles or intracellular pathogens (Kroemer *et al.*, 2010).

GABARAP belongs to a family of mammalian orthologues of the yeast autophagy-related ubiquitin-like protein Atg8 (autophagy-related 8 proteins) (Ohsumi, 2001), it has an essential role in the autophagic process possibly in the elongation of the phagophore membrane by mediating hemi-fusion events (Nakatogawa *et al.*, 2007; Xie *et al.*, 2008; Weidberg *et al.*, 2010). In mammalian cells, three Atg8 homologs have been identified: MAP1LC3 or LC3 (in human: LC3A, LC3B, LC3C), GABARAP and GATE-16 (GABARAPL2). LC3 and GABARAP proteins are the most studied protein in the autophagy machinery and appear to be modified by lipids in the same manner as described in yeasts, and have been shown to localize to the autophagosome (Kabeya *et al.*, 2004). The GABARAP family is not only structurally similar to ubiquitin, but also undergoes a similar posttranslational cascade modification process as occurs in ubiquitinylation (Hochstrasser, 2000). GABARAP contains 117 amino acids and consists of an ubiquitin-like fold with two additional amino terminal helices. *In vivo*, the C-terminal Leu-117 of GABARAP is cleaved off leaving Gly-116 as a C-terminal residue that can be conjugated covalently to proteins and lipids via an E1 (Atg7), E2 (Atg3) and E3 (Atg12/Atg5/Atg16 complex) enzymes cascade (Tanida *et al.*, 1999; Kirisako *et al.*, 2000; Hanada *et al.*, 2007). Although LC3 proteins and GABARAP are known to be conjugated to phosphatidylethanolamine (PE) and incorporated into autophagosomes, the biological relevance of the expansion of Atg8 proteins in higher mammals is largely unknown (Behrends *et al.*, 2010; Wild *et al.*, 2014). This autophagic factor is known to decorate autophagosomes and recruit factors such as p62/SQSTM1 and NBR1 (Bjorkoy *et al.*, 2005; Kirkin *et al.*, 2009; Shvets *et al.*, 2011). However, the exact role of this gene in autophagy is not yet fully understood. Weidberg *et al.* (2010) indicated that LC3 is involved in elongation of the phagophore membrane whereas GABARAP is essential for a later stage of autophagosome maturation, this study have been done by using RNA silencing to target GABARAP and other Atg8 family members in HeLa cells.

The autophagosomes origin is still a matter of debate. Several hypotheses have been generated about the origin of autophagosome, but the most well accepted theories are those which hypothesized ER or mitochondrial origin. In yeast, the cytoplasm of cell contained vesicles forming the phagophore assembly site (PAS). At this site, autophagy machinery proteins have been identified to be coupled to the PAS (Suzuki *et al.*, 2001), which matures from a phagophore to an autophagosome (Kim *et al.*, 2002). In mammals, no PAS has been

identified but the growing and expansion of isolated membranes is induced under the action of ULK1, coupled to the PI3K complex (hVps34, Beclin-1 and p150/hVps35) and to mAtg9, homolog of yeast Atg9 (Young *et al.*, 2006). The further expansion, closure and maturation of the autophagosomes rely on the mammalian homologs of the Atg12/Atg5/Atg16 complex and on Atg8 (Tanida *et al.*, 2004). Figure 4 shows a schematic model of autophagy signaling pathway.

E1-like protein (Atg7) is the first enzyme that activates Atg8 (Tanida *et al.*, 1999), then Atg8 is transmitted to an E2-like protein (Atg3) (Kirisako *et al.*, 2000). Thereafter, Atg8 is conjugated to PE by an amine bond through the free C-terminus of the Atg8 glycine residue. Under the cleavage action of Atg4, PE can be released later from Atg8 to facilitate autophagosome-lysosome fusion (Ichimura *et al.*, 2000). Since the Atg12/Atg5/Atg16 complex stimulates Atg8-PE formation, this complex acts potentially as an E3-like enzyme in the Atg8 conjugation system (Hanada *et al.*, 2007). When Atg8 is conjugated to PE, it joins to the membrane of the autophagosome; therefore Atg8 is used as an autophagosomal marker (Kirisako *et al.*, 1999).

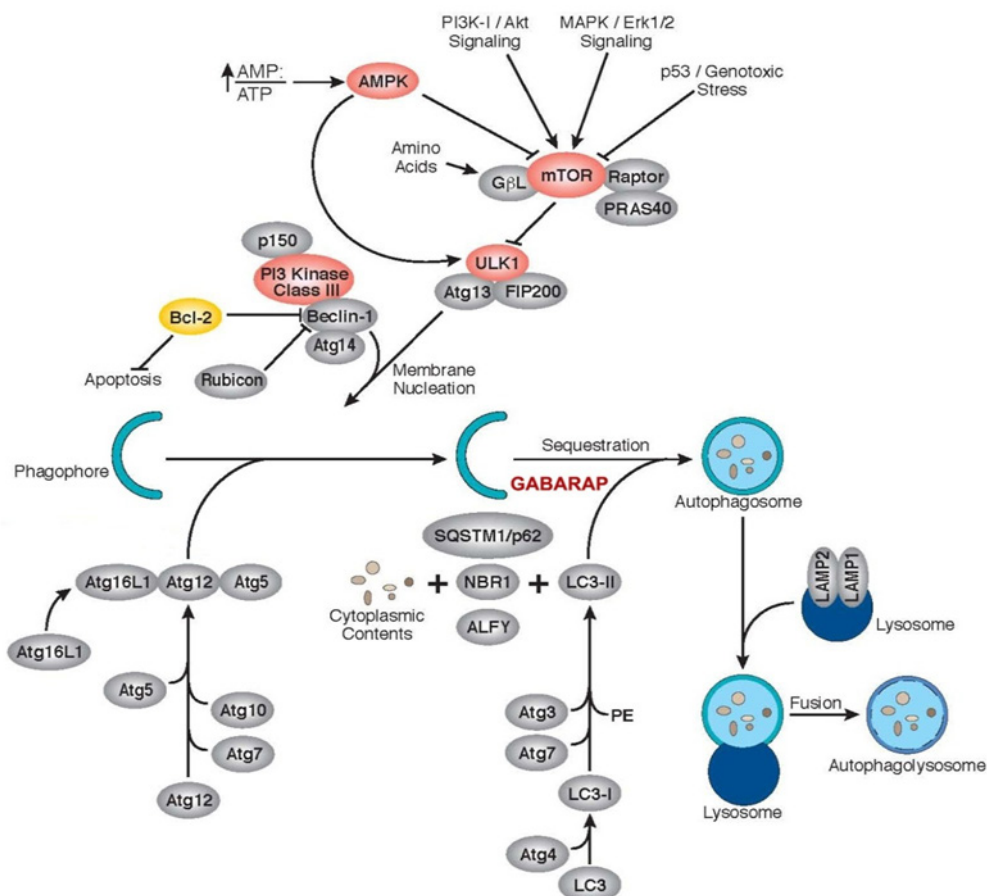


Figure 4. Signaling pathway of autophagy (Source: <http://www.cellsignal.com/>).

1.2.1 Role of autophagy in cellular homeostasis and survival

Autophagy occurs at low basal levels in most normal cells to perform homeostatic functions such as protein and organelle turnover or when the cells need to ‘self-cannibalize’ and to proceed to cell survival under stress in order to maintain cellular integrity (Mizushima *et al.*; 2008). Observations and genetic analyses in patients, as well as studies in transgenic animal models, clearly implicate autophagy in diseases, including neurodegenerative diseases (such as Parkinson’s disease), skeletal muscle diseases (myopathy), cardiac failure, hepatic disorders, infectious diseases, inflammatory disorders (such as Crohn’s disease), aging, diabetes, obesity and cancer (Levine and Kroemer, 2008; Mizushima *et al.*, 2008; Mizushima and Komatsu, 2011). Investigations of the role of autophagy in cellular homeostasis have been performed in liver and brain tissue pathophysiology. Mice with brain-specific Atg5 or Atg7 deletion revealed neuronal degeneration accompanied with protein aggregates and damaged mitochondria accumulation, which are hallmarks of Huntington’s and Parkinson’s diseases (Hara *et al.*, 2006; Komatsu *et al.*, 2006); whereas, mice with liver-specific Atg7 deletion exhibited p62-containing protein aggregations in the liver which prompted liver injury and accelerated the death of hepatocytes (Komatsu *et al.*, 2007). Furthermore, a mouse model with a targeted deletion of Atg7 in adipose tissue displayed unique anti-obesity and insulin sensitization effects with impaired adipogenesis (Singh *et al.*, 2009; Zhang *et al.*, 2009). Survival mechanism of autophagy has been shown in autophagy-deficient mice that die within 1 day of birth due to lack of nutrients (Kuma *et al.*, 2004). In addition, mice with homozygous mutant of Beclin-1 die in early embryonic development (E7.5 or earlier) (Yue *et al.*, 2003); in contrast to mice with other homozygous autophagy gene deficiencies which showed normal embryonic phenotype, for example GABARAP, Atg4 and FIP200 (O’Sullivan *et al.*, 2005; Marino *et al.*, 2007; Wei *et al.*, 2011).

Autophagy proteolysis has been shown to extensively decrease with age (Cuervo *et al.*, 2005; Martinez-Vicente *et al.*, 2005). Diminishing and alteration in the regulation of autophagy leads to the accumulation of altered organelles and membranes, and may start a vicious pro-aging circle (Bergamini *et al.*, 2004). Furthermore, blockage of autophagy genes in long-lived *C. elegans* mutants prevents life-span extension (Melendez *et al.*, 2003).

Moreover, autophagy related gene Atg16L1 is expressed in the intestine and particularly strongly in Crohn’s disease, and the functional knockdown of this gene abrogates autophagy of the intracellular pathogen *Salmonella typhimurium* (Rioux *et al.*, 2007).

1.2.2 Role of autophagy and GABARAP in tumorigenesis

The role of autophagy in cancer is complex and likely tissue and genetic context-dependent. There is evidence that autophagy may be oncogenic in some instances, whereas in others, it clearly contributes to tumor suppression (Levine, 2007; Mathew *et al.*, 2007; Wilkinson and Ryan, 2010; Rosenfeldt and Ryan, 2011). Indeed, the connections between autophagy and cancer occur at two aspects, first at the level of tumor initiation and progression, and the second during cancer treatment. Autophagy is regulated by many sensors involved in tumor suppression (PTEN, TSC1-TSC2, p53, DAPk) or oncogenesis (Akt, Ras), and the signaling pathways of these sensors form part of a cell program that is constantly modified in cancer cells, such as growth, proliferation, survival, death and processes that play important roles in tumor progression, such as tumor immunity and angiogenesis. Botti *et al.* (2006) represented these potential interconnections between autophagy and cell functions that are often disrupted in cancer cells as an integrative model designed by cogwheels moving in a concerted manner to influence autophagy and other cell properties in an alternative manner (Fig. 5).

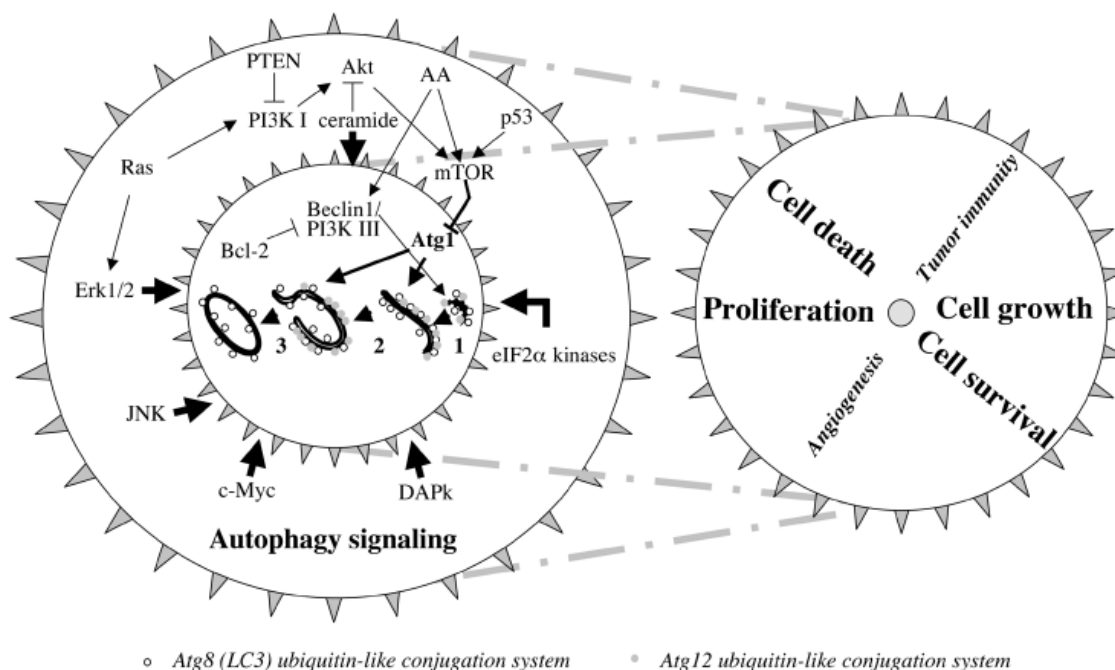


Figure 5. Potential interconnection of autophagy and cellular functions that are constantly disrupted in malignant cells. Autophagy signaling (outer cogwheel on the left), autophagy machinery (inner cogwheel on the left) and cell functions (cogwheel on the right) are symbolized by cogwheels connected by chains. The movement of one cogwheel drives the other two. Bold black arrows and bold black bars indicate the stimulation and inhibition of autophagy, respectively (Source: Botti *et al.*, 2006).

One example of a tumor suppressor sensor of autophagy is p53 that has been demonstrated to play a dual role in autophagy regulation depending on its subcellular location. In the nucleus, p53 executes a pro-autophagic role in a transcription-dependent or independent manner (Feng *et al.*, 2007), whereas the cytoplasmic p53 has been characterized as a master repressor of autophagy (Tasdemir *et al.*, 2008). Ras oncogene is an example of an oncogenic sensor of autophagy; it is a member of the small GTPase family which plays a fundamental role in regulation of cell growth and survival that is frequently activated in cancer (Schubbert *et al.*, 2007). It has been reported that active oncogenic Ras induces autophagy, but depending on the cellular context, autophagy induction can either promotes autophagic cell death (Elgendy *et al.*, 2011) or promotes and facilitates oncogenic transformation by maintaining and improving cell metabolism (Guo *et al.*, 2011; Kim *et al.*, 2011; Lock *et al.*, 2011).

In 2003, Qu *et al.* and Yue *et al.* provided the first genetic link between autophagy and tumorigenesis. They conferred evidence that mice with heterozygous loss of Beclin-1; an autophagy and apoptosis regulating gene (Kang *et al.*, 2011), promoted spontaneous malignancies including lung and liver cancers and lymphomas in aged mice. Many human and murine tissues express Beclin-1, and it localizes primarily within cytoplasmic structures, including the ER, mitochondria and the perinuclear membrane. A monoallelic deletion of Beclin-1 has been frequently observed in sporadic human breast cancers and ovarian cancers (Aita *et al.*, 1999; Kondo and Kondo 2006). In addition, inhibition of autophagy by heterozygous loss of Beclin-1 or homozygous deletion of Atg5 in apoptosis-defective tumor cells induced reactive oxygen species (ROS), mitochondrial damage, and p62 accumulation which led to increased DNA damage and ultimately facilitated cancer progression (Karantza-Wadsworth *et al.*, 2007; Mathew *et al.*, 2009). Paradoxically, Atg5, Atg7, or FIP200 knockout in various tissues did not lead to malignant tumor development *in vivo* (Wei *et al.*, 2011), but the mice with systemic mosaic deletion of Atg5 and liver-specific Atg7 deletion developed benign liver adenomas originating from autophagy-deficient hepatocytes (Takamura *et al.*, 2011). Moreover, Atg4C-deficient mice showed increased susceptibility to fibrosarcoma induction by the chemical carcinogen methylcholanthrene (MCA) (Marino *et al.*, 2007).

It is unlikely that the increased rate of tumorigenesis in mice with heterozygous loss of Beclin-1 is due to autophagy deficiency. First of all, Beclin-1 has been shown to interact with Bcl-2 (B-cell lymphoma 2); an important anti-apoptotic protein. Substantially decreased levels of Beclin-1 in the cells with heterozygous loss of Beclin-1 may promote the activity of Bcl-2 to boost cell survival which in turn promotes tumorigenesis (Pattingre *et al.*, 2005).

Surprisingly, Beclin-1 deficiency has been associated with deficiency in the tumor suppressor p53, suggesting that p53 deficiency, rather than autophagy deficiency, provide a mechanism to promote genomic instability which in turn leads to tumorigenesis in Beclin-1 deficient mice (Liu *et al.*, 2011). Moreover, Liu *et al.* (2011) showed that increased ubiquitination of both Beclin-1 (in the class III PI3K complex) and p53 have been achieved by the inhibition of the deubiquitinating activities of USP10 (ubiquitin specific peptidase 10) and USP13 (ubiquitin carboxyl-terminal hydrolase 13), and subsequently promotes their proteasome-mediated degradation. Beclin-1 by interacting with USP13 regulates the deubiquitinating activities of both USP13 and USP10. Thus, Beclin-1 appears to sit at the center of the mechanisms directing the levels of p53 (Lorina *et al.*, 2013). On the other hand, there is a similarity in the tumor spectra of heterozygous deletions of Beclin-1 and p53 mice. The frequencies of tumors in mice with heterozygous deletions of Beclin-1 and p53 are lung carcinoma, lymphoma and hepatoma (Jacks *et al.*, 1994; Qu *et al.*, 2003), and the Beclin-1 gene is frequently monoallelically deleted in human sporadic ovarian, prostate and breast cancers similar to that of p53 mutations (Liu *et al.*, 2011).

In an elegant study of Wei *et al.* (2011), autophagy inhibition by FIP200 knockout suppressed mammary tumor initiation and progression in a mouse model of breast cancer driven by the PyMT oncogene in association with decreased Cyclin D1 expression, induction of interferon (IFN)-responsive genes, effector T-cell tumor infiltration and increased production of cytokines, such as CXCL10. Furthermore, the consequences of FIP200 deletion resulted in defects in the autophagy machinery including deficient LC3I to LC3II conversion, accumulation of ubiquitinated protein aggregates and p62/SQSTM1, and increased number of abnormal mitochondrial morphology in tumor cells. Mammary tumor cells or Ras-transformed mouse embryonic fibroblasts (MEFs) harbouring FIP200 deletion exhibited decreased cell proliferation in both cell systems with no changes in apoptosis (Wei *et al.*, 2011).

GABARAP is ubiquitously expressed in all tested normal tissues, however, its expression in human tumors has shown diversity; for instance neuroblastoma (Roberts *et al.*, 2004), breast tumors (Klebig *et al.*, 2005), thyroid tumors (Roberts *et al.*, 2009) and colorectal tumors (Miao *et al.*, 2010) were investigated. Roberts *et al.* (2004) studied a cohort of primary neuroblastoma tumor samples and predicted that a low mRNA expression level of GABARAP were associated with decreased survival among patients with neuroblastoma. Moreover, GABARAP transfection into the CAL51 breast cancer cell line influenced the growth rate of cancer cells *in vitro* and the ability of colony formation in soft agar and,

furthermore, suppressed the tumorigenicity of the cells in nude mice (Klebig *et al.*, 2005). They suggested that GABARAP functions as a putative tumor suppressor gene in breast cancer, however, the precise role and mechanism that GABARAP played to inhibit cell growth was not elucidated. In an effort to explore the involvement of neurotransmitter and neurotrophic factors in thyroid carcinogenesis, Roberts *et al.* (2009) showed that the expression level of GABARAP was increased in adenomas and thyroid cancer suggesting its role in early stages of thyroid tumorigenesis. Moreover, Miao *et al.* (2010) found that GABARAP expression was significantly higher in colorectal cancers than that in adjacent matched non-tumor tissues, and the high expression of GABARAP was significantly correlated with a low grade of differentiation and shortened survival.

The second aspect of connection between cancer and autophagy occurs during cancer treatment. Indeed, autophagy induction have been found to spatially localize to hypoxic tumor regions (Mathew *et al.*, 2007), poorly vascularized tumor regions (Degenhardt *et al.*, 2006) or following cytotoxic treatments (Ertmer *et al.*, 2007; Apel *et al.*, 2008; Amaravadi *et al.*, 2011), and thus promotes cancer cell survival under stressful conditions. In general, autophagy induction after both radiation and chemotherapy (Yang *et al.*, 2011), essentially acts as a treatment resistance mechanism, stress-relieving and pro-survival function that is crucial for viability of cancer cell (Lozy and Karantzaa, 2012). In such cases, genetic or pharmacologic autophagy inhibition preferentially sensitizes cancer cells to treatment (Vazquez-Martin *et al.*, 2009; Wang *et al.*, 2011). It has been shown that chloroquine, a non-specific autophagy inhibitor, could enhance the γ -irradiation-induced cell death in glioma cells and enhanced cyclophosphamide-induced tumor cell death in a murine Myc-driven lymphoma model (Firat *et al.*, 2012; Amaravadi *et al.*, 2007). Combination treatment of cisplatin or paclitaxel with chloroquine in non-small cell lung cancer (NSCLC) cell line A549 enhanced the cisplatin- and paclitaxel-induced apoptosis (Liu *et al.*, 2012a). Furthermore, 3-methyladenine, another non-specific autophagy inhibitor, augments 5-fluorouracil chemotherapy by increasing cancer cell apoptosis accompanied by tumor regression in colon cancer xenografts (Li *et al.*, 2010). Pancreatic ductal adenocarcinoma (PDAC) has been shown to require elevated autophagy for growing, and it is highly resistant to chemotherapy. Inhibition of autophagy sensitized PDAC cell lines and xenograft mouse model to gemcitabine; the current standard treatment for PDAC (Donohue *et al.*, 2013). These findings might be a promising approach for augmenting the efficacy of standard anticancer regimens.

1.2.3 Role of autophagy in cancer cell metabolism

Autophagy is a cellular process of self-cannibalization, by which the cells seize their own cytoplasm and organelles and consume them in lysosomes for reusing the resulting metabolites as a source to generate energy and to provide building blocks for the synthesis of new macromolecules. Thus, autophagy is considered being a major cell survival mechanism and deeply integrated into metabolism, stress response and cell death pathways (Rabinowitz and White, 2010; Arroyo *et al.*, 2014). Metabolism function of autophagy is a highly advantageous to cancer cells, which have demonstrated high metabolic demands and a requirement for metabolic reprogramming, as evidenced by the Warburg and reverse Warburg effects (Lozy and Karantzaa, 2012).

Warburg effect is the observation that cancer cells predominantly produce energy by glycolysis followed by lactic acid fermentation in the cytosol, rather than by an oxidation of pyruvate in mitochondria as in most normal cells. Rapidly growing tumor cells have higher glycolytic rates than those of their normal tissues of origin; this occurs even if oxygen is plentiful (aerobic glycolysis) (Warburg, 1956; Kim and Dang, 2006; Vander Heiden *et al.*, 2009). For example, leukemia cells are highly glycolytic despite residing in the bloodstream. Reverse Warburg effect has been elucidated in human epithelial breast cancers. According to this model, aerobic glycolysis (Warburg effect) actually takes place in tumor associated fibroblasts, not in cancer cells. Aerobic glycolysis in cancer associated fibroblasts results in the production of high-energy metabolites (such as lactate and pyruvate), which can then be transferred to adjacent epithelial cancer cells, which are undergoing oxidative mitochondrial metabolism, resulting in increased adenosine triphosphate (ATP) production in cancer cells, driving tumor growth and metastasis (Pavlides *et al.*, 2009; Martinez-Outschoorn *et al.*, 2010; Pavlides *et al.*, 2010). Increased reactive oxygen species (ROS) production and oxidative stress in tumors are caused by the high rates of aerobic glycolysis and glutaminolysis (Lozy and Karantzaa, 2012). ROS act as signal transducers in various intracellular pathways and play critical roles in cell survival, death, and immune defenses. It has been found that ROS production in tumor cells commonly upregulates autophagy for survival (Scherz-Shouval and Elazar, 2007; Huang *et al.* 2011). Furthermore, autophagy in stromal cells stimulates by cancer cell-induced oxidative stress and result in release of metabolites by tumor-associated fibroblasts and their subsequent utilization by neighboring cancer cells (Lozy and Karantzaa, 2012).

The protumorigenic function of autophagy has been demonstrated in recent years through its ability to increase the glucose metabolism in tumor cells in response to diverse stresses.

Lock *et al.* (2011) showed that H-Ras transformation in autophagy-competent MEFs displayed enhancement in glucose uptake compared with their autophagy-deficient counterparts. Increased glycolysis in autophagy-competent cells facilitates Ras-mediated adhesion-independent transformation, indicating a unique mechanism for autophagy to promote Ras-driven tumor growth in specific metabolic microenvironments. In contrast, autophagy-deficiency in Ras-transformed cells and in cancer cells possessing activating Ras mutations has decreased the rate of glycolysis accompanied with decreased the sensitivity to dropped glucose concentrations in comparison with autophagy-competent counterparts, both in terms of proliferation and adhesion-independent transformation (Lock *et al.*, 2011). Implication of autophagy in prevention and progression of cancer has been elucidated in human normal breast epithelial cells (MCF10A). MCF10A cells infected with retroviral MFG-K-RasV¹² undergo cellular transformation with increased levels of autophagy-related genes. In contrast, pharmacological inhibition of autophagy or targeted suppression of Atg5 and Atg7 expression by short hairpin (sh) RNA completely blocked K-RasV¹²-induced anchorage-independent cell growth on soft agar and inhibited tumor formation in nude mice (Kim *et al.*, 2011). Moreover, Kim *et al.* (2011) provided evidence for the cross-talk between ROS and MAPK (mitogen-activated protein kinases) signaling that is required for both autophagy-related gene expression and autophagy induction in cells overexpressing oncogenic K-Ras. Increased ROS production in K-Ras transformed cells resulted in autophagy induction via activation of JNK (c-Jun N-terminal kinase) that lead to MAPK signaling activation.

Because Ras mutations are frequently observed in pancreatic, lung and colon cancers, the role of autophagy has been studied extensively in these cancer models (Guo *et al.*, 2011; Yang *et al.*, 2011). Although Ras mutation is not routinely observed in breast tumors, there is evidence that the Ras pathway is activated in breast cancer cell lines (Eckert *et al.*, 2004), as Ras hyperactivation may occur downstream of ErbB2 signaling, which is often amplified in breast cancers (Birnbaum *et al.*, 2009; Arias-Romero and Chernoff, 2010). High levels of basal autophagy in human cancer cell lines bearing activating Ras mutations have been commonly observed, and down-regulating the expression of essential autophagy genes impaired cell growth through accumulation of abnormal mitochondria and reduced oxygen consumption. In addition, suppression of autophagy in cells transduced with Ras reduced the tumor growth in nude mice, and the tumors displayed abnormal histology, active caspase-3, and p62 and ubiquitin accumulation (Guo *et al.*, 2011).

1.3 Autophagy and apoptosis

Autophagy and apoptosis are both well-controlled biological processes and play fundamental roles in development, maintenance of tissue homeostasis and diseases, and subsequently determining cellular fate. Although autophagy is primarily considered to have a cytoprotective function, it can also promote cell death during normal development and disease, which is called type II programmed cell death (Mizushima *et al.*, 2008; Mizushima and Levine, 2010). There are many crucial factors governing the cross-talk between autophagy and apoptosis. Several autophagic proteins have potential roles in apoptosis, and vice versa, i.e. several proteins known to regulate apoptosis have also been identified as inducers of autophagy (Table 1) (Mukhopadhyay *et al.*, 2014). For example, the functional and structural interaction between Beclin-1 and anti-apoptotic proteins Bcl-2 and Bcl-xL is well documented (Fig. 6) (Pattingre *et al.*, 2005; Takacs-Vellai *et al.*, 2005; Maiuri *et al.*, 2007a; Nikolettou *et al.*, 2013). Inactivation of Beclin-1 triggers apoptotic cell death as evidenced by the increased number of apoptotic cell corpses in somatic tissues and in the germline of animals (Takacs-Vellai *et al.*, 2005). Proteins of Bcl-2 family classified into three groups based on their apoptotic properties. One group inhibits apoptosis (Bcl-2, Bcl-xL, Bcl-w, Bcl-B, Mcl-1, and A1), and two groups of pro-apoptotic proteins: the multi-domain proteins (Bax, Bak, and Bok) contain three Bcl-2 homology (BH) domains, and the BH3-only proteins (Bad, Bid, Bim, Bmf, Bik, Hrk, Noxa, and PUMA), which interact with the anti-apoptotic Bcl-2 protein family to promote apoptosis (Oltvai *et al.*, 1993; Wong and Puthalakath, 2008; Hou *et al.*, 2010). Beclin-1 has a BH3 region, which can bind to BH3 receptors and inhibit anti-apoptotic Bcl-2 proteins, such as Bcl-2 and Bcl-xL, or can stimulate the pro-apoptotic Bcl-2 family members, such as Bax and Bak (Galonek and Hardwick, 2006). Moreover, Bcl-2 inhibits autophagy when it localized to the mitochondria and ER by binding to nutrient-deprivation autophagy factor-1 (NAF-1), which stabilizes the interaction between Bcl-2 and Beclin-1 at the ER surface. Cellular stress conditions cause displacement of Bcl-2 from Beclin-1 and Bax thereby inducing autophagy and apoptosis, respectively. Pro-apoptotic BH3-only protein Bad disrupts the interaction of Bcl-2/Bcl-xL and Beclin-1 to induce autophagy by binding to the BH3-binding domain of Bcl-2 or Bcl-xL (Levine *et al.*, 2008; Marquez and Xu, 2012). In addition, anti-apoptotic Bcl-2 proteins regulate apoptosis at the mitochondrial membrane, where they sequester Bax (pro-apoptotic protein), thus preventing mitochondrial membrane permeability and cytochrome c release to cytosol to execute apoptosis (Wong and Puthalakath, 2008). Recently, specific cellular inhibitors called inhibitor of apoptotic proteins (IAPs), for example Xiap (X-linked inhibitor of apoptosis

protein), have been shown to regulate autophagy via interaction of Xiap with Mdm2 (p53 E3 ubiquitin protein ligase), a negative regulator of p53, and subsequently suppresses autophagy (Huang *et al.*, 2013).

Table 1. Proteins with dual role in autophagy and apoptosis (Source: Mukhopadhyay et al., 2014)

Protein	Role in autophagy	Role in apoptosis
<u>Autophagic proteins</u>		
mTOR	Inactive form involves in initiation	mTOR regulates apoptosis
Beclin-1	Autophagosome nucleation	Cleaved C-fragment induces mitochondrial apoptosis
UVRAG	Upregulates Vps34–Beclin1 interaction	Antiapoptotic, inhibits Bax translocation from cytosol to mitochondria
AMBRA	Upregulates Vps34–Beclin1 interaction	Regulate mitochondrial apoptosis; cleaved by caspases and calpains
Atg3	Conjugates with Atg12	Regulates mitochondrial cell death
Atg5	Conjugates with Atg12, autophagosome elongation	Interacts with FADD to inhibit apoptosis, cleaved N-fragment induces mitochondrial apoptosis
Atg12	Autophagosome elongation	Stimulates mitochondrial apoptosis by inactivating Bcl-2 and Mcl-1
Atg4D	LC3 processing	Cleaved Atg4D localize to mitochondria and induces apoptosis
p62	Binds with LC3, promotes degradation of polyubiquitinated protein aggregates	Caspase-8 processing and activation
<u>Apoptotic proteins</u>		
Bcl-2, Bcl-xL	Interacts with Beclin-1 and inhibit autophagy	Antiapoptotic
Bad, Bak, BNIP3, Nix	Proautophagic, disrupting Beclin-1/Bcl-2 interaction	Proapoptotic
Bax, PUMA	Proautophagic, noncanonical type	Proapoptotic
p53	- Inhibits by cytoplasmic p53 - Induces by nuclear p53 through DRAM	Proapoptotic Proapoptotic
Noxa	Induces autophagy by disrupting Mcl-1/Beclin-1 interaction	Proapoptotic
Bim	Sequesters Beclin-1, inhibits autophagy	Proapoptotic
XIAP	Inhibits by Mdm2-p53 signaling	Inhibits caspase 3,7
cFLIP	Prevent interaction between Atg3 and LC3	Inhibits caspase 8

Furthermore, autophagic proteins have been involved in intrinsic and extrinsic apoptosis pathways (Table 1 and Fig. 6) (Mukhopadhyay *et al.*, 2014; Nikolettou *et al.*, 2013). The extrinsic apoptosis pathway gets stimulation by soluble molecules that bind to plasma-membrane receptors (cell surface death receptors), such as Fas (CD95/APO1), TNF α (tumor necrosis factor- α) and TRAIL (TNF related apoptosis inducing ligand) receptors (Mathew *et al.*, 2009), whereas the intrinsic pathway is triggered by various intracellular (mitochondrial) stimuli resulting from hypoxia, DNA damage, oxidative stress, and growth factor deprivation, which induce outer mitochondrial membrane permeabilization (Galluzzi *et al.*, 2012). In both

circumstances, activation of caspases results in mitochondrial membrane permeabilization, chromatin condensation and DNA fragmentation, thereby leading to the destruction of the cell (Fig. 6) (Green, 2005). Caspases are controlled by IAPs, which bind to and inhibit caspases. Despite this, caspases can escape IAP's inhibitory control through antagonist of IAPs either with Smac/DIABLO and HtrA2/Omi, which are released from the mitochondria (Galluzzi *et al.*, 2012), or Xaf1 (Xiap-associated factor 1) (Liston *et al.*, 2001).

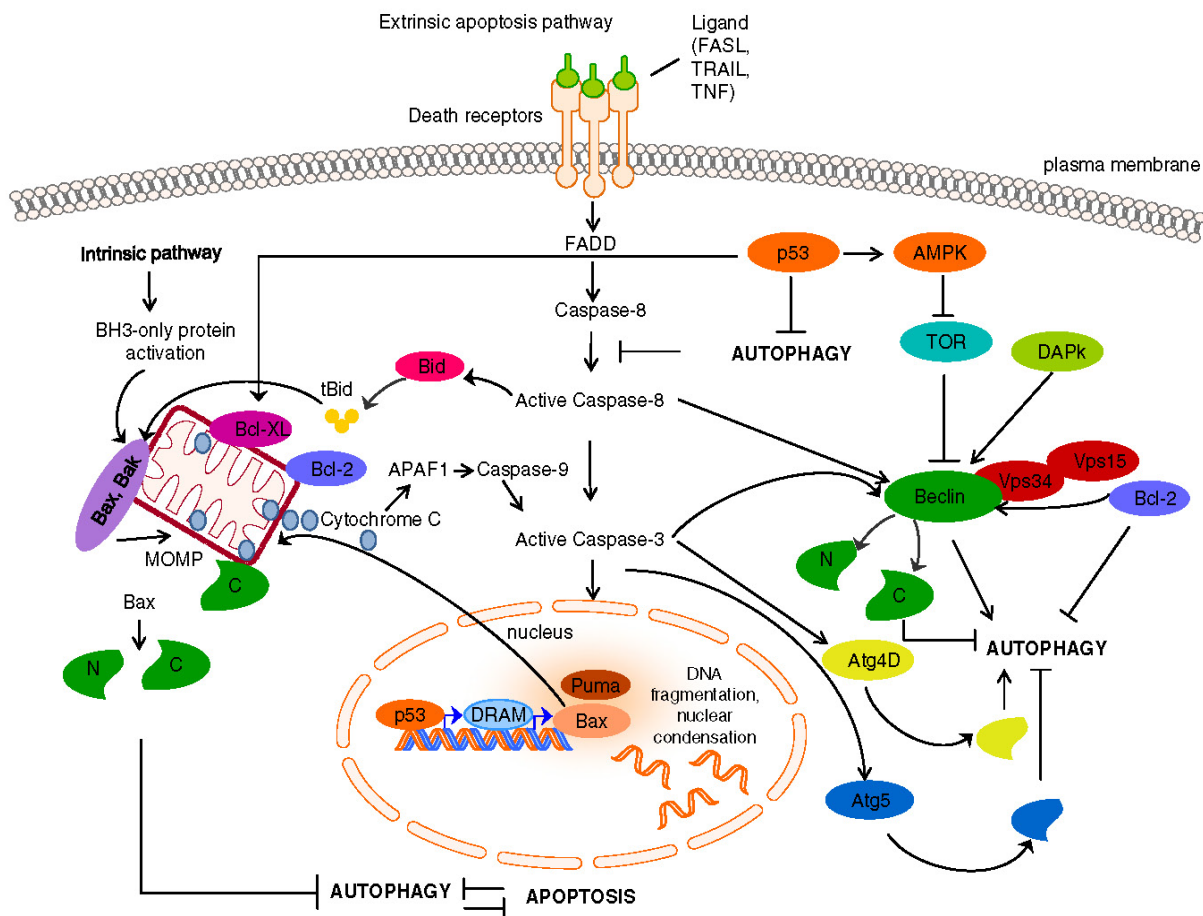


Figure 6. The complex interplay between autophagy and apoptosis (Source: Nikolettou et al., 2013)

The autophagic pathway works as an adaptive response to cellular stress, however, in the case of extreme or prolonged stress, cells are forced to undergo autophagic cell death (Ouyang *et al.*, 2012; Bhutia *et al.*, 2013). It has been shown that autophagy and apoptotic cell death are induced in response of ER stress; for instance perturbation of either ER calcium homeostasis or ER function (Nikolettou *et al.*, 2013). ER-induced autophagy in colon and prostate cancer cells has an essential role in eliminating unwanted polyubiquitinated protein aggregates, thereby safeguarding the cell from death. However, in normal human colon cells

and in non-transformed murine embryonic fibroblasts, autophagy does not mitigate ER stress but rather is engaged in ER-induced apoptosis (Ding *et al.*, 2007).

Searching for a particular binding protein of GABARAP, Lee *et al.* (2005) identified DEAD (Asp-Glu-Ala-Asp/His) box polypeptide 47 (DDX 47), a putative RNA helicase, as a binding partner of GABARAP. Co-transfection of GABARAP and DDX47 cDNA into ovarian cancer cells was shown to induce apoptosis. Moreover, direct interaction of GABARAP and proapoptotic protein Nix/ BNIP3L has been elucidated in mammalian cells (Schwarten *et al.*, 2009). Nix belongs to the BH3-only protein group of Bcl-2 protein family, and is known to localize to mitochondria and to a lesser extent to the ER and nuclear envelope (Imazu *et al.*, 1999; Ohi *et al.*, 1999). Nix induces and contributes to cell death upon transient expression in non-neuronal cells (Imazu *et al.*, 1999, Chen *et al.*, 1999, Yussman *et al.*, 2002). Nix knockout was shown to enhance tumorigenicity, whereas its transient overexpression in a number of cancer cell lines was shown to inhibit colony formation mediated by p53-dependent apoptosis (Fei *et al.*, 2004). Moreover, autophagy has been induced in tumor cells transfected with the Nix homologous gene BNIP3 (Daido *et al.*, 2004). Atg5 overexpression increased autophagy in cells overexpressing BNIP3 compared to BNIP3 alone, and this autophagy enhancement correlated with reduction in BNIP3-mediated cell death (Hamacher-Brady *et al.*, 2007). Atg4, a crucial regulatory component of the autophagosome biogenesis pathway (Scherz-Shouval *et al.*, 2007), has four assumed Atg4 paralogues (autophagins Atg4A-Atg4D) (Marino *et al.*, 2003). Betin and Lane (2009) have shown that caspase-cleaved Atg4D acquires increased priming and delipidation activities against GABARAPL1. The siRNA silencing of Atg4D expression has suppressed the autophagy by abrogating GABARAPL1 autophagosome formation and sensitizes cells to starvation and staurosporine-induced cell death. These findings favor the hypothesis that caspases stimulate Atg4D-mediated autophagy to promote the cellular survival under stress (Betin and Lane, 2009).

Autophagy deficiency or inhibition occurred during knockdown of autophagy related genes or during pharmacological block by chloroquine and 3-methyladenine, resulting in accumulation of ubiquitinated protein aggregates, reactive oxygen species (ROS), p62 accumulation, mitochondrial damage and increased abnormal mitochondrial morphology (Karantza-Wadsworth *et al.*, 2007; Komatsu *et al.*, 2007; Kim *et al.*, 2008; Mathew *et al.*, 2009; Wei *et al.*, 2011). Under cellular stress and anti-cancer therapy, the autophagosome engulfs damaged mitochondria and apoptotic proteins to promote cellular survival, whereas under serum starvation condition, autophagy protects cells by sequestering ROS-producing mitochondria through autophagosome formation (Liu *et al.*, 2012b). Moreover, p62/sequestosome 1 is a

multi-functional and multi-adaptor protein and has been implicated in several cellular signaling pathways, for example the signaling axis that shuttles ubiquitinated proteins to the lysosome during autophagy and the activation of the transcription factor NF- κ B (Moscat and Diaz-Meco, 2009; Huang *et al.*, 2013). Mathew *et al.* (2009) showed that the modulation of p62 by autophagy is a key factor in tumorigenesis, whereas recently, Huang *et al.* (2013) linked p62 activity to the extrinsic apoptosis pathway. In the setting of autophagy inhibition, upregulation of p62 can mediate apoptosis via caspase-8 activation that was Bax-dependent and a consequence of mitochondrial amplification (Huang *et al.*, 2013). Moreover, p62 upregulation and increased level of active caspases-8, in the context of autophagy inhibition, can trigger apoptosis in the presence of H₂O₂ in U87MG cells (Zhang *et al.*, 2013).

In addition to the relationship between autophagy and apoptosis, autophagy also prevents cell death that occurs due to cell detachment from the extracellular matrix (ECM); which is called anoikis, in both nontumorigenic epithelial cell lines and in primary epithelial cells (Fung *et al.*, 2008).

1.4 Autophagy and immune response

Autophagy has been implicated in both innate and adaptive immunity. Published studies suggested that the autophagy machinery is an innate immunity effector against intracellular bacteria and viruses (Nakagawa *et al.*, 2004; Paludan *et al.*, 2005; Yoshimori and Amano, 2009), whereas other studies showed that autophagy has roles in adaptive immunity functions through its impact on MHC (major histocompatibility complex) class II presentation (Dengjel *et al.*, 2005; Gannage and Münz, 2010). The importance of the role of autophagy in immunity (innate and adaptive) is highlighted in part by the association of defects in autophagy with several disease states including metabolic syndrome, inflammatory disorders (Crohn's disease), neurodegeneration, aging and cancer (Levine and Kroemer, 2008).

Autophagy of tumor cell may recruit the immune cells through facilitating of adenosine 5'-triphosphate (ATP) releases from tumor cells in response to chemotherapy. In turn, ATP recruits dendritic cells and a T cell response, thereby stimulating antitumor immune responses (Michaud *et al.*, 2011). Furthermore, Michaud *et al.* (2011) found that inhibiting Atg5 or Atg7 expression in highly immunogenic allograft mouse tumors blunted the ATP release by the tumor cells in response to chemotherapy. The role of autophagy in efficient antigen cross-presentation in tumor cells has been shown in few studies (Li *et al.*, 2008; 2011). Li *et al.* (2008) found that siRNA-mediated knockdown of Beclin-1 or Atg12 in antigen donor tumor cells resulted in less cross-presentation. They postulated a mechanism by which the

autophagosome acted as a carrier of protein antigens from tumor cells (Li *et al.*, 2011). In contrast, autophagy can also limit immune-mediated cytotoxicity (Amaravadi, 2011). Noman *et al.* (2011) found that autophagy prevent T cell-mediated cytotoxicity in the context of hypoxia in lung cancer cells. Moreover, in the B16-F10 melanoma allograft mouse model, inhibition of Beclin-1 resulted in a reduction of tumor growth and increased tumor apoptosis, and combination of autophagy inhibition with melanoma peptide vaccination heightened tumor regression compared to either treatment alone (Noman *et al.*, 2011). Consistent with these results, preclinical data indicated that blocking of autophagy with chloroquine enhanced the efficacy of chemotherapy, targeted therapy, and immunotherapy (Amaravadi *et al.*, 2011). Furthermore, attenuation of autophagy by Atg5 knockdown in human melanoma cells enhanced basal surface exposure of the phagocytosis signal calreticulin, dendritic cell maturation, interleukin-6 (IL-6) production and proliferation of antitumorigenic CD8⁺IFN- γ ⁺ and CD4⁺ IFN- γ ⁺ T cells (Garg *et al.*, 2013).

The tumor stroma consists of tumor cells and tumor-associated cell types including fibroblasts, endothelial cells and immune cells. The accepted current view is that the dynamic interaction and coevolution between tumor cells and stromal cells dictates tumor progression and the response to cancer therapy (Pietras and Ostman, 2010; Maes *et al.*, 2013). Accumulating observations suggest that autophagy may play an important immunomodulatory role by regulating the tumor stroma and surface proteome (Maes *et al.*, 2013). Various stress factors are present in the tumor microenvironment due to intratumoral hypoxia resulting from insufficient vasculature (blood supply) and lack of growth factors as well as tumor acidosis. All of these stress factors stimulate autophagy in the tumor compartment. Increased autophagy in tumor cells can support the energy metabolism, but it can also act as transporter for dangerous signals, proinflammatory cytokines and chemokines, and different intracellular proteins to the extracellular space (Garg *et al.*, 2010; Dupont *et al.*, 2011; Michaud *et al.*, 2011).

It has been shown that innate immunity plays an essential role in controlling the maintenance of tissue homeostasis and reacts to tissue disruption, for example disruption which occurs during breast branching morphogenesis at puberty and pregnancy, and in post-weaning involution (Demaria *et al.*, 2011). These processes are regulated mainly by macrophages, and are associated with inflammation that resolves once tissue homeostasis is restored (Gyorki and Lindeman, 2008). In contrast, carcinogenesis is a chronic process, predominantly characterized by disordered proliferation and death of the neoplastic cells, and the releasing of damage-associated molecular patterns (DAMP) molecules from dying cancer cells can foster

a state of chronic inflammation (Zeh and Lotze, 2005; Mantovani *et al.*, 2008). Moreover, death of epithelial cells during transformation releases tumor-associated antigens which activate tumor specific T and B cell responses, and subsequently prevent tumor outgrowth. On the other hand, genetically unstable cancer cells can become resistant to the recognition and killing by immune effector cells by a process called immunoediting (Schreiber *et al.*, 2011).

There are a wide variety of close interactions between autophagy and the pattern recognition receptors (PRRs) of the innate immune response, for example Toll-like receptors (TLRs) and Nod-like receptors (NLRs) (Araya *et al.*, 2013). During innate immune signaling, TLRs can induce autophagy (Shi and Kehrl, 2010). Disruption of the association between Beclin-1 and Bcl-2 is a proposed mechanism of the induction of autophagy mediated by the TLR adaptors, MyD88 and TIR-domain-containing adapter-inducing interferon- β (TRIF) (Levine *et al.*, 2011). NLRs are components of inflammasomes, an integral part of the innate immune system's response to infections and cellular stress. The activation of inflammasome leads to recruit the apoptosis-associated speck-like protein that contains a caspase recruitment domain and pro-caspase-1, which results in caspase-1 activation. The activation of caspase-1 is required to mature interleukin 1 β (IL-1 β) and IL-18, which are then secreted out of the cells. Autophagy has been shown to negatively regulate inflammasome activation by eliminating dysfunctional mitochondria (Nakahira *et al.*, 2011; Shi *et al.*, 2012). The disruption of autophagy-related genes, including Beclin-1, Atg5, Atg16L1, LC3 and GABARAP, in macrophages have been shown to increase ROS production and translocation of mitochondrial DNA (mtDNA) into the cytosol upon treatment with lipopolysaccharides (LPS), an effective inducer of the inflammatory response, and ATP, an NLRP3 (NLR family, pyrin-domain containing 3) inflammasome inducer (Tal *et al.*, 2009; Nakahira *et al.*, 2011; Zhang *et al.*, 2013). Thereby, secretions of proinflammatory cytokines such as IL-1 β and IL-18 are have augmented, which, in the context of sepsis that is associated with massive infections, can mediate tissue injury and lethal shock (Hotchkiss and Karl, 2003).

Several studies using mouse models demonstrated that developing tumors are indeed recognized and destroyed by the intact immune systems through anti-tumor immune surveillance mechanisms (Shankaran *et al.*, 2001; Bui and Schreiber 2007; Wei *et al.*, 2011). It has been shown that interferon gamma (IFN- γ) inhibited cell growth in various cells (Gooch *et al.*, 2000; Plataniias, 2005), as well as could inhibit growth of mammary tumor cells driven by PyMT (Wei *et al.*, 2011). The protumorigenesis function of autophagy has been evaluated directly by using loss-of-function approaches directed against the FIP200 gene, a regulator of

mammalian autophagy, in a PyMT oncogene driven mouse model of breast cancer *in vivo*. FIP200 knockout halted tumorigenesis by not only affecting cellular energy metabolism and proliferation but also by increasing host antitumor immunosurveillance (Wei *et al.*, 2011). Moreover, FIP200 deletion in mice enhanced infiltration of antitumorigenic CD8⁺IFN- γ ⁺ and CD4⁺IFN- γ ⁺ T cells in the tumor microenvironment, triggered by increased production of chemokines, such as CXCL9 and CXCL10, from FIP200-null tumor cells (Wei *et al.*, 2011). Interestingly, inhibition of cytotoxic T lymphocyte in this model retrieved accelerated mammary tumor initiation (Wei *et al.*, 2011). All together, these observations proposed that cancer cell-associated autophagy plays a key role in subverting antitumor immunity, thereby supporting tumor progression (Maes *et al.*, 2013).

Interestingly, “no inactivating somatic mutations in any autophagy genes have been reported, thus autophagy probably play an essential role in tumorigenesis, and autophagy-deficient tumors may be rare” (Amaravadi, 2011).

1.5 Chemical carcinogens

Carcinogens are a number of agents that can cause tumors in humans and animals. They can be divided into three major groups: chemical carcinogens, physical carcinogens, and oncogenic viruses. Most of them, single or in combination result in tumor initiation by interfering with DNA in cells and thereby impact on cellular function. Chemical carcinogens are environmental factors that act through genotoxic and non-genotoxic mechanisms and they may require metabolic activation to elicit detrimental effects (Fig. 7). The activation of carcinogens is often linked to the activity of ‘xenobiotic metabolizing enzymes’ such as cytochrome P450-dependent monooxygenases, glutathione S-transferases, sulphotransferases and others (Fig. 7) (Luch, 2005).

The most used types of chemical carcinogens are polycyclic aromatic hydrocarbons (PAHs), nitrosoureas and urethane that have been applied in experimental animals to induce tumors (Medina, 1974 and 2007; Uno *et al.*, 2004). Among PAHs, 7,12-dimethylbenz(a)anthracene (DMBA) is a reliable, potent and widely used carcinogen. In addition, it is immunotoxic in various species, tissues, and cell types (Medina, 2007). N-ethyl-N-nitrosourea (ENU) and N-methyl-N-nitrosourea (MNU) are alkylating agents and potent mutagens of the nitrosourea carcinogen family (Medina, 2007). The environmental exposure to DMBA comes from burning of organic matters, including coal, charred foods, cigarette smoke and car exhaust fumes (Gelboin, 1980). DMBA acts at multiple sites and can induce various type of cancer in animal models, for instance mammary, skin, lung neoplasms, lymphoma and oral cavity

tumors (de Oliveira *et al.*, 2013). The response of mice to DMBA is strain-dependent with DBA2f and Sencar mice being the most sensitive and C57BL/6 being the least sensitive (Medina, 2010). Most studies have used DMBA to induce mammary tumors following administration by oral gavage in mouse models (Medina, 1974, Currier *et al.*, 2005).

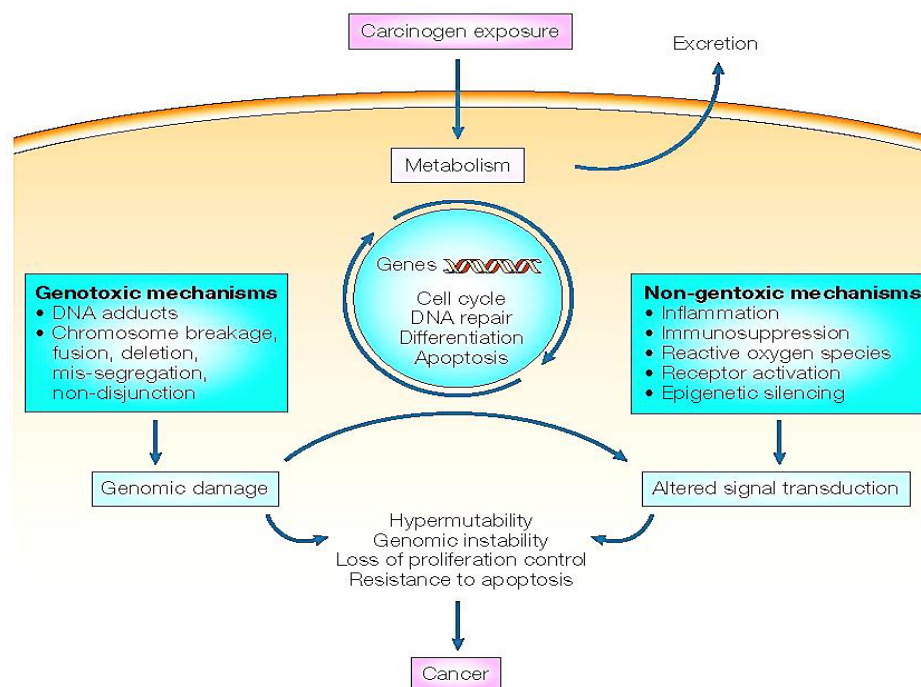


Figure 7. Overview of genotoxic and non-genotoxic effects of carcinogens (Source: Luch, 2005)

In general, chemical carcinogens induce molecular changes in target organ, and the most frequently involved genes are Ras and Tp53 (Hoenerhoff *et al.*, 2009). Many previous studies reported the DNA damaging effect of environmental carcinogens, for example the induction of point mutations in genes such as c-H-ras by DMBA (Dandekar *et al.*, 1986; Cardiff *et al.*, 1988; Qing *et al.*, 1997). Upon DMBA oral gavage treatment, the cellular cytosolic receptor for DMBA, the aryl hydrocarbon receptor (AhR) is upregulated and through its translocation to the nucleus associates with the cofactor ARNT, the AhR nuclear translocation protein (Swanson *et al.*, 1995; Trombino *et al.*, 2000; Denison and Nagy, 2003). Subsequently, the AhR/ARNT complex binds to specific DNA recognition sites and induces gene transcription (Denison and Nagy, 2003). In addition, cytochrome P450 (CYP1A1 and CYP1B1) is upregulated in an AhR-dependent response. Cytochrome P450 has been reported to be involved in the metabolism of DMBA. It converts it into a mutagenic epoxide intermediate that readily forms DNA adduct (Shimada and Fujii-Kuriyama, 2004). These adducts are correlating with DNA mutations and the malignant transformation of PAH-mediated

carcinogenesis (Nebert *et al.*, 1990; Rundle *et al.*, 2000). Moreover, Currier *et al.* (2005) have elucidated the oncogenic signaling of DMBA in mouse mammary tumors. DMBA-induced mammary tumors demonstrated high expression of AhR, c-myc, Cyclin D1, and hyperphosphorylated retinoblastoma (Rb) protein. Moreover, elements of the Wnt signaling pathway, the NF- κ B pathway, and prolyl isomerase Pin-1 have been up-regulated in the tumors when compared to normal mammary glands. They proposed that “environmental carcinogens can produce long-lasting alterations in growth and anti-apoptotic pathways, leading to mammary tumorigenesis” (Currier *et al.*, 2005).

1.5.1 Immunosuppression and immunotoxicity of carcinogen (DMBA)

Suppression of immune response by chemical carcinogens has been reported several decades ago (Malmgren *et al.*, 1952). Chemical carcinogens, especially DMBA, can suppress both cell-mediated immunity and humoral immunity for prolonged periods of time (Prehn, 1963; Ward *et al.*, 1986; Burchiel *et al.*, 1990; Gao *et al.*, 2007, 2008). DMBA suppresses immune response through inhibition of lymphocyte activation, mainly by depressing the ability to generate cytotoxic T-lymphocytes (CTL) and natural killer (NK) cells (Ward *et al.*, 1986; Burchiel *et al.*, 1990). It has been proposed that immunosuppression induced by DMBA, including CTL and NK cell tumoricidal functions, may act as an important mechanism in association with the genotoxic effect, contributing to tumor outgrowth and metastasis (Ward *et al.*, 1986). Microsomal epoxide hydrolase (mEH, EPHX1) has been found as a crucial enzyme for metabolic activation of DMBA *in vivo* leading to immunosuppression of spleen cells (Gao *et al.*, 2007). Furthermore, Gao *et al.* (2008) have shown that genotoxicity of DMBA is responsible for DMBA-induced immunosuppression *in vivo* via activation of p53 and ataxia telangiectasia mutated (ATM) signaling.

Interleukin-2 (IL-2) is a T cell growth factor that has been discovered in the supernatants of activated T cells (Morgan *et al.*, 1976). IL-2 stimulates the growth, differentiation and survival of antigen-specific CD4⁺ T cells and CD8⁺ T cells (Stern and Smith, 1986; Liao *et al.*, 2011). It can modulate effector cell differentiation (T helper type 1 (Th1) cells, Th2, Th17, and regulatory T cells (Tregs)) as well as IL-7 via regulation of cytokine receptor expression (Liao *et al.*, 2011). Several studies demonstrated that DMBA highly suppressed the production of IL-2 from splenocytes in response to mitogenic or allogeneic stimulation *in vivo* and *in vitro* (House *et al.*, 1987; Saas *et al.*, 1996). Recently, IL-2 has been used for the treatment of patients with advanced renal cancer and subsequently of patients with melanoma (Clement and McDermott, 2009; Halama *et al.*, 2010), but it was accompanied

with toxicity. In an effort to reduce the IL-2 toxicity in cancer patients, [Liang *et al.*, \(2012\)](#) provided evidence that inhibition of autophagy by using chloroquine during IL-2 immunotherapy in mouse model lead to regression of tumor growth significantly and prolonged survival.

The immunotoxicity of DMBA is accompanied by a decrease of the spleen weight as well as changes in spleen cellularity (total number of spleen cells reduced) and bone marrow cellularity ([Miyata *et al.*, 2001](#); [Page *et al.*, 2003](#)). These decreases were associated with cell death of splenocytes after DMBA treatment ([Miyata *et al.*, 2001](#); [Gao *et al.*, 2007](#)). Moreover, it has been reported that DMBA induced pre-B-cell apoptosis ([Heidel *et al.*, 1999](#); [Near *et al.*, 1999](#)). For instance, [Page *et al.* \(2003\)](#) have shown that bone marrow toxicity in mice is dependent on p53 activation *in vivo* after DMBA exposure. Further, [Teague *et al.* \(2010\)](#) showed that DMBA activates apoptosis in pro/pre-B cells in a bone marrow stromal cell-dependent manner, via activation of caspase-3.

1.5.2 Carcinogen, autophagy and DNA damage

Modifications in DNA structure (DNA damage) can happen by exogenous environmental agents such as ionizing radiation (IR), ultraviolet (UV) and genotoxic chemicals (for instance, carcinogens) or by endogenous byproducts of regular cellular metabolism including ROS ([Rodriguez-Rocha *et al.*, 2011](#)). In response to genotoxic stimuli or cytotoxic lesions (such as double strand breaks (DSB)), cells trigger several processes in order to retain genomic stability; these processes include DNA damage response (DDR) to repair or remove the lesions and keep DNA integrity, cell cycle checkpoint activation to arrest the progression of the cell cycle and to allow DNA repair and thereby prevent the transmission of the DNA damage, transcriptional response activation to change the transcription profile, and activation of apoptosis pathways in order to remove the damaged or deregulated cells ([Roos and Kaina, 2006](#); [Rodriguez-Rocha *et al.*, 2011](#)). A key player in DNA damage is p53 ([Caspari, 2000](#); [Hickman *et al.*, 2002](#)), however, the response to genotoxic stress is a complex process and requires the activation of several proteins involved in sensing aberrant DNA structures and the initiation of subsequent events ([Rodriguez-Rocha *et al.*, 2011](#)).

DNA damage occurs in several tissues of rat following exposure to DMBA ([Muqbil *et al.*, 2006](#)). In general, PAH-DNA adducts may trigger nucleotide excision repair (NER), including p53-dependent apoptosis in certain cell types, depending on the degree of the DNA lesion and cell cycle progression ([Henkler *et al.*, 2012](#)). [Ganesan *et al.* \(2013\)](#) found that DMBA induces DSB with the subsequent activation of DNA repair as potential mechanism

to prevent the follicle loss in rat ovaries. Moreover, DNA damage activates ATM and/or ATR (ATM and Rad3 related) which in turn phosphorylate a variety of signaling proteins such as checkpoint kinases 1 and 2 (CHK1, CHK2), and p53. Phosphorylated p53 induces transcriptional activation of pro-apoptotic factors such as Fas, Bax and PUMA (Roos and Kaina, 2006). Therefore, DNA-repair deficiency sensitizes cells to apoptosis induced by DNA lesions, such as bulky DNA adducts (Rodriguez-Rocha *et al.*, 2011).

Several studies showed that autophagy was induced in response to DNA damage (Klionsky and Emr, 2000; Polager *et al.*, 2008; Kang *et al.*, 2009), however, the role of autophagy in DDR is still unclear. It has been demonstrated that cells initiate cell cycle arrest and autophagy upon treatment with DNA-damaging agents, for example camptothecin (CPT) (Abedin *et al.*, 2007; Bae and Guan, 2011), etoposide and tomozolomide (Katayama *et al.*, 2007), p-anilinoaniline (Elliott and Reiners, 2008) and IR (Bae and Guan, 2011). Autophagy delayed apoptotic cell death in breast cancer cells treated with CPT (Abedin *et al.*, 2007). The interaction of anti-apoptotic proteins Bcl-2/Bcl-xl with Beclin-1 in ER inhibits autophagy (Maiuri *et al.*, 2007b). The pro-apoptotic and anti-apoptotic Bcl-2 proteins regulate apoptosis induced by DNA damage; this suggests a regulatory role of Bcl-2 family proteins in mediating the crosstalk between autophagy and apoptosis signaling (Zinkel *et al.*, 2006). Furthermore, doxorubicin induced DNA damage in association with autophagy induction which was observed to depend on PARP-1 (poly [ADP-ribose] polymerase 1). Inhibition of autophagy enhanced doxorubicin-mediated cell death suggesting that autophagy acts as a protective mechanism against DNA damage-induced apoptosis (Munoz-Gamez *et al.*, 2009; Huang and Shen, 2009). On the other hand, mitochondrial damage produces ROS which in turn may stimulate mitophagy to remove the damaged organelles, therefore autophagy malfunction lead to increased ROS causing DDR (Mathew *et al.*, 2007). DDR insufficiency could stimulate genomic instability resulting in tumorigenesis; however, extremely increased DNA damage may also result in cell death (Bae and Guan, 2011). Bae and Guan (2011) demonstrated that inhibition of autophagy by FIP200 knockout resulted in deficient repair of DNA damage produced by ionizing radiation and anticancer agents. In this work, persistent DNA damage after CPT treatment was associated with increased apoptosis and reduced survival of FIP200 knockout cells. They suggested that accumulation of p62 protein due to autophagy insufficiency is responsible for impaired DDR and CPT-induced cell death (Bae and Guan, 2011).

1.6 Aims of the study

We previously reported that GABARAP may function as a tumor suppressor in breast cancer cells and that the expression of the gene was associated with larger vesicle formation. However, the precise role and mechanism that GABARAP plays in tumorigenesis could not be elucidated so far. Instead, GABARAP was identified in the meantime as one of the autophagy-related genes that play a role in the maturation of the autophagosome. In the last decade, increasing studies have implicated autophagy in the tumor initiation and progression. Recently, autophagy has been involved in cancer therapy by using autophagy inhibitors, for instance chloroquine. GABARAP is ubiquitously expressed in all tested normal tissues. Its expression has been studied in some cancer types, for example neuroblastoma, breast tumors, thyroid tumors and colorectal tumors. Furthermore, autophagic proteins have been involved in the regulation of both innate and adaptive immunity. Autophagic gene deletions demonstrated an increase in the lethality of sepsis in mouse models and enhanced infiltration of antitumorigenic T cells in the tumor microenvironment.

The primary aim of the study was to explore the role of GABARAP in tumorigenesis by using a knockout mouse model. Specifically the following questions were addressed:

- Does treatment of GABARAP knockout mice with carcinogens or the inoculation of the mice with syngeneic tumor cells affect tumorigenesis differently compared to wild-type mice?
- And if this is the case what are the cellular mechanisms being affected by GABARAP deficiency that govern the differences in the tumor phenotype?

2. Materials and Methods

2.1 Materials

2.1.1 Chemicals

Chemical	Company
7,12-Dimethylbenz(a)anthracene (DMBA)	Sigma-Aldrich, St. Louis, MO, USA
Agarose	Serva, Heidelberg, Germany
Albumin Fraction V (BSA)	Roth, Karlsruhe Germany
Alum potassium sulfate	Merck KGaA, Darmstadt, Germany
Aqua ad injectabilia	Braun, Melsungen, Germany
Ammonium chloride (NH ₄ Cl)	Sigma-Aldrich, St. Louis, MO, USA
Ammonium persulfate (APS)	Sigma-Aldrich, St. Louis, MO, USA
Camptothecin (CPT)	Bio Vision, Milpitas, California, USA
Carmin	Fluka, Bassersdorf, Switzerland
Citric acid monohydrate	Sigma-Aldrich, St. Louis, MO, USA
Chloroquine (CQ) diphosphate salt	Sigma-Aldrich, St. Louis, MO, USA
Deoxycholate	AppliChem, Darmstadt, Germany
Developer	Kodak, Rochester, USA
Diethylether	Otto Fischar, Saarbrücken, Germany
Diethylpyrocarbonate (DEPC)	Sigma-Aldrich, St. Louis, MO, USA
Dimethylsulfoxid (DMSO)	Sigma-Aldrich, St. Louis, MO, USA
Ethylenediaminetetraacetic acid (EDTA)	Sigma-Aldrich, St. Louis, MO, USA
Ethanol	Merck KGaA, Darmstadt, Germany
Fixer	Kodak, Rochester, NY, USA
Formaldehyde	J.T. Baker, Deventer, Netherlands
GelRED	Biotium, Hayward, USA
Glacial acetic acid	J.T. Baker, Deventer, Netherlands
Glycin	Roth, Karlsruhe, Germany
Heparin	Roche, Grenzach-Wyhlen, Germany
Hydrochloric acid (HCl)	J.T. Baker, Deventer, Netherlands
Hydrogen peroxide solution (H ₂ O ₂)	Roth, Karlsruhe, Germany
Isopropanol	Roth, Karlsruhe, Germany
Medroxyprogesteron acetate (MPA)	Pfizer, Madrid, Spain
Methanol	Merck KGaA, Darmstadt, Germany
N-methyl-N-nitrosourea (MNU)	Santa Cruz, CA, USA
N-ethyl-N-nitrosourea (ENU)	Sigma-Aldrich, St. Louis, MO, USA
Non-fat dry milk	BD, Sparks, France
Nonidet P-40 substitute	AppliChem, Darmstadt, Germany
Ortho-phenylenediamine (OPD)	Sigma-Aldrich, St. Louis, MO, USA

Permunt	Fischer Scientific, New Jersey, USA
Potassium chloride (KCl)	Serva, Heidelberg, Germany
Potassium phosphate monobasic (KH ₂ PO ₄)	Merck KGaA, Darmstadt, Germany
Rotiphorese Gel40 (Acrylamide)	Roth, Karlsruhe, Germany
Sesame oil	Local market
Sodium azide (NaN ₃)	Sigma-Aldrich, St. Louis, MO, USA
Sodium bicarbonate (NaHCO ₃)	Merck KGaA, Darmstadt, Germany
Sodium citrate	Merck KGaA, Darmstadt, Germany
Sodium hydroxide (NaOH)	J.T. Baker, Deventer, Netherlands
Sodium lauryl sulfate (SDS)	Roth, Karlsruhe, Germany
Sodium phosphate dibasic (Na ₂ HPO ₄)	Merck KGaA, Darmstadt, Germany
Sodium phosphate dibasic dehydrate (Na ₂ HPO ₄ x 2 H ₂ O)	Merck KGaA, Darmstadt, Germany
Sodium phosphate monobasic monohydrate (Na ₂ HPO ₄ x H ₂ O)	Merck KGaA, Darmstadt, Germany
Sulfuric acid (H ₂ SO ₄)	J.T. Baker, Deventer, Netherlands
Target Retrieval Solution, citrate pH 6	DAKO, Glostrup, Denmark
Tetramethylethylenediamine (TEMED)	Sigma-Aldrich, St. Louis, MO, USA
Tris-Base	EMD Chemicals, San Diego, CA, USA
Tween20	Roth, Karlsruhe, Germany
Xylol	Sigma-Aldrich, St. Louis, MO, USA

2.1.2 PCR and cell culture reagents

Reagent	Company
10 x buffer S	peQlab, Erlangen, Germany
2.0 mM dNTP mix	Thermo Scientific, Rockford, IL, USA
2.5% Trypsin (10 x)	Gibco, Paisley, UK
2-mercapto-ethanol	Sigma-Aldrich, St. Louis, MO, USA
Adenosine triphosphate (ATP)	InvivoGen, Toulouse, France
Dulbecco's MEM (DMEM)	Biochrom, Berlin, Germany
Earle's balanced salt solution (EBSS)	Sigma-Aldrich, St. Louis, MO, USA
FastStart Universal SYBR Green Master (Rox)	Roche, Mannheim, Germany
Fetal calf serum (FCS)	Biochrom, Berlin, Germany
HEPES	Invitrogen, Karlsruhe, Germany
L-glutamine	Invitrogen, Karlsruhe, Germany
Lipopolysaccharide (LPS)	Sigma-Aldrich, St. Louis, MO, USA
Penicillin	Invitrogen, Karlsruhe, Germany
Protease inhibitor cocktail tablets	Roche, Mannheim, Germany
RPMI 1640	Biochrom, Berlin, Germany
Sodium pyruvate	Invitrogen, Karlsruhe, Germany

Streptomycin	Invitrogen, Karlsruhe, Germany
Taq-polymerase (HotStarTaq)	peQlab, Erlangen, Germany
Trypsin-EDTA	Biochrom, Berlin, Germany

2.1.3 Kits and assays

Kit	Company
BCA protein assay kit	Thermo Scientific, Rockford, IL, USA
DAKO REAL™ Detection System Alkaline Phosphatase/RED Rabbit/Mouse	DAKO, Glostrup, Denmark
DNA Clean & Concentrator™ -5 Kit	Zymo Research, Irvine, CA, USA
Horseradish peroxidase-labeled streptavidin	Dianova, Hamburg, Germany
Luminol Reagent (Western Blotting Detection Kit)	Santa Cruz, CA, USA
Maxwell® 16 FFPE Plus LEV DNA Purification Kit	Promega, Madison, WI, USA
QuantiTect® Reverse Transcription Kit	QIAGEN GmbH, Hilden, Germany
REDExtract-N-Amp™ Tissue PCR Kit	Sigma-Aldrich, Seelze, Germany
Trizol reagent (peqGOLD TriFast)	peQlab, Erlangen, Germany

2.1.4 Laboratory equipment and consumables

Material	Company
0.2 ml flexi-PCR-tubes	Kisker Biotech, Steinfurt, Germany
0.5/1.5/2.0 ml microtubes	Sarstedt, Nümbrecht, Germany
10/100/200/1000 µl pipette tips	Sarstedt, Nümbrecht, Germany
5/10/25 ml glass pipette sterile / cell culture	Greiner bio-one, Kremsmünster, Germany
200 µl gel loading pipette tips round	Nerbepplus, Winsen/ Luhe, Germany
6/12/24/96 well cell culture plates sterile	Greiner bio-one, Kremsmünster, Germany
Accu-jet pipette	Integra Bioscience, Fernwald, Germany
Amersham Hyperfilm™ ECL	GE Healthcare, Buckinghamshire, GB
Autoclave	SHP Steriltechnik, Schloss Detzel, Germany
Axio Lab.A1 microscope (Zeiss)	Zeiss, Oberkochen, Germany
Camera Power shot A650 IS	Canon, Tokyo, Japan
Cell culture dishes	Greiner bio-one, Kremsmünster, Germany
Centrifuge 5415 R	Eppendorf, Hamburg, Germany
Centrifuge Universal 320R	Hettich, Tuttlingen, Germany
Cleanbench HERA safe	Thermo Scientific, Waltham, MA, USA
CO ₂ Incubator MCO-17AI	Sanyo, Moriguchi, Japan
Countess automated cell counter	Invitrogen, Carlsbad, CA, USA
Easy-Cast Electrophoresis system Model B2	Owl Scientific, San Francisco, CA, USA
Electrophoresis Power Supply EV231	peQlab, Erlangen, Germany

Hotplate/Stirrer	VWR, Darmstadt, Germany
Hybaid hybridization oven	MWG-Biotech, Ebersberg, Germany
Imager Fluorchem [®] FC2	Alpha Innotec, Minneapolis, MN, USA
Kodak X-ray Film	NEN Life Science Products, MA, USA
Maxwell 16 instrument	Promega, Madison, WI, USA
Microplate absorbance reader	Tecan, Crailsheim, Germany
Microtome	Leica, Nussloch, Germany
Microtome blades	Feather, Seki, Japan
Mini PROTEAN Tetra System for SDS-PAGE	BIO-RAD, Hercules, CA, USA
Mini-Vac eco vacuum pump	peQlab, Erlangen, Germany
NanoDrop Spectrophotometer ND-1000	peQlab, Erlangen, Germany
peQSTAR 96 Universal Gradient cycler	peQlab, Erlangen, Germany
PerfectBlue [™] 'Semi-Dry'-Electro Blotter	peQlab, Erlangen, Germany
PerfectSpin 24 centrifuge	peQlab, Erlangen, Germany
pH-Electrode SenTix 81	inoLab, Weilheim, Germany
Pipettes	peQlab, Erlangen, Germany
Plastic 15 ml and 50 ml falcon tubes	greiner bio-one, Frickenhausen, Germany
Polypropylene cell strainer	BD Biosciences, Sparks, MD, USA
Rotor-Gene Q real-time PCR Machine	QIAGEN, Hilden, Germany
Scout Pro SPU402 scale	Ohaus, Parsipanny, IN, USA
TELAVAL 31 inverse microscope	Zeiss, Oberkochen, Germany
Thriller thermoshaker	peQlab, Erlangen, Germany
Tissue culture flask	Greiner bio-one, Kremsmünster, Germany
Ultra-Turrax T8 (homogeniser)	IKA Labortechnik, Staufen, Germany
Vasco nitril white	Braun, Melsungen, Germany
Vortex-Genie 2	Scientific Industries, Bohemia, NY, USA
Water bath typ 1003	GFL, Burgwedel, Germany
Whatman [™] PVDF Membrane Protran BA83	GE Healthcare, Buckinghamshire, UK

2.1.5 Immunohistochemistry and Western blot primary antibodies

Primary Antibody	Species	Company	Clonality	Dilution
Anti-Cyclin D1	Rabbit	Santa Cruz	polyclonal	1:200 in 5% TBST-Milk
Anti-GABARAP	Rabbit	Abcam	monoclonal	1:2500 in 5% TBST-Milk
Anti-Ki-67 Biotin	Rat	eBioscience	monoclonal	5 µg/ml
Anti-LC3A/B	Rabbit	Cell Signaling	polyclonal	1:1000 in 5% TBST-BSA
Anti-p-γH2AX	Rabbit	Cell Signaling	monoclonal	1:1000 in 5% TBST-BSA
Anti-SQSTM1 (p62)	Rabbit	Novus Biologicals	polyclonal	1:4000 in 5% TBST-Milk
Anti-β-Actin	Mouse	Millipore	monoclonal	1:1000 in 5% TBST-Milk

2.1.6 Secondary antibodies

Secondary antibody	Species	Company	Dilution
HRP-conjugated anti-mouse IgG	Rabbit	DAKO	1:1000
HRP-conjugated anti-rabbit IgG	Goat	Santa Cruz	1:1000

2.1.7 ELISA antibodies

Cytokine	Catalog nr.	Concentration	Marker	Buffer	Company
IFN- γ	551216	1 μ g/ml	none	Na-Phos., pH 9,0	BD Biosciences
	554410	0,5 μ g/ml	Biotin	-	BD Biosciences
IL-17	MAB721	2 μ g/ml	none	PBS	R&D Systems
	BAF421	0,1 μ g/ml	Biotin	-	R&D Systems
IL-1 β	51-26661E	4 μ g/ml	none	NaHCO ₃ , pH 9,5	BD Biosciences
	13-7112	0,5 μ g/ml	Biotin	-	eBioscience
IL-2	554424	1 μ g/ml	none	Na-Phos., pH 9,0	BD Biosciences
	554426	0,5 μ g/ml	Biotin	-	BD Biosciences
IL-6	554400	2 μ g/ml	none	NaHCO ₃ , pH 9,5	BD Biosciences
	554402	0,25 μ g/ml	Biotin	-	BD Biosciences
TNF- α	551225	3 μ g/ml	none	Na-Phos., pH 6,5	BD Biosciences
	554415	0,5 μ g/ml	Biotin	-	BD Biosciences

2.1.8 Cytokine standards

Cytokine	Catalog nr.	Max. concentration	Company
IFN- γ	485-MI/CF	30000 pg/ml	R&D Systems
IL-17	421-ML	10000 pg/ml	R&D Systems
IL-1 β	51-26666E	2000 pg/ml	BD Biosciences
IL-2	212-12	2000 pg/ml	Tebu-bio
IL-6	216-16	5000 pg/ml	Tebu-bio
TNF- α	554589	1000 pg/ml	BD Biosciences

2.1.9 Genotype primer sequences

Primer pairs	Direction	Oligonucleotide sequence	Size (bp)	Annealing temperature
GRAP23FW1	Forward	5'-GCCACCTTCAGCGTAGAAAC-3'	300	62°C
GRAP23BW1	Reverse	5'-GCCTGCTAACATACGCCACT-3'		
GRAP23FW	Forward	5'-ACTGGATGGAGTCCCTGATG-3'	640	62°C
VICTR23C	Reverse	5'-GAGTGATTGACTACCCGTCAGCG-3'		

2.1.10 Quantitative reverse transcriptase PCR (qRT-PCR) primer sequences

Gene	Direction	Oligonucleotide sequence	Accession number	T _a (°C)	Size (bp)
Bax	Forward	5'-TTGGAGATGAACTGGACAGC-3'	NM_007527.3	60	124
	Reverse	5'-CAGTTGAAGTTGCCATCAGC-3'			
Bid	Forward	5'-AGACGAGCTGCAGACAGATG-3'	NM_007544.3	60	137
	Reverse	5'-GGTCCATCTCATCGCCTATT-3'			
GAPDH	Forward	5'-CACACCGACCTTCACCATTTT-3'	NM_008084.2	60	67
	Reverse	5'-GAGACAGCCGCATCTTCTTGT-3'			
p21	Forward	5'-AGGCCCAGTACTTCCTCTGC-3'	NM_007669.4	60	183
	Reverse	5'-CAATCTGCGCTTGGAGTGATA-3'			
Xaf1	Forward	5'-TCCAAGTGTGCAGGAACTG-3'	NM_001037713	60	144
	Reverse	5'-CAACTTCCATGTGCTCTTTCATC-3'			

* T_a, Annealing temperature (°C)

2.1.11 Primer sequences for mutation analysis

Gene	Exon	Oligonucleotide sequence	Accession number	Size (bp)
H-ras1	1	5'-CCTTGGCTAAGTGTGCTTCTCATTGG-3' (F)	NM_008284.2	214
		5'-ACAGCCCACCTCTGGCAGGTAGG-3' (R)		
H-ras1	2	5'-TGTGGATTCTCTGGTCTGAGGAGAG-3' (F)	NM_008284.2	269
		5'-CATAGGTGGCTCACCTGTACTGATG-3' (R)		

* F, Forward primer; R, Reverse primer

* Annealing temperature was 68°C for the first eight cycles, then 60°C for the next 32 cycles of exon 1 primers and 62°C for the next 32 cycles of exon 2 primers.

2.1.12 Solutions and buffers

Western blot & electrophoresis	Composition
10 x electrophoresis buffer (1 l)	250 mM Tris-Base 1.92 M Glycin 1% SDS → pH 8.3

10 x PBS (1 l)	2 g KCl 2 g KH ₂ PO ₄ 14.4 g Na ₂ HPO ₄ 80 g NaCl → pH 7.4
10 x TBST (1 l)	24.2 g Tris-Base 80 g NaCl 14 ml HCl → pH 7.6 10 ml Tween20
10 x Western blot transfer buffer (1 l)	30.03 g Tris-Base 112.6 g Glycine → pH 8.3 → for preparing 1 x buffer add 100 ml methanol
50 x TAE buffer (1 l)	242 g Tris-Base 57.1 ml Glacial acetic acid 100 ml 0.5 M EDTA (pH 8)
Blocking buffer	2.5 g Non-fat dry milk or BSA 50 ml 1 x TBST
RIPA buffer (100 ml)	1 ml NP-40 200 µl 0.5 M EDTA 10 ml 0.5 M Tris pH 7.4 15 ml 1 M NaCl 0.25 g Desoxycholat
RNA isolation	Composition
DEPC-treated H ₂ O	1 l H ₂ O 1 ml Diethylpyrocarbonate (DEPC) → The solution was stirred on a magnetic stirrer overnight and autoclaved the next day.

Carcinogens dissolvent	Composition
0.2 M dibasic sodium phosphate (Na ₂ HPO ₄)	3.56 g Na ₂ HPO ₄ 100 ml H ₂ O
Citrate-buffered saline	1 g KCl 0.44 g Sodium citrate 100 ml H ₂ O → pH 4.5
Citric acid monohydrate	2.1 g Citric acid monohydrate 100 ml H ₂ O
Citric acid-phosphate buffer	36.85 ml Citric acid monohydrate 63.15 ml 0.2 M Na ₂ HPO ₄ → pH 6.0
ELISA buffers	Composition
Ammoniumchlorid/TRIS, pH 7.2	a) 0.83% NH ₄ Cl (7.47 g at 900 ml H ₂ O) b) TRIS (2.059 g at 100 ml H ₂ O), pH 7.65 mix a) and b) 9:1
Citrate buffer, pH 4.8	2.1 g Citric acid 16.2 ml 1 N NaOH 84 ml Aqua dest
Na ₂ HPO ₄ -coating buffer, pH 6.5	1.48 g Na ₂ HPO ₄ x 2 H ₂ O 1.85 g NaH ₂ PO ₄ x H ₂ O 100 ml Aqua dest
NaH ₂ PO ₄ -coating buffer, pH 9.0	1.38 g NaH ₂ PO ₄ x H ₂ O 100 ml Aqua dest
NaHCO ₃ -coating buffer, pH 9.5	0.84 g NaHCO ₃ 100 ml Aqua dest
OPD-solution	2 mg/ml OPD in citrate buffer 20 µl/ml 3% H ₂ O ₂

2.2 Methods

2.2.1 Animals

Female wild-type (Wt) C57BL/6 mice were purchased from Charles River (Sulzfeld, Germany). GABARAP knockout (GABARAP KO) mice were obtained from the Max Planck Institute for Brain Research in Frankfurt, Germany (O'Sullivan *et al.*, 2005). GABARAP KO mice were generated from the Omnibank of embryonic stem cell library by insertion of targeting vector 345 bp upstream of exon 1 of the GABARAP locus (Zambrowicz *et al.*, 1998) (Fig. 8). The heterozygous animals were crossed to produce +/+ (wild-type), +/- (heterozygous) and -/- (homozygous) mice. Mice were housed in standard cages (10 animals per cage) under controlled temperature ($22 \pm 2^\circ\text{C}$) and lighting conditions (monitored 12 h light/12 h dark cycles), and supplied with water and food (Altromin, Lage, Germany) *ad libitum*. All animal experiments were approved by the Thuringian commission for animal protection (No. 02-018/08 and 02-007/13).

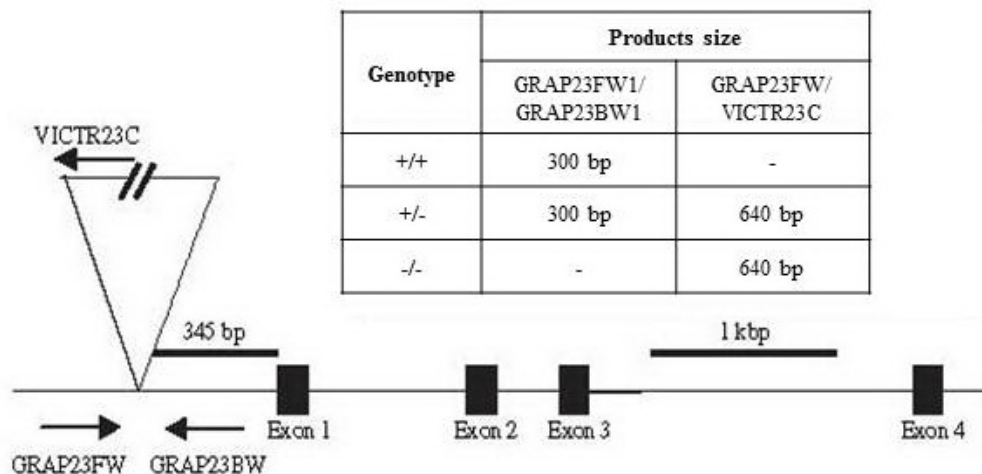


Figure 8. Location of gene-trap vector insertion into the GABARAP gene and primers designed for genotyping (O'Sullivan *et al.*, 2005). The PCR fragment sizes for the different GABARAP genotypes are indicated in the inset.

2.2.2 Genotyping of GABARAP knockout mice

Genomic DNA was extracted from the tails of mice by using REExtract-N-Amp™ Tissue PCR Kit (Sigma-Aldrich, Germany) according to the manufacturer's protocol, as follows:

2.2.2.1 Genomic DNA extraction

First of all, 100 μl of extraction solution was added into 1.5 ml microcentrifuge tube, and then 25 μl of tissue preparation solution was appended to the tube with pipetting up and down to

mix. Fresh mouse tail tips (end down) of about 0.5 cm were cut by using sterile scissors and forceps. The piece of mouse tail tip was transfer into the extraction solution and mixed thoroughly by vortexing. The sample was incubated at room temperature for 10 minutes, and then incubated at 95°C for 3 minutes. After that, 100 µl of neutralization solution B was added to sample and mixed by vortexing. The neutralized tissue extract was used immediately for polymerase chain reaction (PCR); if not, the samples were stored at 4°C.

2.2.2.2 PCR amplification

The following reagents were prepared in duplicate, one reaction for the GRAP23FW1/GRAP23BW1 primer pairs, and the second reaction for the GRAP23FW/VICTR23C primer pairs. The PCR fragment sizes for each primer pairs are indicated in the inset of Figure 8.

Reagent	Volume/reaction
REExtract-N-Amp PCR Reaction Mix	10.0 µl
Forward Primer (100 pmol/µl = 100 µM)	0.08 µl
Reverse Primer (100 pmol/µl = 100 µM)	0.08 µl
H ₂ O	5.84 µl
Tissue Extract	4.00 µl
Total volume	20 µl

Then, the following PCR program was used for each primer pairs:

Step	Temperature	Duration	Cycle
1 Initial denaturation	94°C	1 minute	1
2 Denaturation	94°C	30 seconds	} 35
3 Annealing	62°C	1 minute	
4 Extension	72°C	1 minute	
5 Final elongation	72°C	10 minutes	1

After the program was completed the PCR products were stored at 4°C or loaded directly onto an agarose gel.

2.2.2.3 Agarose gel electrophoresis

PCR products were separated in a 1.5% (w/v) agarose gel. To pour a gel, agarose powder was mixed with 1 x TAE buffer to the desired concentration and heated in a microwave oven until the agarose was completely molten. After cooling down to about 60°C the solution was poured into a casting tray containing a sample comb and allowed to solidify at room temperature. The solid gel was inserted horizontally into the electrophoresis chamber, the

comb removed and the gel covered with 1 x TAE buffer. PCR products were mixed with loading buffer and pipetted into the sample wells. The gel was run with 100 voltages for 40 minutes. Thereafter, the gel was incubated with GelRED for 15 - 30 minutes and a photograph was taken after placing the gel under the imager FluorChem[®] FC2. Figure 9 showed an example of the genotyping results for a group of mice.

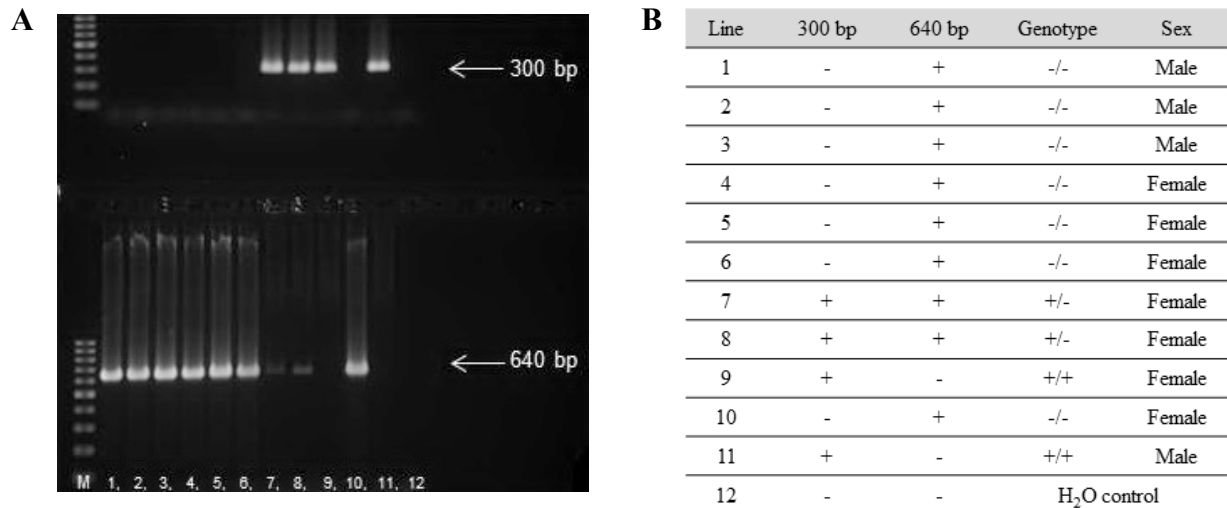


Figure 9. Genotyping results for the different GABARAP genotype mice, wild-type (+/+), heterozygous (+/-) or homozygous (-/-). A) Electrophoresis image for the primer pairs GRAP23FW1/GRAP23BW1 with a band of 300 bp and GRAP23FW/VICTR23C with a band of 640 bp. B) Table to illustrate the results shown in A.

2.2.3 Carcinogen treatment

The genetic background of GABARAP KO mice is C57BL/6 mice. Female C57BL/6 wild-type and GABARAP KO mice at 6 – 8 weeks of age were used in all our experiments for carcinogen treatment. Wild-type and GABARAP KO mice were divided each into 2 groups, control (vehicle-treated) group and carcinogen-treated group. The treatment regimens used in our experiments was according to the literature with some modifications.

2.2.3.1 DMBA treatment

7,12-Dimethylbenz(a)anthracene (DMBA) was dissolved in sesame oil (5 mg/ml) by vortexing for 2 h at room temperature. Several experiments had shown that complete dissolution was obtained using this protocol for DMBA dissolving. All steps in the preparation were carried out under minimum illumination. DMBA-treated groups of wild-type and GABARAP KO mice received 6 weekly doses of 1 mg DMBA/mouse in 200 µl of dissolvent by oral gavage. Control groups received 6 weekly dosed of 200 µl sesame oil. The mice were monitored weekly for palpable tumor formation. The tumor-

bearing mice were anesthetized and killed by cervical dislocation. The tumor specimens were fixed in 5% neutral buffered formalin.

2.2.3.2 ENU treatment

N-Ethyl-N-nitrosourea (ENU) was obtained from Sigma in Isopac bottles containing approximately 1 g of ENU. The desired concentration of ENU was obtained by dissolving it in citric acid-phosphate buffer at pH 6.0, because it is highly decomposition in aqueous media at pH values above 7.0 (Goth and Rajewsky, 1974). In addition, care was taken to prevent decomposition from light during preparation of ENU solution. ENU-treated groups of wild-type and GABARAP KO mice were administered a single intraperitoneal (i.p.) injection of 150 mg ENU/kg of body weight. The mice were monitored weekly for palpable tumor formation. The tumor-bearing mice were anesthetized and killed by cervical dislocation. The tumor specimens were fixed in 5% neutral buffered formalin.

2.2.3.3 Hormone stimulation and MNU treatment

Medroxyprogesterone acetate (MPA) was used together with N-methyl-N-nitrosourea (MNU) in order to increase the incidence of mammary tumors in mice (Pazos *et al.*, 1998). MPA was dissolved in sterile injectable water and MNU was dissolved in citrate-buffered saline pH 4.5. Female mice were administered at 6 weeks of age the first dose of 40 mg MPA/mouse by intramuscular injection. In the next week, i.e. at 7 weeks of age, the mice received a single intraperitoneal (i.p.) injection of 1 mg MNU/mouse in 200 μ l of dissolvent. Four weeks after the first MPA dose, a booster dose of 20 mg MPA/mouse was administered intramuscularly. The mice were monitored every other day for lethality and weekly for palpable tumor formation.

2.2.3.4 MNU and DMBA treatment

In attempt to increase the tumor incidence in our mice model, we used the synergistic treatment of MNU and DMBA in mice (Shirai *et al.*, 1997), which are already promoted with MPA. Female mice at 6 weeks of age were injected with 20 mg MPA/mouse intramuscularly. One week later, the mice were administered i.p. injection of 1 mg MNU/mouse. At 8 weeks of age, the mice received the booster dose of 20 mg MPA/mouse. After that, the mice were given a single oral dose of 1 mg DMBA/mouse at 10 weeks of age. DMBA and MNU were dissolved as mentioned in (2.2.3.1) and (2.2.3.3), respectively. The mice were monitored every other day for lethality and weekly for palpable tumor formation.

2.2.4 Tumor and tissue specimens

2.2.4.1 Haematoxylin and eosin (H & E) staining

Tumor specimens of DMBA-treated mice were fixed and embedded in paraffin. Four- μ m sections were cut from blocks, mounted on glass slides, dewaxed with xylene and gradually hydrated. Subsequently, the sections were stained with haematoxylin and eosin, dehydrated and cleared with xylene. Then the sections were mounted with aqueous mounting medium. The slides were analysed under light microscope and evaluated by Prof. Dr. Iver Petersen.

2.2.4.2 Immunohistochemistry (IHC)

Immunohistochemistry staining of tissue sections from spleen and mammary glands of vehicle-treated (control) and DMBA-treated mice was performed. After 6 weekly oral doses of 1 mg DMBA, spleen specimens and mammary glands were fixed in 5% neutral buffered formalin. Subsequently, paraffin-embedded tissue blocks were constructed, 3 μ m sections were obtained by cutting with a rotation-microtome. The sections were mounted on glass slides (Superfrost Plus, Menzel GmbH), carefully transported to a 50°C water bath to straighten the tissue and dried overnight at 37°C in a heater (Medax). The sections were dewaxed with xylene and gradually hydrated before staining. Antigen retrieval was performed by pressure cooking the slides in citrate buffer (DAKO Target Retrieval Solution, Citrate pH 6) for 5 minutes to break up the proteins cross-links due to fixation. The primary anti-mouse/rat Ki-67 biotin conjugated antibody was incubated at room temperature for 30 minutes in a humidity chamber. Detection was carried out according to the manufacturer's instructions (DAKO REAL[™] Detection System Alkaline Phosphatase / RED). Afterwards the slides were briefly counterstained with haematoxylin and aquaeously mounted.

2.2.4.3 TUNEL assay

The TUNEL reaction was performed on paraffinized sections. Sections were deparaffinized, transferred to antigen retrieval buffer (10 mM sodium citrate pH 6.0), heated in a microwave until boiling and kept at sub-boiling temperature for 10 minutes and then allowed to cool down at room temperature for 30 minutes. The sections were washed three times 5 minutes each with PBS and reacted with terminal deoxynucleotidyl transferase mixture (Fermentas, St. Leon-Rot, Germany) according to the manufacturer's instructions for 1 h in a humidified chamber. After removal of the reaction mixture, sections were washed for three times 5 minutes each with PBS and incubated with Streptavidin-Cy3 (Sigma-Aldrich) at a dilution of 1:500 in PBS containing 1% BSA for 2 h at room temperature. Thereafter, the sections

were washed with PBS three times (5 minutes each) and then mounted with coverslips and a DAPI-containing mounting medium (ProLong Gold, Invitrogen). Tissue section images were taken using a virtual microscope (BX61VS, Olympus, Japan).

2.2.5 Immunology experiments

2.2.5.1 Cytokine analysis from lymphocyte cell cultures

Female wild-type and GABARAP KO mice at 6 - 8 weeks of age were treated with 6 weekly oral doses of 200 μ l sesame oil (vehicle-treated, control group) or 1 mg DMBA/mouse. For analysis of cytokines released from lymphocytes, mice were anesthetized and killed by cervical dislocation after one week of the last DMBA dose. Subsequently the spleen was removed under sterile conditions, and single cell suspensions were made. Thereafter cells were washed with warm cell culture media and erythrocytes were lysed with ammonium chloride/TRIS. The lymphocytes were washed again twice and the cell suspension was adjusted to 2×10^5 cells/ml. Then, the cells were cultured at 1 ml at 37°C with 5% CO₂ in Roswell Park Memorial Institute (RPMI) 1640 medium containing 10% FCS, 2 mM sodium pyruvate, 10 mM HEPES, 15 μ g/ml L-glutamine, 5 μ g/ml streptomycin, 5 U/ml penicillin, and 5×10^{-5} M 2-mercapto-ethanol in 12-well-cell culture plates with or without 1 μ g/ml plate-bound anti-CD3 antibodies (from 1452C11 hybridoma cell supernatant) for T cell receptor stimulation. Supernatants were harvested after 48 h of incubation and frozen at -80°C. To analyse the levels of secreted cytokines a standard sandwich enzyme-linked immunosorbent assay (ELISA) was used. Therefore 96-well-plates were coated with the primary antibodies (IL-2, IFN- γ or IL-17) in the specific coating buffer over night at 4°C (50 μ l/well). Then the plates were washed using a wash buffer containing 0.05% Tween 20 in PBS and unspecific binding sites were blocked by incubation with a solution of 2% BSA in H₂O (300 μ l/well) for 2 h. In the following, the plates were washed again. The probes and standards (recombinant cytokines) were plotted into the wells (100 μ l/well) and incubated over night at 4°C. The next day the plates were washed again and the biotin-labeled secondary antibodies in a solution of 1% BSA were plotted to the wells (100 μ l/well). After 2 h of incubation at room temperature, plates were washed and standard horseradish peroxidase-labeled streptavidin (2 μ l in 10 ml 1% BSA) was pipetted into the wells (100 μ l/well). After 30 minutes incubation at room temperature, plates were washed and 100 μ l/well ortho-phenylenediamine (OPD)-solution was plotted into the wells in the dark. The enzymatic reaction was stopped by adding 50 μ l/well 2N H₂SO₄ and the extinction was measured at 492 nm with a microplate absorbance reader.

2.2.5.2 Cytokine analysis from macrophage cell cultures

The same mice and treatment regimens, which are mentioned above for lymphocytes culture, were used for macrophages culture. For analysis of cytokines released from macrophages, mice were anesthetized and killed by cervical dislocation after one week of the last DMBA dose. Subsequently the peritoneum was exposed under sterile conditions and the abdominal cavity was flushed out with a cold solution containing heparin (20 μ l/100 ml PBS). The cells were collected in centrifuge tubes and washed twice with cold PBS. Then, the cells were adjusted to 2×10^5 cells/ml in RPMI cell culture medium. To separate the macrophages from other cells, the whole pool of cells was incubated for 2 h at 37°C with 5% CO₂ in 24-well-cell culture plates (1 ml/well). Then the non-adhering cells were removed by washing the wells with warm RPMI medium. The adhering cells are suspected to be > 95% macrophages due to former investigations (Yui *et al.*, 1993). In the following the macrophages were stimulated with LPS (1 μ g/ml RPMI medium) and incubated for 4 h at 37°C with 5% CO₂, and then either treated or not with ATP (5 mM) for 1 h. At the end of the incubation the supernatants were harvested and stored at -80°C. To analyse the levels of secreted cytokines (IL-1 β , IL-6 and TNF- α) a standard sandwich enzyme-linked immunosorbent assay (ELISA) was done as previously described in cytokine secretion from lymphocytes (2.2.5.1).

2.2.5.3 Cell surface marker analysis for splenocytes by FACS

For analyses of splenocytes surface marker, mice were anesthetized and killed by cervical dislocation after one week of the last DMBA dose. Subsequently the spleen was removed from vehicle-treated (control) and DMBA-treated groups under sterile conditions, and single cell suspensions were made. The cells were dispersed by gentle pipetting and filtered through a cell strainer to eliminate clumps and debris. Cell suspension was collected in a conical tube, centrifuged 5 minutes at 300 x g at 4°C, and the supernatant was discarded. The cell pellet was washed once again with PBS. Then the cells were resuspended in PBS and cell count and viability analysis was performed. The experiment of cell surface markers was performed in the Institute of Immunology, Jena by kindly support of Martin Böttcher. The cells were decanted into labeled fluorescence-activated cell sorting (FACS) tubes containing 2 ml PBS, centrifuged for 6 minutes at 300 x g (4°C), and the supernatant was discarded. The cell pellet was washed once again with PBS. The cells were permeabilized by washing with 1 ml PBA-S (0.5% saponin in PBA). PBA is a PBS containing 0.25% bovine serum albumin (BSA) and 0.02% sodium azide (NaN₃). Thereafter 25 μ l of antibody master-mix was added and incubated for 20 minutes in the dark on ice. The master-mix was prepared as following:

Blocking reagent	Clone	Source	Dilution factor
α CD16/CD32	2.4G2	Institute of Immunology, Jena	1:100 in PBS
Rat IgG	-	Jackson Immuno Research	1:200 in PBS

Cell type	Antibody	Clone	Source	Dilution factor	Fluorochrome (diluted in 100 μ l PBA)
B cell	B220 ⁺	RA3-6B2	Institute of Immunology, Jena	1:200 in PBS	Pacific Blue
CD4 T cell	CD4 ⁺	GK1.5	Institute of Immunology, Jena	1:200 in PBS	Dye647
CD8 T cell	CD8 ⁺	53-6.7	eBioscience	1:300 in PBS	PE/Cy7
Macrophages	CD11b ⁺	M1/70	eBioscience	1:800 in PBS	Alexa Fluor 700
Neutrophils	CD11b ⁺	M1/70	eBioscience	1:800 in PBS	Alexa Fluor 700
	Ly6G ⁺	RB6-8C5	eBioscience	1:200 in PBS	APC

Thereafter the cells were washed with 1 ml PBA, and resuspended in 200 μ l PBA. The samples were measured with flow cytometer (BD LSR II).

An alternative protocol was used for FoxP3 staining according to the manufacturer's instruction (eBioscience). The splenocytes were prepared as mentioned above. After the last wash with PBS, the supernatant was discarded and the cell pellet was dissociated by pulse vortexing. The surface staining for CD4⁺ and CD25⁺ was performed as described above.

Blocking reagent	Source	Dilution factor
Rat IgG	Jackson Immuno Research	1:200 in PBS

Antibody	Clone	Source	Dilution factor	Fluorochrome (diluted in 100 μ l PBA)
CD4 ⁺	-	eBioscience	1:200 in PBS	APC/Cy7
CD25 ⁺	PC61.5	Institute of Immunology, Jena	1:200 in PBS	Dye647

Then, 1 ml of freshly prepared FoxP3 Fixation/Permeabilization working solution (eBioscience) was added to each tube and mixed by pulse vortexing. The samples were incubated at 4°C for 60 minutes in the dark. Thereafter 2 ml of PBA was added to each tube, centrifuged at 300 x g at room temperature for 5 minutes, and the supernatant was discarded. Subsequently, 25 μ l of antibody was added and incubated for 30 minutes in the dark on ice.

Antibody	Clone	Source	Dilution factor	Fluorochrome (diluted in 100 μ l PBA)
FoxP3	-	eBioscience	1:50 in PBS	FITC

Thereafter, the cells were washed with 1 ml PBA, and resuspended in 200 μ l PBA. The samples were measured with flow cytometer (BD LSR II).

2.2.6 Whole mount analysis of mammary glands

Whole mount of mammary gland is a desirable method to visualize the morphology of the ductal tree; epithelial cell proliferation and ductal branching. Female wild-type and GABARAP KO mice were treated with 6 weekly oral doses of 200 μ l sesame oil as vehicle (control) or 1 mg DMBA/mouse. Mice were anesthetized and killed by cervical dislocation after one week of the last DMBA dose. Whole mount analyses was carried out according to the procedure of [Banerjee *et al.* \(1976\)](#) with small modifications. A longitudinal ventral incision along the midline was made in the skin that extended from the genital to the thoracic region. Then, an inverted V-shaped cut was made on either side of the genitalia and the skin peeled back. The 4th abdominal mammary gland was dissected from the pelt by using surgical scissors and forceps. The 4th abdominal mammary gland was selected for whole mounting because of the presence of the lymph node for orientation. The mammary gland was spread on a glass slide and kept short time (2 - 3 minutes) at room temperature then submerged into a mixture of 1 part glacial acetic acid and three parts 100% ethanol for 3 h. In the following the glands were washed with 70% ethanol for 15 minutes and subsequently rinsed with distilled water for 5 minutes. Subsequently, the glands were stained with alum carmine overnight or until the fat pad was a uniform pink colour (at room temperature with minimum illumination). Then they were rinsed with 70, 90 and 100% ethanol each for 30 minutes. After dehydration, the glands were transferred to xylene for clearing and mounted with aqueous mounting medium (permount). The mammary glands were analysed and evaluated under stereo microscope.

Alum carmine stain:

1 g carmine + 2.5 g alum potassium sulfate in 500 ml distilled water.

Then the mixture were boiled for 20 minutes, the volume adjusted to 500 ml with water, filtered with Whatman filter paper and kept at 4°C with minimum illumination. The alum carmine stain has stored for not more than one week at refrigerator.

2.2.7 Microarray gene expression profiling analysis of mammary glands

Female wild-type and GABARAP KO mice were treated with 6 weekly oral doses of 200 μ l sesame oil as vehicle (control) or 1 mg DMBA/mouse. Mice were anesthetized and killed by cervical dislocation after one week of the last DMBA dose. Abdominal mammary glands

were isolated and directly fixed in 5% neutral buffered formalin, and subsequently paraffin blocks were constructed. Almost all the procedures of tissue preparation, fixation and storage were performed as recommended for successful gene expression profiling analysis of formalin-fixed paraffin-embedded (FFPE) samples, as mentioned by von Ahlfen *et al.* (2007). Microarray analysis was carried out by the Miltenyi Biotec GmbH, Bergisch Gladbach, Germany, using the Agilent Whole Mouse Genome oligo microarrays 8x60K chips according to standard protocols of FFPE samples. The workflow for gene expression analysis of FFPE samples is illustrated in Figure 10.

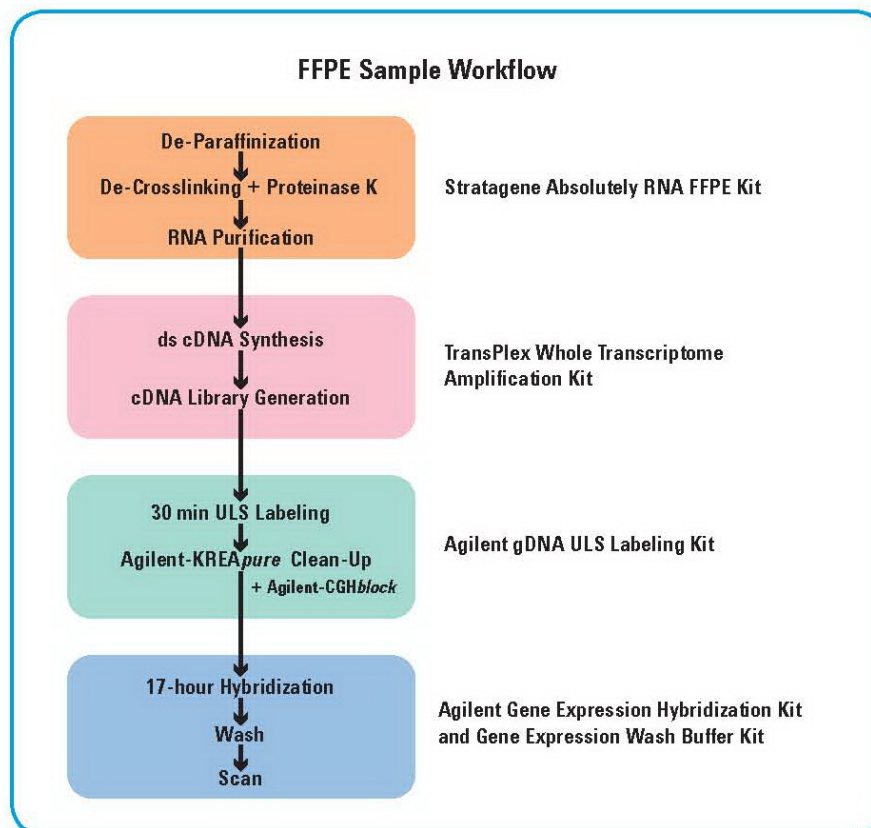


Figure 10. Workflow for Agilent gene expression profile of FFPE samples. Flowchart indicates the various kits and steps involved in the analysis of FFPE samples with the Agilent gene expression microarray workflow (Source: Agilent Technologies).

2.2.7.1 Quality control of total RNA

Eighteen FFPE tissue samples (3 wild-type control (CWt), 3 GABARAP KO control (CKO), 6 wild-type DMBA-treated (DWt), 6 GABARAP KO DMBA-treated (DKO)), each consisting of approximately twenty 10 μm slices, were sent to Miltenyi Biotec. The RNA isolation was performed using the Absolutely RNA FFPE Kit (Stratagene). The quality of total RNA was checked via the Agilent 2100 Bioanalyzer platform (Agilent Technologies). The results of the Bioanalyzer run are visualized in a gel image and an electropherogram

using the Agilent 2100 Bioanalyzer expert software. In addition, RNA Integrity Number (RIN) was generated by the same software to check the integrity and overall quality of total RNA samples. The RIN value is calculated by a proprietary algorithm that takes several quality control parameters into account, for example, 28S RNA/18S RNA peak area ratios and unexpected peaks in the 5S RNA region. A RIN number of 10 indicates high RNA quality, and a RIN number of 1 indicates low RNA quality (Fleige and Pfaffl, 2006). Our RNA samples revealed RIN values ranging from 1.4 to 5.9.

2.2.7.2 Library preparation and WTA amplification of RNA

For the library preparation and Whole Transcriptome Amplification (WTA) step, 200 ng RNA were used. To produce cDNA, the RNA samples were amplified using the Complete TransPlex[®] Whole Transcriptome Amplification Kit (WTA2, Sigma) following the manufacturer's protocol. Yields of cDNA were measured with the ND-1000 Spectrophotometer (NanoDrop).

2.2.7.3 ULS-Labeling

For the ULS-Labeling step, 500 ng of each cDNA sample was used. To produce Cy3-labeled DNA, the DNA samples were labeled using the Genomic DNA ULS Labeling Kit (Agilent Technologies) following the manufacturer's instruction (Gene Expression FFPE Workflow protocol, Agilent). Yields of Cy3-labeled cDNA and the dye-incorporation rate were measured with the ND-1000 Spectrophotometer (NanoDrop). According to the manufacturer's instruction the optimal degree of labeling is between 1.5% and 3%. All our Cy3-labeled cDNA samples revealed an adequate degree of labelling (2.4 - 2.9%).

2.2.7.4 Hybridization of Agilent Whole Genome Oligo Microarrays

The hybridization procedure was performed according to the Agilent Gene Expression FFPE Workflow protocol using the Agilent Gene Expression Hybridization Kit and Agilent CGH*block*. Cy3-labeled DNA in hybridization buffer and CGH*block* were hybridized overnight (17 h, 65°C) to Agilent Whole Mouse Genome Oligo Microarrays 8x60K using Agilent's recommended hybridization chamber and oven. Finally, the microarrays were washed once with Gene Expression Wash Buffer 1 (Agilent Technologies) for 1 minute at room temperature followed by a second wash with Gene Expression Wash Buffer 2 (Agilent Technologies) 37°C for 1 minute. The last washing step was performed with acetonitrile for 5 seconds.

2.2.7.5 Scanning results

Fluorescence signals of the hybridized Agilent Microarrays were detected using Agilent's Microarray Scanner System (Agilent Technologies).

2.2.7.6 Image and data analysis

The analysis of whole genome expression for 18 samples (belonging to four conditions) was kindly performed by the Network Modelling group of Prof. Dr. Rainer König at the Hans-Knöll-Institute (HKI), Jena, Germany. Limma, R package was used to read out and process the microarray image files derived using Agilent's platform (Smyth, 2005). Background correction was performed and arrays were normalized using loess method. 23544 probes were selected having expression intensities above background at least in 3 samples. Expression was averaged for genes having more than one probe set. A total of 15815 genes were finally analyzed further. Differential expression was assessed using Limma for four pairs namely CWT-CKO, CWT-DWT, CKO-DKO and DWT-DKO. Limma calculates a fold change and standard error for each gene by fitting a linear model. Then it calculates empirical Bayes moderated t-test statistics for each gene. P-values derived from moderate t-tests were corrected using the Benjamin and Hochberg approach (Benjamini and Hochberg, 1995). The genes with p-values ≤ 0.05 considered as differentially expressed.

2.2.8 Reverse transcription polymerase chain reaction (RT-PCR)

2.2.8.1 RNA isolation

Total RNA was isolated from several organs of wild-type and GABARAP KO mice by using Trizol reagent (peqGOLD TriFast, peQlab) according to the manufacturer's instruction. For homogenization, the tissue samples (about 100 mg) were lysed directly by addition of 1 ml TriFast. Subsequently the samples were kept on ice during the process of crushing by pestle and power homogeniser (Ultra-Turrax T8). The cell lysate was passed through a pipette several times, transferred to a 1.5 ml tube and kept for 5 minutes at room temperature for dissociation of the nucleoprotein complexes. After addition of 200 μ l chloroform, samples were shaken for 15 seconds and kept at room temperature for another 10 minutes. During centrifugation at 12,000 x g the mixture separated into the lower red phenol-chloroform phase, the interphase and the colourless upper aqueous phase. The upper aqueous RNA containing phase was transferred to a fresh tube and 0.5 ml isopropanol was added to precipitate RNA. Samples were kept on ice for 15 minutes and centrifuged for

10 minutes at 12,000 x g (4°C). Supernatant was removed carefully and the RNA pellet was washed twice with 75% ethanol (prepared with DEPC-treated water) by vortexing and subsequent centrifugation for 10 minutes at 12,000 x g (4°C). RNA pellet was air-dried to remove the excess isopropanol and resuspended in RNase-free water. Concentration was measured with NanoDrop spectrophotometer. RNA was stored at -80°C or immediately used for cDNA synthesis.

2.2.8.2 Complementary DNA (cDNA) synthesis

For reverse transcription of the whole RNA we used the QuantiTect[®] Reverse Transcription Kit (Qiagen) according to the manufacturer's instruction. Genomic DNA elimination reaction was prepared on ice, mixed, incubated for 2 minutes at 42°C and then placed immediately on ice. Reverse transcription master mix was prepared, mixed and kept on ice. The appropriate volume of master mix was distributed into individual tubes. The template RNA (from gDNA elimination reaction) was added, mixed and incubated for 15 minutes at 42°C. To inactivate Reverse Transcriptase, the samples were incubated at 95°C for 3 minutes, immediately placed on ice and stored at -20°C.

2.2.8.3 Quantitative reverse transcriptase PCR (qRT-PCR)

To analyse mRNA related gene expression, a master mix was prepared as following:

Reagent	Volume/reaction
FastStart Universal SYBR Green Master (Rox)	6.250 µl
Forward Primer	0.375 µl
Reverse Primer	0.375 µl
H ₂ O	5.000 µl
cDNA	0.500 µl
Total reaction volume	12.50 µl

The mixture-containing tubes were closed and put in the 72-well-carousel of a Rotor-Gene Q real-time PCR machine. The following program was used:

Cycle(s)	Temperature	Hold Time
1	95°C	10 min
40	95°C	15 seconds
	60°C	60 seconds

Glycerinaldehyd-3-phosphate-dehydrogenase (GAPDH) served as housekeeping gene and was used to normalize gene expression data.

2.2.9 Fibroblasts isolation and treatment

2.2.9.1 Primary culture of mouse embryonic fibroblasts (MEFs)

Mouse embryonic fibroblasts isolation was carried out according to the protocols of culture of animal cells (Freshney, 2005). Mouse embryos were isolated at day 13th of gestation period under sterile conditions. The embryos were transferred into PBS in 10 cm petri dish, rinsed, dissected from unwanted tissue, such as fat and placenta, and transferred to a third dish. In the following they were chopped with scalpels and scissor, washed with PBS and centrifuged. All the pieces were transferred to 500 ml flask filled with 180 ml of PBS plus 20 ml of 2.5% trypsin. The flask was capped, and stirred in a hybridization oven at 100 rpm for 30 minutes at 37°C. In the following the disaggregated cells were collected into a centrifuge tube and placed on ice. Then fresh trypsin was added to the pieces that remained in the flask, and the same steps were repeated for 3 times. Thereafter the collected cell suspensions were centrifuged, resuspended in growth medium (DMEM supplemented with 10% FCS, 2 mM L-glutamine, 1 mM sodium pyruvate, 100 units/ml penicillin, 100 µg/ml streptomycin and 0.1 mM β-mercaptoethanol) and filtered with sterile polypropylene cell strainer. Thereafter the cell suspensions were centrifuged, resuspended with growth medium and cultured in tissue culture flasks at 37°C with 5% CO₂.

2.2.9.2 Mouse embryonic fibroblasts (MEFs) treatment

Wild-type and GABARAP-deficient MEFs at third passage were seeded in 10 cm petri dishes and incubated overnight or until they reached 60 - 70% confluence. To obtain starvation conditions, cells were washed three times with PBS and incubated in EBSS medium in the presence or absence of 10 µM CQ (to inhibit lysosomal degradation) at 37°C for 2 h. For DMBA and camptothecin (CPT) treatment, MEFs were treated with 100 nM DMBA for 24 and 48 h, 5 mM CPT for 4 and 20 h, and medium containing vehicle (0.1% DMSO) as control and subsequently incubated at 37°C and harvested at indicated time point.

2.2.10 Analysis of proteins

2.2.10.1 Protein extraction and measurement

MEFs were harvested after they were washed one time with PBS, trypsinized for 2-5 minutes at 37°C and resuspended in medium. The cell suspension was transferred to a 15 ml Falcon tube and centrifuged for 10 minutes at 300 x g at 4°C. Supernatant was discarded; the pellet washed with 1 ml PBS and centrifuged again at 300 x g at 4°C for 10 minutes. Directly after

aspiration of the supernatant the cell pellets were placed on ice. For cell lysis, a reasonable volume of radioimmunoprecipitation assay (RIPA) buffer (supplemented with protease inhibitors) was added to resuspend the cells, and then incubated for 15 - 20 minutes on ice. The amount of RIPA buffer was determined according to the size of cell pellet. Thereafter the cell debris was removed by centrifugation for 10 minutes at 13,000 x g at 4°C and supernatant was transferred to a fresh 1.5 ml tube. The protein concentration was determined by using the bicinchoninic acid (BCA) protein assay kit according to the manufacturer's instructions. The two solutions of the kit were mixed and distributed to 0.5 ml tubes (20 µl/ tube), and then 2.5 µl of the samples were added and incubated at 37°C for 30 minutes. NanoDrop was used to determine the protein concentration by photometric measurement. A standard curve was set with bovine serum albumin (BSA) and created by preparing 0.5, 0.75, 1, 2, 4, 8, and 10-µg duplicate dilutions of 200 mg/ml stock solution of BSA. Cell lysates were stored in the freezer at -20°C.

2.2.10.2 Western blot analysis

Protein samples were separated by sodium dodecyl sulfate-polyacrylamid gel electrophoresis (SDS-PAGE) using the standard Laemmli method. Prior to loading, the samples were prepared for electrophoresis by addition of 4 fold loading buffer and denatured at 95°C for 5 minutes. Equal amounts of proteins were loaded onto 12% gel. Electrophoresis was run in 1 x electrophoresis buffer for 1-2 hours at 100 V (constant voltage) using Mini PROTEAN Tetra System (BIO-RAD). Protein separation was controlled by running a prestained protein ladder (PageRuler™ Plus, Thermo Scientific).

Separating gel: 10 ml of 12% gel	Stacking gel: 5 ml of 5% gel
4.3 ml H ₂ O	3.7 ml H ₂ O
3 ml 40% Acrylamide	0.63 ml 40% Acrylamide
2.5 ml 1.5 M Tris-HCL, pH 8.8	0.63 ml 1 M Tris-HCL, pH 6.8
100 µl 10% SDS	50 µl 10% SDS
100 µl 10% APS	50 µl 10% APS
10 µl TEMED	5 µl TEMED

Following electrophoresis, the stacking gel was discarded, and the separating gel was submerged in transfer buffer for several minutes (10-20 minutes). Then the protein samples in separating gel were transferred to a nitrocellulose membrane (0.45 µm pore size) using a semidry-transfer method. On a semidry transfer unit (PerfectBlue™ 'Semi-Dry'-Electro Blotter, peQlab) 3 sheets of Whatman paper pre-wetted in transfer buffer, the PVDF

membrane, the gel, and 3 sheets of pre-wetted Whatman paper were assembled. The transfer was performed at 12 V (constant voltage) for 2.5 h. When the blotting was finished, the membrane was submerged in blocking buffer (5% non-fat dry milk powder in TBST or 5% bovine serum albumin in TBST) for 1 - 1.5 h to block the non-specific binding sites. Then the membrane was transferred into 50 ml tubes containing 5 ml primary antibody solution and incubated on a shaker overnight at 4°C. The next day, the membrane was washed with TBST (3 x 5 minutes), and incubated with the corresponding horseradish peroxidase (HRP) conjugated secondary antibody (diluted in blocking buffer) for 1 hour at room temperature. Then the membrane was washed again 3 times in TBST (5 minutes each). For visualization of immuno-reactive bands, the chemiluminescent detecting luminol reagent was used according to manufacturer's instructions (Santa Cruz Biotechnology). Detection solution was applied to the membrane covering it evenly and after a short incubation time excess solution was drained from the membrane. Pictures of the chemiluminescent bands were taken by putting a light sensitive x-ray film on the top of the membrane in a darkroom. The film was developed after different exposure times and fixed according to the standard procedure.

2.2.11 B16 melanoma cell inoculation

B16 melanoma cell line was kindly provided from the Institute of Pathology, Charité in Berlin. Thawing of cells was performed quickly in a 37°C water bath for ~2 minutes. Then, the cells were transferred immediately into a culture flask containing pre-warmed RPMI culture medium supplemented with 10% FCS and incubated at 37°C with 5% CO₂. The next day, the medium was replaced with fresh medium to remove traces of DMSO. The cells were grown to 60 - 70% confluence and harvested by trypsinization (as explain above for MEFs harvesting). The cells were collected in 15 ml centrifuge tubes, pipetted vigorously to obtain single cell suspension and washed with cold PBS. Then, the cells were adjusted to 2.5×10^6 cells/ml in ice-cold PBS and transferred to animal facility while maintaining the cells on ice. The inoculation region was wetted with 70% ethanol before inoculation. The cells were resuspended by inverting the tube several times and a 1 ml syringe attached with 27½-G needle was filled with cell suspension. Female wild-type and GABARAP KO mice were inoculated subcutaneously with 100 µl of cell suspension (2.5×10^5 cells) in the left flank region. After one week of B16 cells injection, we monitored the tumor growth daily and started tumor measurement when it became palpable. Tumor volume was measured using a caliper every other day.

2.2.12 Mutation analysis

Mutation analysis was performed to screen for H-ras mutation in DMBA-induced tumors of wild-type and GABARAP KO mice.

2.2.12.1 DNA extraction

DNA was extracted by using Maxwell[®] 16 FFPE Plus LEV DNA Purification Kit (Promega) according to the manufacturer's instruction. FFPE blocks were sectioned to 10 μm thickness with a rotation microtome. The tumor region within the section was identified by Prof. Dr. Iver Petersen and Dr. Masoud Mireskandari (Institute of Pathology, Jena). Thereafter, the identified tumor region, corresponding to H & E stained section, was scraped from FFPE tissue sections by scalpel. The number of sections for each tumor was determined depending on tumor size (~10 - 20 sections). Then the scraped sections were collected in microtube and briefly centrifuged at full speed to collect the sample at the bottom of the tube. The pellet was resuspended in 180 μl of incubation buffer and 20 μl proteinase K solution. The tumor sample was incubated at 70°C overnight. In the next day, 400 μl of lysis buffer was added to the sample and mixed by vortexing. Then the sample was prepared for Maxwell[®] 16 automated DNA purification instrument (Promega) as illustrated in Figure 11. The cartridge was placed in the rack; the LEV plunger was placed in the last well of cartridge, and elution tube was placed in the front of the Maxwell[®] 16 LEV Cartridge Rack (Fig. 11). Nuclease-free water (35 μl) was added the elution tube. Subsequently, the sample was transferred to well #1 of the cartridge (Fig. 11). Then the rack was transferred to the instrument and we selected the program of DNA extraction of FFPE sample. When the automated purification run was completed, NanoDrop was used to measure the DNA concentration and the purity (260 / 280 nm ratio) of the samples. If not used immediately for PCR the samples were stored at -20°C.

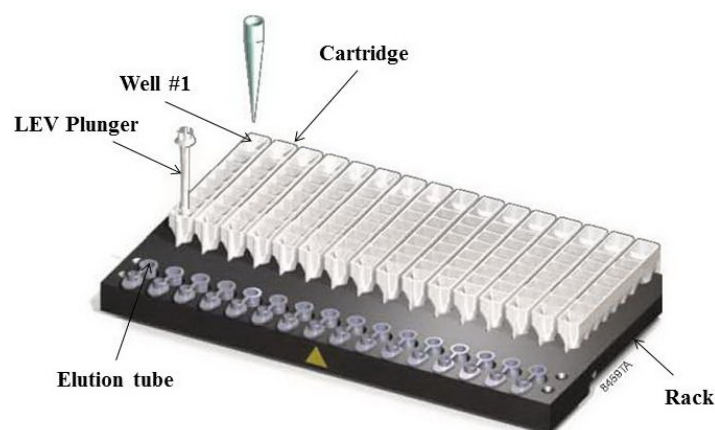


Figure 11. Sample preparation for Maxwell[®] 16 LEV Cartridges of FFPE-DNA purification kit (Promega).

2.2.12.2 Polymerase chain reaction (PCR)

For polymerase chain reaction (PCR) we used the primers shown above in paragraph 2.1.11. 180 ng DNA were used per run and the master mix was prepared as follows:

Reagent	Volume/reaction
10 x buffer S	5 μ l
2.0 mM dNTP mix	5 μ l
Forward Primer (10 pmol/ μ l)	2 μ l
Reverse Primer (10 pmol/ μ l)	2 μ l
Taq-polymerase (HotStarTaq)	0.25 μ l
DNA, 180 ng	Variable
H ₂ O	Variable
Total reaction volume	50 μl

DNA was added to each tube containing master mix as the final step. Tubes were placed in the peQSTAR 96 Universal Gradient cycler (peQlab) and the program was started. The annealing temperature of H-ras primers was 68°C for the first eight cycles, then 60°C for the next 32 cycles of exon 1 primers and 62°C for the next 32 cycles of exon 2 primers.

Step	Temperature	Duration	Cycle
Initial denaturation	95°C	15 minutes	1
Denaturation	94°C	1 minute	} 8
Annealing	68°C	45 seconds	
Extension	72°C	45 seconds	
Denaturation	94°C	1 minute	} 32
Annealing	60°C exon1, 62°C exon 2	45 seconds	
Extension	72°C	45 seconds	
Final elongation	72°C	7 minutes	1

After the program was completed the PCR products were stored at 4°C.

2.2.12.3 Agarose gel electrophoresis

Electrophoresis was performed as described above in paragraph 2.2.2.3.

2.2.12.4 Purification of PCR products for sequencing

The DNA Clean & Concentrator™-5 Kit (Zymo Research) was used for the purification of PCR products for sequencing according to manufacturer's instructions. Two volumes of DNA binding buffer were added to the PCR product and the mixture was transferred to

a Zymo-Spin™ column in a collection tube. Then, centrifugation was carried out for 1 minute at 12,000 x g and the flow-through was discarded. Thereafter, 200 µl of DNA wash buffer per column were added and centrifugation carried out at 12,000 x g for 1 minute. The washing step was repeated once. Ten µl of water were added directly to column matrix and incubated for 1 minute at room temperature. Column was transferred to a fresh 1.5 ml tube and centrifuged for 1 minute at 12,000 x g to elute the DNA. The concentration of purified DNA was measured with NanoDrop.

2.2.12.5 Sequencing and result analysis

Purified PCR products (100 ng) were applied for direct sequencing by capillary electrophoresis (LGC Genomics GmbH, Berlin, Germany), and the sequencing-profiling was analyzed by the Finch TV 1.4.0 software program (Geospiza, PerkinElmer, MA, USA).

2.2.13 Statistical analysis

Data are expressed as mean ± SEM (standard error of the mean). Differences between groups were calculated using the two-tailed Student's *t*-test for unpaired values. Normal distribution of the values was checked using the Kolmogorov-Smirnov test (K-S test). Survival analysis was calculated by the Kaplan-Meier method. Statistical significance was calculated by the SPSS software package (v.16.0, Chicago, USA), p-values below 0.05 were considered as being significant (* $p < 0.05$, ** $p < 0.01$, *** $p = 0$). Statistical analysis for gene expression profiling was explained above in paragraph 2.2.7.6.

3. Results

3.1 GABARAP knockout mice exhibited low tumor formation

In order to investigate the potential roles of GABARAP in the incidence of tumors, we attempted to induce tumors in our transgenic animals by treatment with a reliable potent carcinogen 7,12-dimethylbenz(a)anthracene (DMBA). Female GABARAP knockout (KO) and C57BL/6 wild-type (Wt) mice were given 1 mg doses of DMBA for 6 consecutive weeks by oral gavage beginning at 6 - 8 weeks of age. Mice were checked weekly for the presence of palpable tumor masses. Tumors arose in 14 of 29 (48.3%) of wild-type mice within 35 weeks after the last DMBA dose (Table 2). Surprisingly, the numbers of GABARAP KO mice exhibiting tumors were significantly less than their wild-type counterparts (4 of 33; 12.1%; $p < 0.002$) (Table 2). A variety of tumors developed in each group of mice, for instance mammary, skin, lymphoma and liver tumors. Figure 12 showed gross morphologic and histologic features of tumors induced by DMBA. If only mammary tumors are considered, this represents a reduction from 3 of 14 (21.4%) in wild-type mice to 0 of 4 (0%) in GABARAP KO mice (Table 2).

Table 2. Tumor types and incidence in C57BL/6 wild-type (Wt) and GABARAP KO (KO) mice

<u>Tumor type</u>	<u>C57BL/6 (Wt)</u>	<u>GABARAP^{-/-} (KO)</u>
<i>DMBA treatment</i>	<i>n = 29</i>	<i>n = 33</i>
Mammary	3	-
Skin	7	2
Lymphoma	2	-
Liver	-	1
Undifferentiated tumors	2	1
Total	14 (48.3%)	4 (12.1%)**
<i>Spontaneous tumor</i>	<i>n = 30</i>	<i>n = 35</i>
Mammary	2	-
Lymphoma	-	2
Liver	1	-
Undifferentiated tumors	1	-
Total	4	2

** Significant difference between two groups (p -value < 0.01) calculated by Fisher's exact test.

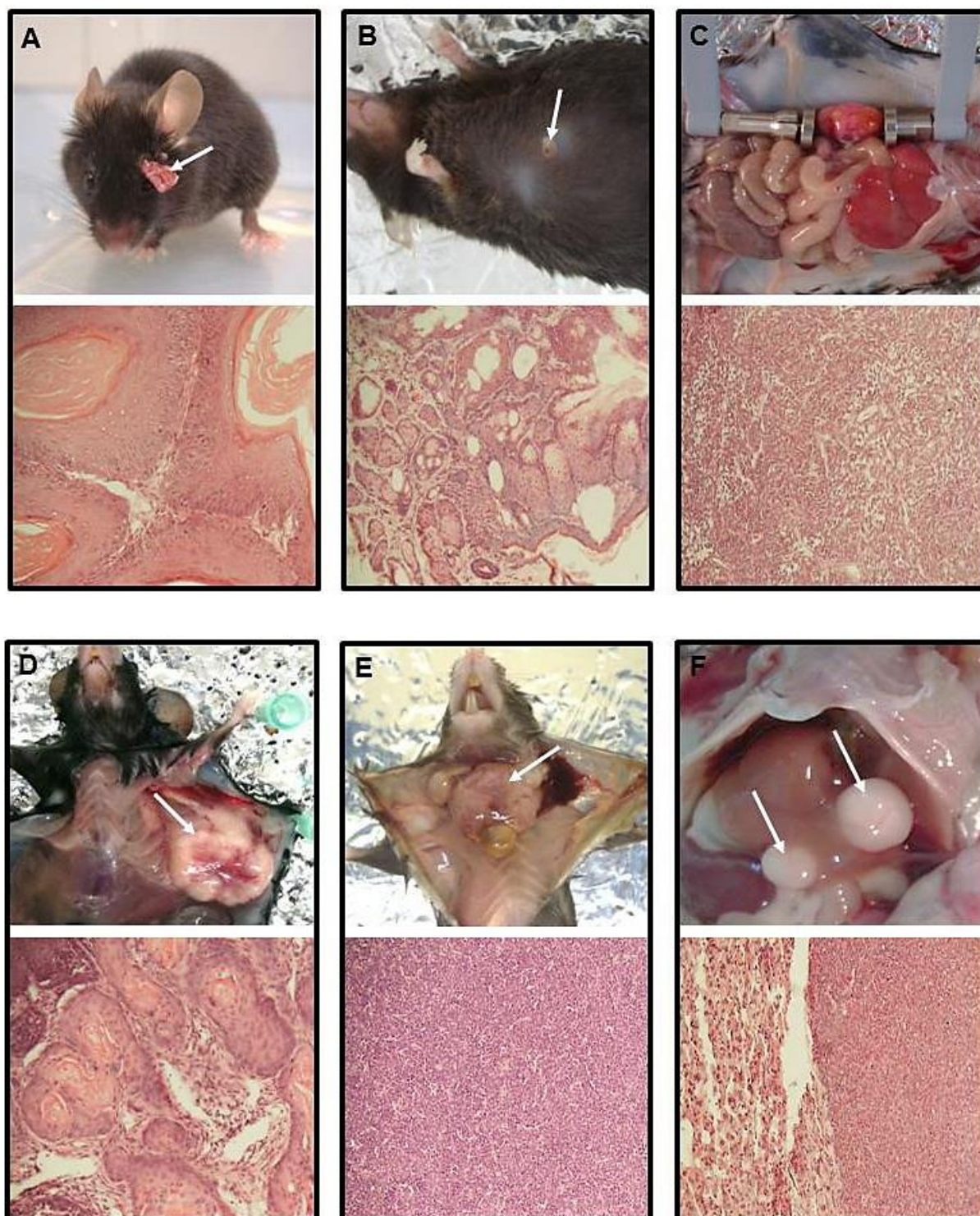


Figure 12. Gross morphologic and histologic features of mice tumors induced by DMBA. **A)** Upper panel: skin tumor in wild-type mouse, bottom panel: H&E staining of skin squamous cell carcinoma. **B)** Upper panel: skin tumor in GABARAP KO mouse, lower panel: H&E staining of skin sebaceous epithelioma. **C)** Upper panel: undifferentiated tumor mass in abdomen of wild-type mouse, bottom panel: H&E staining of histologic section of undifferentiated tumor. **D)** Upper panel: mammary tumor in wild-type mouse, bottom panel: H&E staining of mammary squamous cell carcinoma. **E)** Upper panel: lymphoma in the neck of wild-type mouse, bottom panel: H&E staining of histologic section of lymphoma. **F)** Upper panel: two masses of liver tumor in GABARAP KO mouse, bottom panel: H&E staining of liver cell carcinoma. The magnifications of all histologic sections were 20X.

Regarding the spontaneous tumor incidence in female GABARAP KO and wild-type control mice over the period of 2 years, 4 spontaneous tumors out of 30 (13.3%) developed in wild-type mice compared with 2 out of 35 (5.7%) in GABARAP KO mice (Table 2). Furthermore, no spontaneous mammary tumors developed in GABARAP KO mice in comparison with wild-type control mice group which developed 2 mammary tumors out of 4 spontaneous tumors (Table 2).

The low percentage of tumor incidence in C57BL/6 (Wt) mice is approximately consistent with the data reported by other authors following DMBA treatment and/or spontaneous tumors development, and this is due to the fact that the C57BL/6 mouse strain is less sensitive to DMBA-induced tumorigenesis than other rodent strains (DiGiovanni *et al.*, 1993; Hennings *et al.*, 1993; Woodworth *et al.*, 2004; Medina, 2007).

The median onset time and latency period of tumors induced by DMBA were not available for all tumor types due to a number of mice that had interior tumors; for example liver tumors were difficult to detect by palpation. Figure 13 (A and B) showed the latency periods and sizes of tumors induced by DMBA in mice groups. The tumor occurrence started earlier in wild-type mice compared to GABARAP knockout animals, at the 9th week after the last DMBA dose (Fig. 13 A). The tumor sizes in wild-type mice were obviously larger in most of induced tumors compared to the tumors formed in GABARAP KO mice which were smallest in general (Fig. 13 B). The age in Figure 13 (B) represented the age of mice when they are sacrificed.

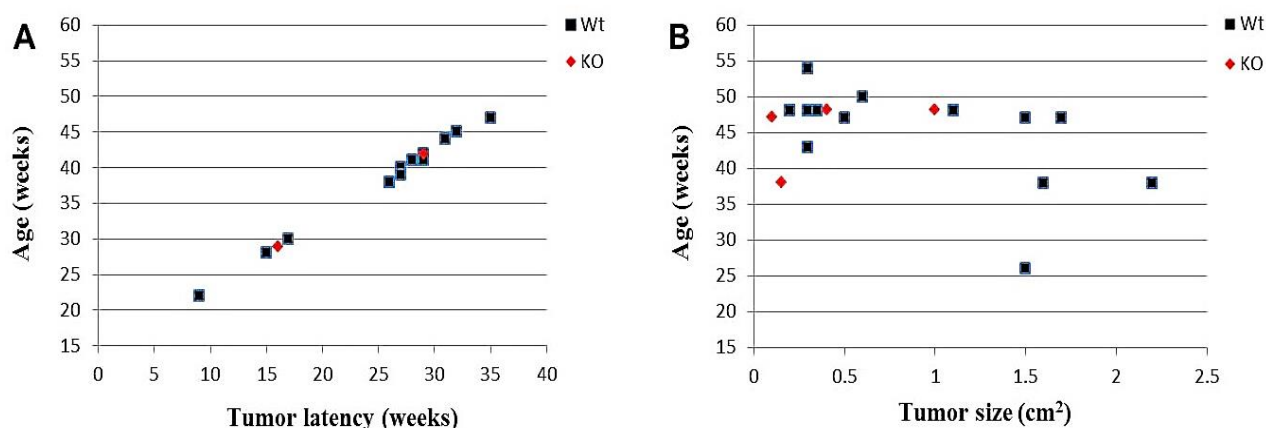


Figure 13. A) Latency period of palpable tumors (skin, lymphoma and mammary tumors) in wild-type (Wt) and GABARAP KO (KO) mice after 6 weekly oral doses of 1 mg DMBA. The latency period represented the date after the last dose of DMBA, which was indicated as (0) in figure. B) Size of all the tumors induced by DMBA in wild-type (Wt) and GABARAP KO (KO) mice. In figure B, the age of mice represented the date when the mice are sacrificed.

3.2 GABARAP knockout mice reduced the survival after different carcinogen treatments

Female GABARAP KO and wild-type mice treated with different carcinogen regimens at 6 – 8 weeks of age in order to increase and improve the tumor incidence. In addition, we wanted to investigate the lethal susceptibility of GABARAP KO mice, since the GABARAP-deficient mice showed a significant survival reduction ($p = 0.006$) after DMBA treatment (Fig. 14 A). In addition to polycyclic aromatic hydrocarbon DMBA, N-ethyl-N-nitrosourea (ENU) and N-methyl-N-nitrosourea (MNU), alkylating agents and potent mutagens, were used in our investigation. Treatment of mice with a single intraperitoneal (i.p.) injection of 150 mg ENU/kg of body weight showed substantial reduction ($p = 0.022$) in survival of GABARAP KO mice compared with wild-type mice through the period of 53 weeks (Fig. 14 B). There was no tumor formation within the period of ENU treatment in GABARAP KO mice, while wild-type mice developed tumors in about 21% of ENU-treated mice ($n = 14$ mice per group).

Furthermore, it was reported that using of medroxyprogesterone acetate (MPA), a steroidal progestin, enhanced the mammary tumorigenesis in BALB/c mice following MNU treatment (Pazos *et al.*, 1998). We attempted to increase the mammary tumors incidence in our mice groups by using the similar treatment regimen; however, we observed that the survival of GABARAP KO mice was significantly decreased ($p = 0.002$) compared with wild-type mice (Fig. 14 C). No tumor formation was observed in both treated groups during the period of 27 weeks of MPA plus MNU treatment. Indeed, non-occurrence of tumor within a short time period after carcinogen treatment consider normal, since those carcinogens (DMBA, ENU and MNU) require more time to initiate and promote tumor development in mouse models.

Moreover, the synergistic effect of MNU and DMBA in mammary carcinogenesis of female rats has been reported in the literature (Shirai *et al.*, 1997). The combined treatment of MNU and DMBA increased the carcinogenic effect and significantly increased the mean number of mammary tumors per rat (Shirai *et al.*, 1997). To further examine tumor susceptibility and lethality of GABARAP KO mice by carcinogen treatment, female mice were treated with MNU and DMBA, which are already promoted with MPA. This combination treatment increased lethality in both mice groups with a faster survival reduction in GABARAP KO mice ($p = 0.002$) than wild-type mice (Fig. 14 D). No tumor formation was observed in both animal groups after this combination of treatment.

In all carcinogen treatment models, deaths were scored when mice were euthanized because of tumors or illness, or were found dead. In our models of carcinogen treatments, almost all GABARAP KO mice were dead without any tumor formation. Finally, GABARAP KO mice have demonstrated higher sensitivity to reduce the survival and tumors incidence than wild-type mice groups after exposure to different carcinogens and treatment regimens.

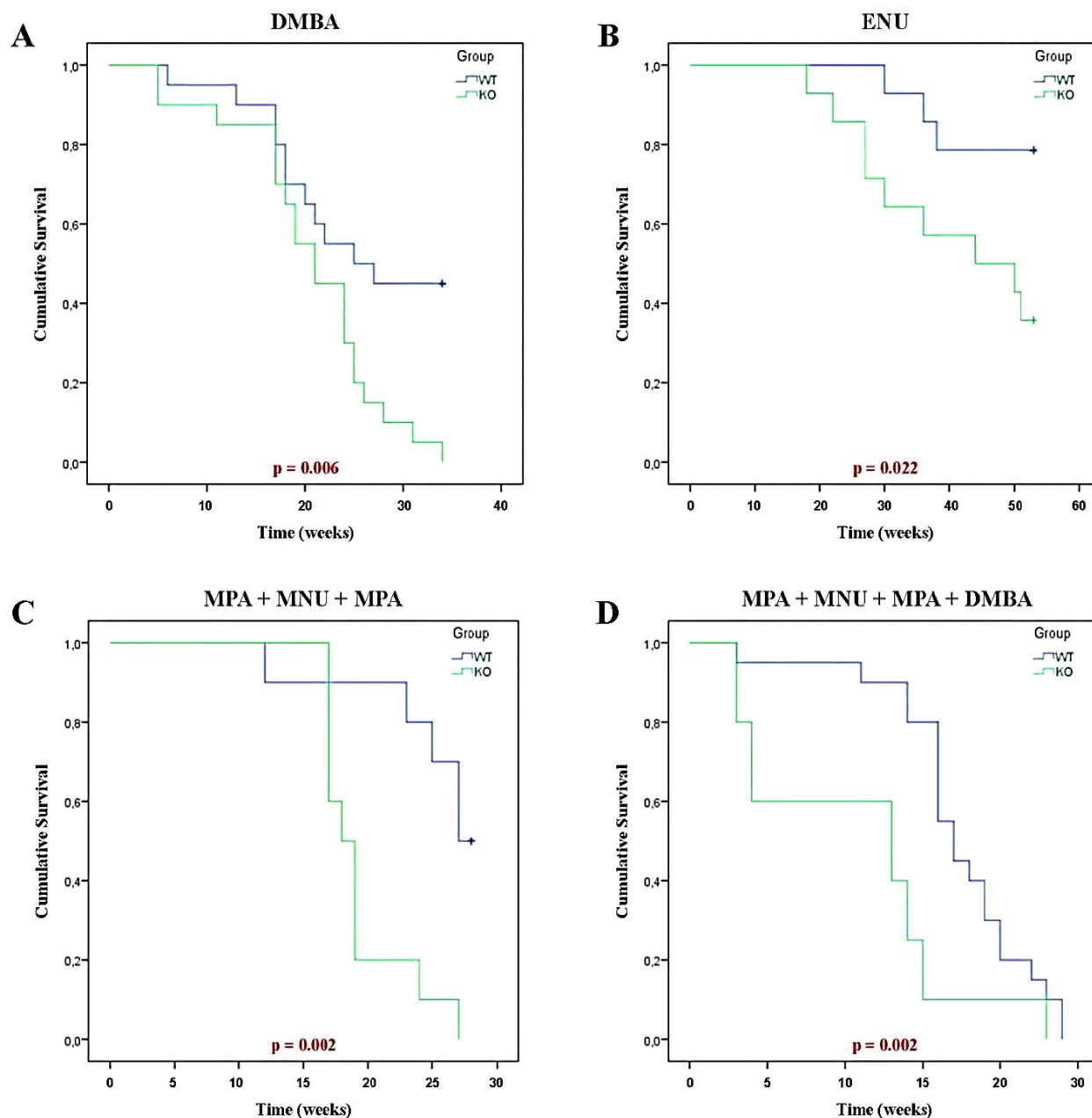


Figure 14. Kaplan-Meier survival plots of GABARAP knockout (KO) and wild-type (Wt) mice after treatment with different carcinogen regimens. (A) DMBA – 6 consecutive weeks of 1 mg/mouse by oral gavage, $n = 20$ mice per group. (B) ENU – single i.p. injection of 150 mg/kg of body weight, $n = 14$ mice per group. (C) MPA 40 mg i.m. + MNU 1 mg i.p. + MPA 20 mg i.m., $n = 10$ mice per group. (D) MPA 20 mg i.m. + MNU 1 mg i.p. + MPA 20 mg i.m. + DMBA 1 mg orally, $n = 20$ mice per group. Deaths were scored when mice were euthanized because of tumors or illness, or were found dead. Almost all GABARAP KO mice were dead without any tumor incidence in all models of carcinogen treatments. P values indicated in each figure.

3.3 High sensitivity of GABARAP KO mice to immunotoxicity of DMBA

During the time of experiments, we noticed that the control GABARAP KO mice groups were phenotypically indistinguishable from wild-type mice and showed no detectable changes in gross anatomy, as reported by O'Sullivan (O'Sullivan *et al.*, 2005). DMBA induced tumors in our mice models with significant tumor and survival reduction in GABARAP KO mice. For this reasons, we wanted to investigate the impact of GABARAP deficiency on the organs cellularity and functions after DMBA treatment. Body weights were monitored at different intervals time starting from the day before DMBA treatment. We noticed that the mean body weights of GABARAP KO mice after 6 weekly oral doses of 1 mg DMBA/mouse were noticeably less than wild-type counterpart group (Fig. 15 A). The body weights progressively increased in wild-type mice after DMBA treatment, in contrast there were only small and tardy increments of body weights in the GABARAP KO mice treated with DMBA (Fig. 15 A).

An immunotoxic effect of DMBA treatment, mainly on the spleen, has been reported (Dean *et al.*, 1985; Miyata *et al.*, 2001; Gao *et al.*, 2005, 2007). In order to explore the immunotoxic effect of DMBA in our mice groups, spleen parameters were observed by different means. Interestingly, the GABARAP KO mice showed a highly decrease of spleen volume compared with wild-type mice after treatment with 6 weekly doses of DMBA (Fig. 15 B). Spleen weights of DMBA-treated wild-type mice were decreased to about 40.5% ($\pm 0.7\%$) of control (vehicle-treated) wild-type mice (Fig. 15 B and C). However, substantial decrease was observed in spleen weights of GABARAP KO mice group treated with DMBA, 13.6% ($\pm 1.8\%$) of control (vehicle-treated) GABARAP KO mice (Fig. 15 B and C).

To inspect the changes in the cellularity of spleen components of GABARAP KO and wild-type mice after DMBA treatment, splenocytes were harvested, counted and differentiated. The alterations in total number of spleen cells were concordant with the spleen weights, and this gives indication that the cell death of splenocytes occurs in both groups of GABARAP KO and wild-type mice treated with DMBA. However, a significant decrease was seen in the total number of GABARAP KO splenocytes after treatment with DMBA; 11.6% ($\pm 2.4\%$) of control splenocytes in GABARAP KO mice compared with 44.7% ($\pm 2.8\%$) of control splenocytes in wild-type mice (Fig. 16). These alterations in total number of splenocytes were in agreement with morphological changes in spleen volumes and weights (Fig. 15 B and C), with a more profound decrease of GABARAP KO cells compared to wild-type cells.

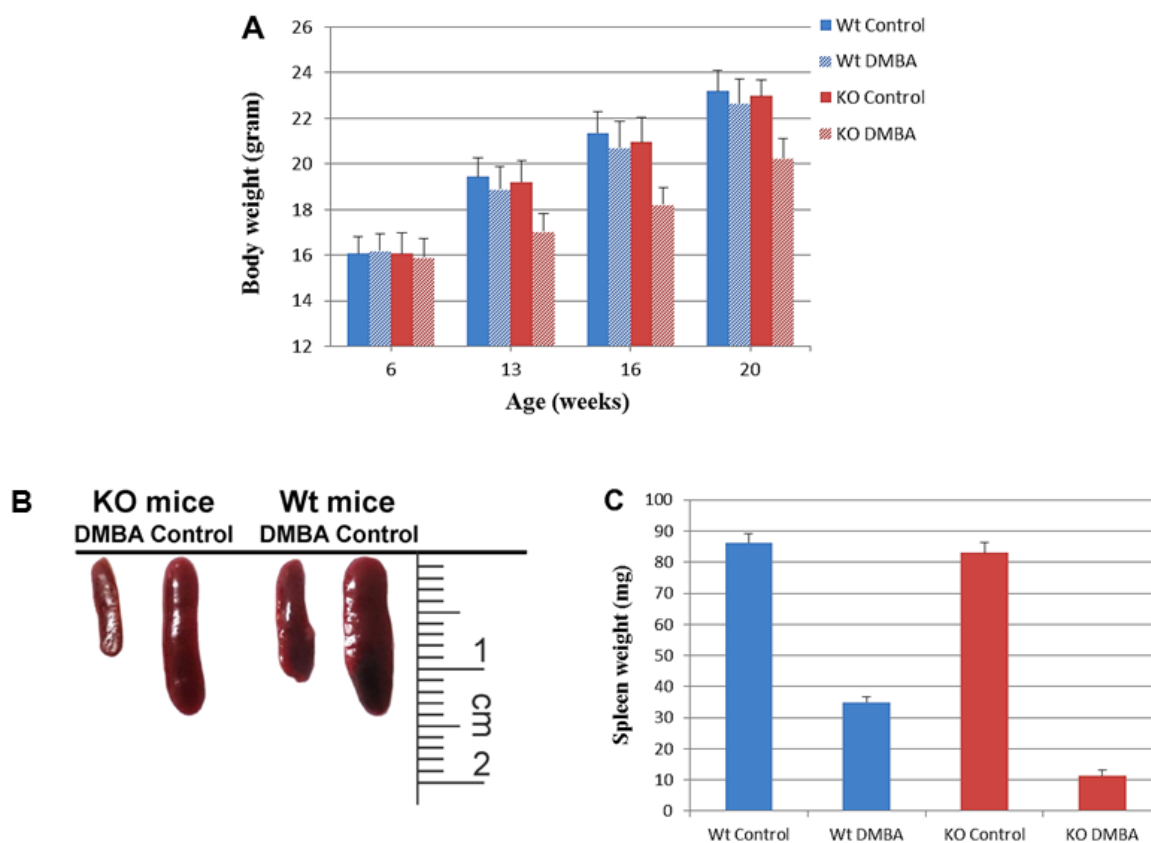


Figure 15. A) Body weights of mice at different intervals time before and after treatment with 6 weekly oral doses of 1 mg DMBA/mouse. Age at 6 weeks represents the day before starting the DMBA treatment. The groups consist of 6 mice per each control (vehicle-treated) group and 16-20 mice for DMBA-treated groups. B) Changes in spleen volume of GABARAP KO (KO) and wild-type (Wt) mice at the same age and treatment condition. C) Spleen weights for mice untreated (control) or treated with DMBA. Data are representative of 7 mice per group. Spleen volumes and weights were measured at 13 weeks of age, i.e. after one week of 6 DMBA doses. All data were shown with means \pm SD.

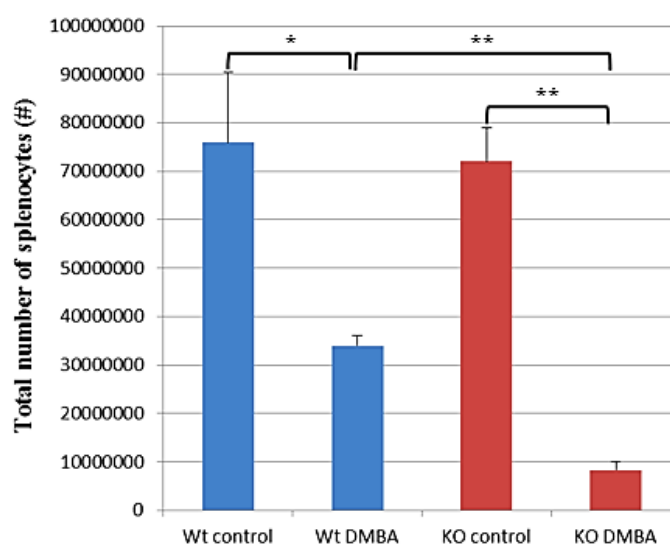


Figure 16. Total number of splenocytes in control (vehicle-treated) and DMBA-treated mice groups. Data are representative of three mice of each group and shown with means \pm SEM. P values shown above each two groups, (*) $p < 0.05$, (**) $p < 0.01$.

Furthermore, the cell surface marker analyses was carried out by using BD™ LSR II flow cytometer to detect the alterations in cellular population of splenocytes after DMBA treatment of GABARAP KO and wild-type mice in comparison with their vehicle control groups. We have detected regulatory T cells (Tregs), B cells, T helper cells (CD4), cytotoxic T cells (CD8), macrophages and neutrophils. The results were compatible with the decrease of total number of splenocytes in both GABARAP KO and wild-type mice (Fig. 17); i.e. GABARAP KO mice showed substantial reduction in populations of splenocytes compared to wild-type mice after DMBA treatment. That means there was no discrimination for the effect of DMBA on particular cell types in both GABARAP KO and wild-type mice.

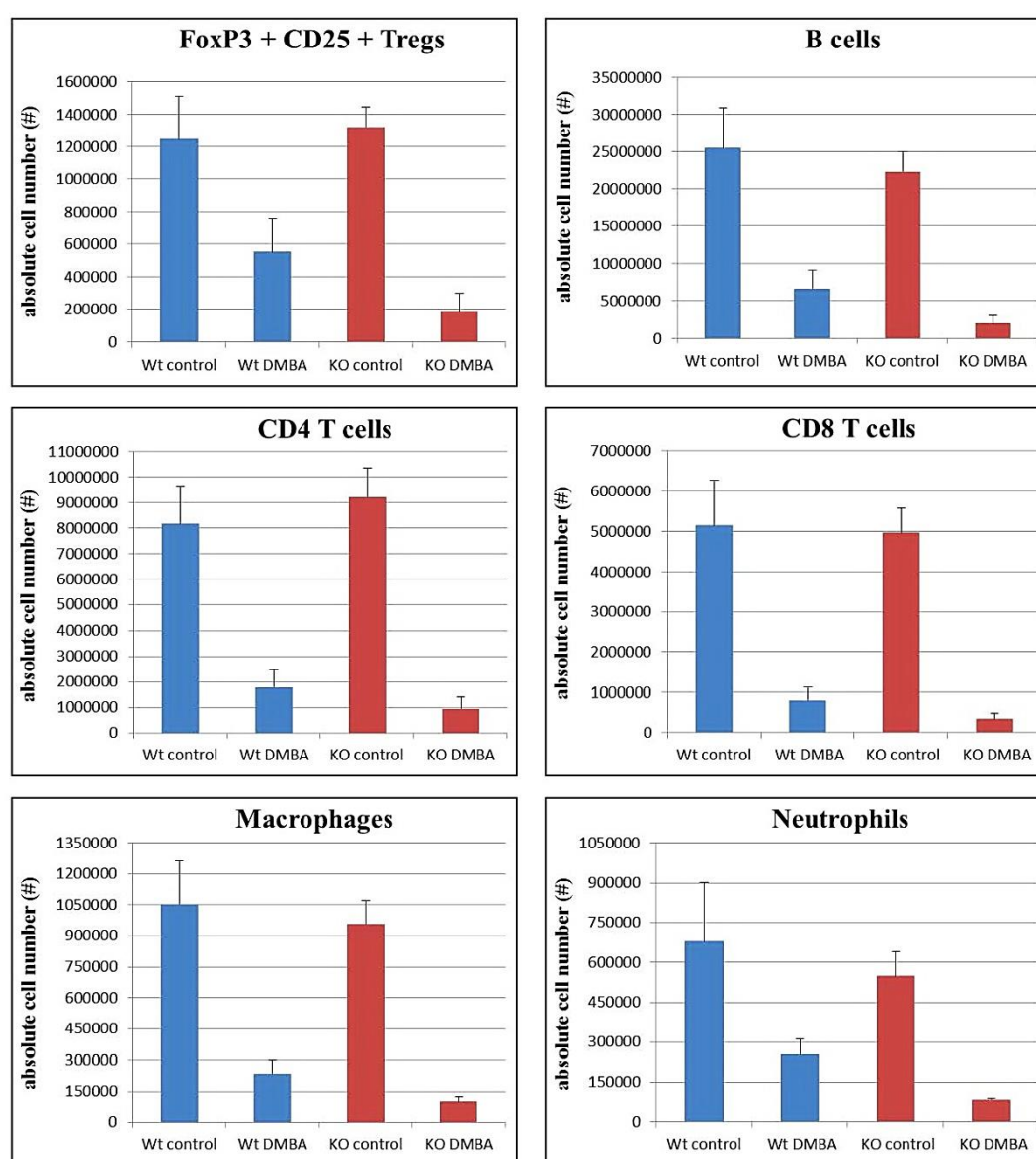


Figure 17. Cell surface markers expression of splenocytes in control (vehicle-treated) and DMBA-treated mice. DMBA treatment was 6 weekly oral doses of 1 mg/mouse. Data are representative of three mice of each group and were shown with means \pm SEM.

These results indicate that the reduced growth of GABARAP KO mice after DMBA treatment was not only due to the effect of DMBA immunotoxicity in the spleen, since wild-type mice showed also reduced spleen weights but their body weights slightly altered after DMBA treatment. This suggests that DMBA treatment in GABARAP-deficient mice may have an impact on other organs in addition to spleen.

3.4 DMBA treatment enhanced cell death in splenocytes of GABARAP KO mice

Our results demonstrated considerable alterations in volumes, weights and total cell numbers in spleens of GABARAP KO mice after DMBA treatment compared with a parallel group of wild-type spleens. In general, it is long believed that autophagy blockade may increase apoptosis in cells when exposed to stress. For these reasons, we have investigated the proliferation and cell death of splenocytes of DMBA-treated and untreated mice. Immunohistochemistry staining was used to detect the expression of Ki-67, a cellular proliferation marker. Female mice have been treated with 6 weekly oral doses of 1 mg DMBA/mouse, and vehicle control groups were given sesame oil orally at the same time points as the DMBA treatment. Splenocytes of both DMBA-treated GABARAP KO and wild-type mice exhibited less Ki-67 expression than their vehicle-treated (sesame oil) groups (Fig. 18 A). Ki-67 expression was obviously decreased at a high level in DMBA-treated GABARAP KO splenocytes compared with DMBA-treated wild-type counterpart (Fig. 18 A).

Moreover, the TUNEL assay was carried out on the spleen sections to detect the apoptotic cells within the spleens. Microscopic examination of TUNEL-stained sections showed an increased number of TUNEL-positive spleen cells after *in vivo* DMBA treatment of both GABARAP KO and wild-type mice (Fig. 18 B). However, the TUNEL-stained sections indicated a substantial increase of TUNEL-positive cells in the spleen tissues of DMBA-treated GABARAP KO mice compared with the DMBA-treated wild-type counterparts (Fig. 18 B).

Our results give an indication that the knockout of GABARAP gene in mice enhanced the incidence of cell death and reduce the proliferation of splenocytes in the DMBA-treated group. Such findings may explain the high reduction of volume, weight and total splenocytes number in GABARAP KO mice after treatment with DMBA by oral gavage.

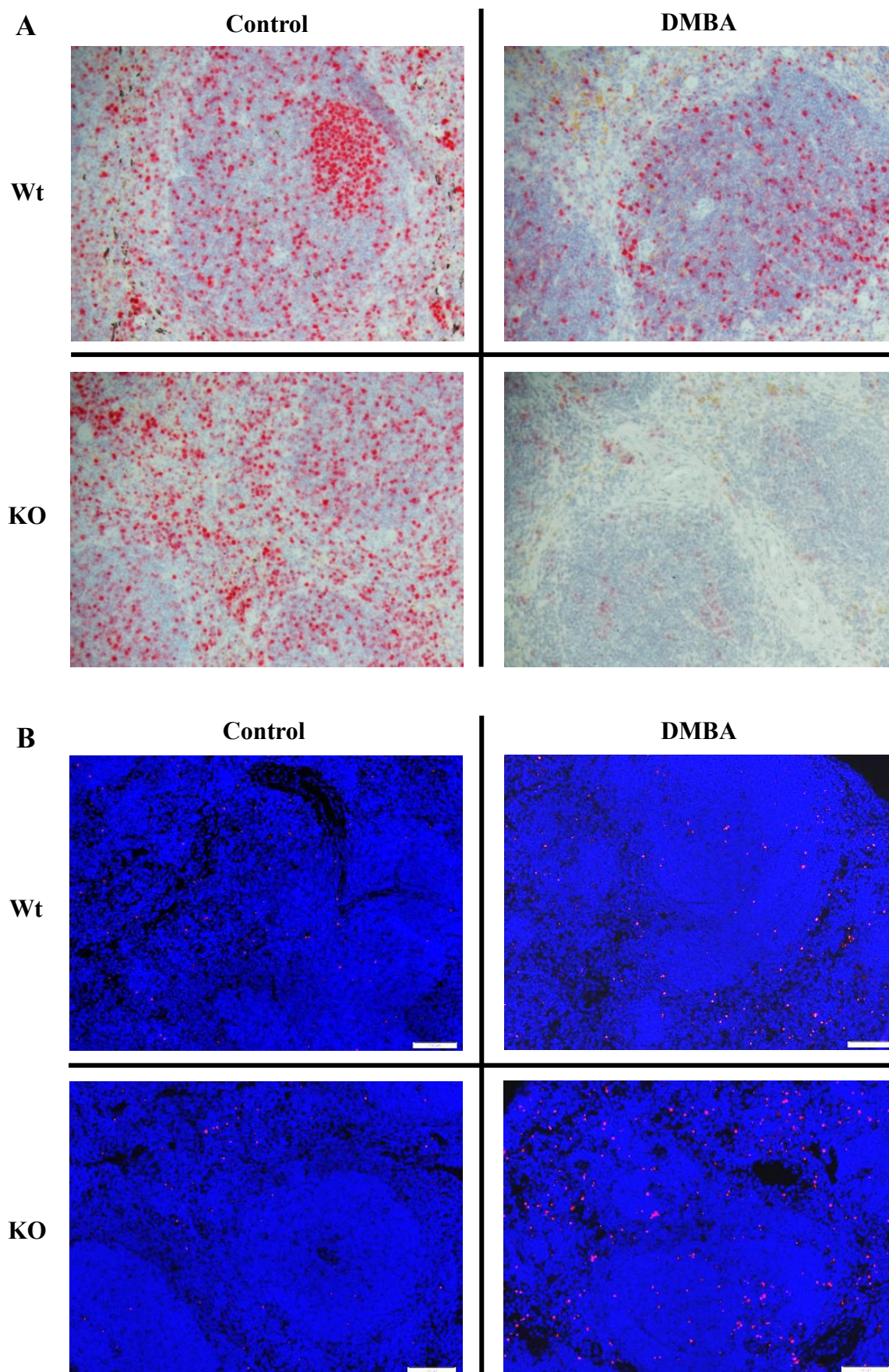


Figure 18. Immunohistochemistry and Immunofluorescence staining for spleen sections of vehicle-treated (control) and DMBA-treated wild-type (Wt) and GABARAP KO (KO) mice. A) Immunohistochemistry staining for Ki-67. Magnifications 20X. B) Immunofluorescence staining/TUNEL assay. Scale bars =100 μm.

3.5 GABARAP-deficient immune cells showed high cytokine secretion

Cytokines secretion can trigger cell signaling toward anti-tumor effects and/or cell death mediated by tissue injury and lethal shock. This capacity of cell signaling relies on a panel of cytokines and the accurate assignment of effector cells. Macrophages and lymphocytes are the major components of the immune system, and both are involved in cytokine secretion as well as effector cells. Many autophagic genes play a role in immunity, and disruption of such genes as LC3B, Atg16l1, Beclin1 and GABARAP increased lethality and IL-1 β expression in sepsis mouse models. For these reasons, we wanted to determine whether GABARAP deficiency upon treatment with DMBA plays role in enhancement of cytokines secretion to a level that may lead to suppress the tumor formation and/or mice death.

Peritoneal macrophages and spleen lymphocytes of GABARAP KO and wild-type mice either treated with sesame oil as vehicle vector (control group) or treated with DMBA were isolated, cultured and stimulated. Lipopolysaccharide (LPS), a component of the outer membrane of Gram-negative bacteria, were used to elicit an immune response by interacting with the macrophage membrane receptor CD14 to induce the generation of cytokines such as IL-1 β , IL-6 and TNF α (Akira *et al.*, 1993; Tracey and Cerami, 1994; Kielian and Blecha, 1995; Meng and Lowell, 1997). Moreover, LPS-primed macrophages treated with adenosine triphosphate (ATP) are an established model for NLRP3 inflammasome-mediated IL-1 β production *in vitro* by stimulation the cleavage of caspase 1 (Saitoh *et al.*, 2008; Nakahira *et al.*, 2011; Zhang *et al.*, 2013). Isolated peritoneal macrophages from vehicle control or DMBA-treated GABARAP KO and wild-type mice were stimulated by treatment with LPS for 4 h or pretreated with LPS for 4 h followed by stimulation with ATP for 1 h. The levels of IL-1 β , IL-6 and TNF α in the medium of cultured macrophages were measured by ELISA. In vehicle control groups, IL-1 β was highly produced after LPS and ATP stimulation in both GABARAP-deficient and wild-type macrophages compared to the macrophages stimulated with LPS alone (Fig. 19 A). GABARAP-deficient macrophages; from mice treated *in vivo* with 6 weekly doses of 1 mg DMBA and stimulated *in vitro* with LPS, generated a significant higher IL-1 β levels than wild-type macrophages (Fig. 19 A). In addition, the level of IL-1 β production was increased in macrophages of both DMBA-treated GABARAP KO and wild-type mice after stimulations with LPS and ATP compared to stimulation with LPS alone (Fig. 19 A). However, the production of IL-1 β was significantly higher in macrophages of DMBA-treated GABARAP KO mice after stimulation with LPS and ATP compared to wild-type counterpart macrophages (Fig. 19 A). Similar results were obtained with IL-6; except that IL-6 secretion was increased in the similar pattern after both stimulations; LPS

alone or LPS and ATP, for macrophages of DMBA-treated groups (Fig. 19 B). Likewise, the production of TNF α in macrophages of vehicle-treated and DMBA-treated GABARAP KO mice was slightly higher in both stimulations compared with wild-type macrophages (Fig. 19 C).

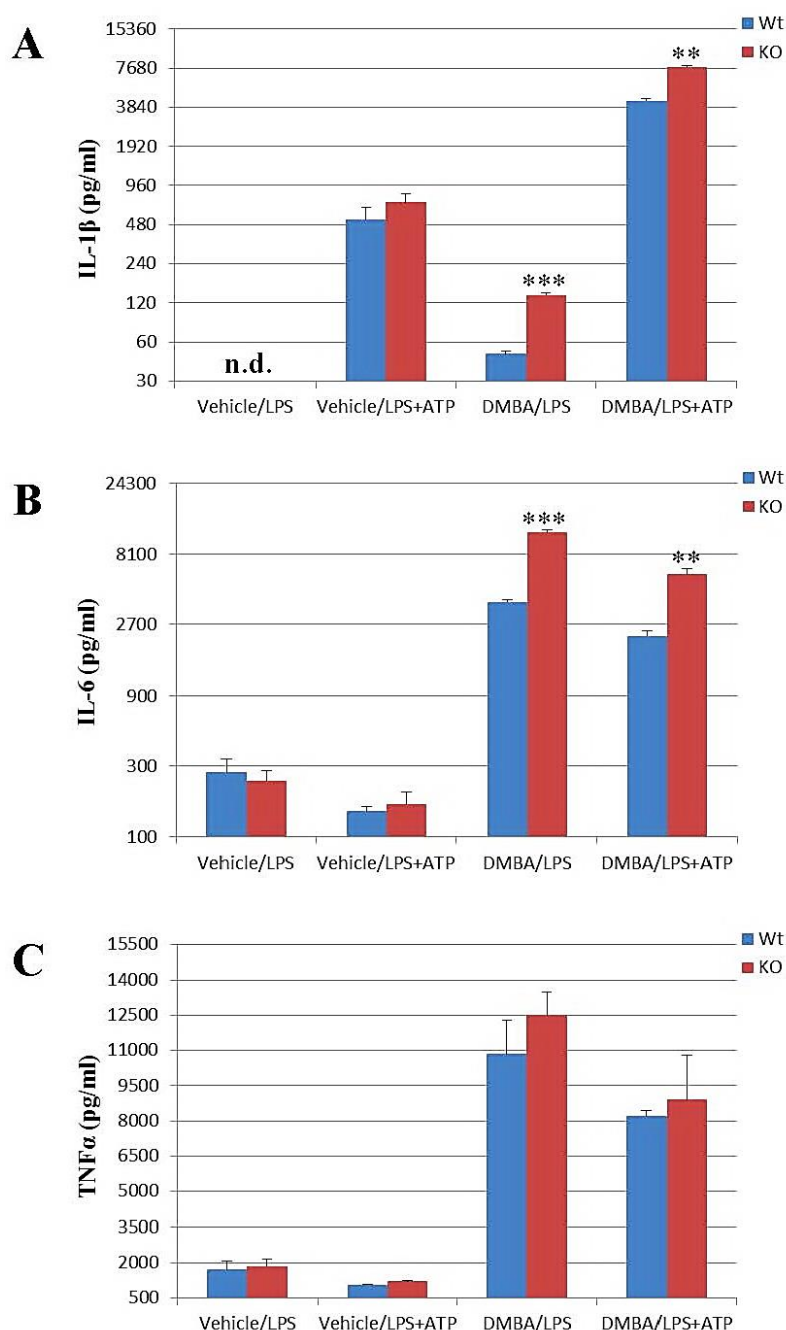


Figure 19. Cytokine secretion from peritoneal macrophages of GABARAP KO (KO) and wild-type (Wt) mice treated with 6 weekly oral doses of sesame oil (vehicle) or 1 mg DMBA/mouse. Macrophages of each group were stimulated with LPS for 4 h or priming 4 h with LPS followed by stimulation with ATP for 1 h (LPS+ATP). A) IL-1 β , B) IL-6 and C) TNF α were measured in the supernatants by ELISA. Data are representative of triplicate experiments and were shown with means \pm SEM. (**) $p < 0.01$; (***) $p = 0.001$; n.d., not detected.

These results could give an indication for sensitivity of GABARAP KO mice after DMBA treatment and could explain the increased lethality in these mice after carcinogen treatment. In addition, IL-1 β has contradictory roles in tumor growth; some studies have shown stimulatory effect on the growth of tumor cells, whereas others have shown that it exerts inhibitory activity. These contradictory effects are controlled by the level of IL-1 β . High concentrations of IL-1 β induced cellular apoptosis, whereas moderate or low levels of IL-1 β in the same cells kept the cell normal or stimulated the cell growth (Roy *et al.*, 2006).

Moreover, isolated lymphocytes from the spleen of vehicle control or DMBA-treated mice were investigated for cytokines secretion. DMBA-treated mice had been reported to be persistently immunosuppressed after treatment, mainly through IL-2 suppression (House *et al.*, 1987; Thurmond *et al.*, 1987, 1988; Burchiel *et al.*, 1990; Saas *et al.*, 1996; Gao *et al.*, 2008). Therefore, lymphocytes were cultured in 6 well plates coated with CD3 to generate an activation signal to T-lymphocytes through association of CD3 with the T-cell receptor (TCR). The stimulation period with CD3 lasted for 48 h, and then the cytokine secretion was measured in the medium of cultured lymphocytes by ELISA. Vehicle control groups showed slightly increased levels of IL-2 in GABARAP-deficient lymphocytes after CD3 stimulation compared with wild-type counterparts (Fig. 20 A). As expected, IL-2 was suppressed in lymphocytes of DMBA-treated wild-type mice after CD3 stimulation compared with CD3-stimulated lymphocytes of vehicle-treated wild-type mice (Fig. 20 A). Surprisingly, GABARAP-deficient lymphocytes of DMBA-treated mice produced more IL-2 after CD3 stimulation than lymphocytes of vehicle-treated GABARAP KO mice (Fig. 20 A). This result indicates that DMBA does not induce suppression of IL-2 production in GABARAP-deficient lymphocytes, in contrast to the normal consequence of DMBA-treated mice which manifested by disruption of T-helper cell function specifically by inhibition of IL-2 production. Likewise, IFN- γ showed similar predisposition of IL-2 after CD3 stimulation of lymphocytes from vehicle-treated and DMBA-treated mice (Fig. 20 B). Stimulated lymphocytes of DMBA-treated GABARAP KO mice showed an increased production of IFN- γ compared either with stimulated lymphocytes of vehicle-treated GABARAP KO or wild-type counterparts. Moreover, the opposite tendency of IFN- γ production was evident between the lymphocytes groups; i.e. less IFN- γ production by stimulated lymphocytes of DMBA-treated wild-type mice than their vehicle-treated wild-type counterparts, and a contrary trend in case of GABARAP-deficient lymphocytes (Fig. 20 B).

It is well known that IFN- γ serves to limit the IL-17-producing T cell population. We measured the IL-17 production from lymphocytes, and we found an antagonist effect between

IL-17 and IFN- γ after stimulation of lymphocytes from DMBA-treated groups; i.e. increased level of IFN- γ led to diminished levels of IL-17 generated by lymphocytes and vice versa (Fig. 20 C).

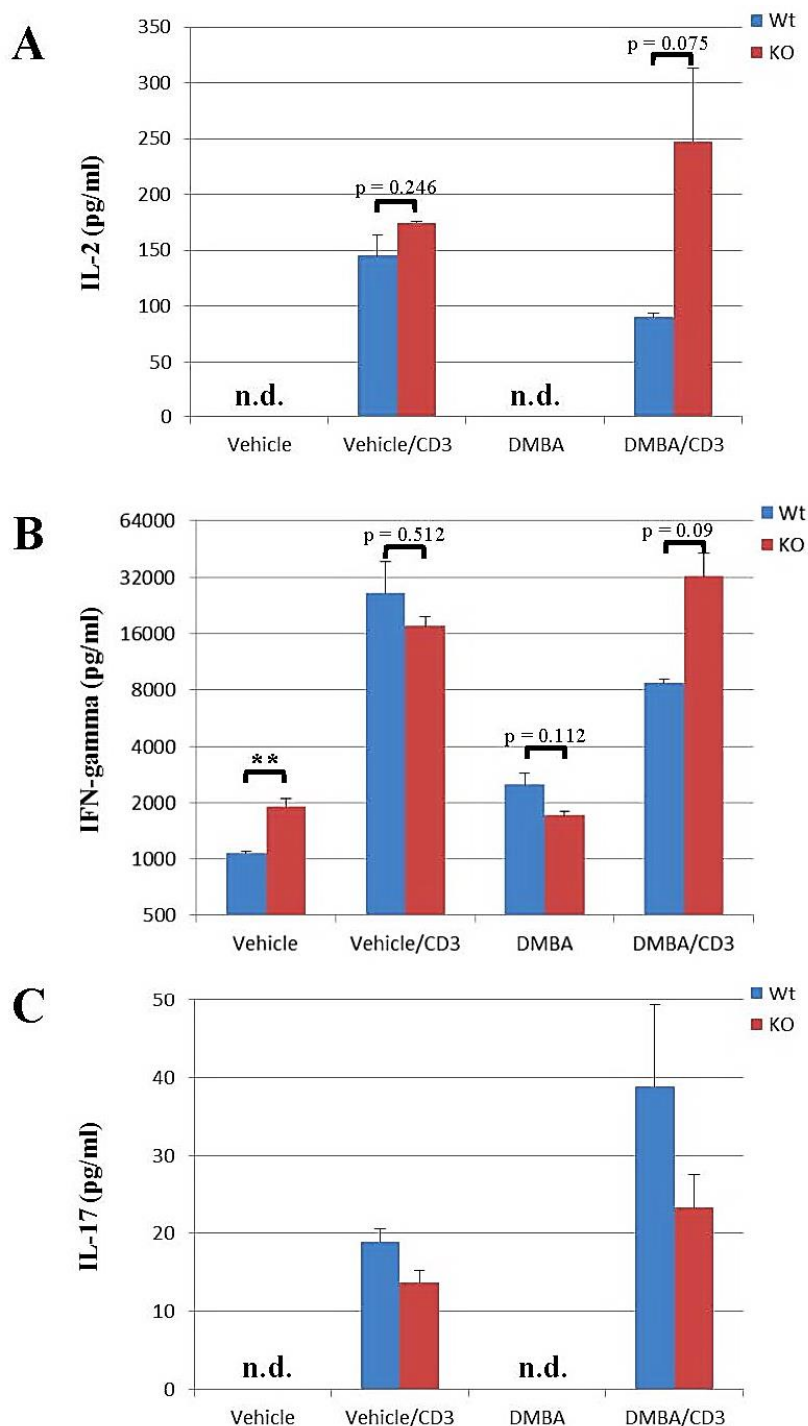


Figure 20. Cytokines secretion from Lymphocytes of GABARAP KO (KO) and wild-type (Wt) mice treated with sesame oil (vehicle) or DMBA. Lymphocytes of each group were stimulated with CD3 for 48 h. A) IL-2, B) IFN- γ and C) IL-17 were measured in the supernatants by ELISA. Data are representative of triplicate experiments and were shown with means \pm SEM. (**) $p < 0.01$. n.d., not detected.

Altogether, these results elucidated that the knockout of GABARAP gene has considerable impact on the immunity of mice through enhancing the secretion of regulatory cytokines, for instance IL-1 β and IL-2. Some of these cytokines, especially IL-2 and IFN- γ , have reliable anti-tumor effects and may explain why GABARAP KO mice developed less tumor formation than wild-type mice after DMBA treatment.

3.6 GABARAP deficiency reduced the growth of mammary glands after DMBA treatment

Our *in vivo* results proved that female GABARAP KO mice did not develop any mammary tumors during the time of experiments whether treated with DMBA or not. DMBA is highly carcinogenic when administered to adult female mice by oral gavage and especially relevant to the study mouse mammary gland tumorigenesis (Ethier and Ullrich, 1982; Medina, 1996; Currier *et al.*, 2005; Klos *et al.*, 2012). For this reason, we explored the mammary epithelial cell growth and ductal trees morphogenesis in our experimental mice groups to evaluate the gland architecture, proliferation and cell death by means of mammary gland whole mount morphology analysis and immunostaining. Female mice were treated with 1 mg doses of DMBA or 200 μ l sesame oil (as vehicle control) for 6 consecutive weeks by oral gavage beginning at 6 - 8 weeks of age.

The abdominal mammary glands of female GABARAP KO and wild-type mice at 14 weeks of age showed normal mammogenesis and there are no obvious phenotypic consequences of GABARAP deficiency on mammary epithelial cell growth at this age (Fig. 21 A). Furthermore, the mammary glands of female wild-type mice treated with 6 weekly doses of 1 mg DMBA/mouse showed a phenotypically normal mammary epithelial trees compared with their age-matched (14 weeks old) control wild-type group (Fig. 21 A). Interestingly, GABARAP deficiency had a significant impact on the mammary epithelial cell growth and ductal branching of female mice after treatment with 6 weekly doses of 1 mg DMBA/mouse. The mammary glands of DMBA-treated female GABARAP KO mice showed a significant reduction of epithelial cell outgrowth and ductal branching compared either with their age matched control GABARAP KO mice or DMBA-treated wild-type mice (Fig. 21 A). Moreover, analysis of mammary gland whole mount morphology was performed by measuring the distance of epithelial growth from the lymph node to the end of epithelial tree by using a ruler, according to de Assis *et al.* (2010). The distances of mammary epithelial growth in DMBA-treated female GABARAP KO mice were significant shorter than their age-matched control GABARAP KO mice or DMBA-treated wild-type mice (Fig. 21 B).

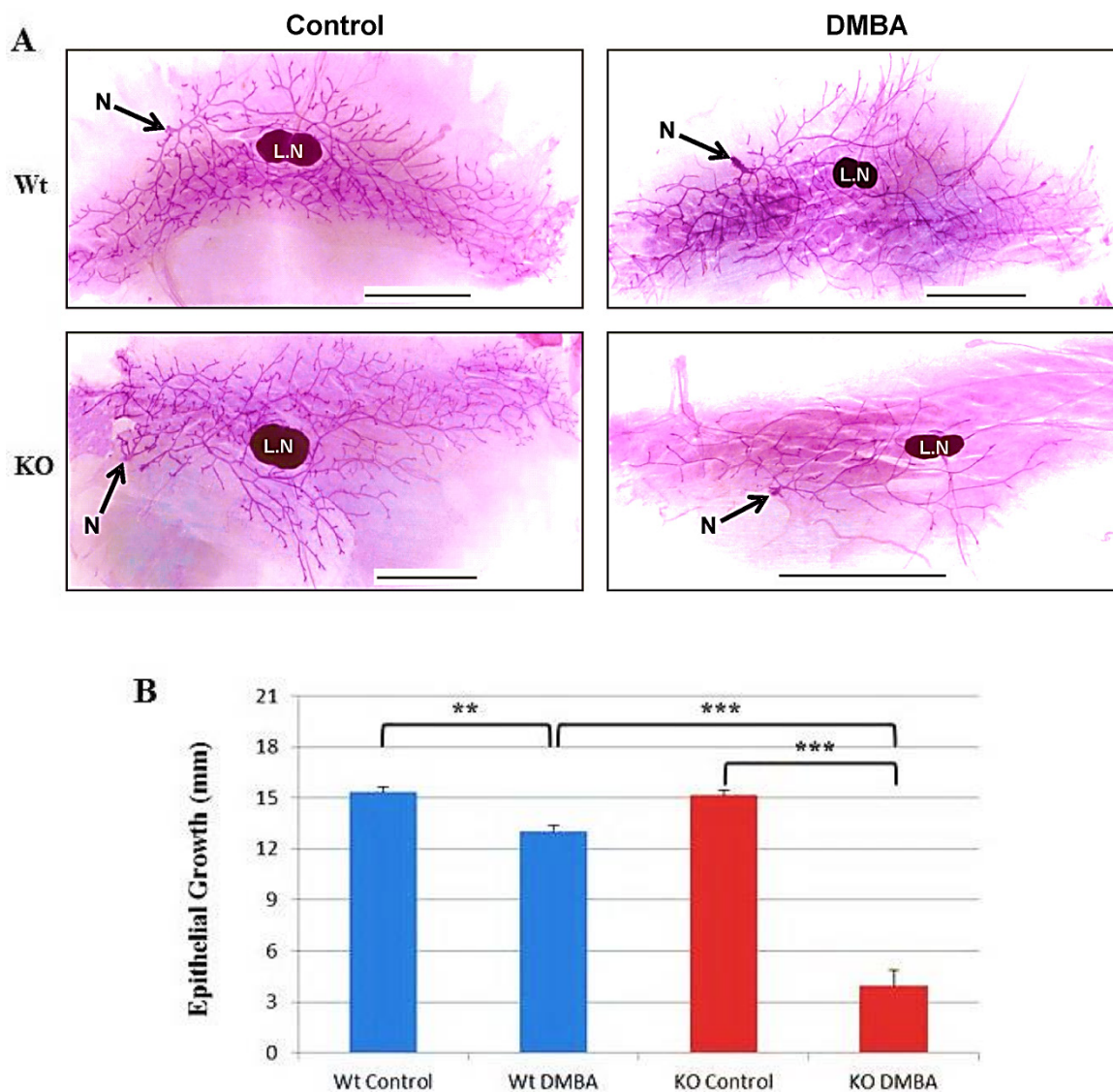


Figure 21. *A) Whole mount analysis of mammary glands from wild-type (Wt) and GABARAP KO (KO) female mice, vehicle-treated (Control) or DMBA-treated. The female mice were either treated with 6 weekly oral doses of 1 mg DMBA/mouse or given sesame oil (vehicle) at the same time of DMBA treatment. L.N = lymph node, N = nipple; scale bars = 5 mm. B) Mammary epithelial growth of female mice treated as described in A. The epithelial growth was determined by measuring the distance from the lymph node to the end of epithelial tree (in millimetres = mm), using a ruler. Values are representative of 6 - 9 mice and were shown with means \pm SEM. (**) $p < 0.01$; (***) $p = 0$.*

Furthermore, immunostaining for mammary gland sections were done by using Ki-67 and TUNEL assay. Similarly to the spleen, mammary glands of DMBA-treated GABARAP KO female mice revealed higher reduction in proliferation by decreased Ki-67 expression compared to mammary glands of vehicle-treated (control) GABARAP KO or DMBA-treated wild-type groups (Fig. 22 A). DMBA-treated wild-type mice showed a slight inhibition of Ki-67 expression in mammary glands compared with their control wild-type counterparts. Moreover, TUNEL staining of mammary gland sections from DMBA-treated GABARAP KO

mice showed an increasing number of TUNEL-positive cells compared with other groups (Fig. 22 B). Altogether, our results showed that cellular deaths were highly elevated in GABARAP KO mice when exposed to genotoxic carcinogen (DMBA) and this may explain the inhibition of tumor formation and the increased lethality of mice after DMBA treatment.

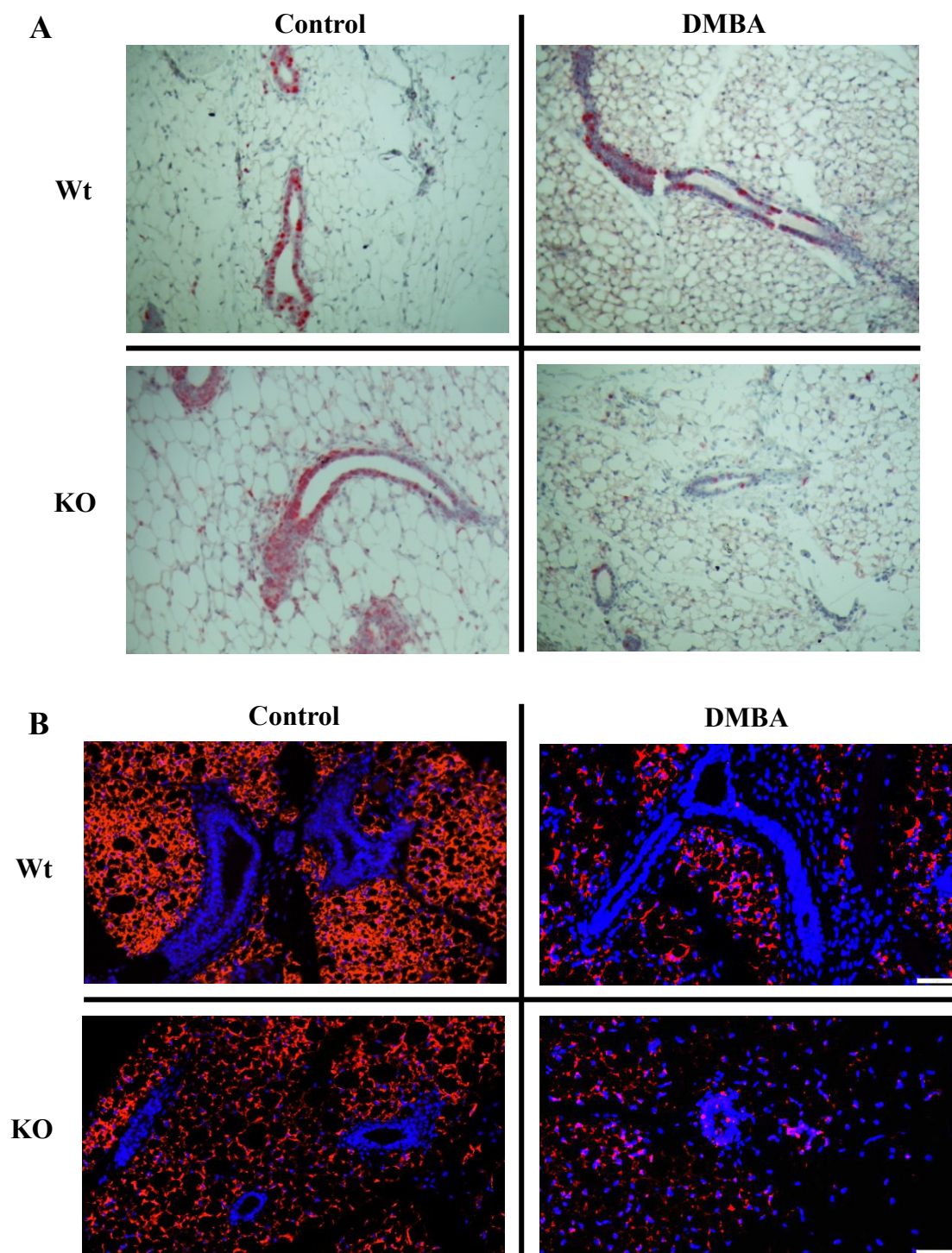


Figure 22. Immunohistochemistry and Immunofluorescence staining for mammary gland sections of vehicle-treated (control) and DMBA-treated wild-type (Wt) and GABARAP KO (KO) mice. A) Immunohistochemistry staining for Ki-67. Magnifications 20X. B) Immunofluorescence staining/TUNEL assay. Scale bars = 50 μ m. Arrows indicate the epithelial cells.

3.7 Gene expression profiling indicated differential expression of tumor suppressor gene *Xafl* in mammary glands of GABARAP KO mice

To further investigate the molecular mechanism by which GABARAP deficiency reduced tumor formation, spontaneously or after genotoxic carcinogen (DMBA) treatment, the workflow of Agilent Whole Mouse Genome expression analysis by microarray gene expression detection was employed. GABARAP KO and wild-type mice were either treated with sesame oil as vehicle (control group) or with 6 weekly oral doses of 1 mg DMBA/mouse beginning at 6 -8 weeks of age. The RNAs from abdominal mammary glands of each group were isolated and hybridized with one-color oligo microarrays 8x60K chips. The data was computed to identify genes that had a significant modification in the expression level in both control and DMBA-treated groups of GABARAP KO and wild-type mammary glands. Four comparisons were generated between control wild-type (CWT), control GABARAP KO (CKO), DMBA-treated wild-type (DWT) and DMBA-treated GABARAP KO (DKO) groups. Next, a subset of genes that had GABARAP-dependent altered expression compared to CWT and DWT was derived from this data, and a selected list of the most differentially expressed genes is represented in a heat map (Fig. 23). In Figure 23, the heat map showed GABARAP gene expression as well as 50 other genes which are exclusively modulated upon GABARAP knockdown. GABARAP expression was shown also in a boxplot (Fig. 24 A). The biological functions for some genes listed in Figure 23 are so far unknown. For instance, five Mup (major urinary protein) family proteins were differentially downregulated in mammary glands of GABARAP KO mice. Mups belong to a larger family of proteins known as lipocalins. The precise role of these genes is not yet clarified, but some authors propose that Mups have beneficial effects on energy metabolism by enhancing mitochondrial function, and also may act as a regulator for glucose and lipid metabolism in mice (Hui *et al.*, 2009; Zhou *et al.*, 2009). Moreover, Rab4a (Ras-related protein), has shown to be upregulated in GABARAP KO mammary glands compared to wild-type counterparts. Rab proteins constitute the largest subfamily of the Ras family of small GTPases and are involved in the regulation of vesicular transport. The encoded protein of this gene is associated with early endosomes and plays a role in regulating the recycling of receptors from endosomes to the plasma membrane (Olkkonen and Stenmark, 1997; Yudowski *et al.*, 2009). Interestingly, tripartite motif-containing protein 16 (Trim16) has been significantly downregulated in GABARAP KO groups (control and DMBA-treated) compared to their wild-type counterparts (Fig. 23 and 24 B). Trim16 is a ubiquitously expressed protein and was identified as an estrogen and anti-estrogen regulated gene in epithelial cells stably expressing estrogen receptor. TRIM proteins

have been reported to have important roles in cell growth, differentiation, ubiquitination, retroviral immunity and cancer (Cao *et al.*, 1998; Beer *et al.*, 2002; Meroni and Diez-Roux, 2005; Marshall *et al.*, 2010; Liu *et al.*, 2014).

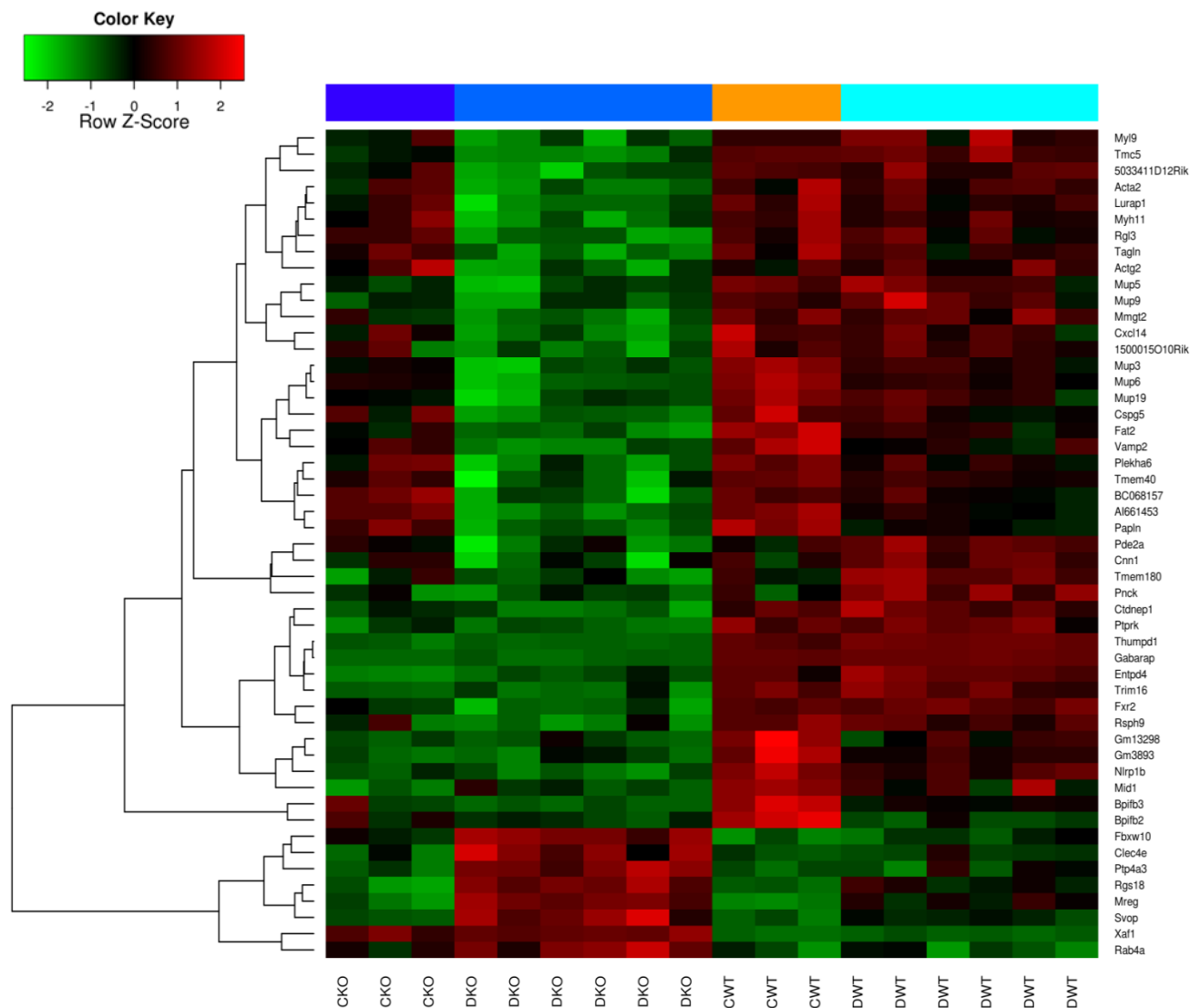


Figure 23. Heatmap of differentially expressed genes in mammary glands of GABARAP KO and wild-type mice. The comparison of control wild-type (CWT) and DMBA-treated wild-type (DWT) with their untreated (CKO) and treated (DKO) GABARAP KO counterparts identified 50 most distinct genes. The control groups included 3 replicates, whereas DMBA-treated groups included 6 replicates.

In our attempt to identify candidate genes related to GABARAP deficiency and interpret our phenotypic results, we found that the knockout of GABARAP resulted in highly and differentially expression of Xiap-associated factor 1 (Xaf1) gene (Fig. 23). Published evidence indicated that Xaf1 functions as a tumor suppressor, and the epigenetic silencing of Xaf1 by aberrant promoter methylation was associated with cancer development and progression (Fong *et al.*, 2000; Byun *et al.*, 2003; Lee *et al.*, 2006; Tu *et al.*, 2009; Huang

et al., 2010; Tu *et al.*, 2010; Sun *et al.*, 2011). GABARAP-deficient mammary glands of control and DMBA-treated mice showed significantly high expression levels of Xaf1 compared with wild-type counterparts (Fig. 23, 24 C and Table 3). Xaf1 was originally identified as a novel negative regulator of X chromosome-linked inhibitor of apoptosis protein (Xiap) (Liston *et al.*, 2001). Xiap is the most potent member of the family of mammalian inhibitor of apoptotic proteins (IAP), and functions through binding to tumor necrosis factor (TNF) receptor-associated factors and caspase family and thereby inhibits apoptosis. Interestingly, Xiap showed a significant upregulation in mammary glands of wild-type mice upon DMBA treatment, whereas mammary glands of DMBA-treated GABARAP KO mice exhibited only modest changes in Xiap expression levels compared to their vehicle control group (Table 3). These finding indicated that Xaf1 upregulation in mammary glands of GABARAP KO mice may contribute to the inhibition of tumor formation and may enhance apoptosis induction upon DMBA treatment.

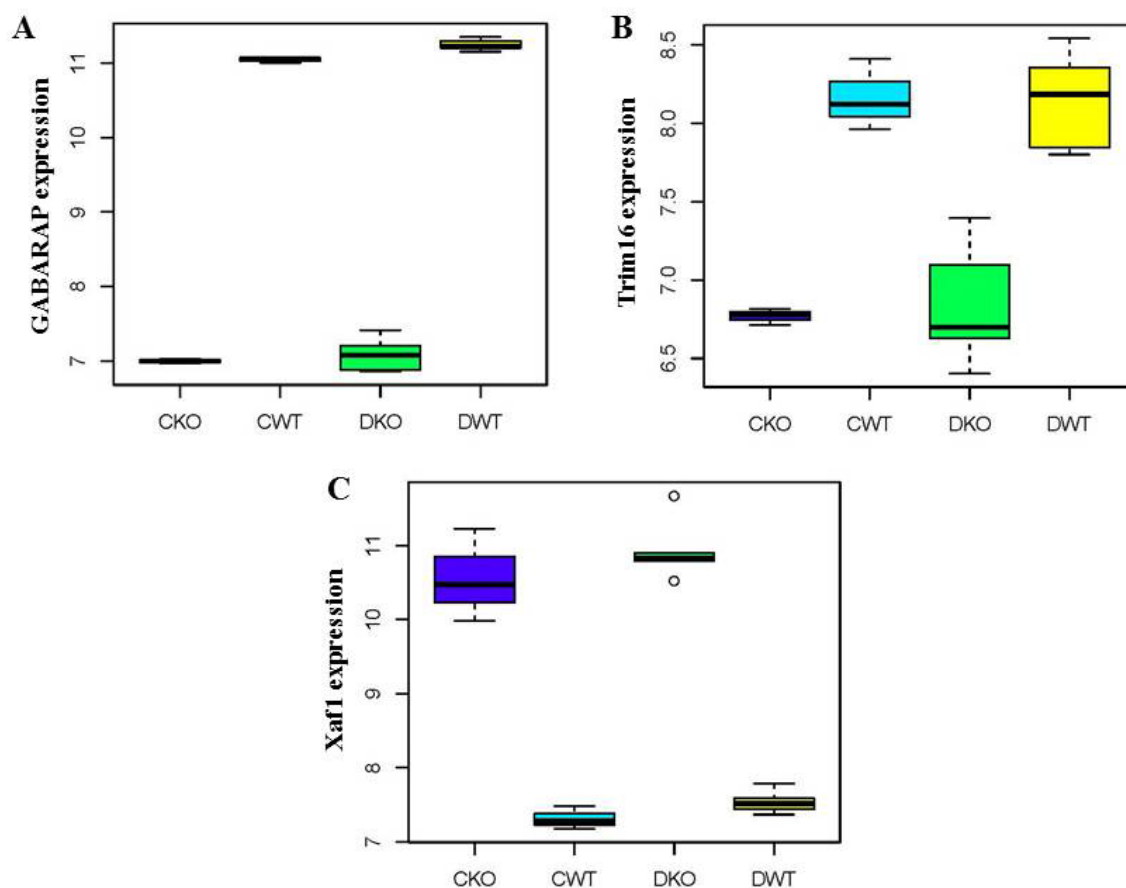


Figure 24. Boxplots of differentially expressed genes in mammary glands of GABARAP KO and wild-type mice. A) GABARAP. B) Trim16. C) Xaf1. Gene expression represents logarithmic fold change in each group. CKO = control (vehicle-treated) GABARAP KO, CWT = control (vehicle-treated) wild-type, DKO = DMBA-treated GABARAP KO, DWT = DMBA-treated wild-type.

Moreover, there are dramatic changes in the genes expression levels when DMBA-treated groups were compared to control (vehicle-treated) groups. The genes listed in Table 3 have been selected according to the phenotypic changes that have been observed in mammary glands (Fig. 21). Most of these genes are involved in apoptosis, cell death, cell cycle control, DNA replication and autophagy, as indicated in the Table 3. Interestingly, GABARAP deficiency boosted the incidence of cell death and cell cycle arrest in mammary glands. The global gene expression profiling of mammary glands of control groups in comparison with DMBA-treated groups, resulted in the identification of a significantly higher expression of pro-apoptotic proteins (Bid, Apaf1 and Bax), tumor necrosis factor receptor superfamily (Tnfrsf10b) and receptor (TNFRSF)-interacting serine-threonine kinase 1 (Ripk1) in mammary glands of DMBA-treated GABARAP KO mice (Table 3). Furthermore, GABARAP-deficient mammary glands of DMBA-treated mice showed a high expression level of cyclin-dependent kinase inhibitor p21 (Cdkn1a) and p18 (Cdkn2c) compared to their control groups (Table 3). In addition, the mammary glands of DMBA-treated wild-type mice exhibited also high expression level of Bax and p21 (Table 3), and this may be due to the genotoxic effect of DMBA; however, there was no massive impact on the epithelial growth of wild-type mammary glands compared with GABARAP KO counterparts (Fig. 21). In contrast, we have found that Cdc7 and Cdk1, essential proteins for G1/S and G2/M phase transitions of eukaryotic cell cycle, were significantly higher expressed in mammary glands of DMBA-treated wild-type mice compared to their control counterparts. Likewise, Siva1, an apoptotic inducer protein (Prasad *et al.*, 1997; Xue *et al.*, 2002; Chu *et al.*, 2005; Du *et al.*, 2009; Resch *et al.*, 2009), was significantly upregulated in mammary glands of DMBA-treated GABARAP KO and wild-type mice. Overexpression of Siva1 had been detected to inhibit stathmin (Stmn), an important regulatory protein of microtubule dynamics, leading to suppression of epithelial-mesenchymal transition (EMT) and metastasis (Li *et al.*, 2011). Interestingly, mammary glands of treated GABARAP KO mice showed downregulated expression levels of Stmn4, in parallel with high expression of Siva1 (Table 3).

There are other genes listed in Table 3 that showed differential expression levels, for instance genes involved in DNA replication or transcriptional factors as well as autophagic genes. For example, NF- κ B1 and E2F were significantly upregulated in the mammary glands of DMBA-treated wild-type mice (Table 3). NF- κ B1 had been reported to play a role in mammary tumorigenesis. The E2F family of transcription factors plays a crucial role in the control of the cell cycle and the action of tumor suppressor genes like pRB (retinoblastoma protein).

Table 3. List of differentially expressed genes in mammary gland of GABARAP KO and wild-type mice with known functions

Gene	Full name	CWT vs CKO	CWT vs DWT	CKO vs DKO	DWT vs DKO	Function
GABARAP	gamma-aminobutyric acid receptor associated protein	-4.05*	0.2	0.09	-4.16*	autophagy
Xaf1	XIAP associated factor 1	3.25*	0.22	0.36	3.39*	apoptosis
Xiap	X-linked inhibitor of apoptosis	0.51	0.86*	0.05	-0.31	apoptosis
Bid	BH3 interacting domain death agonist	0.16	0.53	0.76*	0.39	apoptosis
Apaf1	apoptotic peptidase activating factor 1	-0.33	0.08	0.59*	0.18	apoptosis
Bax	BCL2-associated X protein	0.03	1.79*	2.03*	0.27	apoptosis
Tnfrsf10b	tumor necrosis factor receptor superfamily, member 10b	-0.02	0.62	0.89*	0.25	cell death
Ripk1	receptor (TNFRSF)-interacting serine-threonine kinase 1	0.24	0.29	0.53*	0.48	cell death
Siva1	apoptosis-inducing factor	0.08	1.3*	1.79*	0.57	apoptosis
Stmn4	stathmin-like 4	-0.01	-0.51	-1.14*	-0.65	microtubule destabilizer
Il1r1	interleukin 1 receptor, type I	-0.41	0.08	0.95*	0.45	cytokine receptor
Cdkn1a	cyclin-dependent kinase inhibitor 1A (P21)	-0.1	3.08*	3.73*	0.55	cell cycle control
Cdkn2c	cyclin-dependent kinase inhibitor 2C (p18)	-0.16	0.58	0.86*	0.12	cell cycle control
Rbx1	ring-box 1	0.17	0.49*	0.3	-0.02	cell cycle control
Cdc7	cell division cycle 7	0.29	0.5*	0.23	0.02	cell cycle control
Cdk1	cyclin-dependent kinase 1	0.77	1.06*	0.35	0.07	cell cycle control
Tgfb3	transforming growth factor, beta 3	-0.19	-0.51	-0.86*	-0.55	DNA replication
NF-κB1	nuclear factor of kappa light polypeptide gene enhancer in B-cell 1	0.34	0.71*	0.6	0.23	transcription factor
Smad2	SMAD family member 2	0.42	0.67*	0.38	0.13	transcription factor
E2f1	E2F transcription factor 1	-0.22	-0.9*	-0.62*	0.07	transcription factor
E2f4	E2F transcription factor 4	0.71	1.24*	0.76	0.23	transcription factor
Tfdp2	transcription factor Dp 2	0.17	0.68*	0.47	-0.04	transcription factor
GABARAPL2	GABARAP-like 2	0.09	0.65*	0.62*	0.06	autophagy
Atg12	autophagy related 12	-0.02	0.53*	0.62*	0.07	autophagy
Prkaa1	protein kinase, AMP-activated, alpha 1 catalytic subunit	0.2	0.79*	0.7*	0.11	autophagy
Atg3	autophagy related 3	0.1	0.79*	1.08*	0.4	autophagy
Atg4b	autophagy related 4B, cysteine peptidase	-0.57	-0.65*	-0.15	-0.07	autophagy
Atg5	autophagy related 5	0.33	0.5*	0.28	0.11	autophagy

* Significant expression difference between two groups (p -value ≤ 0.05) calculated by moderate t -test.

- The values in table represent the logarithmic fold change for each gene.

- CWT = control (vehicle-treated) wild-type, CKO = control (vehicle-treated) GABARAP KO, DWT = DMBA-treated wild-type, DKO = DMBA-treated GABARAP KO.

We next performed qRT–PCR analyses to verify the results for a subset of genes using the same set of mRNAs that have been used in oligo microarray chips. We found that the relative mRNA expression of Xaf1 was upregulated more than twofold in mammary glands of control and DMBA-treated GABARAP KO mice in comparison with mammary glands of wild-type counterparts (Fig. 25). Consistent with microarray data, we found that the expression levels of Bid, Bax and p21 were upregulated in both DMBA-treated groups. The relative mRNA expression level of Bid in mammary glands of DMBA-treated GABARAP KO group was upregulated more than twofold in relation to control counterparts, as well as in comparison with their DMBA-treated wild-type counterparts (Fig. 25). The mRNA expression level of Bax was upregulated in mammary glands of both DMBA-treated groups; the level of Bax expression was twofold higher in DMBA-treated GABARAP KO group when compared to wild-type counterpart (Fig. 25). Interestingly, the expression level of p21 in the mammary glands of DMBA-treated GABARAP KO mice was upregulated to 27-fold in relation to the GABARAP KO control group, whereas p21 was upregulated 10-fold in the mammary glands of DMBA-treated wild-type mice relative to their control group (Fig. 25). In comparison of the DMBA-treated groups, we found that p21 was upregulated threefold in the mammary glands of GABARAP KO mice in relation to their wild-type counterparts (Fig. 25).

Considering that upregulated Xaf1 and apoptosis signaling play an important role in antitumor activities (Byun *et al.*, 2003; Brown and Attardi, 2005; Adams and Cory, 2007; Hanahan and Weinberg, 2011; Sun *et al.*, 2011; Wong, 2011), these results suggested that GABARAP deletion might trigger enhanced antitumor activity through augmentation of cell death and cell cycle inhibition, and thus contribute to the suppression of mammary tumorigenesis in these mice.

3.8 Xaf1 highly expressed in organs of GABARAP KO mice

Our results of gene expression microarray analysis showed that the tumor suppressor Xaf1 was differentially expressed in mammary glands of 14 weeks old GABARAP KO mice (control and DMBA-treated). We wanted to check the expression of Xaf1 in different organs and ages of wild-type and GABARAP KO mice. RNA was isolated from mammary gland, liver, lung, spleen and kidney of 6 weeks old mice. qRT–PCR was employed to screen the expression of Xaf1. GABARAP KO organs showed relatively higher mRNA expression of Xaf1 compared with their wild-type counterparts (Fig. 26). It is not doubt that the knockout of GABARAP gene resulted in differential Xaf1 expression in our transgenic mouse model.

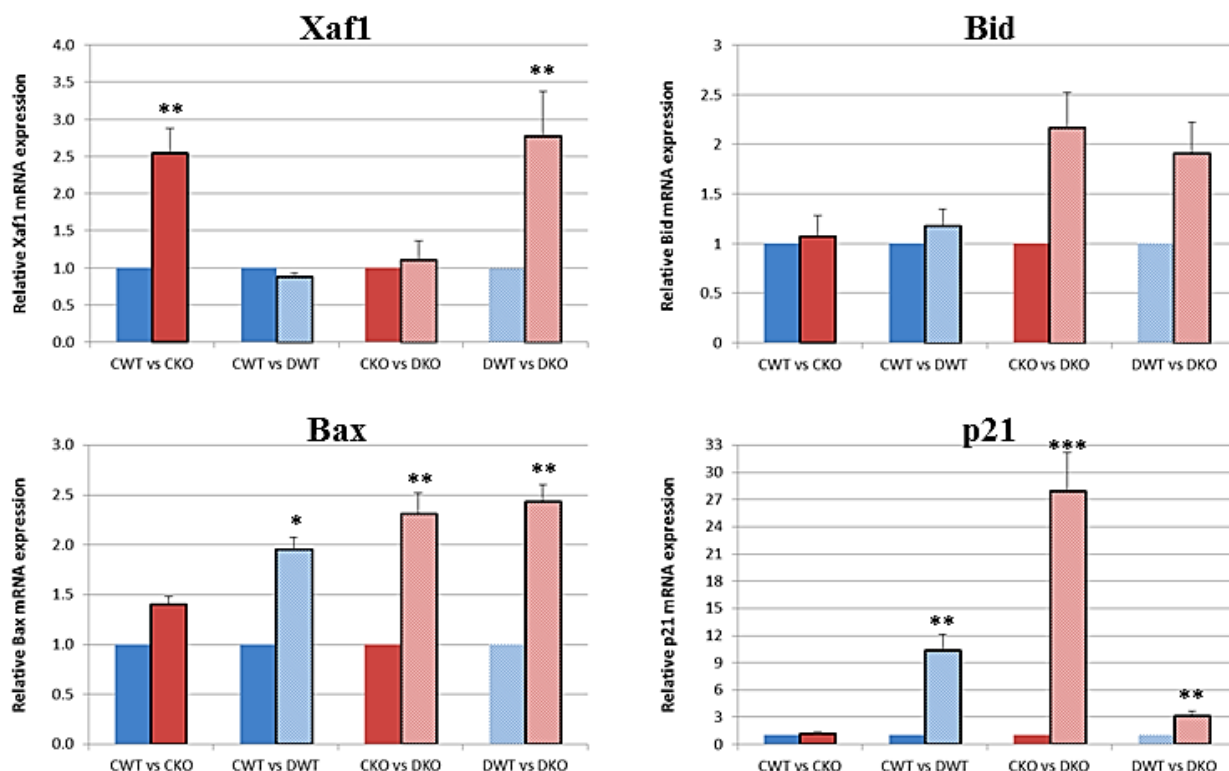


Figure 25. Relative mRNA expression of *Xaf1*, *Bid*, *Bax* and *p21* in mammary glands of vehicle-treated control (C) and DMBA-treated (D) mice measured by quantitative reverse transcriptase PCR (qRT-PCR). The groups are divided as: control wild-type (CWT), DMBA-treated wild-type (DWT), control GABARAP KO (CKO) and DMBA-treated GABARAP KO (DKO) and each figure is representative of four comparisons as indicated. Values are mean \pm SEM of 4-6 samples of each group. The relative expression values of each gene to GAPDH in each sample were calculated and compared. (*) $p < 0.05$; (**) $p < 0.01$; (***) $p = 0$.

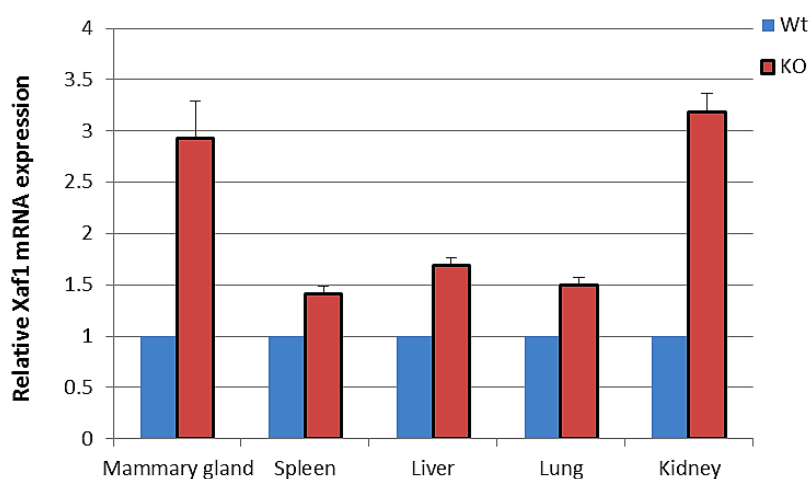


Figure 26. Relative mRNA expression of *Xaf1* in mammary gland, spleen, liver, lung and kidney at 6 weeks old of wild-type (Wt) and GABARAP KO (KO) mice measured by quantitative reverse transcriptase PCR (qRT-PCR). The relative expression value of *Xaf1* to GAPDH in each sample was calculated and compared.

3.9 DNA damage repair impaired in GABARAP-deficient fibroblasts

Fibroblasts are the most ubiquitous cell type within the body and have long been considered to be important investigator tool to identify the functional mechanism of gene in different signaling pathways. Mouse embryonic fibroblasts (MEFs) were isolated from the embryos of GABARAP KO and wild-type mice and cultured for further investigations. Firstly, we were tested whether the GABARAP gene has a crucial role in autophagy machinery. GABARAP-deficient and wild-type MEFs were incubated in starvation medium (EBSS) in the presence or absence of the autophagy inhibitor, chloroquine (CQ), and the autophagic flux was tested by monitoring the autophagic markers LC3 and p62. As depicted in Figure 27 A, both LC3A/B-II and p62 accumulated in GABARAP-deficient MEFs and were not affected by the CQ treatment indicating an inhibition in autophagic flux. Thus, our data suggest that the GABARAP gene has an essential role in the autophagic process in our cell model system.

Furthermore, accumulative evidence indicated that autophagy is involved in DNA damage repair. DMBA has been shown to induce DNA damage in several tissues (Muqbil *et al.*, 2006; Henkler *et al.*, 2012; Ganesan *et al.*, 2013). In addition, camptothecin (CPT) is considered as a DNA damage inducer and showed remarkable anticancer activity in preliminary clinical trials. CPT inhibits replication and transcription by trapping DNA topoisomerase I (Top1) covalently to DNA in a “cleavable complex” (Hsiang *et al.*, 1985; Hsiang and Liu, 1988; Lin *et al.*, 2008; Veloso *et al.*, 2013). To investigate a potential role of GABARAP in the DNA damage response, GABARAP-deficient and wild-type MEFs were treated with DMBA and CPT to induce DNA damage. At various times after treatment with 100 nM DMBA and 5 mM CPT, lysates were prepared from control and treated MEFs and analyzed by western blotting using antibodies against autophagy markers (LC3, p62 and GABARAP), DNA damage repair biomarker (γ H2AX) and Cyclin D1, as a cell cycle progression indicator. As shown in Figure 27 B, induction of autophagy was detected in MEFs after treatment with DMBA and CPT. The conversion of soluble LC3A/B-I to lipid bound LC3A/B-II was shown as an indicator of autophagy induction as well as upregulation of GABARAP in wild-type MEFs and accumulation of p62 protein in GABARAP-deficient MEFs (Fig. 27 B).

Moreover, DNA damage repair was detected by upregulating of phosphorylated γ H2AX (p- γ H2AX) in both GABARAP-deficient and wild-type MEFs after treatment for 24 h (DMBA) or 4 h (CPT) (Fig. 27 B). In wild-type MEFs, p- γ H2AX level thereafter gradually decreased by 48 h (DMBA) or 20 h (CPT) treatment, indicating repair or at least no more accumulation of the DNA damage (Fig. 27 B). In contrast, the protein level of p- γ H2AX

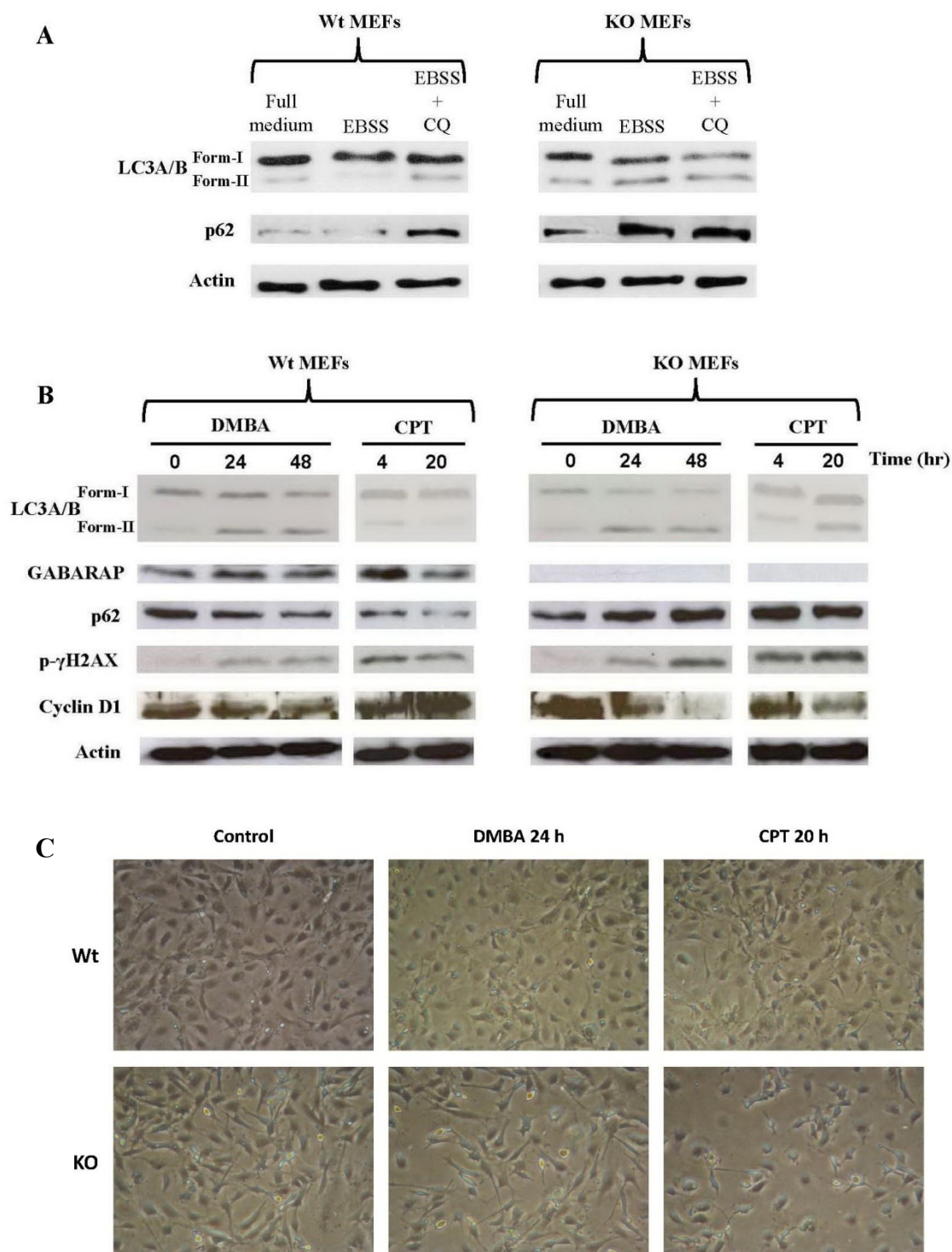


Figure 27. Analysis of autophagy, DNA damage repair and proliferation of wild-type (Wt) and GABARAP KO (KO) MEFs after treatment with DMBA and CPT. A) Wild-type and GABARAP KO MEFs cultured in six well plates, then the cells incubated for 2 h in EBSS medium in the absence or presence of 10 μ M chloroquine (CQ) and subjected to western blot analysis after lysis with RIPA extraction buffer. B) Wild-type and GABARAP KO MEFs cultured and treated with 100 nM DMBA for 24 and 48 h or 5 mM CPT for 4 and 20 h. The cells were then lysed and analyzed by western blotting using antibodies as indicated in figure. C) The cells treated as indicated in B, then the cells photographed after 24 h of DMBA treatment or 20 h of CPT treatment.

remained high and accumulated more at 48 h (DMBA) or 20 h (CPT) after treatment in GABARAP-deficient MEFs, suggesting a defect in the repair of DNA damage induced by DMBA and CPT in these cells. Furthermore, Cyclin D1 was used to detect the progression of cell cycle. Accumulation of p- γ H2AX in GABARAP-deficient MEFs after treatment with DMBA and CPT was accompanied with high reduction in Cyclin D1 protein level compared with their wild-type counterparts (Fig. 27 B). As depicted in Figure 27 C, GABARAP-deficient MEFs showed a decreased proliferation rate after DMBA and CPT treatment compared with their wild-type counterparts.

Together, these results indicated that deletion of GABARAP resulted in defective DNA damage repair and inhibition of cell cycle progression in our cell model system after DMBA and CPT treatments.

3.10 GABARAP KO mice inhibited proliferation of inoculated B16 melanoma cells

To further investigate the potential role of GABARAP gene in tumor progression, GABARAP KO and wild-type mice were subcutaneously inoculated with mouse B16 melanoma cells. After one week of B16 cells injection, we monitored the tumor growth daily and measured the tumor volume every other day beginning from the day when the tumor became palpable. All the wild-type mice presented palpable tumors at 9th day of cell injection compared with 66.7% of GABARAP KO mice showed palpable tumors at this day. The tumor growth increased constantly in wild-type mice. In contrast, tumor growth was clearly reduced in GABARAP KO mice (Fig. 28 A and B). This result suggests that intact GABARAP function in the host animal was advantageous for the growth of the inoculated syngeneic melanoma cells.

3.11 GABARAP-deficient tumors did not exhibit Ras mutation

Many studies indicated that carcinogens, in general, induce molecular changes in target organs (Hoenerhoff *et al.*, 2009). DMBA has been reported to induce point mutations in the H-ras gene resulting in an A > T transversion at the middle adenosine nucleotide of codon 61 (Dandekar *et al.*, 1986; Cardiff *et al.*, 1988; Qing *et al.*, 1997). Recently, the protumorigenic function of autophagy has been demonstrated through its ability to increase the glucose metabolism and thereby facilitating Ras-mediated cell transformation and promoting Ras-driven tumor growth. For this reason, we performed H-ras mutation analysis in DMBA-induced tumors from GABARAP KO and wild-type mice. Our analysis of the hotspot codons

12 and 13 in exon 1 and codon 61 in exon 2 revealed no mutations in the 4 tumors of the GABARAP KO mice compared to 5 mutations in 14 tumors of the wild-type mice (Table 4). The mutations included transversion of CAA > CTA or CAA > CAT (Fig. 29). This result could explain the importance of GABARAP gene, through its involvement in autophagy, in Ras-mediated cellular transformation to induce tumors.

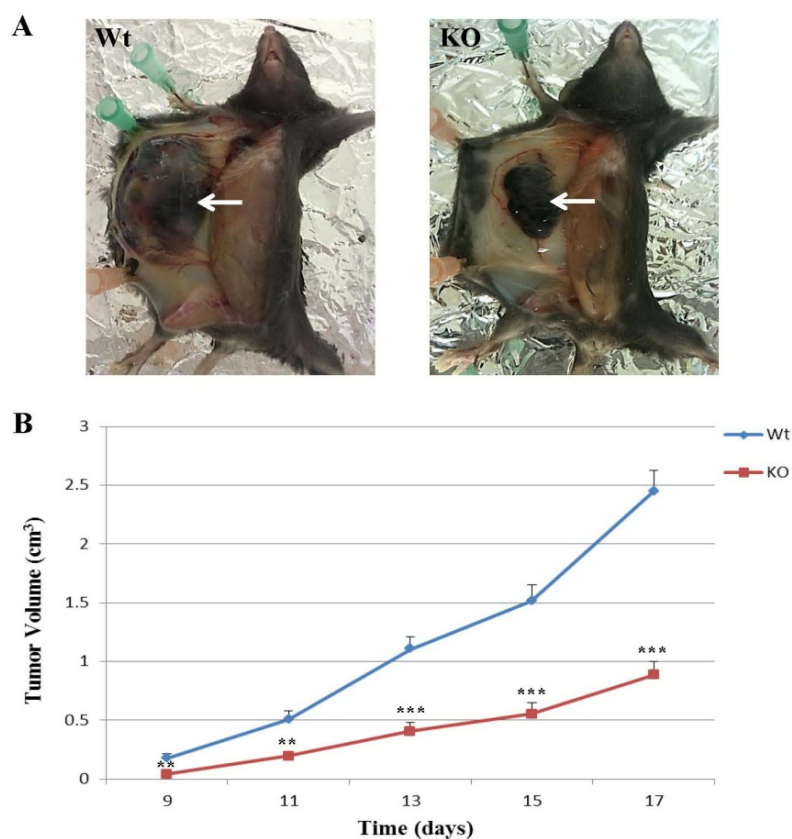


Figure 28. Inhibition of B16 melanoma cells growth in GABARAP KO mice. **A)** Morphologic picture of wild-type (Wt) and GABARAP KO (KO) mice at the 17th day of 2.5×10^5 B16 melanoma cell inoculations. **B)** Growth curve of B16 melanoma cells in Wt and KO mice after inoculation with 2.5×10^5 B16 cells. Values are representative of 12 mice and were shown with means \pm SEM. (**) $p < 0.01$, (***) $p = 0$.

Table 4. Tumor types and H-ras mutation in C57BL/6 wild-type (Wt) and GABARAP KO mice

Tumor type	C57BL/6 (Wt)			GABARAP KO				
	<i>n</i> = 29	H-ras mutation			<i>n</i> = 33	H-ras mutation		
DMBA treatment	Tumors number	12	13	61	Tumors number	12	13	61
Mammary	3	-	-	2	-	-	-	-
Skin	7	-	-	3	2	-	-	-
Lymphoma	2	-	-	-	-	-	-	-
Liver	-	-	-	-	1	-	-	-
Undifferentiated tumors	2	-	-	-	1	-	-	-
Total	14	-	-	5	4	-	-	-

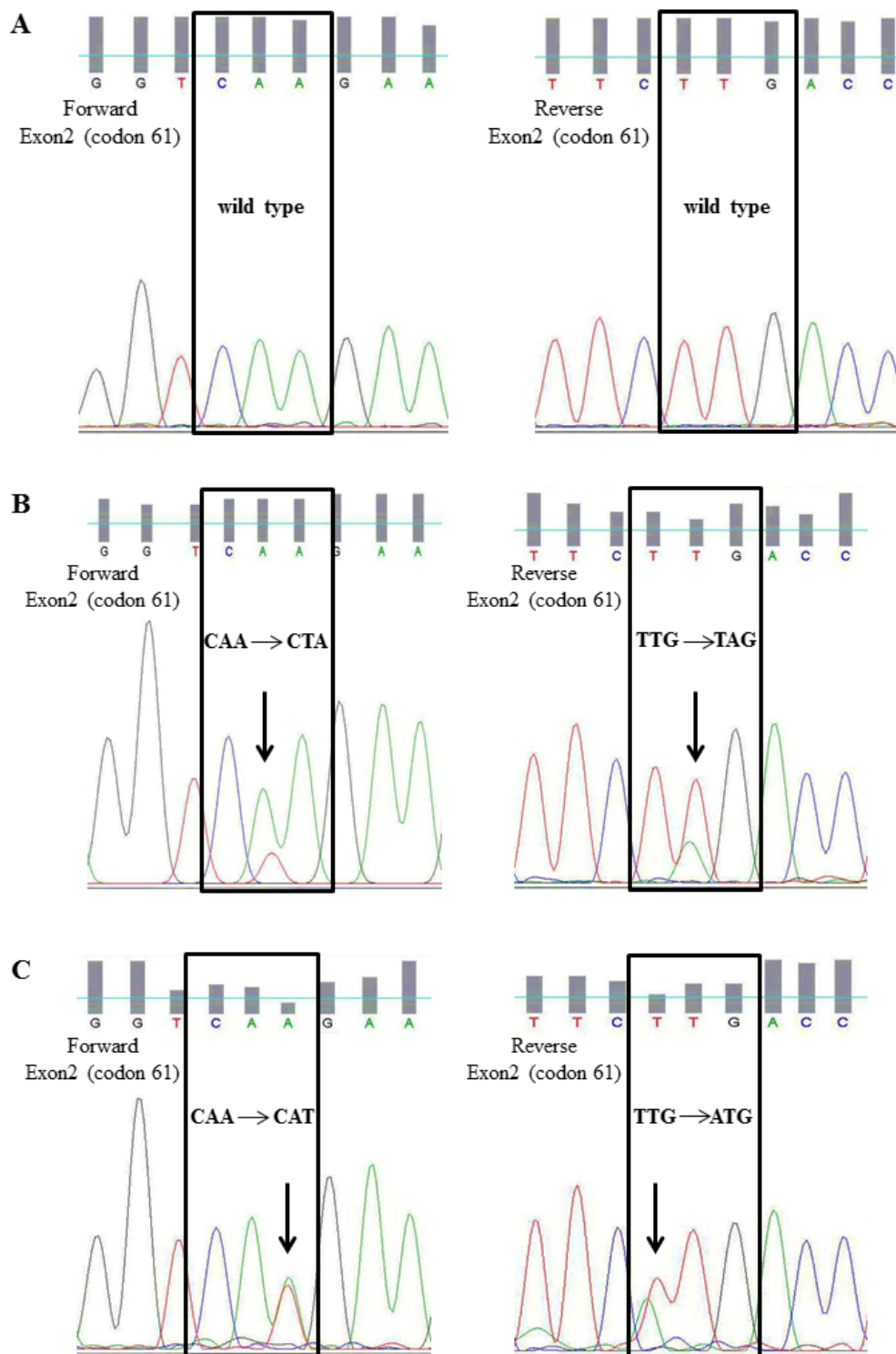


Figure 29. *H-ras* mutation analysis of *GABARAP* KO and wild-type tumors. **A)** Exon 2 (codon 61) of *H-ras* in *GABARAP* tumor showed wild type sequences of forward and reverse primers. **B)** Wild-type tumor showed mutation at forward (CAA > CTA) and reverse (TTG > TAG) sequences of exon 2 (codon 61). **C)** Wild-type tumor showed mutation at forward (CAA > CAT) and reverse (TTG > ATG) sequences of exon 2 (codon 61).

4. Discussion

The main biological role of GABARAP has been previously involved in clustering the neurotransmitter receptors GABA_A by mediating interaction with the cytoskeleton (Wang *et al.*, 1999; Chen *et al.*, 2000). Later on, authors have shown that GABARAP has an essential role in the elongation and maturation of autophagosome, a key structure in the process of autophagy (Nakatogawa *et al.*, 2007; Xie *et al.*, 2008; Weidberg *et al.*, 2010). GABARAP is ubiquitously expressed in all tested normal tissues, and has been explored in primary tumor samples and cancer cell lines and showed a diversity of expression levels. We previously reported that GABARAP may function as a tumor suppressor in breast cancer (Klebig *et al.*, 2005). However, the precise role and mechanism that GABARAP played in tumorigenesis were not elucidated. Our study considered the first attempt to clarify the role of GABARAP in tumorigenesis by using the transgenic mouse model. We used DMBA, a reliable and potent carcinogen, as well as other carcinogens to investigate the potential role of GABARAP in tumorigenesis. In addition, the spontaneous tumor formation was investigated in this mouse model over the period of 2 years. The major findings present in the current study can be summarized as follows: 1) GABARAP KO mice exhibited less tumor formation spontaneously and after carcinogen treatment. 2) High sensitivity of GABARAP KO mice to the toxicity of carcinogens. 3) GABARAP-deficient immune cells enhanced the cytokine production. 4) GABARAP-deficient mammary glands showed a significant decrease in epithelial growth upon DMBA treatment. 5) The tumor suppressor gene and apoptosis inducer Xaf1 differentially expressed in mammary glands of GABARAP KO mice as well as in other organs. 6) DNA damage repair impaired in GABARAP-deficient MEFs. 7) B16 melanoma cell inoculation and Ras mutation in tumor samples showed the potency of GABARAP gene in tumor initiation and progression.

4.1 Less tumor formation in GABARAP KO mice

The role of autophagy in tumorigenesis is complex and likely tissue and genetic context-dependent. Contradictory roles of autophagy in tumor initiation and progression have been mentioned in several reports. In some instances autophagy may serve as protumorigenic mechanism, whereas in others, it contributes to tumour suppression (Levine, 2007; Mathew *et al.*, 2007; Wilkinson and Ryan, 2010; Rosenfeldt and Ryan, 2011). Beclin-1 represented the first genetic link between autophagy and tumorigenesis (Qu *et al.*, 2003; Yue *et al.*, 2003). Heterozygous loss of Beclin-1 promoted spontaneous malignancies in mice. Later on, studies showed that the increased rate of tumor formations in mice with heterozygous loss of

Beclin-1 is not due to autophagy, since that Beclin-1 has been shown to interact and associated with apoptotic protein (Bcl-2) and tumor suppressor p53 (Pattingre *et al.*, 2005; Liu *et al.*, 2011; Lorina *et al.*, 2013). Moreover, Atg4C-deficient mice showed increased susceptibility to fibrosarcoma induced by the intradermal injection of chemical carcinogen MCA in a tissue-specific mode (Marino *et al.*, 2007). In contrast, knockout of FIP200, an important regulator of autophagy, suppressed mammary tumor initiation and progression in a mouse model of breast cancer driven by the PyMT oncogene (Wei *et al.*, 2011). In our investigation, we used the chemical carcinogen (DMBA) in order to enhance the tumor induction and to explore the potential role of GABARAP in tumorigenesis. DMBA is a widely used carcinogen and can induce various types of cancer in animal models (de Oliveira *et al.*, 2013). Most studies have used DMBA to induce mammary tumors following administration by oral gavage in mouse models (Medina, 1974, Currier *et al.*, 2005). We found that GABARAP KO mice significantly reduced the tumor formation after DMBA treatment compared with wild-type mice. In addition, no mammary tumors developed in DMBA-treated GABARAP KO mice. Regarding spontaneous tumor formation, GABARAP KO mice exhibited less tumors compared with wild-type mice, and also without mammary tumorigenesis in GABARAP KO mice. For this reason we concluded that the GABARAP gene may play an influential role in the process of tumor development. Based on our knowledge, this is the first report providing evidence for the role of GABARAP in tumorigenesis in a mouse model.

4.2 High sensitivity of GABARAP KO mice upon carcinogens treatment

Autophagy occurs at low basal levels in most normal cells to maintain cellular homeostatic functions or occurs when the cells need to ‘self-cannibalize’ or to proceed the cell survival under stress in order to maintain cellular integrity (Mizushima *et al.*; 2008). Mice with homozygous mutation of Beclin-1 die in early embryonic development (Yue *et al.*, 2003). In contrast, mice with homozygous deletion of others autophagy gene showed a normal embryonic phenotype (Marino *et al.*, 2007; Wei *et al.*, 2011). During our experiments, we noticed that GABARAP KO mice are viable and fertile and do not display any obvious abnormalities, as reported by O’Sullivan (O’Sullivan *et al.*, 2005). This indicates that GABARAP KO mice are able to develop the autophagic response in demand during the embryogenesis and early neonatal period.

Moreover, administration of genotoxic carcinogens to the mice triggers several processes in order to bypass the stress and the damage induced by such chemicals. Autophagy is one of

these processes which stimulated under such circumstances to overcome stressful conditions (Rodriguez-Rocha *et al.*, 2011; Murrow and Debnath, 2013). In our experiment, we used different carcinogens and different treatment regimens in order to enhance tumor formation. Unlike our expectation, carcinogen-treated GABARAP KO mice manifested higher sensitivity and reduced survival in comparison with treated wild-type mice. Moreover, almost all GABARAP KO mice were died without any tumor formation after carcinogens treatment, except in DMBA treatment. On the other hand, wild-type mice showed tumor formation within the period of some carcinogen treatments, for instance after DMBA and ENU exposure. Normally, carcinogen treatment required several months to initiate and promote tumor development in mouse models. The non-occurrence of tumors in some carcinogen treatment in wild-type mice was due to the shortage of exposure period of carcinogens, because we finished the experiment when all GABARAP KO mice were died. Based on these results, we propose that GABARAP is not essential for autophagy development under normal conditions but may be required for a proper autophagic response under stressful conditions such as genotoxic carcinogen treatment.

DMBA-treated mice have been reported to decrease the spleen weight and cellularity; this decrease was associated with cell death of splenocytes (Dean *et al.*, 1985; Miyata *et al.*, 2001; Gao *et al.*, 2005, 2007). However, the body weight of mice was not substantially affected by DMBA treatment (Miyata *et al.*, 2001; Gao *et al.*, 2005). We found that upon DMBA treatment GABARAP KO mice significantly reduced the spleen cellularity as well as decreased the spleen volume and weight in comparison to DMBA-treated wild-type mice. The body weights of GABARAP KO mice were tardily increased compared to treated wild-type mice. The immunohistochemistry staining revealed a considerable decrease in the proliferation of splenocytes in DMBA-treated GABARAP KO mice, which occurred together with increased cellular death. It seems that GABARAP or “autophagy” deficiency heightened the incidence of cell death and reduced the cellular proliferation rate in spleen under carcinogenic effect which led to a significant reduction in spleen cellularity. The slower growing of GABARAP KO mice upon DMBA treatment may provide insight into the impact of GABARAP deficiency on other organs apart from the spleen. Moreover, the cell surface marker analysis of splenocytes showed a substantial reduction in all cell populations: regulatory T cells (Tregs), B cells, T helper cells (CD4), cytotoxic T cells (CD8), macrophages and neutrophils, which were more profoundly affected by DMBA treatment in GABARAP KO mice than wild-type mice. The pattern of reduction for the populations of splenocytes was consistent with the reduction of the total number of splenocytes, which

means that there was no discrimination for the effect of DMBA on particular cell types of the spleen in both GABARAP KO and wild-type mice groups.

4.3 Enhancement of cytokine secretion in GABARAP-deficient immune cells

The interaction between autophagy and innate immune response has been proven through the capability of TLRs to induce autophagy as well as the negative regulator role of autophagy for inflammasome activation (Shi and Kehrl, 2010; Levine *et al.*, 2011; Nakahira *et al.*, 2011; Shi *et al.*, 2012; Araya *et al.*, 2013). The disruption of autophagy genes in macrophages have been shown to increase ROS production and translocation of mtDNA into the cytosol upon treatment with LPS and ATP, leading to enhance the secretion of proinflammatory cytokines, which can mediate tissue injury and lethal shock in the context of a sepsis model (Hotchkiss and Karl, 2003; Tal *et al.*, 2009; Nakahira *et al.*, 2011; Zhang *et al.*, 2013). In our results, we found that macrophages of DMBA-treated GABARAP KO mice significantly boosted the secretion of IL-1 β and IL-6 upon stimulation with LPS alone or in the combination of LPS and ATP. The high production of proinflammatory cytokines may be responsible for the increase the lethality of GABARAP KO mice upon DMBA treatment. The *in vivo* activation of immune cells may happen during the mice handling or by natural pathogens of laboratory mice as well as the environmental pathogens in the animal houses (Baker, 1998; Connole *et al.*, 2000). Regarding TNF α , the tendencies of secretion from macrophages of DMBA-treated GABARAP KO mice; upon stimulation with LPS alone or LPS and ATP, were higher than macrophages of treated wild-type mice. There was no significant association between TNF α secretion of GABARAP KO and wild-type macrophages upon stimulation possibly due to a relatively few number of macrophages that can be obtained from mice after DMBA treatment. It was reported that autophagy is required for mitochondrial maintenance and preservation of mitochondrial function, as well as the removal of damaged mitochondria by the process called mitophagy (Guo *et al.*, 2011; Aung-Htut *et al.*, 2013; Yang and Yang, 2013). DMBA treatment causes oxidative stress and mitochondrial dysfunction (Frenkel *et al.*, 1995; Arulkumaran *et al.*, 2007; Priyadarsini and Nagini, 2012). It has been shown that accumulation of damaged mitochondria could activate the inflammasome and thereby increased the proinflammatory cytokine secretion (Tal *et al.*, 2009; Nakahira *et al.*, 2011; Zhang *et al.*, 2013). According to these findings we propose that autophagy deficiency, in our case by GABARAP deficiency, under a genotoxic stress of DMBA may activate the inflammasome in macrophages by increasing the damaged mitochondria and ROS production. Thus activation of the inflammasome may be responsible for the increased production of

proinflammatory cytokines (IL-1 β and IL-6) from macrophages of DMBA-treated GABARAP KO mice.

Furthermore, it is known that DMBA treatment resulted in suppression of immune response in mice, both cell-mediated and humoral immunity, for prolonged periods of time (Prehn, 1963; Ward *et al.*, 1986; Burchiel *et al.*, 1990; Gao *et al.*, 2007, 2008). DMBA exerts this effect through inhibition of lymphocyte activation, mainly by suppressing the production of IL-2 from splenocytes and depressing the ability to generate CTL and NK cells (Ward *et al.*, 1986; House *et al.*, 1987; Burchiel *et al.*, 1990; Saas *et al.*, 1996; Gao *et al.*, 2007, 2008). Thereby, this effect of DMBA acts as an important mechanism; in association with its genotoxicity, contributing to tumor outgrowth (Ward *et al.*, 1986). On the other hand, tumor-host cell interaction and tumor microenvironment play an essential role in tumor initiation and progression of breast and other tumor types *in vivo* (Wiseman and Werb 2002; Luo *et al.* 2009; Hanahan and Weinberg 2011). Moreover, the host immune defense mechanisms play a crucial role in tumor immune surveillance and removal of cancerous cells (Koebel *et al.* 2007; Finn 2008). For example, De Palma *et al.* (2008) and Wei *et al.* (2011) showed effective inhibition of PyMT-driven tumor growth and metastasis through upregulation of interferon target genes. In our results, lymphocytes of DMBA-treated GABARAP KO mice produced higher levels of IL-2 and IFN- γ after *in vitro* stimulation with CD3 than lymphocytes of their untreated control group. In contrast, it was clear that lymphocytes of DMBA-treated wild-type mice suppress IL-2 and IFN- γ production after CD3 stimulation. That means our results demonstrated immune enhancement, rather than immunosuppression, in GABARAP KO mice upon DMBA treatment. The levels of IL-2 and IFN- γ secretion did not reach statistical significance possibly due to a relatively few number of lymphocytes that can be obtained from GABARAP KO mice after DMBA treatment.

The high production of some cytokines has a critical mechanism in the inhibition of tumor outgrowth and metastasis. For instance, IL-1 β was shown to be engaged in different cellular signaling pathways. The engagement of IL-1 β in specific signaling pathways relies on its concentration or level. At high levels, cells received genotoxic insults and triggered cellular apoptosis, whereas moderate or low levels in the same cells may keep the cells normal or stimulate cell growth (Roy *et al.*, 2006). Moreover, the outcome of antigen-specific T cell responses is mainly regulated by cytokines. When a T cell responds to an antigen, its cytokine profile engages certain T-helper cell pathway stimulated by the antigen-presenting cell. Moreover, the existence of IL-2 and IFN- γ can modulate effector cell differentiation, for instance Th1 cells, via regulation of cytokine receptor expression (Liao *et al.*, 2011). Many

investigations indicated the importance of IL-2 and IFN- γ in immunological reactions to tumor cell growth and promoting innate and adaptive immune responses (Yang *et al.*, 2003). IL-2 displayed significant anti-tumor activity for a different type of tumors, for instance advanced renal cancer and melanoma (Clement and McDermott, 2009; Halama *et al.*, 2010) since it supports the proliferation and clonal expansion of T cells (CD4⁺T cells and CD8⁺T cells) that specifically attack certain tumor types (Stern and Smith, 1986; Liao *et al.*, 2011). However, high doses of IL-2 were found to be accompanied by severe toxicity. To overcome the toxicity of IL-2, they found that inhibition of autophagy by using chloroquine during IL-2 immunotherapy in a mouse model led to significantly regression of tumor growth and prolonged survival (Liang *et al.*, 2012). This finding may support our results of tumor inhibition in GABARAP KO mice, since autophagy already attenuated in this mouse model by GABARAP knockout as well as IL-2 was found to be upregulated in lymphocytes of DMBA-treated group upon stimulation with CD3.

Our finding of immunomodulation upon DMBA treatment represents the first report for enhancement of immunity and/or “anti-tumor immunity” in our GABARAP KO mouse model of autophagy, which requires further investigation to explore the mechanism by which GABARAP executes this modulation.

4.4 Inhibition of epithelial growth in mammary glands of GABARAP KO mice after DMBA treatment

Mouse models have provided information for understanding the biological, cellular and molecular alterations involved in mammary tumorigenesis (Medina, 2007). The mammary gland is one of dominant target organs for the carcinogenicity of DMBA when administered by oral gavage (Medina, 1974, Currier *et al.*, 2005). Terminal end buds (TEB) are specialized structures in the mammary gland responsible for duct elongation during the immediate post pubertal period of development. TEBs of mammary glands are thought to be the target sites for the origin of tumors. Since the presence of TEBs in the time period of 4 - 8 weeks of age, the susceptibility of the mammary gland to DMBA carcinogenesis is highly age-dependent (Williams and Daniel, 1983 Medina, 2007). For this reason we used the female mice of 6 - 8 week age in all our investigations. Our results for tumor induction by DMBA revealed no mammary tumors in GABARAP KO mice compared to 21.4% mammary tumors in wild-type mice. We investigated the mammary epithelial cell growth and ductal tree morphogenesis after 6 weekly doses of 1 mg DMBA/mouse in both GABARAP KO and wild-type mice to evaluate the gland architecture and proliferation by means of mammary gland whole mount

morphology analysis. The impact of DMBA on the epithelial cell growth and ductal branching was obvious in mammary gland of GABARAP KO mice. Although the mammary glands of DMBA-treated female wild-type mice appeared to have a significant alteration in epithelial growth compared to aged-matched control wild-type counterparts, this change could be a normal consequence of treatment with genotoxic carcinogen like DMBA. The ability of DMBA to induce apoptosis has been indicated in lymphoid organs and bone marrow (Miyata *et al.*, 2001; Page *et al.*, 2003). Recently, Stolpmann *et al.* (2012) showed that activation of AhR (aryl hydrocarbon receptor) sensitised the cells to induce apoptosis. We propose that DMBA can induce apoptosis in mammary glands, since AhR has been showed to be upregulated upon DMBA treatment in mammary glands (Swanson *et al.*, 1995; Trombino *et al.*, 2000; Denison and Nagy, 2003; Currier *et al.*, 2005).

Furthermore, immunohistochemistry staining for Ki-67 revealed inhibition of epithelial cell growth in mammary glands of DMBA-treated GABARAP KO mice as well as increased incidence of cell death compared to mammary glands of DMBA-treated wild-type mice. In general, knockout of GABARAP seems to sensitise the cell to inhibit the proliferation and increases cell death induction which was obvious in spleen and mammary gland.

4.5 Gene expression profiling indicated differential expression of tumor suppressor and apoptosis inducer genes in GABARAP KO mice

Microarray analysis is a widely used technology for studying gene expression on a global scale that can be used to investigate the molecular mechanisms that contribute to disease. Several studies have shown that microarray gene expression profiling results in improved diagnosis and risk stratification in cancer (van 't Veer *et al.*, 2002; Jackson *et al.*, 2013). To explore the molecular mechanisms by which deficiency of GABARAP led to reduced tumor formations, we employed Agilent Whole Mouse Genome expression microarrays to analyse mammary glands of vehicle-treated (control) and DMBA-treated GABARAP KO and wild-type mice. We found a subset of genes that had GABARAP-dependent alterations in both control and DMBA-treated groups. Xaf1 is the most important gene that was differentially expressed in mammary gland of both control and DMBA-treated GABARAP KO mice. This gene has been widely studied in the last decade and characterized as an apoptosis inducer and tumor suppressor gene. Xaf1 is expressed ubiquitously in all normal cells (Fong *et al.*, 2000). In contrast, extremely low or undetectable Xaf1 expression is a frequent event in several cancer cell lines (Fong *et al.*, 2000), as well as in many types of human cancer tissues (Byun *et al.*, 2003; Ma *et al.*, 2005; Lee *et al.*, 2006; Tu *et al.*, 2009; Huang *et al.*, 2010). Moreover,

Kempkensteffen *et al.* (2007) found that loss of Xaf1 expression correlated strongly with tumor staging, implicating loss of Xaf1 function in tumor progression. The epigenetic silencing of Xaf1 by aberrant promoter methylation (hypermethylation) has been associated with cancer development and progression (Byun *et al.*, 2003; Lee *et al.*, 2006; Zou *et al.*, 2006; Huang *et al.*, 2010). The restoration of Xaf1 expression induced cancer cell apoptosis and inhibited tumor growth in various types of cancers including gastric, colon, liver, pancreatic and prostate cancers, as well as increased cell sensitivity to drug-induced apoptosis (Byun *et al.*, 2003; Lee *et al.*, 2006; Arora *et al.*, 2007; Tu *et al.*, 2009, 2010; Huang *et al.*, 2010). Recently, Zhang *et al.* (2011) showed that Xaf1 inhibited cell invasion, it interacts with and attenuates the trans-activity of Four and a Half LIM protein 2. Moreover, Straszewski-Chavez *et al.* (2007) showed that Xaf1 re-localized to mitochondria in response to TRAIL and promoted translocation of Bax into mitochondria and cytochrome C release from mitochondria, and thereby induced apoptosis. Interestingly, our results demonstrated enhancement of pro-apoptotic gene (Bid, Apaf1 and Bax) expression in mammary glands of DMBA-treated GABARAP KO mice. Bax expression was elevated also in DMBA-treated wild-type mammary glands and this may be due to the genotoxic effect of DMBA.

Furthermore, Xaf1 has been shown to induce cell cycle arrest in G2/M phase and mitotic catastrophe (Tu *et al.*, 2009; Wang *et al.*, 2009a; Zhang *et al.*, 2011). In our results, mammary glands of DMBA-treated GABARAP KO mice exhibited differential expression of cyclin-dependent kinase inhibitors p21 (Cdkn1a) and p18 (Cdkn2c) that could explain the inhibition of epithelial cell growth. The results of relative mRNA expression of Bax and p21 by using qRT-PCR revealed differences in the expression of these genes when we compared the DMBA-treated groups. In addition, Zou *et al.* (2012) showed recently that Xaf1 is a novel target of p53 and that it enhances p53-mediated apoptosis via post-translational modification. We proposed that despite the high expression of Xaf1 in mammary gland of GABARAP KO mice, its extreme effect as an apoptosis inducer may not detect entirely at the mRNA level. Nevertheless, high Xaf1 expression in mammary glands of GABARAP KO mice fits well with the observed phenotype, i.e. high Xaf1 expression predisposes mammary gland epithelium to undergo apoptosis after genotoxic insult thereby preventing tumor formation and favoring inhibition of branching/growth of the glandular tissue.

Xaf1 was originally identified as a binding partner and a novel negative regulator of apoptosis inhibitor protein Xiap thereby acting itself as an apoptosis inducer. Xaf1 directly interacts with endogenous Xiap and results in Xiap sequestration to nuclear inclusions, thereby antagonizing the anti-caspase activity of Xiap and reverses the protective effect of Xiap

overexpression in cell lines (Liston *et al.*, 2001). High relative expression of Xiap compared to Xaf1 expression in cancer cells has provided a survival preference through increasing the Xiap anti-apoptotic function (Fong *et al.*, 2000). We found that Xiap was significantly upregulated in the mammary glands of DMBA-treated wild-type mice. This may be an indication that the gene provides a protective mechanism for wild-type mammary glands against cellular death signaling. Moreover, Xiap overexpression may confer a possibility for mammary tumor formation in wild-type mice. In contrast, the mammary glands of DMBA-treated GABARAP KO mice demonstrated insignificant alterations in the expression level of Xiap.

However, Xaf1 have been reported to induce cell death also by Xiap-independent pathways (Xia *et al.*, 2006; Yu *et al.*, 2007; Tu *et al.*, 2010). Xia *et al.* (2006) showed that Xaf1 activates the mitochondrial apoptotic pathway that was dramatically enhanced by TNF α ; they found no evidence for an interaction between Xaf1 and Xiap. Thus, Xaf1 induces apoptosis through multiple mechanisms. Interestingly, we found that Tnfrsf10b and Ripk1, both are TNF receptors, significantly upregulated in mammary glands of DMBA-treated GABARAP KO mice. Tnfrsf10b is a member of the tumor necrosis factor (TNF) receptor superfamily and contains an intracellular death domain that can induce apoptosis in many physiological events, such as autoimmunity and activation-induced cell death (Chaudhary *et al.*, 1997; Zhao *et al.*, 2014).

We screened the expression level of Xaf1 in several organs and found that Xaf1 was highly expressed in the investigated organs of GABARAP KO mice compared to the wild-type mice. This indicates that Xaf1 is a general event of GABARAP deficiency, and may explain the reduction of tumor formation in general and the cytotoxic effect of DMBA in the spleen of GABARAP KO mice.

Expression profiles displayed several differentially expressed genes upon GABARAP deficiency. We reviewed most of these genes to identify the biological functions that may provide an interpretation for the phenotypic changes in the mammary glands as well as the reduction in tumor formation of GABARAP KO mice. Many of these genes are with unknown functions so far, but some of them have been reported to play a role in tumorigenesis and/or cell death or may function as a transcription factor. For instance, we found Trim16 significantly downregulated in mammary glands of both control and DMBA-treated GABARAP KO mice. Trim16 is a ubiquitously expressed protein and was identified as an estrogen and anti-estrogen regulated gene in epithelial cells stably expressing estrogen receptor. The family of this protein play essential roles in cell growth, differentiation,

ubiquitination, retroviral immunity and cancer (Cao *et al.*, 1998; Beer *et al.*, 2002; Meroni and Diez-Roux, 2005; Marshall *et al.*, 2010; Liu *et al.*, 2014). The expression of Trim16 is induced by estrogen in breast cancer cells and keratinocyte growth factor in keratinocytes, when the cells are forced to proceed into a differentiation pathway (Beer *et al.*, 2002; Marshall *et al.*, 2010). There is evidence that Trim16 reduced the cell viability in retinoid-sensitive neuroblastoma cells and retinoid-resistant breast and lung cancer cells, however the viability of non-cancer cells was unaffected by Trim16 overexpression (Cheung *et al.*, 2006; Raif *et al.*, 2009; Marshall *et al.*, 2010). Recently, Liu *et al.*, (2014) showed that inhibition of one protein of the Trim family, Trim24, promoted apoptosis in hepatocellular carcinoma by increasing the protein levels of p53, Bax, and caspase-8, and decreasing the expression of Bcl-2, Survivin, Cyclin D1, and CDK4. They also proved the involvement of Trim24 in EMT. These findings provide an indication for the essential role of the Trim family in tumor initiation and progression. However, the exact role of Trim16 in our studies is not clear and requires further investigations to clarify it.

Moreover, Siva1 has been proven as an apoptotic inducer protein (Prasad *et al.*, 1997; Xue *et al.*, 2002; Chu *et al.*, 2005; Du *et al.*, 2009; Resch *et al.*, 2009). Li *et al.*, (2011) showed that overexpression of Siva1 inhibited stathmin (Stmn), an important regulatory protein of microtubule dynamics, leading to suppression of EMT and metastasis. In our results, Siva1 was upregulated in DMBA-treated groups; GABARAP KO and wild-type mice, but the expression level of Stmn4 was significantly downregulated in DMBA-treated GABARAP KO mice. This finding may explain the inhibition of mammary gland proliferation and tumorigenesis of GABARAP KO mice upon DMBA treatment, since EMT is an essential process for epithelial cells to develop, migrate, invade and initiate metastasis and tumor progression (Yang and Weinberg, 2008; Kalluri and Weinberg, 2009; Thiery *et al.*, 2009).

Furthermore, several transcription factors have been shown to be upregulated in mammary glands of wild-type mice upon DMBA treatment, for instance NF- κ B1, Smad2, E2f4 and Tfdp2. NF- κ B is an important regulator of mammary gland development, where it controls proliferation and branching (Brantley *et al.*, 2001; Cao *et al.*, 2001), and also protects the epithelial cells during apoptotic alveolar involution (Clarkson *et al.*, 2000). These findings support our results of the occurrence of mammary tumorigenesis in wild-type mice upon DMBA treatment in contrast to GABARAP KO mice. Mammary glands of wild-type mice can develop protective mechanisms upon DMBA treatment against cellular death represented by a significant upregulation of NF- κ B as well as Xiap. In addition, constitutive activation of NF- κ B factors have been demonstrated in breast cancer; high nuclear NF- κ B levels were

found in the majority of specimens from DMBA-induced rat mammary tumor and primary human breast tumor, carcinogen transformed human mammary epithelial cells and breast cancer cell lines (Sovak *et al.*, 1997). Kim *et al.* (2000) and Currier *et al.* (2005) showed that NF- κ B upregulation occurs as an early event and can precede DMBA-induced mammary tumor formation in rats and mice. Moreover, overexpression of NF- κ B family member c-Rel in the mammary gland promotes breast cancer in transgenic mice (Romieu-Mourez *et al.*, 2003). Thus, the expression profile analysis is consistent with our experimental observation that wild-type mice exhibited mammary tumor formation in contrast to GABARAP KO mice. Tumor development is a result of aberrant cellular proliferation and failure to undergo apoptosis in response to normal signaling cues (Green and Evan, 2002). One “hallmark” of cancer is the dysregulation of cell death pathways (Igney and Krammer, 2002), and this dysregulation is required for tumor initiation and progression (Hanahan and Weinberg, 2011). Autophagy and apoptosis are both well-controlled biological processes and play fundamental roles in development, maintenance of tissue homeostasis and diseases. Accumulating evidence revealed that autophagy and apoptosis can cooperate, antagonize or assist each other, for subsequently determining the fate of cells. Recently, many studies have delineated pathways that mediate the complex interplay between autophagy and apoptosis providing molecular insight into the signaling network that regulates both processes, as we showed in Figure 6. Indeed, there are many crucial factors governing the cross-talk between autophagy and apoptosis, several autophagic proteins showed essential roles in apoptosis and vice versa, as elucidated in Table 1 (Mukhopadhyay *et al.*, 2014). Autophagy has been well established as an important cell survival mechanism, especially in cells under stress conditions (Cecconi and Levine, 2008; Kroemer and Levine, 2008). Elliott and Reiners (2008) showed that suppression of autophagy enhanced the cytotoxicity of DNA-damaging agents. This let us to propose that attenuation of autophagy, or GABARAP deletion, deprives the cells from essential survival mechanisms leading to an increase of sensitivity against exposure to stress like genotoxic carcinogens.

Finally, the mechanisms linking autophagy and apoptosis are not fully defined. However, our results demonstrated a unique interaction between GABARAP and Xaf1 expression. The high expression of Xaf1 was not only detectable in mammary glands but also in different organs of GABARAP KO mice. This observation requires further study to clarify how GABARAP knockout influences Xaf1 expression. We propose two possibilities of interaction; one could be by direct genetic interaction of GABARAP and Xaf1 and the second by indirect interaction. Indeed, several regulatory pathways of Xaf1 expression have been reported.

Wang *et al.* (2006a) demonstrated heat shock factor 1 (Hsf1) as a negative regulator of Xaf1. Moreover, Xaf1 has been recognized as an interferon-stimulated gene and its expression has been promoted by both IFN and TNF α (Leaman *et al.*, 2002). The mechanism by which IFN induced Xaf1 expression was either through interaction with the interferon regulatory factor 1-binding element (Irf-E) or demethylation of CpG sites within the Xaf1 promoter (Wang *et al.*, 2006b; Micali *et al.*, 2007; Wang *et al.*, 2009b). Micali *et al.* (2007) showed that Xaf1 knockdown in cancer cells led to complete loss of IFN- β -mediated TRAIL-induced cell death. It has been reported that IFN- β -induced Xaf1 expression was mediated by Stat1 through the interaction with IFN stimulated response element-Xaf1. Stat1 knockdown and blocking its phosphorylation decreased IFN- β -induced Xaf1 expression (Sun *et al.*, 2008). Recently, Qiu *et al.* (2014) showed that Irf-1-enhanced Xaf1 gene activation in glomerular mesangial cells in a rat nephritis model. Therefore, Xaf1 appears to be a mediator or effector of cytokine-induced apoptosis. Interestingly, we found that GABARAP deficiency modulated cytokine secretion, for instance IFN- γ (Fig. 20 B). According to our findings we would like to promote the idea of cytokines being involved in the enhancement of Xaf1 expression thus pointing to an indirect mechanism of Xaf1 regulation by GABARAP knockout.

4.6 Impairment of DNA damage repair in GABARAP-deficient MEFs

There are many factors that can cause DNA damage and DNA damage response (DDR). These factors are either exogenous environmental agents, like genotoxic chemicals and chemotherapeutic drugs, or endogenous byproducts of regular cellular metabolism (Rodriguez-Rocha *et al.*, 2011). Recently, autophagy has been showed to be induced in response to DNA damage; however the precise role of autophagy in DDR is still unclear (Klionsky and Emr, 2000; Polager *et al.*, 2008; Kang *et al.*, 2009). We observed that autophagy was induced after treatment of GABARAP-deficient and wild-type MEFs with DMBA and CPT, both are DNA-damaging agents. Autophagy induction after treatment with DNA-damaging agents may represent a pro-survival function to maintain cellular integrity. However, GABARAP-deficient MEFs have been shown to accumulate p62 as an indicator of autophagy impairment; p62 is associated with the autophagosome membrane and in case of intact autophagy p62 undergoes degradation by the action of the lysosome.

One important event in DDR activation is phosphorylation of histone H2AX (termed γ H2AX) which leads to recruitment of DNA repair molecules to the site of damage. Therefore it is considered as a marker for DNA double-strand break (DSB) formation (Kinner *et al.*, 2008; Svetlova *et al.*, 2010). After DSB re-joining γ H2AX foci are eliminated from the nucleus and

this elimination can serve as a useful marker of DSB repair in normal cells and tissues (Svetlova *et al.*, 2010). We found that γ H2AX was accumulated in the GABARAP-deficient MEFs in a time-dependent manner after treatment with DMBA and CPT; in contrast wild-type MEFs showed no change or decrease in amount of γ H2AX protein at 48 h (DMBA) or 20 h (CPT) treatment. These findings denoted that GABARAP deficiency resulted in the impairment of the DNA damage repair mechanism induced by the genotoxic chemical DMBA and the chemotherapeutic agent CPT. Moreover, lack of DNA damage repair in GABARAP-deficient MEFs was accompanied with decrease in cell survival and reduction in Cyclin D1 protein expression.

The mechanisms underlying GABARAP deficiency leading to defective DNA damage repair are not well understood at present. However, Bae and Guan (2011) showed that p62 accumulation may be responsible for defective DDR and reduced cellular survival in FIP200-deletion MEFs upon CPT treatment. In addition, inhibition of autophagy by heterozygous loss of Beclin-1 or homozygous deletion of Atg5 in apoptosis-defective tumor cells induced p62 accumulation which led to increased DNA damage (Karantza-Wadsworth *et al.*, 2007; Mathew *et al.*, 2009). Interestingly, we also observed accumulated p62 in GABARAP-deficient MEFs upon DMBA and CPT treatment. Furthermore, Bae and Guan (2011) indicated that direct inhibition of p62 expression by using RNA interference suppressed accumulation of γ H2AX in FIP200-deficient MEFs and rescued the increased sensitivity of CPT-induced cell death. We suggest that upregulation of p62 in GABARAP-deficient MEFs may mediate the reduction of DNA damage repair and the inhibition of cell proliferation.

Indeed, it is known that p62 is localized primarily in the cytoplasm as a cargo protein of ubiquitinated proteins for autophagic degradation (Moscat and Diaz-Meco, 2009). However, Pankiv *et al.* (2010) showed that p62 contains two nuclear localization signals and a nuclear export signal. It is required for polyubiquitinated protein interaction with promyelocytic leukemia (PML) nuclear bodies. PML nuclear bodies are implicated in DNA damage repair, they contain several DDR proteins such as TopBP1 (Lallemant-Breitenbach and de Thé, 2010). Despite this, Moscat and Diaz-Meco (2009) pointed out that accumulation of p62 in the cytoplasm also impact on DNA damage repair through its indirect interaction with multiple other proteins. The other possibility of defective DNA damage repair is increased production of ROS in autophagy-deficient cells (Mathew *et al.*, 2007; Liu *et al.*, 2010). Finally, our results showed that DNA-damaging agents extremely increased inhibition of proliferation of GABARAP-deficient cells. This is consistent with the observed increased vulnerability of autophagy-defective cell to DNA damage and the rationale for using drugs

like camptothecin in chemotherapy together with autophagy inhibitors in cancer therapy. However, further investigations are required to explore the exact mechanisms of GABARAP in this process.

4.7 *In vivo* inhibition of B16 melanoma cells growth in GABARAP KO mice

Using the GABARAP KO mice we also addressed the question whether the genetic background may affect the *in vivo* tumor growth of inoculated tumor cells. To address this issue, we used the transplantable murine melanoma B16 cell line. The subcutaneous inoculation of melanoma B16 cells is widely used for the evaluation of gene deletion consequences and/or therapy (Overwijk and Restifo, 2001). Several studies have shown a significant decrease of tumor cells growth, *in vivo* and *in vitro*, treated with autophagy inhibitor chloroquine (Fan *et al.*, 2006; Zheng *et al.*, 2009; Noman *et al.*, 2011). Our investigation of tumor cells inoculation in GABARAP-deficient mice model represents the first inspection for the role of the *in vivo* effect of autophagy-related gene deletion on tumor growth. Noman *et al.* (2011) showed that targeting Beclin-1 in B16 melanoma cells reduced tumor growth, which was associated with an increase in apoptotic cells. In the same study, they found that autophagy prevented T cell-mediated cytotoxicity in the context of hypoxia in lung cancer cells (Noman *et al.*, 2011). Our *in vivo* results showed that GABARAP knockout reduced B16 melanoma cells growth.

The molecular mechanisms how autophagy-related gene deficiency in the mouse model could influence the growth of the inoculated tumor cells is unknown so far. GABARAP-deficient immune cells demonstrated modulation in the cytokine secretion upon CD3 stimulation. It might be speculated that this effect may influence the growth of B16 melanoma cells by increased anti-tumor immunity. However, the precise role of tumor growth reduction in GABARAP KO mice needs to be clarified by studying microenvironment factors which represent an essential demand for tumor growth *in vivo*. Tumor microenvironment can enhance tumor cell growth by recruitment of angiogenesis-promoting factors, in addition to the role of immune system as a key determinant in the regulation of tumor growth or rejection (Witz and Levy-Nissenbaum, 2006).

4.8 Absence of Ras mutation in DMBA-induced tumors of GABARAP KO mice

Many chemical carcinogens induce molecular alterations in target organ, and the most frequently involved genes are Ras and Tp53 (Hoenerhoff *et al.*, 2009). It is well known

that DNA damaging effect of DMBA mostly induced point mutations in genes such as c-H-ras (Dandekar *et al.*, 1986; Cardiff *et al.*, 1988; Qing *et al.*, 1997). Ras oncogenes play a fundamental role in regulation of cell growth and survival and they are frequently activated in cancer (Schubbert *et al.*, 2007). Previous studies showed that active oncogenic Ras induced autophagy to promote and facilitate oncogenic transformation by maintaining and improving cell metabolism (Guo *et al.*, 2011; Kim *et al.*, 2011; Lock *et al.*, 2011). Indeed, Ras-transformed cells have been shown to enhance glucose uptake, whereas autophagy-deficient counterparts have decreased rates of glycolysis (Lock *et al.*, 2011). Moreover, Wei *et al.* (2011) observed that FIP200-null mammary tumor cells and transformed MEFs had reduced glycolysis and suppressed mammary tumor initiation and progression in a mouse model of breast cancer driven by the PyMT oncogene. These findings elucidated the essential role of autophagy-related genes in tumorigenesis induced by oncogenic signaling. Since DMBA has been reported to induce point mutations in H-ras gene leading to A > T transversion in codon 12, 13 and 61 (Dandekar *et al.*, 1986; Cardiff *et al.*, 1988; Qing *et al.*, 1997), we wanted to investigate the H-ras status in the tumors obtained from GABARAP KO and wild-type mice after treatment with 6 weekly oral doses of DMBA. Interestingly, we did not find any mutations within the hot spots of exon 1 (codon 12, 13) and exon 2 (codon 61) of H-ras in the tumors of GABARAP KO mice. In contrast, tumors of wild-type mice were shown to harbour H-ras mutation within codon 61 of exon 2 in about 36% of total tumors number.

We suggested an essential role of GABARAP gene in tumorigenesis, and this role may be through its involvement in the autophagy process. Furthermore, the non-occurrence of H-ras mutations in the tumors of GABARAP KO mice may indicate the involvement of autophagy/GABARAP in Ras-mediated cellular transformation.

4.9 Conclusions

By using a mouse model, we have identified a novel role of GABARAP in tumor formation and progression. GABARAP knockout (KO) mice showed less tumor formation, spontaneously and after carcinogen treatment. The tumor inhibition of GABARAP knockout mice was characterized by absence of mammary tumors in the both conditions. We found that GABARAP plays a role in immunomodulation after carcinogen treatment and that the gene knockout induced alterations of the gene expression profile.

Treatment by chemical carcinogens was accompanied by less tumor formation and increased lethality of GABARAP KO mice. Moreover, DMBA showed a massive impact to decrease the cellularity of splenocytes of GABARAP KO compared to the wild-type counterparts. This

effect was due to decreased proliferation rates and increased cellular death of GABARAP-deficient splenocytes. The *in vitro* stimulation of macrophages and lymphocytes from GABARAP KO mice resulted in a high increment in cytokine secretion. Proinflammatory cytokines, IL-1 β and IL-6, were significantly produced by macrophages of DMBA-treated GABARAP KO mice compared to wild-type counterparts. Lymphocytes of DMBA-treated GABARAP KO mice showed immune enhancement by increasing the production of IL-2 and IFN- γ . In contrast, lymphocytes of DMBA-treated wild-type mice demonstrated immunosuppression represented by repression of IL-2 and IFN- γ production.

Mammary epithelial cell growth of GABARAP KO mice showed an inhibition in the growth and branching of the glandular tissue upon DMBA treatment compared to wild-type counterparts. This inhibition was accompanied by a decreased proliferation rate and increased cellular death of mammary gland epithelium. Gene expression profiling analysis indicated high and differential expression of the tumor suppressor gene Xaf1 in mammary glands of GABARAP KO mice. Studies on expression of Xaf1 in several cancer cells identified it as an apoptosis inducer and tumor suppressor gene as well as a potential inhibitor of invasion. In addition, several cell death/apoptosis genes were found to be upregulated in mammary glands of DMBA-treated GABARAP KO mice compared to wild-type counterparts. In our view the high Xaf1 expression predisposed the mammary gland epithelium to undergo apoptosis after genotoxic insult thereby preventing tumor formation.

Mouse embryonic fibroblasts (MEFs) revealed impairment of DNA damage repair and reduction in proliferation rate after genotoxic agents (DMBA and camptothecin (CPT)) treatment in GABARAP-deficient cells. Failure of DNA damage repair has evidenced by accumulation of histone H2AX (γ H2AX) protein in a time-dependent manner in association with downregulation of the Cyclin D1 protein.

The growth of mouse B16 melanoma cells inoculated subcutaneously in GABARAP KO mice was inhibited. Furthermore, the mutation analysis of H-ras in DMBA-induced tumors revealed no mutation within the hot spots of exon 1 and 2 in tumors of GABARAP KO mice which may indicate that these neoplasms develop in an alternative way compared to the classical, DMBA-induced, Ras-mediated activation of tumorigenesis.

Altogether, our results demonstrated different aspects for the role of GABARAP in tumorigenesis. The challenge of future investigations will be to explore the molecular mechanisms of GABARAP in the regulation of gene expression, more specifically of Xaf1 expression, and immunomodulation after genotoxic stress. Figure 30 summarizes our working model for the potential mechanisms of tumor inhibition in GABARAP KO mice.

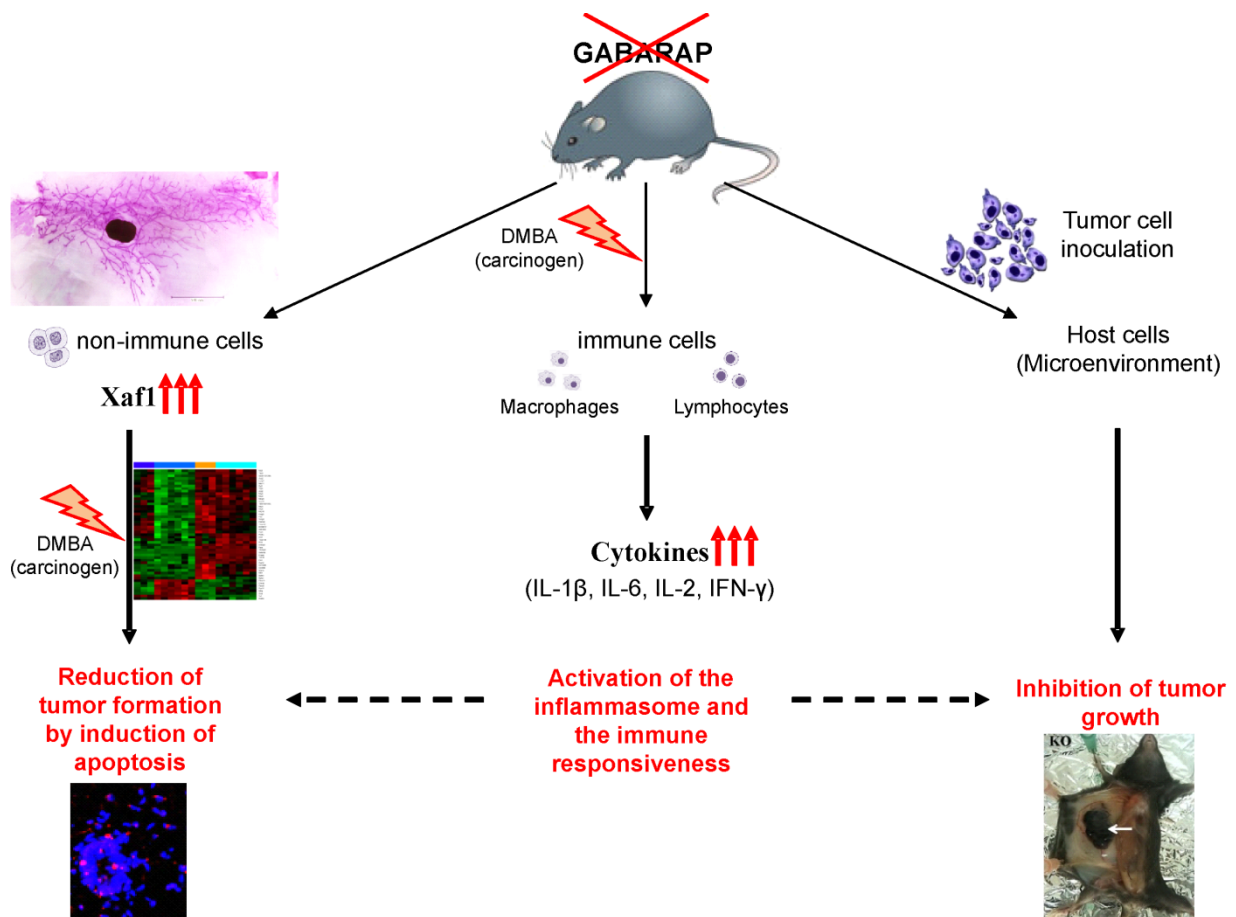


Figure 30. Working model summarizing the potential mechanisms of tumor suppression in GABARAP KO mice subjected to genotoxic stress (DMBA). GABARAP deletion results in impairment of autophagy in the cells. In non-immune cells, knockout of GABARAP gene leads to over- and differential expression of tumor suppressor gene *Xaf1* that may trigger cell death events under stress leading to the inhibition of tumor formation. Under genotoxic stress, GABARAP-deficient immune cells highly produce several cytokines which could suppress tumor formation and/or may trigger cell death. Similarly, tumor cell inoculation might induce inflammasome activation and cytokine secretion leading to inhibition of tumor growth by the enhancement of antitumor immunity.

5. References

- Abedin MJ, Wang D, McDonnell MA, Lehmann U, Kelekar A (2007). Autophagy delays apoptotic death in breast cancer cells following DNA damage. *Cell Death Differ*; 14: 500-10.
- Adams JM, Cory S (2007). The Bcl-2 apoptotic switch in cancer development and therapy. *Oncogene*; 26: 1324-37.
- Aita VM, Liang XH, Murty VV, Pincus DL, Yu W, Cayanis E, Kalachikov S, Gilliam TC, Levine B (1999). Cloning and genomic organization of beclin 1, a candidate tumor suppressor gene on chromosome 17q21. *Genomics*; 59: 59-65.
- Akira S, Taniuchi T, Kishimoto T (1993). Interleukin-6 in biology and medicine. *Adv Immunol*; 54: 1-78.
- Amaravadi RK, Yu D, Lum JJ, Bui T, Christophorou MA, Evan GI, Thomas-Tikhonenko A, Thompson CB (2007). Autophagy inhibition enhances therapy-induced apoptosis in a Myc-induced model of lymphoma. *J Clin Invest*; 117: 326-36.
- Amaravadi RK (2011). Cancer. Autophagy in tumor immunity. *Science*; 334: 1501-2.
- Amaravadi RK, Lippincott-Schwartz J, Yin X-M, Weiss WA, Takebe N, Timmer W, DiPaola RS, Lotze MT, White E (2011). Principles and current strategies for targeting autophagy for cancer treatment. *Clin Canc Res*; 17: 654-66.
- Apel A, Herr I, Schwarz H, Rodemann HP, Mayer A (2008). Blocked autophagy sensitizes resistant carcinoma cells to radiation therapy. *Cancer Res*; 68: 1485-94.
- Araya J, Hara H, Kuwano K (2013). Autophagy in the pathogenesis of pulmonary disease. *Intern Med*; 52: 2295-303.
- Arias-Romero LE, Chernoff J (2010). p21-activated kinases in ErbB2-positive breast cancer: A new therapeutic target?. *Small GTPases*; 1: 124-8.
- Arora V, Cheung HH, Plenchette S, Micali OC, Liston P, Korneluk RG (2007). Degradation of survivin by the X-linked inhibitor of apoptosis (XIAP)-XAF1 complex. *J Biol Chem*; 282: 26202-9.
- Arroyo DS, Gaviglio EA, Ramos JMP, Bussi C, Rodriguez-Galan MC, Iribarren P (2014). Autophagy in inflammation, infection, neurodegeneration and cancer. *Int Immunopharmacol*; 18: 55-65.
- Arulkumaran S, Ramprasath VR, Shanthi P, Sachdanandam P (2007). Alteration of DMBA-induced oxidative stress by additive action of a modified indigenous preparation-Kalpaamruthaa. *Chem Biol Interact*; 167: 99-106.
- Aung-Htut MT, Lam YT, Lim YL, Rinnerthaler M, Gelling CL, Yang H, Breitenbach M, Dawes IW (2013). Maintenance of mitochondrial morphology by autophagy and its role in high glucose effects on chronological lifespan of *Saccharomyces cerevisiae*. *Oxid Med Cell Longev*; 2013: 636287.
- Bae H, Guan JL (2011). Suppression of autophagy by FIP200 deletion impairs DNA damage repair and increases cell death upon treatments with anticancer agents. *Mol Cancer Res*; 9: 1232-41.
- Baker DG (1998). Natural pathogens of laboratory mice, rats, and rabbits and their effects on research. *Clin Microbiol Rev*; 11: 231-66.

- Banerjee MR, Wood BG, Lin FK, Crump LR (1976). Organ culture of the whole mammary gland of the mouse. *Tissue Cult Assoc Manual*; 2: 457-61.
- Bavro VN, Sola M, Bracher A, Kneussel M, Betz H, Weissenhorn W (2002). Crystal structure of the GABA(A)-receptor-associated protein, GABARAP. *EMBO Rep*; 3: 183-9.
- Beer HD, Munding C, Dubois N, Mamie C, Hohl D, Werner S (2002). The estrogen-responsive B box protein: a novel regulator of keratinocyte differentiation. *J Biol Chem*; 277: 20740-9.
- Behrends C, Sowa ME, Gygi SP, Harper JW (2010). Network organization of the human autophagy system. *Nature*; 466: 68-76.
- Benjamini Y, Hochberg Y (1995). Controlling the false discovery rate: a practical and powerful approach to multiple testing. *J Roy Statist Soc Ser B*; 57: 289–300.
- Bergamini E, Cavallini G, Donati A, Gori Z (2004). The role of macroautophagy in the ageing process, anti-ageing intervention and age-associated diseases. *Int J Biochem Cell Biol*; 36: 2392-404.
- Betin VM, Lane JD (2009). Caspase cleavage of Atg4D stimulates GABARAP-L1 processing and triggers mitochondrial targeting and apoptosis. *J Cell Sci*; 122: 2554-66.
- Bhutia SK, Mukhopadhyay S, Sinha N, Das DN, Panda PK, Patra SK, Maiti TK, Mandal M, Dent P, Wang XY, Das SK, Sarkar D, Fisher PB (2013). Autophagy: cancer's friend or foe? *Adv Cancer Res*; 118: 61-95.
- Birnbaum D, Sircoulomb F, Imbert J (2009). A reason why the ERBB2 gene is amplified and not mutated in breast cancer. *Cancer Cell Int*; 9: 5.
- Bjorkoy G, Lamark T, Brech A, Outzen H, Perander M, Overvatn A, Stenmark H, Johansen T (2005). p62/SQSTM1 forms protein aggregates degraded by autophagy and has a protective effect on huntingtin-induced cell death. *J Cell Biol*; 171: 603-14.
- Boileau AJ, Pearce RA, Czajkowski C (2005). Tandem subunits effectively constrain GABA_A receptor stoichiometry and recapitulate receptor kinetics but are insensitive to GABA_A receptor-associated protein. *J Neurosci*; 25: 11219-30.
- Botti J, Djavaheri-Mergny M, Pilatte Y, Codogno P (2006). Autophagy signaling and the cogwheels of cancer. *Autophagy*; 2: 67-73.
- Brantley DM, Chen CL, Muraoka RS, Bushdid PB, Bradberry JL, Kittrell F, Medina D, Matrisian LM, Kerr LD, Yull FE (2001). Nuclear factor-kappaB (NF-kappaB) regulates proliferation and branching in mouse mammary epithelium. *Mol Biol Cell*; 12: 1445-55.
- Brown JM, Attardi LD (2005). The role of apoptosis in cancer development and treatment response. *Nat Rev Cancer*; 5: 231-7.
- Bui JD, Schreiber RD. 2007. Cancer immunosurveillance, immunoediting and inflammation: independent or interdependent processes? *Curr Opin Immunol*; 19: 203-208.
- Burchiel SW, Davis DA, Gomez MP, Montano RM, Barton SL, Seamer LC (1990). Inhibition of lymphocyte activation in splenic and gut-associated lymphoid tissues following oral exposure of mice to 7,12-dimethylbenz[a]anthracene. *Toxicol Appl Pharmacol*; 105: 434-42.
- Byun DS, Cho K, Ryu BK, Lee MG, Kang MJ, Kim HR, Chi SG (2003). Hypermethylation of XIAP-associated factor 1, a putative tumor suppressor gene from the 17p13.2 locus, in human gastric adenocarcinomas. *Cancer Res*; 63: 7068-75.

- Cao T, Duprez E, Borden KL, Freemont PS, Etkin LD (1998). Ret finger protein is a normal component of PML nuclear bodies and interacts directly with PML. *J Cell Sci*; 111: 1319-29.
- Cao Y, Bonizzi G, Seagroves TN, Greten FR, Johnson R, Schmidt EV, Karin M (2001). IKKalpha provides an essential link between RANK signaling and cyclin D1 expression during mammary gland development. *Cell*; 107: 763-75.
- Cardiff RD, Gumerlock PH, Soong MM, Dandekar S, Barry PA, Young LJ, Meyers FJ (1988). c-H-ras-1 expression in 7,12-dimethyl benzanthracene-induced Balb/c mouse mammary hyperplasias and their tumors. *Oncogene*; 3: 205-13.
- Caspari T (2000). How to activate p53. *Curr Biol*; 10: R315-7.
- Cecconi F, Levine B (2008). The role of autophagy in mammalian development: cell makeover rather than cell death. *Dev Cell*; 15: 344-57.
- Chaudhary PM, Eby M, Jasmin A, Bookwalter A, Murray J, Hood L (1997). Death receptor 5, a new member of the TNFR family, and DR4 induce FADD-dependent apoptosis and activate the NF-kappaB pathway. *Immunity*; 7: 821-30.
- Chen G, Cizeau J, Vande Velde C, Park JH, Bozek G, Bolton J, Shi L, Dubik D, Greenberg A (1999). Nix and Nip3 form a subfamily of pro-apoptotic mitochondrial proteins. *J Biol Chem*; 274: 7-10.
- Chen L, Wang H, Vicini S, Olsen RW (2000). The gamma-aminobutyric acid type A (GABA_A) receptor-associated protein (GABARAP) promotes GABA_A receptor clustering and modulates the channel kinetics. *Proc Natl Acad Sci USA*; 97: 11557-62.
- Chen ZW, Chang CS, Leil TA, Olcese R, Olsen RW (2005). GABA_A receptor associated protein regulates GABA_A receptor cell-surface number in *Xenopus laevis* oocytes. *Mol Pharmacol*; 68: 152-9.
- Chen ZW, Olsen RW (2007). GABAA receptor associated proteins: a key factor regulating GABAA receptor function. *J Neurochem*; 100: 279-94.
- Chu F, Barkinge J, Hawkins S, Gudi R, Salgia R, Kanteti PV (2005). Expression of Siva-1 protein or its putative amphipathic helical region enhances cisplatin-induced apoptosis in breast cancer cells: effect of elevated levels of BCL-2. *Cancer Res*; 65: 5301-9.
- Ciechanover A (2005). Proteolysis: From the lysosome to ubiquitin and the proteasome. *Nat Rev Mol Cell Biol*; 6: 79-87.
- Clarkson RW, Heeley JL, Chapman R, Aillet F, Hay RT, Wyllie A, Watson CJ (2000). NF-kappaB inhibits apoptosis in murine mammary epithelia. *J Biol Chem*; 275: 12737-42.
- Clement JM, McDermott DF (2009). The high-dose aldesleukin (IL-2) "select" trial: a trial designed to prospectively validate predictive models of response to high-dose IL-2 treatment in patients with metastatic renal cell carcinoma. *Clin Genitourin Cancer*; 7: E7-9.
- Connole MD, Yamaguchi H, Elad D, Hasegawa A, Segal E, Torres-Rodriguez JM (2000). Natural pathogens of laboratory animals and their effects on research. *Med Mycol*; 38: 59-65.
- Coyle JE, Qamar S, Rajashankar KR, Nikolov DB (2002). Structure of GABARAP in two conformations: implications for GABA(A) receptor localization and tubulin binding. *Neuron*; 33: 63-74.

- Cuervo AM, Bergamini E, Brunk UT, Dröge W, French M, Terman A (2005). Autophagy and Aging: The Importance of Maintaining “Clean” Cells. *Autophagy*; 1: 131-40.
- Currier N, Solomon SE, Demicco EG, Chang DL, Farago M, Ying H, Dominguez I, Sonenshein GE, Cardiff RD, Xiao ZX, Sherr DH, Seldin DC (2005). Oncogenic signaling pathways activated in DMBA-induced mouse mammary tumors. *Toxicol Pathol*; 33: 726-37.
- Daido S, Kanzawa T, Yamamoto A, Takeuchi H, Kondo Y, Kondo S (2004). Pivotal role of the cell death factor BNIP3 in ceramide-induced autophagic cell death in malignant glioma cells. *Cancer Res*; 64: 4286-93.
- Dandekar S, Sukumar S, Zarbl H, Young LJ, Cardiff RD (1986). Specific activation of the cellular Harvey-ras oncogene in dimethylbenzanthracene-induced mouse mammary tumors. *Mol Cell Biol*; 6: 4104-8.
- de Assis S, Warri A, Cruz MI, Hilakivi-Clarke L (2010). Changes in mammary gland morphology and breast cancer risk in rats. *J Vis Exp*; (44).
- De Duve C, Wattiaux R (1966). Functions of lysosomes. *Annu Rev Physiol*; 28: 435-92.
- de Oliveira KD, Tedardi MV, Cogliati B, Dagli ML (2013). Higher incidence of lung adenocarcinomas induced by DMBA in connexin 43 heterozygous knockout mice. *Biomed Res Int*; 2013: 618475.
- De Palma M, Mazziere R, Politi LS, Pucci F, Zonari E, Sitia G, Mazzoleni S, Moi D, Venneri MA, Indraccolo S, Falini A, Guidotti LG, Galli R, Naldini L (2008). Tumor-targeted interferon-alpha delivery by Tie2-expressing monocytes inhibits tumor growth and metastasis. *Cancer Cell*; 14: 299-311.
- Dean JH, Ward EC, Murray MJ, Lauer LD, House RV (1985). Mechanisms of dimethylbenzanthracene-induced immunotoxicity. *Clin Physiol Biochem*; 3: 98-110.
- Degenhardt K, Mathew R, Beaudoin B, Bray K, Anderson D, Chen G, Mukherjee C, Shi Y, Gélinas C, Fan Y, Nelson DA, Jin S, White E (2006). Autophagy promotes tumor cell survival and restricts necrosis, inflammation, and tumorigenesis. *Cancer Cell*; 10: 51-64.
- Demaria S, Pilonis KA, Adams S (2011). Cross-Talk of Breast Cancer Cells with the Immune System, *Breast Cancer - Carcinogenesis, Cell Growth and Signalling Pathways*, Prof. Mehmet Gunduz (Ed.), ISBN: 978-953-307-714-7.
- Dengjel J, Schoor O, Fischer R, Reich M, Kraus M, Müller M, Kreymborg K, Altenberend F, Brandenburg J, Kalbacher H, Brock R, Driessen C, Rammensee HG, Stevanovic S (2005). Autophagy promotes MHC class II presentation of peptides from intracellular source proteins. *Proc Natl Acad Sci USA*; 102: 7922-7.
- Denison MS, Nagy SR (2003). Activation of the aryl hydrocarbon receptor by structurally diverse exogenous and endogenous chemicals. *Annu Rev Pharmacol Toxicol*; 43: 309-34.
- DiGiovanni J, Bhatt TS, Walker SE (1993). C57BL/6 mice are resistant to tumor promotion by full thickness skin wounding. *Carcinogenesis*; 14: 319-21.
- Ding WX, Ni HM, Gao W, Hou YF, Melan MA, Chen X, Stolz DB, Shao ZM, Yin XM (2007). Differential effects of endoplasmic reticulum stress-induced autophagy on cell survival. *J Biol Chem*; 282: 4702-10.
- Donohue E, Thomas A, Maurer N, Manisali I, Labouebe MZ, Zisman N, Anderson HJ, Ng SSW, Webb M, Bally M, Roberge M (2013). The autophagy inhibitor Verteporfin

- moderately enhances the antitumor activity of gemcitabine in a pancreatic ductal adenocarcinoma model. *J Cancer*; 4: 585-96.
- Du W, Jiang P, Li N, Mei Y, Wang X, Wen L, Yang X, Wu M (2009). Suppression of p53 activity by Siva1. *Cell Death Differ*; 16: 1493-504.
- Dupont N, Jiang S, Pilli M, Ornatowski W, Bhattacharya D, Deretic V (2011). Autophagy-based unconventional secretory pathway for extracellular delivery of IL-1 β . *EMBO J*; 30: 4701-11.
- Eckert LB, Repasky GA, Ulku AS, McFall A, Zhou H, Sartor CI, Der CJ (2004). Involvement of Ras activation in human breast cancer cell signaling, invasion, and anoikis. *Cancer Res*; 64: 4585-92.
- Elgendy M, Sheridan C, Brumatti G, Martin SJ (2011). Oncogenic Ras-induced expression of Noxa and Beclin-1 promotes autophagic cell death and limits clonogenic survival. *Mol Cell*; 42: 23-35.
- Elliott A, Reiners JJ (2008). Suppression of autophagy enhances the cytotoxicity of the DNA damaging aromatic amine p-anilinoaniline. *Toxicol Appl Pharmacol*; 232: 169-79.
- Ertmer A, Huber V, Gilch S, Yoshimori T, Erfle V, Duyster J, Elsässer HP, Schätzl HM (2007). The anticancer drug imatinib induces cellular autophagy. *Leukemia*; 21: 936-42.
- Ethier SP, Ullrich RL (1982). Induction of mammary tumors in virgin female BALB/c mice by single low doses of 7,12-dimethylbenz[a]anthracene. *J Natl Cancer Inst*; 69: 1199-203.
- Fan C, Wang W, Zhao B, Zhang S, Miao J (2006). Chloroquine inhibits cell growth and induces cell death in A549 lung cancer cells. *Bioorg Med Chem*; 14: 3218-22.
- Fei P, Wang W, Kim SH, Wang S, Burns TF, Sax JK, Buzzai M, Dicker DT, McKenna WG, Bernhard EJ, El-Deiry WS (2004). Bnip3L is induced by p53 under hypoxia, and its knockdown promotes tumor growth. *Cancer Cell*; 6: 597-609.
- Feng Y, He D, Yao Z, Klionsky DJ (2014). The machinery of macroautophagy. *Cell Research*; 24: 24-41.
- Feng Z, Hu W, de Stanchina E, Teresky AK, Jin S, Lowe S, Levine AJ (2007). The regulation of AMPK beta1, TSC2, and PTEN expression by p53: stress, cell and tissue specificity, and the role of these gene products in modulating the IGF-1–AKT–mTOR pathways. *Cancer Res*; 67: 3043-53.
- Finn OJ (2008). Cancer immunology. *N Engl J Med*; 358: 2704-15.
- Firat E, Weyerbrock A, Gaedicke S, Grosu AL, Niedermann G (2012). Chloroquine or chloroquine-PI3K/Akt pathway inhibitor combinations strongly promote γ -irradiation-induced cell death in primary stem-like glioma cells. *PLoS One*; 7: e47357.
- Fleige S, Pfaffl MW (2006). RNA integrity and the effect on the real-time qRT-PCR performance. *Mol Aspects Med*; 27: 126-39.
- Fong WG, Liston P, Rajcan-Separovic E, St Jean M, Craig C, Korneluk RG (2000). Expression and genetic analysis of XIAP-associated factor 1 (XAF1) in cancer cell lines. *Genomics*; 70: 113-22.
- Frenkel K, Wei L, Wei H (1995). 7,12-dimethylbenz[a]anthracene induces oxidative DNA modification *in vivo*. *Free Radic Biol Med*; 19: 373-80.
- Freshney RI (2005). Culture of animal cells: A manual of basic technique. (5th edition) John Wiley & Sons, Inc., New York. Pages: 176-199.

- Funderburk SF, Wang QJ, Yue Z (2010). The Beclin 1-VPS34 complex - at the crossroads of autophagy and beyond. *Trends Cell Biol*; 20: 355-62.
- Fung C, Lock R, Gao S, Salas E, Debnath J (2008). Induction of autophagy during extracellular matrix detachment promotes cell survival. *Mol Biol Cell*; 19: 797-806.
- Galluzzi L, Kepp O, Kroemer G (2012). Mitochondria: master regulators of danger signalling. *Nat Rev Mol Cell Biol*; 13: 780-8.
- Galonek HL, Hardwick JM (2006). Upgrading the BCL-2 network. *Nat Cell Biol*; 8: 1317-9.
- Ganesan S, Bhattacharya P, Keating AF (2013). 7,12-Dimethylbenz(a)anthracene exposure induces the DNA repair response in neonatal rat ovaries. *Toxicol Appl Pharmacol*; 272:690-6.
- Gannage M, Münz C (2010). MHC presentation via autophagy and how viruses escape from it. *Semin Immunopathol*; 32: 373-81.
- Gao J, Lauer FT, Dunaway S, Burchiel SW (2005). Cytochrome P450 1B1 is required for 7,12-dimethylbenz(a)-anthracene (DMBA) induced spleen cell immunotoxicity. *Toxicol Sci*; 86: 68-74.
- Gao J, Lauer FT, Mitchell LA, Burchiel SW (2007). Microsomal epoxide hydrolase is required for 7,12-dimethylbenz[a]anthracene (DMBA)-induced immunotoxicity in mice. *Toxicol Sci*; 98: 137-44.
- Gao J, Mitchell LA, Lauer FT, Burchiel SW (2008). p53 and ATM/ATR regulate 7,12-dimethylbenz[a]anthracene-induced immunosuppression. *Mol Pharmacol*; 73: 137-46.
- Garg AD, Nowis D, Golab J, Vandenabeele P, Krysko DV, Agostinis P (2010). Immunogenic cell death, DAMPs and anticancer therapeutics: an emerging amalgamation. *Biochim Biophys Acta*; 1805: 53-71.
- Garg AD, Dudek AM, Ferreira GB, Verfaillie T, Vandenabeele P, Krysko DV, Mathieu C, Agostinis P (2013). ROS-induced autophagy in cancer cells assists in evasion from determinants of immunogenic cell death. *Autophagy*; 9: 1292-307.
- Gelboin HV (1980). Benzo[alpha]pyrene metabolism, activation and carcinogenesis: role and regulation of mixed-function oxidases and related enzymes. *Physiol Rev*; 60: 1107-66.
- Gooch JL, Herrera RE, Yee D. 2000. The role of p21 in interferon-mediated growth inhibition of human breast cancer cells. *Cell Growth Differ*; 11: 335-42.
- Goth R, Rajewsky MF (1974). Persistence of O6-ethylguanine in rat-brain DNA: correlation with nervous system-specific carcinogenesis by ethylnitrosourea. *Proc Natl Acad Sci U S A*; 71: 639-43.
- Green DR, Evan GI (2002). A matter of life and death. *Cancer Cell*; 1: 19-30.
- Green DR (2005). Apoptotic pathways: ten minutes to dead. *Cell*; 121: 671-4.
- Green F, O'Hare T, Blackwell A, Enns CA (2002). Association of human transferrin receptor with GABARAP. *FEBS Lett*; 518: 101-6.
- Guo JY, Chen HY, Mathew R, Fan J, Strohecker AM, Karsli-Uzunbas G, Kamphorst JJ, Chen G, Lemons JMS, Karantza V, Collier HA, DiPaola RS, Gelinas C, Rabinowitz JD, White E (2011). Activated Ras requires autophagy to maintain oxidative metabolism and tumorigenesis. *Genes Dev*; 25: 460-70.
- Gyorki DE, Lindeman GJ (2008). Macrophages, more than just scavengers: their role in breast development and cancer. *ANZ J Surg*; 78: 432-6.

- Halama N, Zoernig I, Jaeger D (2010). Advanced malignant melanoma: immunologic and multimodal therapeutic strategies. *J Oncol*; 2010: 689893.
- Hamacher-Brady A, Brady NR, Logue SE, Sayen MR, Jinno M, Kirshenbaum LA, Gottlieb RA, Gustafsson AB (2007). Response to myocardial ischemia/reperfusion injury involves Bnip3 and autophagy. *Cell Death Differ*; 14: 146-57.
- Hanada T, Noda N, Satomi Y, Ichimura Y, Fujioka Y, Takao T, Inagaki F, Ohsumi Y (2007). The Atg12-Atg5 conjugate has a novel E3-like activity for protein lipidation in autophagy. *J Biol Chem*; 282: 37298-302.
- Hanahan D, Weinberg RA (2011). Hallmarks of cancer: the next generation. *Cell*; 144: 646-74.
- Hara T, Nakamura K, Matsui M, Yamamoto A, Nakahara Y, Suzuki-Migishima R, Yokoyama M, Mishima K, Saito I, Okano H, Mizushima N (2006). Suppression of basal autophagy in neural cells causes neurodegenerative disease in mice. *Nature*; 441: 885-9.
- Hay N, Sonenberg N (2004). Upstream and downstream of mTOR. *Genes Dev*; 18: 1926-45.
- Hayashi-Nishino M, Fujita N, Noda T, Yamaguchi A, Yoshimori T, Yamamoto A (2009). A subdomain of the endoplasmic reticulum forms a cradle for autophagosome formation. *Nat Cell Biol*; 11: 1433-37.
- Heidel SM, Holston HK, Buters JTM, Gonzalez FJ, Jefcoate CR and Czuprynski CJ (1999). Bone marrow stromal cell cytochrome P4501B1 is required for pre-B cell apoptosis induced by 7,12 dimethylbenz[a]anthracene. *Mol Pharmacol*; 56: 1317-23.
- Henkler F, Stolpmann K, Luch A (2012). Exposure to polycyclic aromatic hydrocarbons: bulky DNA adducts and cellular responses. *EXS*; 101: 107-31.
- Hennings H, Glick AB, Lowry DT, Krsmanovic LS, Sly LM, Yuspa SH (1993). FVB/N mice: an inbred strain sensitive to the chemical induction of squamous cell carcinomas in the skin. *Carcinogenesis*; 14: 2353-8.
- Hickman ES, Moroni MC, and Helin K (2002). The role of p53 and pRB in apoptosis and cancer. *Curr Opin Genet Dev*; 12: 60-6.
- Hochstrasser M (2000). Biochemistry. All in the ubiquitin family. *Science*; 289: 563-4.
- Hoenerhoff MJ, Hong HH, Ton TV, Lahousse SA, Sills RC (2009). A review of the molecular mechanisms of chemically induced neoplasia in rat and mouse models in National Toxicology Program bioassays and their relevance to human cancer. *Toxicol Pathol*; 37: 835-48.
- Hotchkiss RS, Karl IE (2003). The pathophysiology and treatment of sepsis. *N Engl J Med*; 348: 138-50.
- Hou W, Han J, Lu C, Goldstein LA, Rabinowich H (2010). Autophagic degradation of active caspase-8: a crosstalk mechanism between autophagy and apoptosis. *Autophagy*; 6: 891-900.
- House RV, Lauer LD, Murray MJ, Dean JH (1987). Suppression of T-helper cell function in mice following exposure to the carcinogen 7,12-dimethylbenz[a]anthracene and its restoration by interleukin-2. *Int J Immunopharmacol*; 9: 89-97.
- Hsiang YH, Hertzberg R, Hecht S, Liu LF (1985). Camptothecin induces protein-linked DNA breaks via mammalian DNA topoisomerase I. *J Biol Chem*; 260: 14873-8.

- Hsiang YH, Liu LF (1988). Identification of mammalian DNA topoisomerase I as an intracellular target of the anticancer drug camptothecin. *Cancer Res*; 48: 1722-6.
- Huang J, Yao WY, Zhu Q, Tu SP, Yuan F, Wang HF, Zhang YP, Yuan YZ (2010). XAF1 as a prognostic biomarker and therapeutic target in pancreatic cancer. *Cancer Sci*; 101: 559-67.
- Huang J, Lam GY, Brumell JH (2011). Autophagy signaling through reactive oxygen species. *Antioxid Redox Signal*; 14: 2215-31.
- Huang Q, Shen HM (2009). To die or to live: the dual role of poly(ADP-ribose) polymerase-1 in autophagy and necrosis under oxidative stress and DNA damage. *Autophagy*; 5: 273-6.
- Huang S, Okamoto K, Yu C, Sinicrope FA (2013). p62/sequestosome-1 up-regulation promotes ABT-263-induced caspase-8 aggregation/activation on the autophagosome. *J Biol Chem*; 288: 33654-66.
- Huang X, Wu Z, Mei Y, Wu M (2013). XIAP inhibits autophagy via XIAP-Mdm2-p53 signalling. *EMBO J*; 32: 2204-16.
- Hui X, Zhu W, Wang Y, Lam KS, Zhang J, Wu D, Kraegen EW, Li Y, Xu A (2009). Major urinary protein-1 increases energy expenditure and improves glucose intolerance through enhancing mitochondrial function in skeletal muscle of diabetic mice. *J Biol Chem*; 284: 14050-7.
- Ichimura Y, Kirisako T, Takao T, Satomi Y, Shimonishi Y, Ishihara N, Mizushima N, Tanida I, Kominami E, Ohsumi M, Noda T, Ohsumi Y (2000). A ubiquitinlike system mediates protein lipidation. *Nature*; 408: 488-92.
- Ieguchi K, Ueda S, Kataoka T, Satoh T (2007). Role of the Guanine Nucleotide Exchange Factor Ost in Negative Regulation of Receptor Endocytosis by the Small GTPase Rac1. *J Biol Chem*; 282: 23296-305.
- Igney FH, Krammer PH (2002). Death and anti-death: tumour resistance to apoptosis. *Nat Rev Cancer*; 2: 277-88.
- Imazu T, Shimizu S, Tagami S, Matsushima M, Nakamura Y, Miki T, Okuyama A, Tsujimoto Y (1999). Bcl-2/E1B 19 kDa-interacting protein 3-like protein (Bnip3L) interacts with bcl-2/Bcl-xL and induces apoptosis by altering mitochondrial membrane permeability. *Oncogene*; 18: 4523-9.
- Jacks T, Remington L, Williams BO, Schmitt EM, Halachmi S, Bronson RT, Weinberg RA (1994). Tumor spectrum analysis in p53-mutant mice. *Curr Biol*; 4: 1-7.
- Jackson AF, Williams A, Moffat I, Phillips SL, Recio L, Waters MD, Lambert IB, Yauk CL (2013). Preparation of archival formalin-fixed paraffin-embedded mouse liver samples for use with the Agilent gene expression microarray platform. *J Pharmacol Toxicol Methods*; 68: 260-8.
- Jung CH, Jun CB, Ro SH, Kim YM, Otto NM, Cao J, Kundu M, Kim DH (2009). ULK-Atg13-FIP200 complexes mediate mTOR signaling to the autophagy machinery. *Mol Biol Cell*; 20: 1992-2003.
- Kabeya Y, Mizushima N, Yamamoto A, Oshitani-Okamoto S, Ohsumi Y, Yoshimori T (2004). LC3, GABARAP and GATE16 localize to autophagosomal membrane depending on form-II formation. *J Cell Sci*; 117: 2805-12.
- Kalluri R, Weinberg RA (2009). The basics of epithelial-mesenchymal transition. *J Clin Invest*; 119: 1420-8.

- Kanematsu T, Jang I, Yamaguchi T, Nagahama H, Yoshimura K, Hidaka K, Matsuda M, Takeuchi H, Misumi Y, Nakayama K, Yamamoto T, Akaike N, Hirata M, Nakayama K (2002). Role of the PLC-related, catalytically inactive protein p130 in GABA(A) receptor function. *EMBO J*; 21: 1004-11.
- Kang KB, Zhu C, Yong SK, Gao Q, Wong MC (2009). Enhanced sensitivity of celecoxib in human glioblastoma cells: Induction of DNA damage leading to p53-dependent G1 cell cycle arrest and autophagy. *Mol Cancer*; 8:66.
- Kang R, Zeh HJ, Lotze MT, Tang D (2011). The Beclin 1 network regulates autophagy and apoptosis. *Cell Death Differ*; 18: 571-80.
- Karantza-Wadsworth V, Patel S, Kravchuk O, Chen G, Mathew R, Jin S, White E (2007). Autophagy mitigates metabolic stress and genome damage in mammary tumorigenesis. *Genes Dev*; 21: 1621-35.
- Katayama M, Kawaguchi T, Berger MS, Pieper RO (2007). DNA damaging agent-induced autophagy produces a cytoprotective adenosine triphosphate surge in malignant glioma cells. *Cell Death Differ*; 14: 548-58.
- Kempkensteffen C, Hinz S, Schrader M, Christoph F, Magheli A, Krause H, Schostak M, Miller K, Weikert S (2007). Gene expression and promoter methylation of the XIAP-associated Factor 1 in renal cell carcinomas: correlations with pathology and outcome. *Cancer Lett*; 254: 227-35.
- Kielian TL, Blecha F (1995). CD14 and other recognition molecules for lipopolysaccharide: a review. *Immunopharmacology*; 29: 187-205.
- Kim DH, Sarbassov DD, Ali SM, King JE, Latek RR, Erdjument-Bromage H, Tempst P, Sabatini DM (2002). mTOR interacts with raptor to form a nutrient-sensitive complex that signals to the cell growth machinery. *Cell*; 110: 163-75.
- Kim DW, Sovak MA, Zanieski G, Nonet G, Romieu-Mourez R, Lau AW, Hafer LJ, Yaswen P, Stampfer M, Rogers AE, Russo J, Sonenshein GE (2000). Activation of NF-kappaB/Rel occurs early during neoplastic transformation of mammary cells. *Carcinogenesis*; 21: 871-9.
- Kim J, Huang WP, Stromhaug PE, Klionsky DJ (2002). Convergence of multiple autophagy and cytoplasm to vacuole targeting components to a perivacuolar membrane compartment prior to de novo vesicle formation. *J Biol Chem*; 277: 763-73.
- Kim JW, Dang CV (2006). Cancer's molecular sweet tooth and the Warburg effect. *Cancer Res*; 66: 8927-30.
- Kim MJ, Woo SJ, Yoon CH, Lee JS, An S, Choi YH, Hwang SG, Yoon G, Lee SJ (2011). Involvement of autophagy in oncogenic K-Ras-induced malignant cell transformation. *J Biol Chem*; 286: 12924-32.
- Kim PK, Hailey DW, Mullen RT, Lippincott-Schwartz J (2008). Ubiquitin signals autophagic degradation of cytosolic proteins and peroxisomes. *Proc Natl Acad Sci USA*; 105: 20567-74.
- Kinner A, Wu W, Staudt C, Iliakis G (2008). Gamma-H2AX in recognition and signaling of DNA double-strand breaks in the context of chromatin. *Nucleic Acids Res*; 36: 5678-94.
- Kirisako T, Baba M, Ishihara N, Miyazawa K, Ohsumi M, Yoshimori T, Noda T, Ohsumi Y (1999). Formation process of autophagosome is traced with Apg8/Aut7p in yeast. *J Cell Biol*; 147: 435-46.

- Kirisako T, Ichimura Y, Okada H, Kabeya Y, Mizushima N, Yoshimori T, Ohsumi M, Takao T, Noda T, Ohsumi Y (2000). The reversible modification regulates the membrane-binding state of Apg8/Aut7 essential for autophagy and the cytoplasm to vacuole targeting pathway. *J Cell Biol*; 151: 263-76.
- Kirkin V, Lamark T, Sou YS, Bjorkoy G, Nunn JL, Bruun JA, Shvets E, McEwan DG, Clausen TH, Wild P, Bilusic I, Theurillat JP, Overvatn A, Ishii T, Elazar Z, Komatsu M, Dikic I, Johansen T (2009). A role for NBR1 in autophagosomal degradation of ubiquitinated substrates. *Mol Cell*; 33: 505-16.
- Kittler JT, Rostaing P, Schiavo G (2001) The subcellular distribution of GABARAP and its ability to interact with NSF suggest a role for this protein in the intracellular transport of GABA_A receptors. *Mol Cell Neurosci*; 18: 13-25.
- Kittler JT, Arancibia-Carcamo IL, Moss SJ (2004). Association of GRIP1 with a GABA_A receptor associated protein suggests a role for GRIP1 at inhibitory synapses. *Biochem Pharmacol*; 68: 1649-54.
- Klebig C, Seitz S, Arnold W, Deutschmann N, Pacyna-Gengelbach M, Scherneck S, Petersen I (2005). Characterization of γ -aminobutyric acid type A receptor-associated protein, a novel tumor suppressor, showing reduced expression in breast cancer. *Cancer Res*; 65: 394-400.
- Klionsky DJ, Emr SD (2000). Autophagy as a regulated pathway of cellular degradation. *Science*; 290: 1717-21.
- Klionsky DJ, Cregg JM, Dunn WA, Emr SD, Sakai Y, Sandoval IV, Sibirny A, Subramani S, Thumm M, Veenhuis M, Ohsumi Y (2003). A unified nomenclature for yeast autophagy related genes. *Dev Cell*; 5: 539-45.
- Klos KS, Kim S, Alexander CM (2012). Genotoxic exposure during juvenile growth of mammary gland depletes stem cell activity and inhibits Wnt signaling. *PLoS One*; 7: e49902.
- Koebel CM, Vermi W, Swann JB, Zerafa N, Rodig SJ, Old LJ, Smyth MJ, Schreiber RD (2007). Adaptive immunity maintains occult cancer in an equilibrium state. *Nature*; 450: 903-7.
- Komatsu M, Waguri S, Chiba T, Murata S, Iwata J, Tanida I, Ueno T, Koike M, Uchiyama Y, Kominami E, Tanaka K (2006). Loss of autophagy in the central nervous system causes neurodegeneration in mice. *Nature*; 441: 880-4.
- Komatsu M, Waguri S, Koike M, Sou YS, Ueno T, Hara T, Mizushima N, Iwata J, Ezaki J, Murata Sh, Hamazaki J, Nishito Y, Iemura S, Natsume T, Yanagawa T, Uwayama J, Warabi E, Yoshida H, Ishii T, Kobayashi A, Yamamoto M, Yue Z, Uchiyama Y, Kominami E, Tanaka K (2007). Homeostatic levels of p62 control cytoplasmic inclusion body formation in autophagy deficient mice. *Cell*; 131: 1149-63.
- Kondo Y, Kondo S (2006). Autophagy and cancer therapy. *Autophagy*; 2: 85-90.
- Kroemer G, Levine B (2008). Autophagic cell death: the story of a misnomer. *Nat Rev Mol Cell Biol*; 9: 1004-10.
- Kroemer G, Mariño G, Levine B (2010). Autophagy and the integrated stress response. *Mol Cell*; 40: 280-93.
- Kuma A, Hatano M, Matsui M, Yamamoto A, Nakaya H, Yoshimori T, Ohsumi Y, Tokuhiisa T, Mizushima N (2004). The role of autophagy during the early neonatal starvation period. *Nature*; 432:1032-6.

- Lallemand-Breitenbach V, de Thé H (2010). PML nuclear bodies. *Cold Spring Harb Perspect Biol*; 2: a000661.
- Laplante M, Sabatini DM (2009). mTOR signaling at a glance. *J Cell Sci*; 122: 3589-94.
- Leaman DW, Chawla-Sarkar M, Vyas K, Reheman M, Tamai K, Toji S, Borden EC (2002). Identification of X-linked inhibitor of apoptosis-associated factor-1 as an interferon-stimulated gene that augments TRAIL Apo2L-induced apoptosis. *J Biol Chem*; 277: 28504-11.
- Lee JH, Rho SB, Chun T (2005). GABAA receptor associated protein (GABARAP) induces apoptosis by interacting with DEAD (Asp-Glu-Ala-Asp / His) box polypeptide 47 (DDX 47). *Biotechnol Lett*; 27: 623-8.
- Lee MG, Huh JS, Chung SK, Lee JH, Byun DS, Ryu BK, Kang MJ, Chae KS, Lee SJ, Lee CH, Kim JI, Chang SG, Chi SG (2006). Promoter CpG hypermethylation and downregulation of XAF1 expression in human urogenital malignancies: implication for attenuated p53 response to apoptotic stresses. *Oncogene*; 25: 5807-22.
- Leil TA, Chen ZW, Chang CS, Olsen RW (2004). GABA_A receptor-associated protein traffics GABA_A receptors to the plasma membrane in neurons. *J Neurosci*; 24: 11429-38.
- Levine B (2007). Cell biology: autophagy and cancer. *Nature*; 446: 745-47.
- Levine B, Kroemer G (2008). Autophagy in the pathogenesis of disease. *Cell*; 132: 27-42.
- Levine B, Sinha S, Kroemer G (2008). Bcl-2 family members: dual regulators of apoptosis and autophagy. *Autophagy*; 4: 600-6.
- Levine B, Mizushima N, Virgin HW (2011). Autophagy in immunity and inflammation. *Nature*; 469: 323-35.
- Li J, Hou N, Faried A, Tsutsumi S, Kuwano H (2010). Inhibition of autophagy augments 5-fluorouracil chemotherapy in human colon cancer *in vitro* and *in vivo* model. *Eur J Cancer*; 46: 1900-9.
- Li N, Jiang P, Du W, Wu Z, Li C, Qiao M, Yang X, Wu M (2011). Siva1 suppresses epithelial-mesenchymal transition and metastasis of tumor cells by inhibiting stathmin and stabilizing microtubules. *Proc Natl Acad Sci USA*; 108: 12851-6.
- Li Y, Wang LX, Yang G, Hao F, Urba WJ, Hu HM (2008). Efficient cross-presentation depends on autophagy in tumor cells. *Cancer Res*; 68: 6889-95.
- Li Y, Wang LX, Pang P, Cui Z, Aung S, Haley D, Fox BA, Urba WJ, Hu HM (2011). Tumor-derived autophagosome vaccine: mechanism of cross-presentation and therapeutic efficacy. *Clin Cancer Res*; 17: 7047-57.
- Liang X, De Vera ME, Buchser WJ, Romo de Vivar Chavez A, Loughran P, Beer Stolz D, Basse P, Wang T, Van Houten B, Zeh HJ 3rd, Lotze MT (2012). Inhibiting systemic autophagy during interleukin 2 immunotherapy promotes long-term tumor regression. *Cancer Res*; 72: 2791-801.
- Liao W, Lin JX, Leonard WJ (2011). IL-2 family cytokines: new insights into the complex roles of IL-2 as a broad regulator of T helper cell differentiation. *Curr Opin Immunol*; 23: 598-604.
- Lin CP, Ban Y, Lyu YL, Desai SD, Liu LF (2008). A ubiquitin-proteasome pathway for the repair of topoisomerase I-DNA covalent complexes. *J Biol Chem*; 283: 21074-83.

- Liston P, Fong WG, Kelly NL, Toji S, Miyazaki T, Conte D, Tamai K, Craig CG, McBurney MW, Korneluk RG (2001). Identification of XAF1 as an antagonist of XIAP anti-Caspase activity. *Nat Cell Biol*; 3: 128-33.
- Liu B, Bao J, Yang J, Cheng Y (2012a). Targeting autophagic pathways for cancer drug discovery. *Chin J Cancer*; 32: 113-20.
- Liu F, Lee JY, Wei H, Tanabe O, Engel JD, Morrison SJ, Guan JL (2010). FIP200 is required for the cell-autonomous maintenance of fetal hematopoietic stem cells. *Blood*; 116: 4806-14.
- Liu J, Xia H, Kim M, Xu L, Li Y, Zhang L, Cai Y, Norberg HV, Zhang T, Furuya T, Jin M, Zhu Z, Wang H, Yu J, Li Y, Hao Y, Choi A, Ke H, Ma D, Yuan J (2011). Beclin1 controls the levels of p53 by regulating the deubiquitination activity of USP10 and USP13. *Cell*; 147: 223-34.
- Liu SY, Chen CL, Yang TT, Huang WC, Hsieh CY, Shen WJ, Tsai TT, Shieh CC, Lin CF (2012b). Albumin prevents reactive oxygen species-induced mitochondrial damage, autophagy, and apoptosis during serum starvation. *Apoptosis*; 17: 1156-69.
- Liu X, Huang Y, Yang D, Li X, Liang J, Lin L, Zhang M, Zhong K, Liang B, Li J (2014). Overexpression of TRIM24 is associated with the onset and progress of human hepatocellular carcinoma. *PLoS One*; 9: e85462.
- Lock R, Roy S, Kenific CM, Su JS, Salas E, Ronen SM, Debnath J (2011). Autophagy facilitates glycolysis during Ras-mediated oncogenic transformation. *Mol Biol Cell*; 22: 165-78.
- Lorina S, Hamaïb A, Mehrpourb M, Codognob P (2013). Autophagy regulation and its role in cancer. *Semin Cancer Biol*; 23: 361-79.
- Lozy F, Karantzaa V (2012). Autophagy and cancer cell metabolism. *Semin Cell Dev Biol*; 23: 395-401.
- Luch A (2005). Nature and nurture - lessons from chemical carcinogenesis. *Nat Rev Cancer*; 5: 113-25.
- Luo J, Solimini NL, Elledge SJ (2009). Principles of cancer therapy: oncogene and non-oncogene addiction. *Cell*; 136: 823-37.
- Ma TL, Ni PH, Zhong J, Tan JH, Qiao MM, Jiang SH (2005). Low expression of XIAP-associated factor 1 in human colorectal cancers. *Chin J Dig Dis*; 6: 10-4.
- Maes H, Rubio N, Garg AD, Agostinis P (2013). Autophagy: shaping the tumor microenvironment and therapeutic response. *Trends Mol Med*; 19: 428-46.
- Maiuri MC, Le Toumelin G, Criollo A, Rain JC, Gautier F, Juin P, Tasdemir E, Pierron G, Troulinaki K, Tavernarakis N, Hickman JA, Geneste O, Kroemer G (2007a). Functional and physical interaction between Bcl-X(L) and a BH3-like domain in Beclin-1. *EMBO J*; 26: 2527-39.
- Maiuri MC, Criollo A, Tasdemir E, Vicencio JM, Tajeddine N, Hickman JA, Geneste O, Kroemer G (2007b). BH3-only proteins and BH3 mimetics induce autophagy by competitively disrupting the interaction between Beclin 1 and Bcl-2/Bcl-X(L). *Autophagy*; 3: 374-6.
- Malmgren RA, Benneson BE, McKinley TW (1952). Reduced antibody titers in mice treated with carcinogenic and cancer chemotherapeutic agents. *Proc Soc Exp Biol Med*; 79: 484-8.

- Mantovani A, Allavena P, Sica A, Balkwill F (2008). Cancer-related inflammation. *Nature*; 454: 436-44.
- Marino G, Uria JA, Puente XS, Quesada V, Bordallo J, Lopez-Otin C (2003). Human autophagins, a family of cysteine proteinases potentially implicated in cell degradation by autophagy. *J Biol Chem*; 278: 3671-8.
- Marino G, Salvador-Montoliu N, Fueyo A, Knecht E, Mizushima N, Lopez-Otin C (2007). Tissue-specific autophagy alterations and increased tumorigenesis in mice deficient in Atg4C/autophagin-3. *J Biol Chem*; 282: 18573-83.
- Marquez RT, Xu L (2012). Bcl-2:beclin-1 complex: multiple, mechanisms regulating autophagy/apoptosis toggle switch. *Am J Cancer Res*; 2: 214-21.
- Marshall GM, Bell JL, Koach J, Tan O, Kim P, Malyukova A, Thomas W, Sekyere EO, Liu T, Cunningham AM, Tobias V, Norris MD, Haber M, Kavallaris M, Cheung BB (2010). TRIM16 acts as a tumour suppressor by inhibitory effects on cytoplasmic vimentin and nuclear E2F1 in neuroblastoma cells. *Oncogene*; 29: 6172-83.
- Martinez-Outschoorn UE, Trimmer C, Lin Z, Whitaker-Menezes D, Chiavarina B, Zhou J, Wang C, Pavlides S, Martinez-Cantarín MP, Capozza F, Witkiewicz AK, Flomenberg N, Howell A, Pestell RG, Caro J, Lisanti MP, Sotgia F (2010). Autophagy in cancer associated fibroblasts promotes tumor cell survival: Role of hypoxia, HIF1 induction and NFκB activation in the tumor stromal microenvironment. *Cell Cycle*; 9: 3515-33.
- Martinez-Vicente M, Sovak G, Cuervo AM (2005). Protein degradation and aging. *Exp Gerontol*; 40: 622-33.
- Mathew R, Karantza-Wadsworth V, White E (2007). Role of autophagy in cancer. *Nat Rev Cancer*; 7: 961-67.
- Mathew R, Karp CM, Beaudoin B, Vuong N, Chen G, Chen HY, Bray K, Reddy A, Bhanot G, Gelinas C, DiPaola RS, Karantza-Wadsworth V, White E (2009). Autophagy suppresses tumorigenesis through elimination of p62. *Cell*; 137: 1062-75.
- Mathew SJ, Haubert D, Krönke M, Leptin M (2009). Looking beyond death: a morphogenetic role for the TNF signalling pathway. *J Cell Sci*; 122: 1939-46.
- Matsuura A, Tsukada M, Wada Y, Ohsumi Y (1997). Apg1p, a novel protein kinase required for the autophagic process in *Saccharomyces cerevisiae*. *Gene*; 192: 245-50.
- Medina D (1974). Mammary tumorigenesis in chemical carcinogen-treated mice. I. Incidence in BALB-c and C57BL mice. *J Natl Cancer Inst*; 53: 213-21.
- Medina D (1996). The mammary gland: a unique organ for the study of development and tumorigenesis. *J Mammary Gland Biol Neoplasia*; 1: 5-19.
- Medina D (2007). Chemical carcinogenesis of rat and mouse mammary glands. *Breast Dis*; 28: 63-8.
- Medina D (2010). Of mice and women: A short history of mouse mammary cancer research with an emphasis on the paradigms inspired by the transplantation method. *Cold Spring Harb Perspect Biol*; 2: a004523.
- Mehrpour M, Esclatine A, Beau I, Codogno P (2010). Overview of macroautophagy regulation in mammalian cells. *Cell Research*; 20: 748-62.
- Melendez A, Talloczy Z, Seaman M, Eskelinen EL, Hall DH, Levine B (2003). Autophagy genes are essential for dauer development and life-span extension in *C. elegans*. *Science*; 301: 1387-91.

- Meng F, Lowell CA (1997). Lipopolysaccharide (LPS)-induced macrophage activation and signal transduction in the absence of Src-family kinases Hck, Fgr, and Lyn. *J Exp Med*; 185: 1661-70.
- Meroni G, Diez-Roux G (2005). TRIM/RBCC, a novel class of 'single protein RING finger' E3 ubiquitin ligases. *Bioessays*; 27: 1147-57.
- Miao Y, Zhang Y, Chen Y, Chen L, Wang F (2010). GABARAP is overexpressed in colorectal carcinoma and correlates with shortened patient survival. *Hepatogastroenterology*; 57: 257-61.
- Micali OC, Cheung HH, Plenchette S, Hurley SL, Liston P, LaCasse EC, Korneluk RG (2007). Silencing of the XAF1 gene by promoter hypermethylation in cancer cells and reactivation to TRAIL-sensitization by IFN-beta. *BMC Cancer*; 7: 52.
- Michaud M, Martins I, Sukkurwala AQ, Adjemian S, Ma Y, Pellegatti P, Shen S, Kepp O, Scoazec M, Mignot G, Rello-Varona S, Tailler M, Menger L, Vacchelli E, Galluzzi L, Ghiringhelli F, di Virgilio F, Zitvogel L, Kroemer G (2011). Autophagy-dependent anticancer immune responses induced by chemotherapeutic agents in mice. *Science*; 334: 1573-7.
- Miyata M, Furukawa M, Takahashi K, Gonzalez FJ, Yamazoe Y (2001). Mechanism of 7,12-dimethylbenz[a]anthracene-induced immunotoxicity: role of metabolic activation at the target organ. *Jpn J Pharmacol*; 86: 302-9.
- Mizushima N, Levine B, Cuervo AM, Klionsky DJ (2008). Autophagy fights disease through cellular self-digestion. *Nature*; 451: 1069-75.
- Mizushima N, Levine B (2010). Autophagy in mammalian development and differentiation. *Nat Cell Biol*; 12: 823-30.
- Mizushima N, Komatsu M (2011). Autophagy: Renovation of cells and tissues. *Cell*; 147: 728-41.
- Mohrlüder J, Stangler T, Hoffmann Y, Wiesehan K, Mataruga A, Willbold D (2007). Identification of calreticulin as a ligand of GABARAP by phage display screening of a peptide library. *FEBS J*; 274: 5543-55.
- Mohrlüder J, Schwarten M, Willbold D (2009). Structure and potential function of γ -aminobutyrate type A receptor-associated protein. *FEBS J*; 276: 4989-5005.
- Morgan DA, Ruscetti FW, Gallo R (1976). Selective *in vitro* growth of T lymphocytes from normal human bone marrows. *Science*; 193: 1007-8.
- Moscat J, Diaz-Meco MT (2009). p62 at the crossroads of autophagy, apoptosis, and cancer. *Cell*; 137: 1001-4.
- Mukhopadhyay S, Panda PK, Sinha N, Das DN, Bhutia SK (2014). Autophagy and apoptosis: where do they meet? *Apoptosis*; 19: 555-66.
- Munoz-Gamez JA, Rodriguez-Vargas JM, Quiles-Perez R, Aguilar-Quesada R, Martin-Oliva D, de Murcia G, Menissier de Murcia J, Almendros A, Ruiz de Almodovar M, Oliver FJ (2009). PARP-1 is involved in autophagy induced by DNA damage. *Autophagy*; 5: 61-74.
- Muqbil I, Azmi AS, Banu N (2006). Prior exposure to restraint stress enhances 7,12-dimethylbenz(a)anthracene (DMBA) induced DNA damage in rats. *FEBS Lett*; 580: 3995-9.

- Murrow L, Debnath J (2013). Autophagy as a stress-response and quality-control mechanism: implications for cell injury and human disease. *Annu Rev Pathol*; 8: 105-37.
- Nakagawa I, Amano A, Mizushima N, Yamamoto A, Yamaguchi H, Kamimoto T, Nara A, Funao J, Nakata M, Tsuda K, Hamada S, Yoshimori T (2004). Autophagy defends cells against invading group A *Streptococcus*. *Science*; 306: 1037-40.
- Nakahira K, Haspel JA, Rathinam VA, Lee SJ, Dolinay T, Lam HC, Englert JA, Rabinovitch M, Cernadas M, Kim HP, Fitzgerald KA, Ryter SW, Choi AM (2011). Autophagy proteins regulate innate immune responses by inhibiting the release of mitochondrial DNA mediated by the Nalp3 inflammasome. *Nat Immunol*; 12: 222-30.
- Nakatogawa H, Ichimura Y, Ohsumi Y (2007). Atg8, a ubiquitin-like protein required for autophagosome formation, mediates membrane tethering and hemifusion. *Cell*; 130: 165-78.
- Near RI, Matulka RA, Mann KK, Gogate SU, Trombino AF, Sherr DH (1999). Regulation of preB cell apoptosis by aryl hydrocarbon receptor/transcription factor-expressing stromal/adherent cells. *Proc Soc Exp Biol Med*; 221: 242-52.
- Nebert DW, Petersen DD, Fornace AJ Jr (1990). Cellular responses to oxidative stress: the [Ah] gene battery as a paradigm. *Environ Health Perspect*; 88: 13-25.
- Nikoletopoulou V, Markaki M, Palikaras K, Tavernarakis N (2013). Crosstalk between apoptosis, necrosis and autophagy. *Biochim Biophys Acta*; 1833: 3448-59.
- Noman MZ, Janji B, Kaminska B, Van Moer K, Pierson S, Przanowski P, Buart S, Berchem G, Romero P, Mami-Chouaib F, Chouaib S (2011). Blocking hypoxia-induced autophagy in tumors restores cytotoxic T-cell activity and promotes regression. *Cancer Res*; 71: 5976-86.
- O'Sullivan GA, Kneussel M, Elazar Z, Betz H (2005). GABARAP is not essential for GABA receptor targeting to the synapse. *Eur J Neurosci*; 22: 2644-8.
- Ohi N, Tokunaga A, Tsunoda H, Nakano K, Haraguchi K, Oda K, Motoyama N, Nakajima T (1999). A novel adenovirus E1B19K-binding protein B5 inhibits apoptosis induced by Nip3 by forming a heterodimer through the C-terminal hydrophobic region. *Cell Death Differ*; 6: 314-25.
- Ohsumi Y (2001). Molecular dissection of autophagy: two ubiquitin-like systems. *Nat. Rev. Mol. Cell. Biol.*; 2: 211-6.
- Olkkonen VM, Stenmark H (1997). Role of Rab GTPases in membrane traffic. *Int Rev Cytol*; 176: 1-85.
- Oltvai ZN, Milliman CL, Korsmeyer SJ (1993). Bcl-2 heterodimerizes *in vivo* with a conserved homolog, Bax, that accelerates programmed cell death. *Cell*; 74: 609-19.
- Ouyang L, Shi Z, Zhao S, Wang FT, Zhou TT, Liu B, Bao JK (2012). Programmed cell death pathways in cancer: a review of apoptosis, autophagy and programmed necrosis. *Cell Prolif*; 45: 487-98.
- Overwijk WW, Restifo NP (2001). B16 as a mouse model for human melanoma. *Curr Protoc Immunol*; Chapter 20: Unit 20.1.
- Page TJ, O'Brien S, Holston K, MacWilliams PS, Jefcoate CR, and Czuprynski CJ (2003). 7,12-Dimethylbenz[a]anthracene-induced bone marrow toxicity is p53-dependent. *Toxicol Sci*; 74: 85-92.

- Paludan C, Schmid D, Landthaler M, Vockerodt M, Kube D, Tuschl T, Münz C. (2005). Endogenous MHC class II processing of a viral nuclear antigen after autophagy. *Science*; 307: 593-6.
- Pankiv S, Lamark T, Bruun JA, Øvervatn A, Bjørkøy G, Johansen T (2010). Nucleocytoplasmic shuttling of p62/SQSTM1 and its role in recruitment of nuclear polyubiquitinated proteins to promyelocytic leukemia bodies. *J Biol Chem*; 285: 5941-53.
- Pattingre S, Tassa A, Qu X, Garuti R, Liang XH, Mizushima N, Packer M, Schneider MD, Levine B (2005). Bcl-2 antiapoptotic proteins inhibit Beclin 1-dependent autophagy. *Cell*; 122: 927-39.
- Pavlidis S, Whitaker-Menezes D, Castello-Cros R, Flomenberg N, Witkiewicz AK, Frank PG, Casimiro MC, Wang C, Fortina P, Addya S, Pestell RG, Martinez-Outschoorn UE, Sotgia F, Lisanti MP (2009). The reverse Warburg effect: aerobic glycolysis in cancer associated fibroblasts and the tumor stroma. *Cell Cycle*; 8: 3984-4001.
- Pavlidis S, Tsirigos A, Migneco G, Whitaker-Menezes D, Chiavarina B, Flomenberg N, Frank PG, Casimiro MC, Wang C, Pestell RG, Martinez-Outschoorn UE, Howell A, Sotgia F, Lisanti MP (2010). The autophagic tumor stroma model of cancer: Role of oxidative stress and ketone production in fueling tumor cell metabolism. *Cell Cycle*; 9: 3485-505.
- Pazos P, Lanari C, Elizalde P, Montecchia F, Charreau EH, Molinolo AA (1998). Promoter effect of medroxyprogesterone acetate (MPA) in N-methyl-N-nitrosourea (MNU) induced mammary tumors in BALB/c mice. *Carcinogenesis*; 19: 529-31.
- Pietras K, Ostman A (2010). Hallmarks of cancer: interactions with the tumor stroma. *Exp Cell Res*; 316: 1324-31.
- Platanias LC. 2005. Mechanisms of type-I- and type-II-interferon- mediated signalling. *Nat Rev Immunol* 5: 375-386.
- Polager S, Ofir M, Ginsberg D (2008). E2F1 regulates autophagy and the transcription of autophagy genes. *Oncogene*; 27: 4860-4.
- Prasad KV, Ao Z, Yoon Y, Wu MX, Rizk M, Jacquot S, Schlossman SF (1997). CD27, a member of the tumor necrosis factor receptor family, induces apoptosis and binds to Siva, a proapoptotic protein. *Proc Natl Acad Sci USA*; 94: 6346-51.
- Prehn RT (1963). Function of depressed immunologic reactivity during carcinogenesis. *J Natl Cancer Inst*; 31: 791-805.
- Priyadarsini RV, Nagini S (2012). Quercetin suppresses cytochrome P450 mediated ROS generation and NFκB activation to inhibit the development of 7,12-dimethylbenz[a]anthracene (DMBA) induced hamster buccal pouch carcinomas. *Free Radic Res*; 46: 41-9.
- Qing WG, Conti CJ, LaBate M, Johnston D, Slaga TJ, MacLeod MC (1997). Induction of mammary cancer and lymphoma by multiple, low oral doses of 7,12-dimethylbenz[a]anthracene in SENCAR mice. *Carcinogenesis*; 18: 553-9.
- Qiu W, Zhou J, Zhu G, Zhao D, He F, Zhang J, Lu Y, Yu T, Liu L, Wang Y (2014). Sublytic C5b-9 triggers glomerular mesangial cell apoptosis via XAF1 gene activation mediated by p300-dependent IRF-1 acetylation. *Cell Death Dis*; 5: e1176.

- Qu X, Yu J, Bhagat G, Furuya N, Hibshoosh H, Troxel A, Rosen J, Eskelinen EL, Mizushima N, Ohsumi Y, Cattoretti G, Levine B (2003). Promotion of tumorigenesis by heterozygous disruption of the beclin 1 autophagy gene. *J Clin Invest*; 112: 1809-20.
- Rabinowitz JD, White E (2010). Autophagy and metabolism. *Science*; 330: 1344-8.
- Resch U, Schichl YM, Winsauer G, Gudi R, Prasad K, de Martin R (2009). Siva1 is a XIAP-interacting protein that balances NFkappaB and JNK signalling to promote apoptosis. *J Cell Sci*; 122: 2651-61.
- Rioux JD, Xavier RJ, Taylor KD, Silverberg MS, Goyette P, Huett A, Green T, Kuballa P, Barmada MM, Datta LW, Shugart YY, Griffiths AM, Targan SR, Ippoliti AF, Bernard EJ, Mei L, Nicolae DL, Regueiro M, Schumm LP, Steinhart AH, Rotter JI, Duerr RH, Cho JH, Daly MJ, Brant SR (2007). Genome-wide association study identifies new susceptibility loci for Crohn disease and implicates autophagy in disease pathogenesis. *Nat Genet*; 39: 596-604.
- Roberts SS, Mori M, Pattee P, Lapidus J, Mathews R, O'Malley JP, Hsieh YC, Turner MA, Wang Z, Tian Q, Rodland MJ, Reynolds CP, Seeger RC, Nagalla SR (2004). GABAergic system gene expression predicts clinical outcome in patients with neuroblastoma. *J Clin Oncol*; 22: 4127-34.
- Roberts SS, Mendonça-Torres MC, Jensen K, Francis GL, Vasko V (2009). GABA receptor expression in benign and malignant thyroid tumors. *Pathol Oncol Res*; 15: 645-50.
- Rodriguez-Rocha H, Garcia-Garcia A, Panayiotidis MI, Franco R (2011). DNA damage and autophagy. *Mutat Res*; 711: 158-66.
- Romieu-Mourez R, Kim DW, Shin SM, Demicco EG, Landesman-Bollag E, Seldin DC, Cardiff RD, Sonenshein GE (2003). Mouse mammary tumor virus c-rel transgenic mice develop mammary tumors. *Mol Cell Biol*; 23: 5738-54.
- Roos WP, Kaina B (2006). DNA damage-induced cell death by apoptosis. *Trends Mol Med* 12: 440-50.
- Rosenfeldt MT, Ryan KM (2011). The multiple roles of autophagy in cancer. *Carcinogenesis*; 32: 955-63.
- Roy D, Sarkar S, Felty Q (2006). Levels of IL-1 beta control stimulatory/inhibitory growth of cancer cells. *Front Biosci*; 11: 889-98.
- Rundle A, Tang D, Hibshoosh H, Estabrook A, Schnabel F, Cao W, Grumet S, Perera FP (2000). The relationship between genetic damage from polycyclic aromatic hydrocarbons in breast tissue and breast cancer. *Carcinogenesis*; 21: 1281-9.
- Saas P, Bohuon C, Pallardy M (1996). Effects of methyl substitutions on benz[a]anthracene derivatives-induced immunosuppression. *J Toxicol Environ Health*; 49: 371-87.
- Saitoh T, Fujita N, Jang MH, Uematsu S, Yang BG, Satoh T, Omori H, Noda T, Yamamoto N, Komatsu M, Tanaka K, Kawai T, Tsujimura T, Takeuchi O, Yoshimori T, Akira S (2008). Loss of the autophagy protein Atg16L1 enhances endotoxin-induced IL-1beta production. *Nature*; 456: 264-8.
- Sarbassov DD, Ali SM, Sengupta S, Sheen JH, Hsu PP, Bagley AF, Markhard AL, Sabatini DM (2006). Prolonged rapamycin treatment inhibits mTORC2 assembly and Akt/PKB. *Mol Cell*; 22: 159-68.
- Scherz-Shouval R, Elazar Z (2007). ROS, mitochondria and the regulation of autophagy. *Trends Cell Biol*; 17: 422-7.

- Scherz-Shouval R, Shvets E, Fass E, Shorer H, Gil L, Elazar Z (2007). Reactive oxygen species are essential for autophagy and specifically regulate the activity of Atg4. *EMBO J*; 26: 1749-60.
- Schreiber RD, Old LJ, Smyth MJ (2011). Cancer immunoediting: integrating immunity's roles in cancer suppression and promotion. *Science*; 331: 1565-70.
- Schubbert S, Shannon K, Bollag G (2007). Hyperactive Ras in developmental disorders and cancer. *Nat Rev Cancer*; 7: 295-308.
- Schwarten M, Mohrlüder J, Ma P, Stoldt M, Thielmann Y, Stangler T, Hersch N, Hoffmann B, Merkel R, Willbold D (2009). Nix directly binds to GABARAP: a possible crosstalk between apoptosis and autophagy. *Autophagy*; 5: 690-8.
- Shankaran V, Ikeda H, Bruce AT, White JM, Swanson PE, Old LJ, Schreiber RD (2001). IFN γ and lymphocytes prevent primary tumour development and shape tumour immunogenicity. *Nature* 410: 1107-11.
- Shi CS, Kehrl JH (2010). Traf6 and A20 differentially regulate tlr4- induced autophagy by affecting the ubiquitination of beclin 1. *Autophagy*; 6: 986-7.
- Shi CS, Shenderov K, Huang NN, Kabat J, Abu-Asab M, Fitzgerald KA, Sher A, Kehrl JH (2012). Activation of autophagy by inflammatory signals limits IL-1 β production by targeting ubiquitinated inflammasomes for destruction. *Nat Immunol*; 13: 255-63.
- Shimada T, Fujii-Kuriyama Y (2004). Metabolic activation of polycyclic aromatic hydrocarbons to carcinogens by cytochromes P450 1A1 and 1B1. *Cancer Sci*; 95: 1-6.
- Shirai K, Uemura Y, Fukumoto M, Tsukamoto T, Pascual R, Nandi S, Tsubura A (1997). Synergistic effect of MNU and DMBA in mammary carcinogenesis and H-ras activation in female Sprague-Dawley rats. *Cancer Lett*; 120: 87-93.
- Shvets E, Abada A, Weidberg H, Elazar Z (2011). Dissecting the involvement of LC3B and GATE-16 in p62 recruitment into autophagosomes. *Autophagy*; 7: 683-88.
- Singh R, Xiang Y, Wang Y, Baikati K, Cuervo AM, Luu YK, Tang Y, Pessin JE, Schwartz GJ, Czaja MJ (2009). Autophagy regulates adipose mass and differentiation in mice. *J Clin Invest*; 119: 3329-39.
- Smyth GK (2005). Limma: linear models for microarray data. In: 'Bioinformatics and Computational Biology Solutions using R and Bioconductor'. R. Gentleman, V. Carey, S. Dudoit, R. Irizarry, W. Huber (eds), Springer, New York. Pages: 397-420.
- Sovak MA, Bellas RE, Kim DW, Zanieski GJ, Rogers AE, Traish AM, Sonenshein GE (1997). Aberrant nuclear factor-kappaB/Rel expression and the pathogenesis of breast cancer. *J Clin Invest*; 100: 2952-60.
- Stern JB, Smith KA (1986). Interleukin-2 induction of T-cell G1 progression and c-myc expression. *Science*; 233: 203-6.
- Stolpmann K, Brinkmann J, Salzmann S, Genkinger D, Fritsche E, Hutzler C, Wajant H, Luch A, Henkler F (2012). Activation of the aryl hydrocarbon receptor sensitises human keratinocytes for CD95L- and TRAIL-induced apoptosis. *Cell Death Dis*; 3: e388.
- Straszewski-Chavez SL, Visintin IP, Karassina N, Los G, Liston P, Halaban R, Fadiel A, Mor G (2007). XAF1 mediates tumor necrosis factor-alpha-induced apoptosis and X-linked inhibitor of apoptosis cleavage by acting through the mitochondrial pathway. *J Biol Chem*; 282: 13059-72.

- Sun PH, Zhu LM, Qiao MM, Zhang YP, Jiang SH, Wu YL, Tu SP (2011). The XAF1 tumor suppressor induces autophagic cell death via upregulation of Beclin-1 and inhibition of Akt pathway. *Cancer Lett*; 310: 170-80.
- Sun Y, Qiao L, Xia HH, Lin MC, Zou B, Yuan Y, Zhu S, Gu Q, Cheung TK, Kung HF, Yuen MF, Chan AO, Wong BC (2008). Regulation of XAF1 expression in human colon cancer cell by interferon beta: activation by the transcription regulator STAT1. *Cancer Lett*; 260: 62-71.
- Suzuki K, Kirisako T, Kamada Y, Mizushima N, Noda T, Ohsumi Y (2001). The preautophagosomal structure organized by concerted functions of APG genes is essential for autophagosome formation. *EMBO J*; 20: 5971-81.
- Svetlova MP, Solovjeva LV, Tomilin NV (2010). Mechanism of elimination of phosphorylated histone H2AX from chromatin after repair of DNA double-strand breaks. *Mutat Res*; 685: 54-60.
- Swanson HI, Chan WK, Bradfield CA (1995). DNA binding specificities and pairing rules of the Ah receptor, ARNT, and SIM proteins. *J Biol Chem*; 270: 26292-302.
- Takacs-Vellai K, Vellai T, Puoti A, Passannante M, Wicky C, Streit A, Kovacs AL, Muller F (2005). Inactivation of the autophagy gene bec-1 triggers apoptotic cell death in *C. elegans*. *Curr Biol*; 15: 1513-7.
- Takamura A, Komatsu M, Hara T, Sakamoto A, Kishi C, Waguri S, Eishi Y, Hino O, Tanaka K, Mizushima N (2011). Autophagy-deficient mice develop multiple liver tumors. *Genes Dev*; 25: 795-800.
- Tal MC, Sasai M, Lee HK, Yordy B, Shadel GS, Iwasaki A (2009). Absence of autophagy results in reactive oxygen species-dependent amplification of RLR signaling. *Proc Natl Acad Sci USA*; 106: 2770-5.
- Tanida I, Mizushima N, Kiyooka M, Ohsumi M, Ueno T, Ohsumi Y, Kominami E (1999). Apg7p/Cvt2p: A novel protein-activating enzyme essential for autophagy. *Mol Biol Cell*; 10: 1367-79.
- Tanida I, Ueno T, Kominami E (2004). LC3 conjugation system in mammalian autophagy. *Int J Biochem Cell Biol*; 36: 2503-18.
- Tasdemir E, Maiuri MC, Galluzzi L, Vitale I, Djavaheri-Mergny M, D'Amelio M, Criollo A, Morselli E, Zhu C, Harper F, Nannmark U, Samara Ch, Pinton P, Vicencio JM, Carnuccio R, Moll UM, Madeo F, Paterlini-Brechot P, Rizzuto R, Szabadkai G, Pierron G, Blomgren K, Tavernarakis N, Codogno P, Cecconi F, Kroemer G (2008). Regulation of autophagy by cytoplasmic p53. *Nat Cell Biol*; 10: 676-87.
- Teague JE, Ryu HY, Kirber M, Sherr DH, Schlezinger JJ (2010). Proximal events in 7,12-dimethylbenz[a]anthracene-induced, stromal cell-dependent bone marrow B cell apoptosis: stromal cell-B cell communication and apoptosis signaling. *J Immunol*; 185: 3369-78.
- Thiery JP, Acloque H, Huang RY, Nieto MA (2009). Epithelial-mesenchymal transitions in development and disease. *Cell*; 139: 871-90.
- Thumm M, Egner R, Koch B, Schlumpberger M, Straub M, Veenhuisb M, Wolf DH (1994). Isolation of autophagocytosis mutants of *Saccharomyces cerevisiae*. *FEBS Lett*; 349: 275-80.

- Thurmond LM, Lauer LD, House RV, Cook JC, Dean JH (1987). Immunosuppression following exposure to 7,12-dimethylbenz[a]anthracene (DMBA) in Ah-responsive and Ah-nonresponsive mice. *Toxicol Appl Pharmacol*; 91: 450-60.
- Thurmond LM, House RV, Lauer LD, Dean JH (1988). Suppression of splenic lymphocyte function by 7,12-dimethylbenz[a]anthracene (DMBA) *in vitro*. *Toxicol Appl Pharmacol*; 93: 369-77.
- Tracey KJ, Cerami A (1994). Tumor necrosis factor: a pleiotropic cytokine and therapeutic target. *Annu Rev Med*; 45: 491-503.
- Trombino AF, Near RI, Matulka RA, Yang S, Hafer LJ, Toselli PA, Kim DW, Rogers AE, Sonenshein GE, Sherr DH (2000). Expression of the aryl hydrocarbon receptor/transcription factor (AhR) and AhR-regulated CYP1 gene transcripts in a rat model of mammary tumorigenesis. *Breast Cancer Res Treat*; 63: 117-31.
- Tsukada M, Ohsumi Y (1993). Isolation and characterization of autophagy-defective mutants of *Saccharomyces cerevisiae*. *FEBS Lett*; 333: 169-74.
- Tu SP, Liston P, Cui JT, Lin MC, Jiang XH, Yang Y, Gu Q, Jiang SH, Lum CT, Kung HF, Korneluk RG, Wong BC (2009). Restoration of XAF1 expression induces apoptosis and inhibits tumor growth in gastric cancer. *Int J Cancer*; 125: 688-97.
- Tu SP, Sun YW, Cui JT, Zou B, Lin MC, Gu Q, Jiang SH, Kung HF, Korneluk RG, Wong BC (2010). Tumor suppressor XIAP-Associated factor 1 (XAF1) cooperates with tumor necrosis factor-related apoptosis-inducing ligand to suppress colon cancer growth and trigger tumor regression. *Cancer*; 116: 1252-63.
- Uno S, Dalton TP, Derkenne S, Curran CP, Miller ML, Shertzer HG, and Nebert DW (2004). Oral exposure to benzo[a]pyrene in the mouse: detoxication by inducible cytochrome P450 is more important than metabolic activation. *Mol Pharmacol*; 65: 1225-37.
- van 't Veer LJ, Dai H, van de Vijver MJ, He YD, Hart AA, Mao M, Peterse HL, van der Kooy K, Marton MJ, Witteveen AT, Schreiber GJ, Kerkhoven RM, Roberts C, Linsley PS, Bernards R, Friend SH (2002). Gene expression profiling predicts clinical outcome of breast cancer. *Nature*; 415: 530-6.
- Vander Heiden MG, Cantley LC, Thompson CB (2009). Understanding the Warburg effect: the metabolic requirements of cell proliferation. *Science*; 324: 1029-33.
- Vazquez-Martin A, Oliveras-Ferraros C, Menendez JA (2009). Autophagy facilitates the development of breast cancer resistance to the anti-HER2 monoclonal antibody trastuzumab. *PLoS One*; 4: e6251.
- Veloso A, Biewen B, Paulsen MT, Berg N, Carmo de Andrade Lima L, Prasad J, Bedi K, Magnuson B, Wilson TE, Ljungman M (2013). Genome-wide transcriptional effects of the anti-cancer agent camptothecin. *PLoS One*; 8: e78190.
- von Ahlfen S, Missel A, Bendrat K, Schlumpberger M (2007). Determinants of RNA quality from FFPE samples. *PLoS One*; 2: e1261.
- Wang H, Bedford FK, Brandon NJ, Moss SJ, Olsen RW (1999). GABAA-receptor-associated protein links GABA_A receptors and the cytoskeleton. *Nature*; 397:69-72.
- Wang H, Olsen RW (2000). Binding of the GABA_A Receptor-Associated Protein (GABARAP) to Microtubules and Microfilaments Suggests Involvement of the Cytoskeleton in GABARAP-GABA_A Receptor Interaction. *J Neurochem.*; 75: 644-55.

- Wang J, He H, Yu L, Xia HH, Lin MC, Gu Q, Li M, Zou B, An X, Jiang B, Kung HF, Wong BC (2006a). HSF1 down-regulates XAF1 through transcriptional regulation. *J Biol Chem*; 281: 2451-9.
- Wang J, Peng Y, Sun YW, He H, Zhu S, An X, Li M, Lin MC, Zou B, Xia HH, Jiang B, Chan AO, Yuen MF, Kung HF, Wong BC (2006b). All-trans retinoic acid induces XAF1 expression through an interferon regulatory factor-1 element in colon cancer. *Gastroenterology*; 130: 747-58.
- Wang J, Gu Q, Li M, Zhang W, Yang M, Zou B, Chan S, Qiao L, Jiang B, Tu S, Ma J, Hung IF, Lan HY, Wong BC (2009a). Identification of XAF1 as a novel cell cycle regulator through modulating G(2)/M checkpoint and interaction with checkpoint kinase 1 in gastrointestinal cancer. *Carcinogenesis*; 30: 1507-16.
- Wang J, Zhang W, Zhang Y, Chen Y, Zou B, Jiang B, Pang R, Gu Q, Qiao L, Lan H, Kung HF, Wong BC (2009b). c-Jun N-terminal kinase (JNK1) upregulates XIAP-associated factor 1 (XAF1) through interferon regulatory factor 1 (IRF-1) in gastrointestinal cancer. *Carcinogenesis*; 30: 222-9.
- Wang K, Liu R, Li J, Mao J, Lei Y, Wu J, Zeng J, Zhang T, Wu H, Chen L, Huang C, Wei Y (2011). Quercetin induces protective autophagy in gastric cancer cells: involvement of Akt-mTOR- and hypoxia-induced factor 1alpha-mediated signaling. *Autophagy*; 7: 966-78.
- Warburg O (1956). On the origin of cancer cells. *Science*; 123: 309-14.
- Ward EC, Murray MJ, Lauer LD, House RV, Dean JH (1986). Persistent suppression of humoral and cell-mediated immunity in mice following exposure to the polycyclic aromatic hydrocarbon 7,12-dimethylbenz[a]anthracene. *Int J Immunopharmacol*; 8: 13-22.
- Wei H, Wei S, Gan B, Peng X, Zou W, Guan J (2011). Suppression of autophagy by FIP200 deletion inhibits mammary tumorigenesis. *Genes Dev*; 25: 1510-27.
- Weidberg H, Shvets E, Shpilka T, Shimron F, Shinder V, Elazar Z (2010). LC3 and GATE-16/GABARAP subfamilies are both essential yet act differently in autophagosome biogenesis. *EMBO J*; 29: 1792-1802.
- Wild Ph, McEwan DG, Dikic I (2014). The LC3 interactome at a glance. *J Cell Sci*; 127: 3-9.
- Wilkinson S, Ryan KM (2010). Autophagy: an adaptable modifier of tumourigenesis. *Curr Opin Genet Dev*; 20: 57-64.
- Williams JM, Daniel CW (1983). Mammary ductal elongation: differentiation of myoepithelium and basal lamina during branching morphogenesis. *Dev Biol*; 97: 274-90.
- Wirawan E, Berghe TV, Lippens S, Agostinis P, Vandenabeele P (2012). Autophagy: for better or for worse. *Cell Research*; 22: 43-61.
- Wiseman BS, Werb Z (2002). Stromal effects on mammary gland development and breast cancer. *Science*; 296: 1046-9.
- Witz IP, Levy-Nissenbaum O (2006). The tumor microenvironment in the post-PAGET era. *Cancer Lett*; 242: 1-10.
- Wong RS (2011). Apoptosis in cancer: from pathogenesis to treatment. *J Exp Clin Cancer Res*; 30: 87.

- Wong WW, Puthalakath H (2008). Bcl-2 family proteins: the sentinels of the mitochondrial apoptosis pathway. *IUBMB Life*; 60: 339-90.
- Woodworth CD, Michael E, Smith L, Vijayachandra K, Glick A, Hennings H, Yuspa SH (2004). Strain-dependent differences in malignant conversion of mouse skin tumors is an inherent property of the epidermal keratinocyte. *Carcinogenesis*; 25: 1771-8.
- Wu M, Yin G, Zhao X, Ji C, Gu S, Tang R, Dong H, Xie Y, Mao Y (2006). Human RAB24, interestingly and predominantly distributed in the nuclei of COS-7 cells, is colocalized with cyclophilin A and GABARAP. *Int J Mol Med*; 17: 749-54.
- Xia Y, Novak R, Lewis J, Duckett CS, Phillips AC (2006). Xaf1 can cooperate with TNFalpha in the induction of apoptosis, independently of interaction with XIAP. *Mol Cell Biochem*; 286: 67-76.
- Xie Z, Nair U, Klionsky DJ (2008). Atg8 controls phagophore expansion during autophagosome formation. *Mol Biol Cell*; 19: 3290-98.
- Xue L, Chu F, Cheng Y, Sun X, Borthakur A, Ramarao M, Pandey P, Wu M, Schlossman SF, Prasad KV (2002). Siva-1 binds to and inhibits BCL-X(L)-mediated protection against UV radiation-induced apoptosis. *Proc Natl Acad Sci USA*; 99: 6925-30.
- Yang J, Weinberg RA (2008). Epithelial-mesenchymal transition: at the crossroads of development and tumor metastasis. *Dev Cell*; 14: 818-29.
- Yang JY, Yang WY (2013). Bit-by-bit autophagic removal of parkin-labelled mitochondria. *Nat Commun*; 4: 2428.
- Yang L, Ng KY, Lillehei KO (2003). Cell-mediated immunotherapy: a new approach to the treatment of malignant glioma. *Cancer Control*; 10: 138-47.
- Yang S, Wang X, Contino G, Liesa M, Sahin E, Ying H, Bause A, Li Y, Stommel JM, Dell'antonio G, Mautner J, Tonon G, Haigis M, Shirihai OS, Doglioni C, Bardeesy N, Kimmelman AC (2011). Pancreatic cancers require autophagy for tumor growth. *Genes Dev*; 25: 717-29.
- Yang ZJ, Chee CE, Huang S, Sinicrope FA (2011). The role of autophagy in cancer: therapeutic implications. *Mol Cancer Ther*; 10: 1533-41.
- Yla-Anttila P, Vihinen H, Jokitalo E, Eskelinen EL (2009). 3D tomography reveals connections between the phagophore and endoplasmic reticulum. *Autophagy*; 5: 1180-85.
- Yoshimori T, Amano A (2009). Group A Streptococcus: a loser in the battle with autophagy. *Curr Top Microbiol Immunol*; 335: 217-26.
- Young AR, Chan EY, Hu XW, Kochl R, Crawshaw SG, High S, Hailey DW, Lippincott-Schwartz J, Tooze SA (2006). Starvation and ULK1-dependent cycling of mammalian Atg9 between the TGN and endosomes. *J Cell Sci*; 119: 3888-900.
- Yu LF, Wang J, Zou B, Lin MC, Wu YL, Xia HH, Sun YW, Gu Q, He H, Lam SK, Kung HF, Wong BC (2007). XAF1 mediates apoptosis through an extracellular signal-regulated kinase pathway in colon cancer. *Cancer*; 109: 1996-2003.
- Yudowski GA, Puthenveedu MA, Henry AG, von Zastrow M (2009). Cargo-mediated regulation of a rapid Rab4-dependent recycling pathway. *Mol Biol Cell*; 20: 2774-84.
- Yue Z, Jin S, Yang C, Levine AJ, Heintz N (2003). Beclin 1, an autophagy gene essential for early embryonic development, is a haploinsufficient tumor suppressor. *PNAS*; 100: 15077-82.

- Yui S, Sasaki T, Yamazaki M (1993). Augmentation and suppression of TNF release from macrophages by inflammatory polymorphonuclear leukocytes. *Microbiol Immunol*; 37: 801-8.
- Yussman MG, Toyokawa T, Odley A, Lynch RA, Wu G, Colbert MC, Aronow BJ, Lorenz JN, Dorn GW II (2002). Mitochondrial death protein Nix is induced in cardiac hypertrophy and triggers apoptotic cardiomyopathy. *Nat Med*; 8: 725-30.
- Zambrowicz BP, Friedrich GA, Buxton EC, Lilleberg SL, Person C, Sands AT (1998). Disruption and sequence identification of 2,000 genes in mouse embryonic stem cells. *Nature*; 392: 608-11.
- Zeh HJ 3rd, Lotze MT (2005). Addicted to death: invasive cancer and the immune response to unscheduled cell death. *J Immunother*; 28: 1-9.
- Zhang W, Yang Y, Jiang B, Peng J, Tu S, Sardet C, Zhang Y, Pang R, Hung IF, Tan VP, Lam CS, Wang J, Wong BC (2011). XIAP-associated factor 1 interacts with and attenuates the trans-activity of four and a Half LIM protein 2. *Mol Carcinog*; 50: 199-207.
- Zhang Y, Goldman S, Baerga R, Zhao Y, Komatsu M, Jin S (2009). Adipose-specific deletion of autophagy-related gene 7 (*atg7*) in mice reveals a role in adipogenesis. *PNAS*; 106: 19860-5.
- Zhang YB, Zhao W, Zeng RX (2013). Autophagic degradation of caspase-8 protects U87MG cells against H₂O₂-induced oxidative stress. *Asian Pac J Cancer Prev*; 14: 4095-9.
- Zhang Z, Xu X, Ma J, Wu J, Wang Y, Zhou R, Han J (2013). Gene deletion of Gabarap enhances Nlrp3 inflammasome-dependent inflammatory responses. *J Immunol*; 190: 3517-24.
- Zhao X, Liu X, Su L (2014). Parthenolide induces apoptosis via TNFRSF10B and PMAIP1 pathways in human lung cancer cells. *J Exp Clin Cancer Res*; 33: 3.
- Zheng Y, Zhao YL, Deng X, Yang S, Mao Y, Li Z, Jiang P, Zhao X, Wei Y (2009). Chloroquine inhibits colon cancer cell growth *in vitro* and tumor growth *in vivo* via induction of apoptosis. *Cancer Invest*; 27: 286-92.
- Zhou Y, Jiang L, Rui L (2009). Identification of MUP1 as a regulator for glucose and lipid metabolism in mice. *J Biol Chem*; 284: 11152-9.
- Zinkel S, Gross A, Yang E (2006). BCL2 family in DNA damage and cell cycle control. *Cell Death Differ*; 13: 1351-9.
- Zou B, Chim CS, Zeng H, Leung SY, Yang Y, Tu SP, Lin MC, Wang J, He H, Jiang SH, Sun YW, Yu LF, Yuen ST, Kung HF, Wong BC (2006). Correlation between the single-site CpG methylation and expression silencing of the XAF1 gene in human gastric and colon cancers. *Gastroenterology*; 131: 1835-43.
- Zou B, Chim CS, Pang R, Zeng H, Dai Y, Zhang R, Lam CS, Tan VP, Hung IF, Lan HY, Wong BC (2012). XIAP-associated factor 1 (XAF1), a novel target of p53, enhances p53-mediated apoptosis via post-translational modification. *Mol Carcinog*; 51: 422-32.

6. Appendix

6.1 Acknowledgment

My PhD study has been a challenging journey both scientifically and personally and it has taken me several years far away from my darling homeland (**IRAQ**). I have met many inspiring people who in one way or another have contributed to this PhD study.

I am extremely grateful to the Deutscher Akademischer Austauschdienst (DAAD) for the scholarship which allowed me to do my doctoral study in Germany. I would like also to thank the Interdisciplinary Centre for Clinical Research (IZKF) of Jena University Hospital and the Graduate Academy of Friedrich Schiller University for their financial support for my project.

It is with immense gratitude that I acknowledge the support and help of my supervisors for their guidance, understanding, patience, and most importantly, their friendship during my PhD study at the Institute of Pathology / University Hospital / Friedrich-Schiller University of Jena. They encouraged me to not only grow as an experimentalist but also as an instructor and an independent thinker. I would like to thank my primary supervisor, Prof. Dr. Iver Petersen for his invaluable contribution and supervision acceptance that supported me to get the DAAD scholarship. Despite his busy schedule, he has always made time for discussion. I have always appreciated his calm and carefully evaluating manner. I have truly learned a lot during my thesis, which go beyond science itself, and thank Prof. Petersen for this. My second supervisor, Prof. Dr. Rolf Bräuer, is also invaluable. Without his support and active participation in every step of the process, this thesis may never have been completed. Thank Prof. Bräuer very much for your encouragement, assistance, guidance and understanding over these past five years.

During my thesis work, I am lucky to have Kristin Zöllner, Dr. Yuan Chen, Claudia Seliger, Melanie Gerth, Linlin Yang, Tiantian Cui, Christina Polasky, Friederike Saabler and Qing Zhang as my colleagues in the lab. I cherish the friendship with them. I am very grateful to Dr. Chen for her stimulating and enthusiastic discussions during my experimental work.

I cannot honestly find words to express my gratitude to Kristin Zöllner for all that she has done for me. Her knowledge and expert in routine procedures of DNA extraction, mutation analysis, and processing and sectioning tissue have greatly supported me to achieve a part of my results. Kristin is not only an excellent scientific laboratory technician that helps me in research work, but also warm-heartedly introduced me to living in Germany. For everything you've done for me, Kristin, I thank you.

I would like to thank Dr. Matthias Ebbinghaus, from the Institute of Physiology 1, for his great assistance in the immunological experiments and for his actively motivation and enthusiastic discussion about the project. I would like also to thank all the members of the Institute of Pathology, especially Mrs. Renate Stöckigt and Mrs. Cornelia Hüttich for their fantastic help in animal experiments and tissue samples preparation. I wish to thank Dr. Petra Richter for her support to show me the correct procedures of different techniques used in the laboratory. I am also very thankful to Dr. Masoud Mireskandari for his help in evaluation the histology sections.

I am very grateful for Prof. Dr. Rainer König and Dr. Vijaykumar Muley, from Network Modelling group at Hans-Knöll-Institute (HKI), for their support for analysing the data of whole mouse genome expression and their motivation and enthusiastic discussions about the project.

My sincere thanks to Prof. Dr. Zhao-Qi Wang and Dr. Zhongwei Zhou, from the Leibniz Institute for Age Research Fritz-Lipmann-Institut e.V. (FLI), they helped me to perform the TUNEL assay, as well as valuable discussions. I wish also to thank Martin Böttcher, from the Institute of Immunology, for his assistance to carry out the FACS analysis.

I would like to thank my wife Khansaa. Her support, encouragement, quiet patience and unwavering love were undeniably the bedrock upon which the past seven years of my life have been built. Her tolerance of my occasional tough mood during the writing of my thesis is a testament in itself of her love. I would also to thank Khansaa for her help in some experiments of my project. I thank my parents for their prayer to me, faith in me and allowing me to be as ambitious as I wanted. My special thanks to my brothers Omar, Ali and Raed and my sister Suha, with whom I shared my pleasant life in our parent's home and also I would like to thank them for their support during my graduate study. Also, I thank Khansaa's family, her mother Muna, her brothers Abdel-Latif and Labid, and her sisters Amna and Asma, for providing me an unending encouragement and support.

Finally, and most importantly, I would like to thank my soul and sweet little daughter **Myriam** for her existence in my life. She gave me an immense motivation and encouragement to do my best to finish this thesis and to continue my research in Iraq.

6.2 Curriculum vitae

Firas Subhi Salah

Nationality: Iraqi

Born: on April 10, 1977 in Diyala, Iraq

- 1983 - 1989 Elementary school, Diyala, Iraq
- 1989 - 1992 Middle school, Diyala, Iraq
- 1992 - 1995 High school (gymnasium), Diyala, Iraq
- June 1995 School-leaving exams (Baccalaureate)
- 1995 - 2000 Student at College of Veterinary Medicine, University of Baghdad, Baghdad, Iraq
- June 2000 Bachelor degree in Veterinary Medicine and Surgery
- 2000 - 2001 Resident doctor in Diyala veterinary hospital
- 2000 - 2004 Master of science student at Pathology department / College of Veterinary Medicine, University of Baghdad, Baghdad, Iraq
- Feb 2004 Master degree of science in Veterinary Medicine / Pathology. Thesis title "Pathological and cytogenetic study on some epithelial skin tumors in human and bovine"
- April 2004 Work at Iraqi Centre for Cancer and Medical Genetics Research (ICCMGR), Baghdad, Iraq
- 2004 - 2009 Researcher and assistant lecturer at Iraqi Centre for Cancer and Medical Genetics Research (ICCMGR), Baghdad, Iraq
- 2007 - 2009 Editorial secretary of Iraqi Journal of Cancer (IJC) and Iraqi Journal of Genetic (IJG) issued by Iraqi centre for cancer and medical genetics research (ICCMGR).
- Since Oct 2009 PhD student at Institute of Pathology / University Hospital Jena / Friedrich Schiller University, Jena, Germany

.....

Jena, den 26. Juni 2014

Firas Subhi Salah

6.3 List of publication and presentations

- F. S. Salah, I. Petersen. LCD-array for molecular diagnosis of Synovial Sarcoma. 2nd Postgraduate Symposium on Cancer Research, Altes Schloss Dornburg / Jena, Germany, April 2010 (**poster**).
- I. Petersen, B. Günther, K. Nitsche, F. Subhi, T. Knösel, A. Altendorf-Hofmann, D. Katenkamp (2011). Neues aus dem Jenaer Weichteiltumor-Register. Der Pathologe; 32: 40-46. (**publication**)
- F. S. Salah, R. Bräuer, M. Pacyna-Gengelbach, G. O’Sullivan, H. Betz, I. Petersen. The role of GABARAP in the onset and progression of solid tumors with special emphasis on breast cancer. 3rd Postgraduate Symposium on Cancer Research, Altes Schloss Dornburg / Jena, Germany, April 2011 (**poster**).
- F. S. Salah, R. Bräuer, M. Pacyna-Gengelbach, G. O’Sullivan, H. Betz, I. Petersen. The role of GABARAP in the onset and progression of solid tumors with special emphasis on breast cancer. 95th Annual Meeting of the German Society of Pathology, Leipzig, Germany, June 2011 (**poster**). Der Pathologe, 2011, 32(Supplement 1): 91.
- F.S. Salah, R. Bräuer, S. Nietzsche, Y. Chen, I. Petersen. Re-expression of GABARAP by p38 inhibitor Induces Autophagy and Inhibits Growth in Breast Cancer Cells. 5th Postgraduate Symposium on Cancer Research, Altes Schloss Dornburg / Jena, Germany, April 2013 (**poster**).
- F.S. Salah, R. Bräuer, S. Nietzsche, Y. Chen, I. Petersen. Re-expression of GABARAP by p38 inhibitor Induces Autophagy and Inhibits Growth in Breast Cancer Cells. 97th Annual Meeting of the German Society of Pathology, Heidelberg, Germany, May 2013 (**poster**). Der Pathologe, 2013, 34(Supplement 1): 117.
- F.S. Salah, M. Ebbinghaus, R. Bräuer, I. Petersen. Anti-tumor activity of GABARAP-deficient mice treated with 7,12-Dimethylbenz(a)anthracene (DMBA). 6th Postgraduate Symposium on Cancer Research, Altes Schloss Dornburg / Jena, Germany, April 2014 (**poster**).
- F.S. Salah, M. Ebbinghaus, R. Bräuer, I. Petersen. Anti-tumor activity of GABARAP-deficient mice treated with 7,12-Dimethylbenz(a)anthracene (DMBA). 98th Annual Meeting of the German Society of Pathology, Berlin, Germany, June 2014 (**poster**). Der Pathologe, 2014, 35(Supplement 1): 132-133.

.....

Jena, den 26. Juni 2014

Firas Subhi Salah

6.4 Ehrenwörtliche Erklärung

Hiermit erkläre ich, dass mir die Promotionsordnung der Medizinischen Fakultät der Friedrich-Schiller-Universität bekannt ist,

ich die Dissertation selbst angefertigt habe und alle von mir benutzten Hilfsmittel, persönlichen Mitteilungen und Quellen in meiner Arbeit angegeben sind,

mich folgende Personen bei der Auswahl und Auswertung des Materials sowie bei der Herstellung des Manuskripts unterstützt haben:

Prof. Dr. med. Iver Petersen

Prof. Dr. rer. nat. Rolf Bräuer

Prof. Dr. Rainer König

Dr. Matthias Ebbinghaus

Dr. Vijaykumar Muley

Dr. Zhongwei Zhou

Frau Dipl. Ing. Renate Stöckigt

Frau Cornelia Hüttich

Frau Kristin Zöller

die Hilfe eines Promotionsberaters nicht in Anspruch genommen wurde und dass Dritte weder unmittelbar noch mittelbar geldwerte Leistungen von mir für Arbeiten erhalten haben, die im Zusammenhang mit dem Inhalt der vorgelegten Dissertation stehen,

dass ich die Dissertation noch nicht als Prüfungsarbeit für eine staatliche oder andere wissenschaftliche Prüfung eingereicht habe und

dass ich die gleiche, eine in wesentlichen Teilen ähnliche oder eine andere Abhandlung nicht bei einer anderen Hochschule als Dissertation eingereicht habe.

Jena, 26.06.2014

Ort, Datum

Unterschrift des Verfassers